Longitudinal high-throughput single-B-cell exploration of the broadly neutralizing antibody repertoire in an HIV-1 elite-neutralizer

Benjamin Nemoz

THÈSE

Pour obtenir le grade de

DOCTEUR DE L'UNIVERSITÉ GRENOBLE ALPES

École doctorale : CSV- Chimie et Sciences du Vivant
Spécialité : Virologie - Microbiologie - Immunologie
Unité de recherche : Institut de Biologie Structurale

Exploration longitudinale à haut débit et en cellule unique du répertoire d'anticorps neutralisants à large spectre chez un neutraliseur d'élite du VIH-1

Longitudinal high-throughput single-B-cell exploration of the broadly neutralizing antibody repertoire in an HIV-1 elite-neutralizer

Présentée par :

Benjamin NEMOZ

Direction de thèse :

Pascal POIGNARD — Directeur de thèse
PROFESSEUR DES UNIVERSITES - PRATICIEN HOSPITALIER, Université Grenoble Alpes

Giovanna CLAVARINO — Co-encadrante de thèse
MAITRESSE DE CONFERENCES - PRATICIENNE HOSPITALIERE, Université Grenoble Alpes

Rapporteurs :

Dorian McILROY
MAITRE DE CONFERENCES, Université de Nantes

Marit VAN GILS
ASSOCIATE PROFESSOR, Amsterdam UMC

Bernard VERRIER
DIRECTEUR DE RECHERCHE, CNRS Rhônes Auvergne

Thèse soutenue publiquement le **24 avril 2024**, devant le jury composé de :

Pascal POIGNARD — Directeur de thèse
PROFESSEUR DES UNIVERSITES - PRATICIEN HOSPITALIER, Université Grenoble Alpes

Winfried WEISSENHORN — Président du Jury
PROFESSEUR, Université Grenoble Alpes

Katie DOORES — Examinatrice
PROFESSEURE, King's College London

Dorian McILROY — Rapporteur
MAITRE DE CONFERENCES, Université de Nantes

Marit VAN GILS — Rapporteure
ASSOCIATE PROFESSOR, Amsterdam UMC

Bernard VERRIER — Rapporteur
DIRECTEUR DE RECHERCHE, CNRS Rhône Auvergne

Invités :

Giovanna CLAVARINO — Co-encadrante de thèse
MAITRESSE DE CONFERENCES - PRATICIENNE HOSPITALIERE, Université Grenoble Alpes

Bryan BRINEY
ASSOCIATE PROFESSOR, Scripps Research

Longitudinal high-throughput single B-cell exploration of the broadly neutralizing antibody repertoire in an HIV elite-neutralizer

-

Exploration à haut débit et en cellule-unique du répertoire d'anticorps neutralisants à large spectre chez un neutraliseur d'élite du VIH-1

by

Benjamin Nemoz

A thesis submitted in fulfillment
of the requirements for the Doctor of Philosophy degree
in Virology & Immunology
in the Ecole Doctorale Chimie et Sciences du Vivant
of the University of Grenoble - Alpes

24 April 2024

Thesis Committee: Pr. Pascal Poignard, Thesis Supervisor
Pr. Katie Doores
Pr. Winfried Wissenhorn
Dr. Marit Van Gils
Dr. Dorian McIlroy
Dr. Bernard Verrier

"Evolution is a general condition to which all theories, all hypotheses, all systems must bow and which they must satisfy henceforward if they are to be thinkable and true. Evolution is a light which illuminates all facts, a curve that all lines must follow"

– Pierre Teilhard de Chardin

ACKNOWLEDGMENTS

I would first like to thank my PhD supervisor Pr. Pascal Poignard for giving me the opportunity to complete the present work. I am thankful for his scientific input, without which none of this would have been possible. I would also like to extend my warmest thanks to Dr Giovanna Clavarino for her help and guidance in carrying out this work.

I would like to express my infinite gratitude to Dr. Bryan Briney, who, without being given the opportunity to refuse, welcomed me into his team in the most generous way. This event probably changed the course of my life in a lasting way. Thanks also to Pr. Dennis Burton, who was instrumental in making this opportunity a reality.

I would now like to thank the members of the jury who agreed to judge my work, Prs. Katie Doores and Winfried Weissenhorn, with special thanks to Drs. Marit Van Gils, Dorian McIlroy and Bernard Verrier, rapporteurs of this work, for their very constructive feedback on the present manuscript.

To all my colleagues, from the Institute of Structural Biology, along with the wonderful team at the Virology Laboratory of Grenoble's Hospital, I would like to express my deepest gratitude and admiration. You have been remarkable all these years. I will miss you deeply.

Finally, I would like to express my heartfelt gratitude to my family and friends, who have consistently stood by my side and continue to inspire me each day. Their unwavering support encourages me to strive for excellence in everything I do.

ABSTRACT

Human Immunodeficiency Virus type 1 (HIV-1) infection remains a major global health concern, with an estimated 39 million people living with the virus worldwide and new contaminations above a million cases yearly. Efficient anti-retroviral therapies are available, allowing a sustained relief for infected individuals. These therapeutics have also contributed to better prevention and helped curb the epidemic, notably in high-income countries. However, a vaccine is still eagerly awaited for controlling this epidemic, especially in lower-income regions and precarious settings.

The protective role of neutralizing antibodies (NAbs) has been unequivocally demonstrated in both animal models of HIV infection and in human settings. Consequently, the development of a B-cell-based vaccine capable of eliciting antibodies (Abs) with the ability to neutralize the majority of circulating viruses, namely broadly NAbs (bNAbs), could be foreseen as an answer to the HIV pandemic. The investigation of bNAb development in HIV-1 elite neutralizers provides valuable insights to inform the design of such vaccines. To date, most of the undertaken studies have relied on conventional single B-cell FACS sorting to isolate bNAbs. In the present study, we have used the Chromium Single Cell Immune Profiling approach to conduct a high-throughput longitudinal single-cell exploration of the B-cell repertoire in an HIV-1 elite neutralizer. Importantly, this novel method enables the use of a much greater number of HIV envelope glycoprotein (Env) baits compared to regular FACS-based Ab isolation studies, providing a more comprehensive view of the anti-Env Ab repertoire. In addition, this approach yields a wealth

of information on the nature of the specific Abs identified and the corresponding B-cells.

The study enabled the uncovering of the sequence of 12,130 putative HIV Env specific Abs. Antibodies from 39 lineages were produced and tested for neutralization, revealing 21 distinct neutralizing lineages. The results thus demonstrated the ability of the method to explore large antigen-specific Ab repertoires from longitudinal samples. The neutralizing activity of Abs from four neutralizing lineages together recapitulated the serum activity of the donor, achieving neutralization against 62.4% of a large predictive panel of 126 pseudoviruses. One of these neutralizing Ab lineages was shown to target the gp120 high-mannose patch supersite with great breadth and potency; Abs from this lineage were sensitive to the presence of a glycan in position N332. A single of those Abs achieved most of the neutralization breadth (51.1%) with a high potency (mean IC_{50} of 91.1 $ng.mL^{-1}$). This Ab exhibited a 23 AA-long CDR_H3 and 20% somatic hypermutation (SMH). The lineage showed continuous evolution over 6.5 years of maturation, with observed SHM rates ranging from 2.0% to 30.6% for the heavy chain, without any insertions or deletions. Conventional FACS-based sorting was previously used to isolate bNAbs from the same donor. In comparison, the single cell high-throughput approach made possible the isolation of orders of magnitude more Abs. Furthermore, the newly isolated NAbs were overall more potent and broader than those isolated previously, indicating the superiority of the novel method in recovering neutralizing lineages. Ongoing structural studies will elucidate the epitopes responsible for the broad neutralization observed in this donor. Together, the findings may help the design of reverse vaccine approaches, which show promise in the development of an effective AIDS vaccine.

RÉSUMÉ

L'infection par le virus de l'immunodéficience humaine de type 1 (VIH-1) reste un problème majeur de santé publique à l'échelle mondiale, avec environ 39 millions de personnes vivant avec le virus et de nouvelles contaminations dépassant le million de cas par an. Des antirétroviraux efficaces permettent maintenant de traiter durablement les personnes infectées. Ces thérapies contribuent également à améliorer la prévention et à ralentir la progression de l'épidémie. Cependant, un vaccin reste nécessaire, en particulier pour contrôler l'épidémie dans les régions à faible revenu et les environnements précaires.

Le rôle protecteur des anticorps neutralisants (AcN) a été démontré sans équivoque dans les modèles animaux d'infection par le VIH et chez l'homme. Par conséquent, le développement d'un vaccin visant à la production, par les cellules B, d'anticorps (Ac) capables de neutraliser la majorité des virus en circulation, à savoir des AcN à large spectre (AcNLS), pourrait être envisagé comme une réponse à la pandémie de VIH.

L'étude du développement des AcNLS chez certains individus, dénommés neutraliseurs d'élite du VIH-1, fournit des informations précieuses pour la conception de tels vaccins. Jusqu'à présent, la plupart des études entreprises se sont appuyées sur le tri conventionnel de cellules B uniques par cytométrie en flux (FACS) pour isoler les AcNLS. Dans la présente étude, nous avons utilisé l'approche "Chromium Single Cell Immune Profiling" à haut débit sur cellules uniques (scRNA-seq) pour réaliser une exploration longitudinale du répertoire des cellules B chez un neutraliseur d'élite du VIH-1. Cette méthode

permet d'utiliser comme appâts pour l'identification des cellules B spécifiques un nombre beaucoup plus important de glycoprotéines d'enveloppe (Env) du VIH par rapport aux approches d'isolement d'Ac basées sur le FACS, ce qui permet d'obtenir une analyse plus complète du répertoire en Ac anti-Env. En outre, cette approche fournit une multitude d'informations sur la nature des Ac spécifiques identifiés et sur les cellules B correspondantes.

Notre étude a permis d'identifier la séquence de 12 130 anticorps spécifiques de la protéine Env du VIH. Des Ac de 39 lignées ont été produits et testés pour leurs capacités de neutralisation, révélant 21 lignées neutralisantes. Ces résultats démontrent la capacité de la méthode à explorer de vastes répertoires spécifiques d'antigènes à partir d'échantillons longitudinaux. L'activité neutralisante des Ac de quatre lignées récapitulait l'activité sérique du donneur, permettant de neutraliser 62,4% d'un large panel prédictif de 126 pseudovirus. Une de ces lignées neutralisantes ciblait la région riche en mannose de la gp120. Par ailleurs, les Ac de cette lignée étaient sensibles à la présence d'un glycane en position N332. Un seul de ces Ac était responsable de la plus grande partie de cette neutralisation (51,1%) avec une activité à faible concentration (IC_{50} moyenne de 91,1 $ng.mL^{-1}$). Cet Ac possède un CDR_H3 de 23 AA de long et 20% d'hypermutation somatique (SMH). La lignée a montré une maturation continue sur 6,5 ans, avec des taux de SMH observés de 2,0% à 30,6% pour la chaîne lourde, sans insertion ou délétion.

Un tri conventionnel basé sur la méthode FACS avait été utilisé précédemment pour isoler des AcNLS du même donneur. En comparaison, l'approche scRNA-seq a permis d'isoler des Ac en nombre bien supérieur. En outre, les AcN nouvellement isolés étaient globalement plus neutralisants et de plus large spectre que ceux isolés précédemment, ce qui indique la supériorité de la nouvelle méthode pour l'identification de lignées neutralisantes. Les études structurales

en cours permettront d'élucider les épitopes responsables de la neutralisation observée chez ce donneur. L'ensemble de ces résultats pourrait contribuer à la conception d'approches de "vaccinologie inverse", qui représentent à l'heure actuelle un espoir pour la mise au point d'un vaccin contre le VIH.

CONTENTS

LIST OF FIGURES

LIST OF TABLES

Chapter 1

INTRODUCTION

1.1 Human Immunodeficiency Virus (HIV)

The human Acquired Immuno-Deficiency Syndrome (AIDS) was described in 1981, following initial reports of clusters of cases of Pneumocystis pneumonia [55] and Kaposi's sarcoma [56]. Two years later, the etiological agent of this syndrome, the human immunodeficiency virus type 1 (HIV-1), was isolated by Françoise Barré-Sinoussi and Luc Montagnier [18]. The findings were confirmed the following year by research conducted by Robert Gallo [255] and Jay Levy [198]. Since then, HIV infection has been deeply studied, resulting in one of the most abundant scientific literature corpus and contributing significantly to our understanding of the human immune system.

1.1.1 The virus

HIV is a zoonotic virus that originated in non-human primates (NHPs) and spread to humans circa 1900 [105]. Since then, new infections have occurred through sexual contact, by vertical transmission, through percutaneous exposure, or by means of transplantation or blood transfusions. To date, an estimated 39 million individuals live with HIV worldwide [329], with an uneven distribution: some countries and regions bear a much larger fraction of the infections. Sub-Saharan African countries concentrate the largest burden of the pandemic. HIV-related mortality peaked in 2006, however the progression of new infections has continued at a relatively stable pace, thus underlining the need for a sustained response at a global level.

HIV is classified in two types: HIV-1 and HIV-2. HIV-1 originates from several individual zoonotic spillover events. HIV-1 is related to chimpanzee strains of the Simian Immunodeficiency Virus (SIVcpz) isolated in *P. t. troglodytes* and in *P. t. schweinfurthii* [113] and to gorilla strains of the SIV endemic to this species (SIVgor) [79]. The existence of HIV-2 was suspected in 1985 [14], the virus was successfully isolated in 1986 [64] and sequenced in 1987 [132]. Analysis of the sequence demonstrated that the virus derived from a Sooty

Mangabey SIV [140]. HIV-2 is less transmissible, mainly owing to overall lower viral loads and more frequent spontaneous immunological control of the virus by the host [336]. HIV-2 represents only a fraction of worldwide infections, mainly in a geographical area limited to West-Africa [349].

Both HIVs are highly variable viruses [19]. This is mainly attributed to the high viral mutation rate paired with a rapid and continuous viral replication rate [25, 239]. HIV-1 has been classified into four groups: groups M, N, O and P, reflecting the existence of the different spillover transmission events. Groups N, O and group P are of limited geographic diversity and concern few individuals. Group M (Major) is the main cause of worldwide infections and can be divided in clades, or subtypes. Main clades are phylogenetically pure, i.e. monophyletic, and designated with a single letter (A, B, C, D, F, G, H J and K). In contrast, and due to frequent recombination events, circulating recombinant forms (CRF) are designated by the clade letters from which they arise followed by a number. To date, there are over 95 CRFs of diverse geographic origin. Prevalence and incidence of different clades are highly dependent on the region or country as well as on the mode of transmission. Subtype C is the most prevalent worldwide, accounting for the majority of infections in Africa and Asia.

This extraordinary diversity is a major obstacle for vaccine design. Indeed, to be successful, a vaccine needs to elicit an immune response capable of recognizing this diversity [48].

HIV-1 is an exogenous retrovirus [39, 112]; it integrates its genomic material – about 10 kilobases [356] – into the host's cellular genome [185], thus constituting a reservoir of proviruses. The reservoir consists mainly of $CD4^+$ T lymphocytes. A small proportion of these cells are resting T-cells, constituting a latent reservoir [67]. Decay of this latent reservoir is slow, with an estimated half-life of 44 months [75], making HIV elimination based on antiretroviral therapy (ART) alone impossible [153, 240].

HIV-1 uses the CD4 cell-surface receptor as an entry receptor [202, 201]. Entry occurs at the cell surface, is pH-independent [314] and does not require endocytosis [212]. Viral- and cellular-membranes fuse together to unload viral

content in the cytosol [346]. Entry also requires the engagement of a co-receptor. The two main ones are CCR5 [2, 61, 84, 93, 97] and CXCR4 [106]. The viral molecule that engages the cellular receptors is the Env protein [57]. The Env protein is a trimer of heterodimers of the glycoproteins gp120 (120 kDa) and gp41 (41 kDa). A precursor of Env with a molecular weight of 160 kDa is cleaved to generate these two subunits that remain non-covalently bound after cleavage [332, 99]. Six to twenty Env proteins are present at the surface of the infectious particle [372, 371], although it is estimated that only one to three molecules may be sufficient for the virus to gain cellular entry [32].

Due to the nature of the cellular receptors involved in viral infection, target cells are mainly the $CD4^+$ T lymphocytes, but other cells including monocytes, macrophages and dendritic cells can be infected [254].

1.1.2 Env structure

Complete structural determination of the Env trimer has long remained elusive, due to its relative unstable pre-fusion conformation. The structure of monomeric gp120 (mgp120) was solved early on in 1998 [359]. A first relatively complete picture of the trimer was only obtained in 2008 [204] partly owing to the recently obtained stable constructs.

A first recombinant, soluble and stable construct of HIV Env trimer that successfully mimicked the conformation of native trimers was achieved with the insertion of a disulfide bond (SOS) stabilizing the interaction between gp120 and gp41 subunits, and by an additional Isoleucine to Proline (IP) mutation in the N-terminal region of the gp41 heptad repeat domain [23]. Further optimizations (enhancing cleavage site, truncation of the hydrophobic C-terminus part of the MPER, ...) were used to obtain the soluble, stable and natively-conformed BG505.SOSIP. Truncation at residue 664 allowed the production of the highly producing, stable and soluble heterotrimer known as BG505.SOSIP.664 [281]. This will serve as the foundation to the constructs used in the present work.

The HIV Env trimer has the inner organization of a type I membrane fusion protein. Highly variable parts containing the receptor binding site are located at the extremity. The more conserved viral fusion machinery occupies the

space situated at the base of the trimer [168, 209]. The gp120 subunit is composed in an inner and an outer domain, separated by a bridging sheet. The outer domain has five highly variable loops (V1-V5) that shield the conserved residues of the inner domain. The Env trimer is stabilized by the variable loops V1, V2 and V3 that make contacts between gp120 monomers. The V1 and V2 loops form the apex of the trimer. The V1 loop extends towards the exterior side of the trimer, towards a convex region. The V2 loop protrudes orthogonally to the trimer axis, above the CD4 binding site (CD4bs). Both loops can withstand large conformational variability, including length modifications as they protrude towards the outer side of the gp120 trimer. The intrinsically disordered nature of the V2 loop is debated as its conformation is especially variable, with no defined tridimensional structures visualized in corresponding studies [209].

The V3 loop lies beneath these two V1 and V2 loops [165] and is more constrained. The base of this loop arises from the outer part of the gp120 subunit, and the loop progresses laterally to finally make contact at the extremity with the neighboring gp120 protomer, near the base of the V2 loop. Thus, this loop cannot vary greatly in length without destabilizing the trimer as a whole. The tip of the V3 loop making contact with the adjacent protomer harbors a conserved binding motif (-**GPGX**- with X being an arginine or a glutamine). The V3 loop is also home to conserved potential N-linked glycosylation sites (PNGS) at positions N295, N301, N332 and N334. These are located close to the base of the loop [343].

As a functional region, the CD4bs is the unique part of the exposed Env surface to be conserved (the co-receptor binding site is shielded/buried behind the V3-loop) and relatively devoid of glycan shielding. Nevertheless, in addition to a relatively constrained size, the surface concerned is half-buried at the interface of two adjacent monomers of gp120, thus limiting exposure of this vulnerability site to immune recognition. Surrounding hypervariable loops (V1, V2 and V3) and glycans (especially the glycan moiety at position N276) further enclose the CD4bs in a partially protected groove, or cryptic region, narrowing the available angles of approach [223].

1.1.3 Glycosylation of Env

Glycans account for about half of the total molecular weight of the gp120 subunit [368] and coat the vast majority (50-70%) of the surface of the trimer. N-linked glycan occupancy is in part defined by the presence of a PNGS and the subsequent glycan expression at this site. PNGS are defined by the Asn-X-Ser/Thr motif, where X can be any amino acid except proline. Between 18 and 33 PNGS are present on each gp120 monomer. Despite the PNGS positions being mostly constant across viral clades, the glycan occupancy is highly variable, with up to 90% differences between strains at any given position [122].

These glycans are added during post-translational modifications. A first $Glc_3Man_9GlcNAc_2$ residue is added at each PNGS site by the oligosaccharyl transferase complex [26]. These high-mannose glycans are then trimmed by the endoplasmic reticulum mannosidases. Additional sugar residues are added by the glycosyltransferases. However, due to limited accessibility at certain sites, the modifications of the initial oligosaccharides may be impaired, leading to high levels of heterogeneity. Overall, only a relatively small proportion of PNGS bear complex or hybrid glycans. This heterogeneity makes recognition of the Env glycoprotein by the immune system more complex [179, 21]. Furthermore, the recognition of N-linked glycans by antigen-presenting cells (APC) can steer antibody class switching towards less effective antibody subclasses [139].

HPLC and mass spectrometry analyses of glycosylated residues from native-like soluble SOSIP constructs have helped map in detail the overall glycan content of the HIV Env trimer (**Figure 1.1**).

The apex region of the trimer harbors some PNGS, notably at positions N156, N160 and N173 [165]. But most of the PNGS are located at the base of the V3-loop, where they are present at an exceptional density (23 PNGS in the clade B isolate 'BaL'). This forms a dense array of glycans, whose high density prevents the action of the mannosidases. This results in a region of high mannose content which has been termed the high-mannose patch (HMP) [26]. The stability of this dense array of glycans has been demonstrated [262]. These regions, defined by the heterogeneity of the distribution of PNGS in

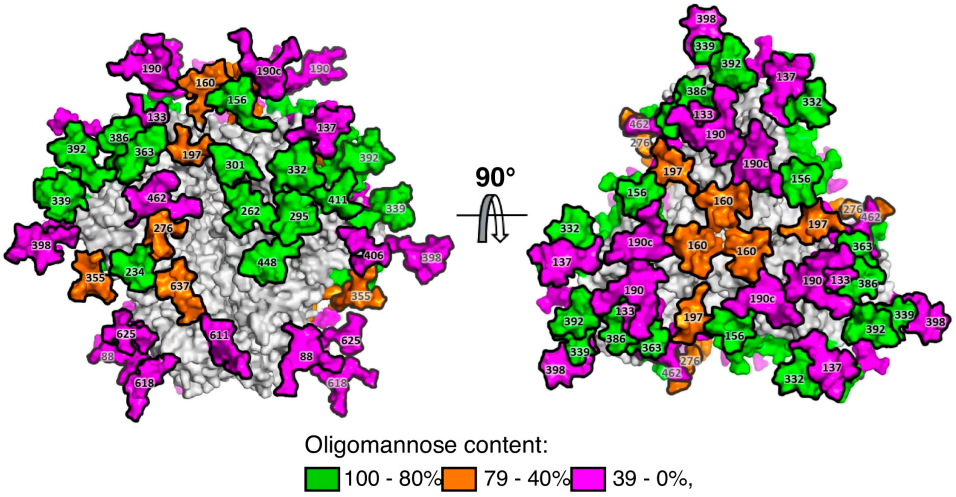

Figure 1.1. Overall glycosylation and glycan content of the BG505.SOSIP.664 trimer construct. The high-mannose patch is seen at the center of the side representation (left) in green, comprising the glycan in position N332. Figure adapted from [20]

the Env sequence, do not vary between different cell types of origin, and are termed protein-directed effects.

Glycosylation of the Env was first studied in monomers. However, the glycan content of trimers differs from that of monomers [90]. Trimerization brings some of the PNGS present on adjacent monomers closer together. This, along with supplementary protein-glycan interactions reduces mannosidase access to these glycans. Compared to mgp120s, trimers have a higher content in oligo-mannose glycans [121, 261, 263]. This is particularly true for the V2-Apex region and the glycan at position N160 [20].

The glycan shield of HIV Env trimer can also vary between cell type of production [179]. These discrepancies are referred to as cell-directed effects. This is particularly important for the gp41 subunit, the glycosylation of the gp120 remaining fairly similar [90].

1.1.4 HIV infection

Sexual transmission is responsible for the majority of infections, and, in particular, transmission via heterosexual relations accounts for 85% of new infections worldwide [301].

In the case of sexual transmission, a single HIV virion is thought to be transmitted during the contaminating intercourse in most cases [174, 279]. Consequently, at the individual level, the genetic diversity of the Env glycoprotein in early viruses is almost nonexistent [353, 366, 373]. This demonstrates the presence of a strong selective pressure during the transmission. At the population level, the diversity of transmitted viruses also seems to be reduced. There seems to be a preferential transmission of ancestral (transmitted) strains compared to contemporary strains circulating in the transmitting partner [268]. This has been attributed to a higher infectivity of transmitted/founder strains [142]. In particular, these viruses seem to have a reduced sensitivity to the α-interferon-mediated innate immune responses [8] and a notable resilience to cell-mediated immune reactions [138]. Furthermore, it has been demonstrated that sexually transmitted HIV exhibits an almost exclusive CCR5 tropism [373, 174], concurring with the dominant presence of $CCR5^+$ cells in the mucosal tissues, such as dendritic cells (DC) and macrophages (reviewed in [216]).

One study reported an accumulation of mutations in the region of the V3-loop, significantly shorter Env sequences, and a diminished charge of the V3-loop in transmitted/founder viruses[280]. The glycosylation of the Env protein of transmitted/founder virions was also reported to be substantially inferior to the one of circulating viruses [85, 62, 120, 170]. In these studies, recombinant trimers bearing the *env* sequence of transmitted/founder viruses seemed to be more compact and glycan-restricted [85], with modification of sequences favoring shorter V1-V2 loops [62] and an overall loss of PNGS in the V3-loop [170] or at positions 413-415 [120]. This reduction in glycan content however was not reported in all studies [280]. Overall, glycan content of the Env glycoprotein seems to be lower in transmitted/founder viruses, owing in part to shorter V1/V2/V3 loops but also to a reduced number of occupied PNGS and shortened glycan residues. These different glycosylation patterns could have an impact on the protection that is mediated by antibodies that target these glycans in the sexual transmission.

The period between the transmission of a founder virus and the detection of the virus in the plasma is known as the eclipse phase of the HIV infection [325]. This phase corresponds to a 10-day to 2-week phase during which the virus

first replicates at a focal point of infection before spreading undetected through the lymphatic system to the proximal lymph node first, and subsequently to distal lymph nodes [231]. The early phase of the eclipse period has been termed the 'window of opportunity' as this period seems to hold the key to transmission-blocking possibilities [250].

In early phases of the infection, viral load peaks in about 2 to 3 weeks to reach between 10^6 and 10^8 copies.mL^{-1}. The host initiates an initial immune response upon infection: it is thought that DC and natural killer (NK) cells exercise most of the initial antiviral response [4]. Through cytolysis of infected cells and by means of antiviral cytokines and chemokines, these cells exert substantial pressure on the nascent infection. This innate immune response precedes the adaptive immune response mediated by specific $CD4^+$ T-cells, $CD8^+$ T-cells and B cells. Nevertheless, HIV successfully overcomes this initial innate immune response [227]. Indeed, it is estimated that about 80% of the gut-associated lymphoid tissue $CD4^+$ T-cells, that consist predominantly of $CCR5^+$ activated cells, are depleted within the first three weeks of the infection [33]. Despite this early loss, an adaptive immune response is subsequently mounted. Cytotoxic T lymphocytes (CTL, or $CD8^+$ lymphocytes) are an essential component of this response to HIV-1 infection, as their depletion translates into an uncontrolled viral replication [287]. However, the reduction in HIV viremia does not seem to be related to the clearance of productively infected cells by those CTLs [354]. Furthermore, the $CD8^+$ mediated response does not impact the constitution of the reservoir [311].

Notwithstanding, the host immune response to this invasion reduces the initial viral load to the set-point viral load, usually orders of magnitude lower [238]. Several factors (host genetics, environmental factors and viral genetics) influence the value of the set-point viral load [109]. Early on in the initial infection, the virus establishes its persistence in a cellular reservoir. Studies in macaques have shown that the reservoir constitution begins as early as 3 days after the transmission event [348].

1.2 The antibody response to HIV infection

1.2.1 Overview of antibody development

Immunoglobulins (Ig), also known as Antibodies (Abs) when in their soluble form, are proteins composed of two identical heavy-chains and two identical light-chains that interact to form a Y-shaped macromolecule with a molecular weight of approximately 150 kDa. This multimeric complex is held together by several disulfide bonds. Different isotypes are defined by the type of heavy-chain these Abs possess, and the conformation of secreted Ig differs according to this isotype. The interface between the N-terminal domain of the light-chain and the N-terminal domain of the heavy-chain defines the variable region of the Ab, the Fab region, that contains the paratope responsible for the specific recognition of the antigen (Ag). The surface of the antigen recognized by the paratope is termed epitope. The C-terminal extremities of the heavy-chains interact to form the crystallizable fragment of the Ig (Fc), showcasing a relatively conserved sequence.

The same Ig can be present in two forms: either bound to the membrane of a B cell where it takes part in the B cell receptor (BCR), or in the form of a secreted Ab. BCRs and Abs produced by a single B cell share the same Ag specificity and the same underlying genetic sequence.

Immunoglobulin germline genes

Complete Ig genes are obtained through the recombination of three gene segments named V for variable, D for diversity and J for junction in the lymphoid progenitors (pre-B cells) in the bone marrow [69]. These three gene segments are required for the heavy-chain and only two (V and J) are required for light-chains. Light-chain encoding gene segments are available in two types, producing kappa ($\varkappa$) or lambda (λ) chains. These Ig gene segments are identified in a nomenclature put together by the IMunoGeneTics (IMGT) consortium [194] and later endorsed by the World Health Organization (WHO). In their 2001 database, IMGT reported between 77 and 84 functional alleles for V_H-gene segments in the human species, along with 37-43 functional alleles for V_L-gene segments and 37-41 functional alleles for V_K-gene segments.

The genomic sequences of these gene segments were obtained from a limited number of studies. Indeed, these studies require the sequencing of genomic (constitutional) DNA and have been carried out mainly in subjects of Caucasian origin. As a result, the sequence diversity observed for these gene segments and their alleles probably underestimates the true sequence diversity in the entire human population. Other approaches have leveraged the accessibility of recombined RNA sequences encoding functional BCR/Abs [331] to infer the possible germline alleles from which they arise [70]. By sampling a larger number of individuals of broader geographical origins and ethnicity, this offers the possibility to build an alternative reference dataset of available germline sequences in both human and other species [249].

However, the diversity of the Ab repertoire is not limited to the recombination of these gene segments as additional mechanisms build on this combinatorial diversity to create the extraordinary diversity of the human BCR/Ab repertoire that enables us to cope with the antigenic landscape we are exposed to.

In addition to the aforementioned combinatorial diversity, other mechanisms are at play to further increase the total diversity of the immunoglobulin repertoire. One of these mechanisms is the templated (junctional diversity) and untemplated diversity added upon recombination by the terminal deoxynucleotidyl transferase (TdT) enzyme. This process takes place in naïve B cells and allows for insertion and/or deletion of a small number of nucleotides at the junction sites between two recombining gene segments. The sequence of the CDR3 arises from the recombining region between the V-gene segment and the J-gene segment, fully encompassing the D-gene segment in heavy-chains. The D-gene segment can be rearranged in various reading frames, and can therefore contribute to a great degree of diversity in the CDR_H3 region. These mechanisms explain the high variability and the untemplated nature of the CDR3. This variability allows the CDR3, and more especially the CDR_H3, to be a major determinant of antigen specificity. This region usually bears most of the contacts with the antigen.

Somatic hypermutation

In activated B cells, the activation-induced cytidine deaminase enzyme (AID) inserts somatic hypermutations (SHM) into the variable parts of the BCR/Ab sequences [365]. This process, at the root of Ab maturation, further increases the BCR/Ab repertoire diversity. Mutations are situated in mutational hotspots. Indeed, the AID enzyme targets the cytidine present in the -**WRCY**- motif (W for a weak base: A or T, R for a purine: A or G, C for a cytidine, and Y for a pyrimidine: C or T) of Ig genes [86, 248, 244]. This enables specific targeting of highly variable regions [58] with a frequency of mutation that directly depends upon mutational hotspot accessibility [363], and prevents the excessive maturation of Ig genes corresponding to high affinity BCR, as these are relatively depleted of these mutational motifs.

The observed diversity of human immune repertoires has been described in great detail in recent studies [37], owing to the development of both high-throughput sequencing technologies (NGS) and novel computational methods. It is now estimated that the healthy human immune system can theoretically generate B cells/Abs with 10^{16} to 10^{18} different specificities.

Hence, Ab repertoires of healthy individuals are extraordinarily diverse. However, Abs in unrelated individuals seem to organize into clonal families of limited variability. It is thought that this apparent proximity in lineages is the consequence of the negative selection process of autoreactive B cells that takes place in the bone marrow. Another hypothesis that has been proposed is that shared antigens will produce convergent immune response and skew the repertoire diversity in the same direction. However, this hypothesis has recently been disregarded [37]. The evolution of related B cells in a single clonal lineage makes it possible to reconstruct the developmental history of such lineage. In particular, the unmutated common ancestor (UCA) of a given lineage can be found or at least approached through NGS exploration of the B cell repertoire. This can approximate the original naïve B cell that sparked the development of such lineage.

In the field of vaccine design, the genetic background diversity of the targeted population should be taken into account. Genetic background varies between individuals. The maturation of Abs can only be achieved through a

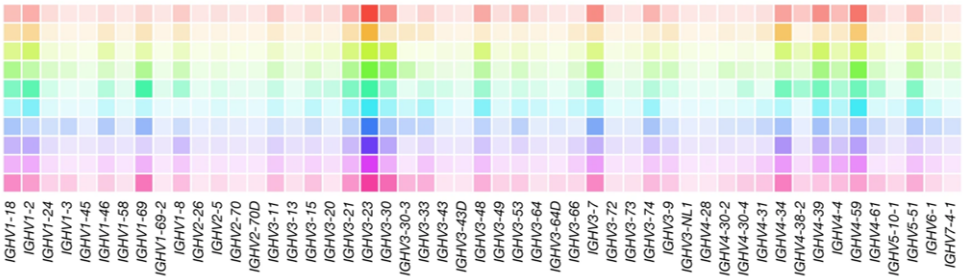

Figure 1.2. Heatmap representation of the observed frequencies of V_H-gene usage across ten healthy subjects sampled in [37].

limited number of mutations. Possible mutations are limited to certain positions where they occur, and require time to happen. Therefore, some Abs might prove very difficult, if not impossible, to elicit. For example, eliciting Abs that require a specific V-segment allele for antigen binding will not be achievable for individuals who lack the corresponding germline sequence. Also, Abs that have high levels of SHM are difficult to elicit. Indeed, they require sustained activation of the AID enzyme to reach these SHM levels. It is worth noting that SHM accumulate with time spent by the B cell in the germinal center (GC), either in a single stay, or through-out several cycles.

From the genomic sequences available, different individuals use Ig gene segments in different proportions, although with some shared preferences. The comparison of Ig gene segment and allele usage between those of healthy subjects (**Figure 1.2**) and those observed in patients with infectious or autoimmune diseases can inform on the immune response involved in these diseases.

In the context of HIV infection, to our knowledge, few systematic reviews of adaptive immune receptor repertoire (AIRR) response have been conducted [173]. Some studies mention the overall differences in Ab repertoires between healthy donors and HIV-infected patients [294]. These authors mention the enrichment of the repertoire with IG_HV3-30 and IG_HJ4 genes, without providing biological hypotheses to explain these findings.

Class switch, isotypes

The process of class-switch recombination (CSR) is mediated by the AID enzyme among others, and leads to the recombination of the Ig C-gene segments, while retaining the specificity of the Ab. This process involves the deletion of the previously used C-gene segment. This results in a complete loss of the DNA encoding the precedent constant domain of the Ig, thus making the process irreversible [60]. The order in which CSR is performed is fixed and follows the distribution of constant-chain encoding genes on the genomic DNA strand: IgG3, IgG1, IgA1, IgG2, IgG4, IgE and IgA2.

Class-switch recombination depends on the activation signal delivered through the CD40 molecule and its cognate ligand CD40L present at the surface of $CD4^+$ T-cells. In HIV infection, there seems to be a reduced possibility for B cells to undergo CSR [258] resulting in an increase in IgM and a decrease in IgG. Paradoxically, it has been shown that the virus itself could trigger CSR by a polyclonal activation of B cells through other mechanisms (CD40-independent) [166].

Maturation of B cells

In lymph nodes, follicular dendritic cells (FDC) organize a complex network where naïve B cells are initially situated [3]. After a first encounter with their antigen, and with the help of T-cells, these pre-GC B cells start to multiply. A small subset of the generated B cells will form the early GC within the network formed by the FDC [116]. These FDC serve as a reservoir for antigens that will drive the maturation process [137].

The newly-formed GC separates into the light-zone (LZ) and the dark-zone (DZ). B cells from the DZ proliferate and undergo successive rounds of SHM. The newly-formed population of B cells, harboring a wide range of slightly mutated BCRs then reenters the LZ to test their antigen binding capacities on FDC-bound antigens. This process is called cyclic reentry [175]. The competitive nature of antigen-binding and successful $CD4^+$ T follicular helper-cells (Tfh-cells) activation acts as a positive selection, and allows B cells to further proliferate back in the DZ [335]. This process accounts for most

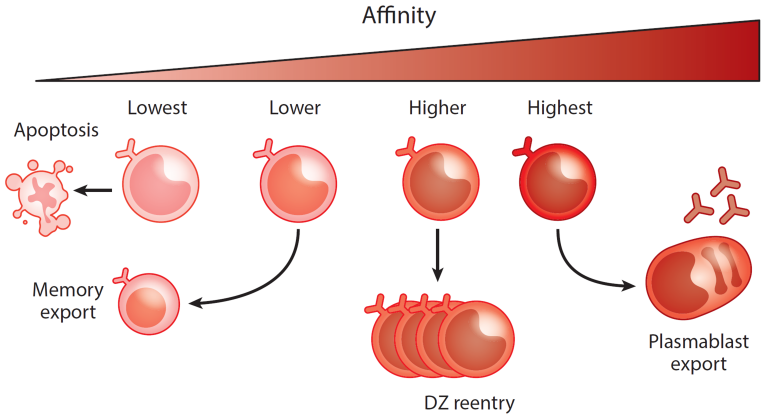

Figure 1.3. Schematic representation of one of the proposed models for affinity maturation and cell fate determination. High affinity GC B cells tend to evolve into Ab-secreting cells, whereas lower-affinity might predispose cells to enter the memory compartment. This simplistic view does not take into account other mechanisms that allow for MBCs to exhibit high affinities. Adapted from [334]. GC: germinal-center, DZ: dark zone, MBC: memory B cell

of the B cell maturation. However, some B cells can undergo non-canonical extra-follicular (EF) responses outside the GC [102].

B cell cycling in the GC relies upon a differential expression of cell-surface markers that can be used to identify these populations. Down-regulation of surface IgD mainly differentiates the naive B cells from activated, GC-forming B cells [22]. Metabolic phenotype also clearly separates those cells: proliferating B cells undergo high metabolic activity (reviewed in [334]).

The affinity of the matured BCR seems to act as a determinant for cellular differentiation. A proposed model is presented in **Figure 1.3**. A higher affinity seems to cause GC B cells to transform in proliferative plasmablasts (PB). These PBs can evolve into Ab-productive plasma-cells (PC) or into resting PCs [243]. Conversely, memory B cells (MBC) tend to arise from lower-affinity GC B cells [296, 333, 355]. However, this seems to only partly explain the origin of MBCs. A time-dependent mechanism seems to also participate in the MBC differentiation of B cells. Indeed, high affinity pre-MBCs are often found in late-stage GCs, and high-affinity Abs bearing high levels of SHM are often recovered from circulating MBCs [318].

1.2.2 Neutralization and other mechanisms of action of antibodies

Antibodies have several mechanisms of action. They can act either through cellular or molecular effectors, or independently. Indeed, some immune cells or molecular effectors exert their functions through Abs. These functions are referred to as Fc-dependent functions. The Fc domain is engaged by the Fc-receptor (FcR). Fc-dependent functions encompass Ab-dependent cell-mediated cytotoxicity (ADCC), complement activation culminating in the formation of the Membrane Attack Complex (MAC), opsonization of pathogens, leading to phagocytosis (ADCP), and the induction of agglutination.

Conversely, neutralization is an Fc-independent function of Abs: it does not require the engagment of an external effector via the Fc. Neutralization is the ability to induce a loss of infectivity (partial or complete) by the binding of Abs to viral particles, independently of Fc engagement [47, 46]. In the context of HIV infection, neutralization occurs through the binding of Abs to the sole accessible viral protein found on the surface of viral particles: the Env glycoprotein.

Neutralizing Abs (NAbs) are of great interest for vaccine design as most viral vaccines rely on NAbs. Their use has been proposed for prophylactic uses as NAbs protect against HIV infection in animal models. Moreover, NAbs could be part of new HIV treatments, in addition to, or in replacement of antiretroviral therapy (ART).

Mechanisms of neutralization have been extensively reviewed in [46]. In the context of HIV, various have been described:

- NAbs are able to aggregate viral particles
- NAbs can prevent access to the receptor-binding site (through obstruction/steric clash). For example, the bNAb PGT121 binds to an epitope situated proximal to the CD4 binding site and the CCR5 binding site. However, the distances between the epitope and both receptor sites is short and the presence of the NAb induces a steric clash with the CD4 and/or the CCR5 and prevents attachment to the cellular target [167]

- It has been demonstrated that NAbs can provoke Env trimer disassembly. Some NAbs targeting the base of the gp41 subunit can destabilize the Env trimer and induce the shedding of gp120 subunits [277]

- Some NAbs induce Env trimer conformational changes. For example, NAbs 3BC315 and 3BC176 induce conformational changes to the Env glycoprotein by binding to an epitope situated at the interface between two gp41 protomers [193]

- Finally, NAbs can block virus and cellular membrane fusion. Some NAbs have been demonstrated to stabilize the pre-fusion conformation, thus impeding the membrane fusion [129]

In addition, NAbs can block viral egress. However, this mechanism does not prevent the initial cellular infection. Therefore, this is not measured by in-vitro neutralization assays that rely on single-round infection. Other neutralization mechanisms have been described that do not apply to HIV, such as the inhibition of the endosome formation or the inhibition of internalization in endosomes.

Neutralization is assessed in-vitro by assays that are now standardized. Briefly, Abs are put in presence of viral particles or pseudo-viruses (PVs) at different concentrations and incubated together for a determined amount of time. PVs are virions bearing genetic material defective for the Env encoding region, thus rendering them non-infectious after gaining entry to the cell. After this incubation period, the mixture is brought in contact with cells permissive to HIV infection. In the case of non-neutralizing Abs (NNAbs), the viral particles infect the cells. Conversely, in presence of NAbs, their presence prevents the infection of the cells. Cell infection is usually measured through the expression of a reporter gene induced by viral elements [282].

In some cases, neutralization by a NAb may plateau at less than 100% regardless of the Ab concentration, suggesting that the Ab is active against only a fraction of the population of viruses. This partial neutralization has been observed both with PV strains and fully-infectious primary viral isolates, produced either in cell lines or in primary cells [221]. Ab-mediated aggregation of viral particles has been suggested as an explanation of this behavior [213]. In

this case, an aggregated fraction has a reduced to no remaining infectivity, and a second fraction, termed the persistent fraction, retains infectious capacity.

However, it has been suggested that the overall antigenic heterogeneity of the Env glycoprotein could be the main driver of such incomplete neutralization [68]. Multiple factors are involved in the heterogeneity of the Env. One of these is the nature of the glycan shield which, as stated above, can be highly heterogeneous, thus potentially explaining incomplete neutralization [118].

In the context of HIV-1 infection, a large fraction of infected individuals seem to be capable of mounting a neutralizing response directed at the autologous viruses [266]. However, neutralization does not appear to hinder viral progression, or only temporarily [1]. Indeed, under this selective pressure, viruses with mutated residues in the epitopes of these NAbs can easily escape neutralization. Furthermore, neutralization does not protect against superinfection [292].

Despite this, certain individuals develop Ab responses capable of neutralizing heterologous viruses, that is to say viruses isolated from other infected patients. Furthermore, for a small subset of these individuals, the serum of these infected patients can neutralize a large number of viral strains. These elite-neutralizers are capable of developing NAb responses with remarkably broad neutralizing activity. In a number of cases, a single or a few NAbs responsible for this neutralizing activity can be isolated from the B cells of these individuals. Hence the breadth of neutralization of the serum can sometimes be recapitulated by a limited number of exceptional NAbs. These are termed broadly neutralizing antibodies (bNAbs) [159]. These bNAbs display cross-neutralization capabilities by targeting epitopes that are highly conserved across viral strains. Given their exceptional neutralizing abilities, they are extensively studied. Indeed, these bNAbs can protect from the infection (see below) and eliciting these bNAbs in uninfected individuals could result in an effective vaccine.

Broadly NAbs exhibit different breadths of neutralization, corresponding to the number of viral strains neutralized. To assess this breadth, neutralization is measured against various panels of viruses or PVs [299, 291, 81], some of

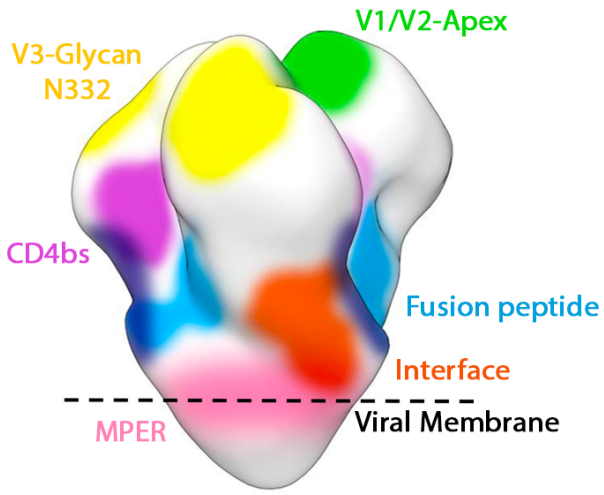

Figure 1.4. Schematic representation of the most commonly described antigenic supersites of the HIV Env glycoprotein (side view). In addition, the Silent Face (SF) epitope should be considered. Adapted from [343]. CD4bs: CD4 binding site, MPER: Membrane-proximal external region

which have been designed to be predictive of a neutralization against a much larger viral population. Depending on the studies, elite neutralizers accounted for 1% [299] to 23% [126] of tested individuals using such panels against the polyclonal sera. These discrepancies can be notably explained by the nature of the panel utilized and the use of different thresholds to define elite neutralizers.

1.2.3 Broadly NAbs define antigenic supersites on the Env trimer

The successful isolation of bNAbs has made possible the delineation of conserved epitopes or regions of the Env trimer often referred to as supersites of vulnerability. Here we briefly review these main antigenic sites depicted in **Figure 1.4**. To date, more than a hundred bNAbs have been successfully isolated from infected donors, whether in longitudinal studies or in cohorts with single-point samples. The following paragraph does not aim at recapitulating all the previously isolated bNAbs and neutralizing lineages. However, I will discuss some of most prominent ones.

The first bNAbs to be isolated in the 1990s were b12 (anti-CD4bs) [44], 2G12 (anti-V3-glycan) [326], 4E10 and 2F5 (both anti-MPER) [316, 376]. A

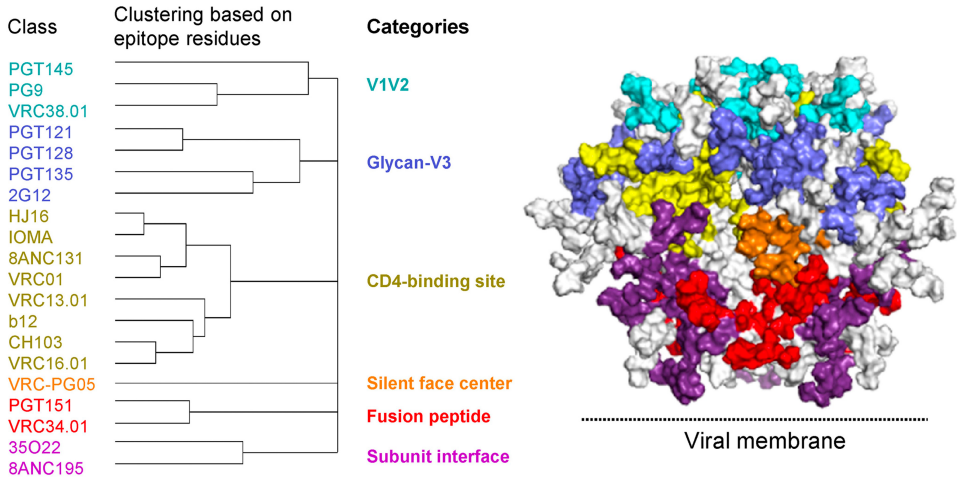

Figure 1.5. Selected bNAbs can be grouped in major classes of bNAbs depending on their targeted epitopes, defining six neutralizing categories. Anti-membrane proximal external region (MPER) Abs targeting the gp41 subunit should also be considered. Adapted from [63].

second generation of bNAbs were isolated circa 2009 using single B cell sorting with FACS and novel cloning techniques [339, 370, 340, 104].

As of 2021, twenty classes of gp120-targeting bNAbs have been described, organized in six groups (**Figure 1.5**) corresponding to their targeted epitope [145]. An additional class of bNAbs targets the membrane-proximal external region (MPER) of the gp41 subunit. Because CD4bs and anti-MPER bNAbs target regions that are highly-conserved across all viral clades, they tend to exhibit larger breadth than other bNAb categories.

The CD4-binding site

The CD4bs was initially described from structural studies revealing the structure of the mgp120 in complex with the contact-bearing domains of the CD4 receptor [188]. Between the inner domain and the outer domain of the gp120 subunit lies a cavity, delineated by the bridging sheet that accommodates the CD4 most distal residues. The CD4bs is a discontinuous region that sits at this interface between the inner and outer domains of the gp120. Contact of the CD4 cellular receptor induces important conformational changes in the gp120 to allow interaction with the co-receptor. Although the CD4bs

is clearly defined by CD4 receptor contact residues, the antigenic site corresponding to the CD4bs epitope corresponds to a larger area.

Among the first NAbs isolated to target the CD4bs, hence participating in the definition of the latter, was b12 [44]. This NAb along with other moderately potent NAbs [377] helped modify the definition of the CD4bs epitope to include nearby residues from V1, V2 and V3 loops. Further isolated bNAbs against the CD4bs encompass VRC01 [370, 358], 3BNC117 [54], VRC07-523LS [276], N6 [148], among others.

VRC01 is probably one of the most studied and well understood bNAbs. The isolation of VRC01 was reported in 2010 [370]. Early studies have demonstrated the ability of VRC01 to overcome glycan and conformational masking through usage of substantially mutated V-gene regions. VRC01-class bNAbs require the use of the $IG_HV1\text{-}2*02$ gene paired with a light-chain with a short CDR_L3 of 5 amino acids. Structural studies described the conserved viral epitope recognized by this class of bNAbs [357]. The glycan residue at position N276 participates in the definition of the CD4bs epitope, as it shields the rest of the CD4bs and bNAbs are required to accommodate its presence [80].

A study conducted by G. Karlsson Hedestam in 2012 [319] identified other key residues of the CD4bs antigenic site by comparing their use by CD4-binding ligands, by induced NAbs in non-human primates (NHPs) and by the CD4bs-canonical bNAb VRC01 (see in particular figure 5b of the cited study).

Following the isolation of VRC01, VRC07-523 was isolated and demonstrated a 5- to 8-fold increase in neutralization compared with VRC01, neutralizing about 96% of tested viral isolates with no signs of autoreactivity [276].

Worth citing here, the isolation of CH103 bNAb was reported in the same period [200]. This bNAb was less mutated than other bNAbs hence sparking great interest (see below). It was first seen at week 14 post-infection as a member of a lineage of 5 NAbs, neutralizing 55% of a 196-virus panel. However, the potency remained moderate ($mean_{IC50}$ around 4 $\mu g.mL^{-1}$).

CD4bs bNAbs seem to be relatively rarely elicited: only 5% of infected donors in a large cohort developed anti-CD4bs specificities [189]. They are particularly interesting for passive immunization and vaccination approaches as they typically display large breadth and strong potency. However, CD4bs bNAbs tend to require higher SHM rates to reach full potential [306], hence potentially rendering more complicated their elicitation in a vaccinal approach.

The V1/V2-Apex region

The V1/V2-Apex region was initially defined by four anti-parallel β-strands bound together by disulfide bonds [226]. Sitting at the apex of the trimer, this domain remains overall accessible to NAbs with a greater diversity in angle of approach and modes of recognition than those targeting the CD4bs. Furthermore, a subset of the V2-forming residues are conserved [374], enabling broad recognition for NAbs that are able to accommodate shielding glycans. This major antigenic site has been further separated into three epitopes exhibiting slightly different footprint and key features: the V2i epitope encompasses residues from C and D β-strands [220]. A second epitope was termed V2p. This V2p epitope is a non-neutralizing epitope, but interestingly, it seems to be the preferential target of protective responses observed in the RV144 'Thai' study reviewed below [199]. Finally, a third epitope lies in the V1/V2-apex region. Termed V2q for quaternary, this epitope arises from relatively conserved residues within the V2 loop in addition to surrounding glycans, and in particular the N160 glycan. bNAbs targeting this epitope include PG9 and PG16 [339], along with bNAbs of the PGT145 family [340] among others. Interestingly, these bNAbs share common features such as extensive breadth, long CDR_H3 loops and high germline divergence, attesting the important level of maturation required to target this epitope [219].

The PG9 bNAb was the first to be isolated among bNAbs targeting the V1/V2 region. It does so with an angle of approach that aligns with the trimer three-fold axis [165], and makes contacts with two of the three gp120 protomers in a quaternary mode of recognition (V2q epitope described above), allowing a stoichiometry of 1:1 in binding with the complete Env trimer. Structural analysis revealed the importance of mannose residues in the epitope for PG9 binding [226] as well as for PG16 [242]. Overall, PG9-class bNAbs require the presence of a glycan at position N160 to sustain neutralization. Viruses

produced in cells treated with kifunensine (an α-mannosidase I inhibitor [101]) displaying unprocessed $Man_9GlcNAc_2$ residues at PNGS, are resistant to neutralization by PG9-like NAbs. The presence of glycosylated residues at positions N156 and N160 has proven to be of paramount importance to the formation of the quaternary epitope of bNAbs targeting this region such as PG9 or PG16 [91].

The CAP256-VRC26 neutralizing lineage encompasses twelve members isolated from a superinfected donor, between 59 and 206 weeks post-infection (14 to 51 months post-infection). These Abs demonstrate relatively good breadth and potency, achieving neutralization against 47% viral strains of a 47 PV panel at a potency of 0.07 $\mu g.mL^{-1}$ [95]. This lineage uses the IG_HV3-30 and IG_LV1-51 V-genes and displays a very long CDR_H3 with 35 to 37 AA, the mature Abs exhibiting SHM rates that are not exceptionally high (15%). The mode of recognition of the HIV Env trimer recalls that of the PG9-class bNAbs, targeting the V1-V2 region at the apex of the trimer. One single Ab is bound per trimer, with a quaternary specificity for the native trimeric conformation. Similarity with the PG9-class Abs is not complete: CAP256-VRC26 NAbs did not show strict sensitivity to glycans at positions N156 and N160, with an epitope closer to the trimer axis.

PGT145 bNAb has been isolated from the donor 84 of the IAVI Protocol G study [340], along with other members of the PGT14x family. PGT145 shares the same mode of recognition as PG9 (and as CH04), relying on extended anionic loops to penetrate through glycan shield.

CH01 and CH04 bNAbs also target the V1/V2 conformational epitope described above. While of relatively moderate potency, they neutralized a maximum of 49% viral isolates of 92 tier 2 viruses. Interestingly, the reverted unmutated ancestor retained some neutralization activity, with neutralization of 16% of the same viral isolates [27].

Another anti-V2-apex bNAb worth mentioning here is PGDM1400. This bNAb was isolated in 2014 [309] and exhibits both exceptional breadth and potency, making it one of the best bNAbs available to date. PGDM1400-1412 bNAbs belong to the same lineage as PGT140-145 bNAbs. They share gene

usage (IG_HV1-8, IG_HJ6, IG_KV2-28, IG_KJ1), CDR_H3 length (33-34 AA) and have related CDR_H3 sequences. PGDM1400-1412 bNAbs have been isolated from a single timepoint using BG505.SOSIP.664 to select for quaternary Abs.

The V3-loop sites

The V3-loop antigenic supersite is separated into more specific epitopes. The crown of the V3-loop, its stem and its base [144]. The V3-loop region is involved in the co-receptor recognition. Its deletion renders the modified viruses non-infectious [330], thus demonstrating a vital functional role. This region is also strictly conserved in terms of length: the V3-loop seems to always encompass 34 or 35 AA residues to confer trimer stability. Several additional structural features are also conserved such as glycosylation positions, especially in the N- and C-terminal regions of the loop. The crown corresponds to the extremity of the V3-loop, and encompasses the conserved residues -**GPGX**- mentioned earlier and involved in the contact with the adjacent protomer. Next to it, the stem of the V3-loop holds a great amount of flexibility, thus rendering its precise description uneasy. Finally, the base of the loop is organized around the loop-making disulfide bond.

The so-called high-mannose patch corresponds to the base of the V3 loop and was termed a supersite of vulnerability, owing to its high conservation and bNAbs targeting this region with a variety of modes of recognition [180]. This region indeed seems to protrude outside of the gp120 structure hence exposing most of the surface with a large degree of freedom regarding the angle of approach. A number of bNAbs isolated to date target this region, and in many cases depend on the glycan at position N332 situated at the center of this supersite. The bNAbs binding to this region are termed V3 glycan-dependent bNAbs and differ from the glycan-independent NAbs that target the crown and stem of the V3-loop.

Among the first isolated bNAbs directed against this V3-region, 2G12 neutralized clade A viruses but not clade E, and showed complete dependency on the glycans, especially the one at position N295. It is worth noting that 2G12 remains a special case: the paratope is formed by an unusual Ab-domain swap [49].

The PGT121 bNAb, along with other members of the PGT12x and PGT13x bNAbs were isolated from different donors (17 and 36) of the IAVI Protocol G cohort [340]. The related bNAbs PGT128 and PGT130 are two branches of a same lineage. PGT128 bears a 6 AA insertion in the CDR_H2, required for neutralization, and it recognizes the glycans at position N332. NAbs in the PGT120 branch are notably good at recognizing glycans present at position N334 and lack the CDR_H2 insertion [92].

The QA013.2 bNAb has been isolated from a clade D-infected and clade A-superinfected donor with around one year between both infections [350]. This bNAb was isolated from samples at 6 years post initial infection. Forty-two members of this neutralizing lineage have been recovered, making it one of the most expanded neutralizing lineages studied. These NAbs utilize the IG_HV3-7*01, IG_HD1-1*01, and IG_HJ5*02 genes and harbor a 21-residue long CDR_H3 region. The heavy-chain of the best NAb of the lineage was calculated to have 20.0% SHM. This bNAb demonstrated typical contacts of the V3/Glycan-specific bNAbs: QA013.2 interacts with glycans at position N301 (with the CDR_H1 and CDR_H2 loops) and N332 (with the CDR_H3) as well as with the GDIR motif at the base of the V3 loop [297]. This mode of recognition is similar to that shown by bNAbs 10-1074 or PGT121.

The donor PC39 of the IAVI Protocol C cohort was infected with two transmitted/founder viruses and developed broad neutralization, allowing for bNAb isolation in a study similar to ours [161]. Broadly neutralizing responses appeared relatively rapidly (9-11 months post-infection). The isolated lineage comprised 36 members and was defined by usage of the IG_HV4–34*01 and IG_HJ6*02 heavy-chain genes and the IG_KV3–20*01 and IG_KJ2*01 light-chain genes. CDR_H3 was 22 AA long and all members demonstrated a significant insertion in the CDR_H1 region, spanning either 4 or 11 AA. Neutralization reached 76.0% of a 37 PV panel with a potency reaching 0.08 $\mu g.mL^{-1}$. Structural packing of the CDR_H3 depended on the length of the insertion, separating these bNAbs into two clades: the 11 AA-inserted clade had modes of recognition resembling the PGT135 bNAb while the mode of recognition of the 4 AA-inserted NAbs was not completely uncovered due to an increased flexibility.

Interestingly, glycan-dependent bNAb might have been primed with glycans originating from the self, and those displayed by different life stages of parasitic infections. In an original study, Huettner and colleagues demonstrate that the unmutated common ancestor (UCA) of a neutralizing lineage targeting the N332/V3 region cross-reacted with self- and non-self N-glycans, some of those present as surface antigens of *Schistosoma mansoni*, a parasitic worm highly prevalent in sub-Saharan African countries. Some of these bNAbs could have been primed by the parasitic infection before targeting the glycosylated Env from the HIV [150].

MPER region

The MPER region spans over 24 AA in the C-terminal extremity of the gp41 subunit and contains mostly hydrophobic AA, enriched in tryptophan residues. Because this sequence is highly conserved across all viral clades, NAbs targeting this supersite can in rare cases display extraordinary breadth, reaching $\geq$ 98% for some bNAbs. However, bNAbs targeting this epitope are often polyreactive. Furthermore, eliciting Abs targeting this site has proven arduous as the proximity of the membrane narrows angles of approach. Two modes of recognition can be distinguished for this region: broadest bNAbs recognize a small α-helix while less broad NAbs make use of additional residues surrounding this secondary structure.

4E10 is a powerful NAb that recognizes the linear epitope in the C-terminal part of the MPER region of gp41. While this epitope is highly conserved, some mutations and especially the F673L substitution can confer resistance to 4E10, at the cost of viral infectivity. In the primary study, F673L mutation was present in about 33% of the tested viral isolates [125].

Besides the aforementioned 4E10 and 2F5, and among bNAbs with significant breadth and potency and directed against the MPER region, we can cite 10E8 [147]. This bNAb 10E8 successfully neutralizes around 98% of a 181-virus panel of tested viruses, making it one of the broadest bNAbs available to date.

Interface and Fusion peptide

The region spanning between the gp120 and gp41 protomers is known as the interface. Several bNAbs targeting this region have helped delineate multiple contiguous epitopes within this region. Residues E83, V85, E87 and N229 are often participating in the epitope definition, along with the glycan in position N88. Among epitopes situated in this region, we can cite the Fusion Peptide (FP) region and the Fusion Peptide Proximal Region (FPPR). The FP region is a chain of 15 to 20 hydrophobic AAs located in the N-terminal part of the gp41 subunit. The bNAb 35O22 targets this interface epitope, neutralizing 62% of 181 viruses with a $\text{median}_{\text{IC50}}$ of 0.033 $\mu g.mL^{-1}$. Due to the nature of the epitope, these NAbs do not bind mgp120 but bind a conserved stretch of residues spanning across both gp120 and gp41 subunits. The serum analysis conducted by the authors suggested that this type of response could be commonly elicited by natural infection [146]. However, 35022 seemed to show enhanced binding to Env with pre-fusion conformation after CD4 engagement, rendering difficult its elicitation.

The definition of the fusion-peptide supersite was obtained with the isolation of N123-VRC34.01 bNAb. A study of the mechanism of action unveiled an inhibition of conformational changes that are required for viral entry. Furthermore, the crystal structure was made available in complex with the Env trimer [182], and anti-fusion peptide Abs were later successfully elicited in macaques [181]. Demonstration of protection in passive immunization studies in macaques with this VRC34 bNAb has recently been published [246]. The bNAb PGT151 and its cognate NAbs from the family PGT15x have been isolated from a single donor (31) of the IAVI Protocol G. They also target this fusion-peptide epitope of the HIV Env trimer [104].

Overview of the breadth and potency of current bNAbs

Current bNAbs can be characterized by both their potency and breadth of coverage against the diversity of global viruses, as shown in **Figure 1.6**. The first generation bNAbs, 2G12 and b12 are situated on the lower side of the plot (narrow breadth and low potency). Since their isolation, novel generation of isolated bNAbs have shown greater potency and breadth. The most potent bNAb shown here, CAP256-VRC26.25 exhibits an outstanding

potency of around 1 ng.mL^{-1}, more than 3 orders of magnitude more potent than first generation bNAbs. Topping the chart, N6 is the broadest bNAb known to date, neutralizing between 98 and 100% of viruses, a feat acheived by targeting the CD4bs supersite.

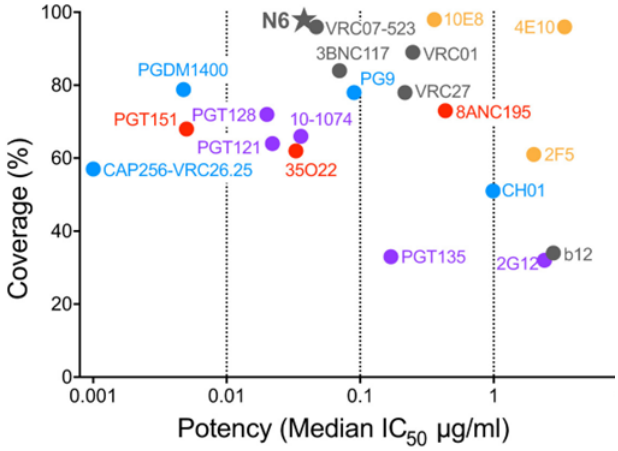

Figure 1.6. Breadth of coverage and potency of selected broadly neutralizing antibodies (bNAbs). Targeted epitopes are color-coded: anti-V2-apex are shown in blue, anti-V3-glycan are in purple, the bNAbs targeting the interface are shown in red. Anti-CD4-binding site (CD4bs) are shown in grey and yellow depicts anti-MPER (membrane-proximal external region). Adapted from [305].

1.2.4 Viral and hosts determinants of broad neutralizing responses

The identification of bNAbs raised questions about whether all individuals are capable of mounting a broadly neutralizing response, or whether such a response relies on specific characteristics from either the host or the virus.

It appears that neutralization can arise independently of the age of the infected individual: broad neutralization has been described in children, sometime with limited Ab maturation [302], and often developing sooner in the infection than in adults [123, 87]. Children seem to elicit broad neutralization more frequently, and to be capable of reaching higher Abs maturation rates [108]. Among key determinants of this immune response in young individuals, the presence of IL-21-secreting HIV-specific Tfh-cells in the GC was highlighted [271], as well as higher levels of plasma IL-5 [192].

There appears to be no role for geographical origin, route of HIV-transmission, race or ethnicity in the genesis of broad neutralizing activity [94, 189]. Some studies however nuanced this: it was described that Black individuals developed bNAb responses with a higher frequency [278], and in a recent study, Schommers *et al.* showed that increased neutralization was observed in female recipients of younger age and originating from Asia or Central Africa [288]. This might be attributed to the pre-existence in certain populations of Abs targeting exogenous and endogenous glycan motifs due to previous parasitic infection [150]. However this has not been widely demonstrated.

The probability of developing bNAbs is associated with the duration of infection without treatment and also with a higher viral load [278]. However, after several years of infection, this association does not hold: in a longitudinal study of more than 400 untreated primary-infected individuals, no significant broad neutralization appeared after 4 years of infection [189]. Furthermore, in individuals who developed broadly neutralizing serum activity, the broad neutralization appeared at 3.5 years on average. A recent study of more than 2,000 HIV-infected individuals showed that neutralization and breadth of neutralization was better predicted by a longer time spent off ART [288].

A high viral load is linked to development of broad neutralization [251], as well as a lower $CD4^+$ T-cell count [283, 127, 288], these two observations being potentially related. In one study however, breadth of neutralization against the Env glycoprotein has been associated with the presence of a strong $CD4^+$ T-cell response [265]. In this study, the association was particularly strong for Gag-specific $CD4^+$ T-cells and, at lower level, for the gp41-specific $CD4^+$ T-cells. Notably, the association was not observed for gp120-specific $CD4^+$ T-cells.

Also concerning immune cells, a higher frequency of circulating Tfh-cells, as well as the early preservation of both Tfh-cells and B cells were linked to more frequent and broader neutralization [206, 65, 189]. The high frequency of circulating Tfh-cells is thought to be a proxy to the presence of these cells in GCs. Their higher frequency in GCs could be in part responsible for the broad neutralization. Furthermore, the levels of $CD4^+$ $PD\text{-}1^+$ $CXCR3^-$ $CCR5^+$ memory Tfh-cells have been shown to correlate positively with broad neutralizing ac-

tivity [206]. These cells are key factors to induce the SHM in B cells. Because bNAbs tend to require higher SHM rates, an increased number of these cells could favor the elicitation of bNAbs.

Regarding Ig levels in serum, a positive correlation between neutralization and total plasma IgG levels and anti-Env IgG binding titers was assessed [189]. Neutralization levels were also associated with plasmatic titers of anti-gp41 and anti-p24 IgG in the same cohort.

On the HIV side, some viral determinants of neutralization have been discussed, albeit these findings should be taken cautiously. A stronger content in glycan at transmission seems to correlate with quicker elicitation of neutralization in the host [337]. Overall glycan occupancy seems to increase over time in chronically infected individuals, suggesting that glycans participate in viral escape. Linking these two observations, some authors have suggested that neutralization would arise more quickly in individuals infected by heavily glycosylated viruses because the possibilities of glycan-mediated viral escape are thinner. In addition, antigen presentation by DCs seems to increase as mannose content rises, thereby potentially favoring stronger CD4 help to B cells and the elicitation of NAb responses [155]. Regardless of these, infection with a non-clade B virus seems to be correlated with broader and more potent neutralization [288].

As stated above, the immune response appears to be usually insufficient to prevent superinfection events. Whether superinfection leads to an increase in the breadth and potency of neutralizing Ab responses has been debated. Superinfected individuals tend to see their neutralizing response boosted [73, 114]. Furthermore, some highly potent bNAbs have been isolated from superinfected donors [95, 297]. One possible boosting mechanism is the induction of a more diverse polyclonal repertoire [350]. However, this has not been consistently reported, some recipients showing an absence of broadening of their neutralization activity following superinfection [72, 295].

1.2.5 Isolation of bNAbs in longitudinal studies

A relatively low number of studies of infected individuals for which a longitudinal follow-up is available have been published. Several of them have been

made possible thanks to the IAVI Protocol C cohort. Here, I briefly review key features of selected studies.

In 2013, Liao and colleagues [200] described the isolation of CH103. This bNAb targets the CD4bs. The donor was enrolled in a cohort of acute HIV-1 infections (CHAVI001) and was followed up for more than 3 years. An initial screening step demonstrated that the serum activity targeted the CD4bs. Autologous neutralization appeared at 14 weeks post infection (wpi) and heterologous neutralization was seen from 41 to 92 wpi. Successful bNAb isolation was performed at 136 wpi by FACS-based sorting. B cells that bound to the RSC3 construct were sorted, among which CH103, CH104, CH105 and CH106 were recovered. These belonged to a single lineage using V_H4-59, D_H3-16, J_H4 heavy-chain genes and V_L3-1, J_L1 light-chain genes of lambda subtype. Second generation sequencing of PBMCs allowed the recovery of 457 heavy-chains along with 171 unpaired light-chains from this lineage. The inferred UCA mAbs from this lineage did not bind to heterologous Env proteins. However, the isolated autologous transmitted/founder virus CH505 was successfully recognized by the UCA candidates. Polyreactivity was acquired during maturation and bNAbs CH103, CH104 and CH106 were polyreactive. A strong selection pressure was observed in the viral isolates from 30 to 53 wpi, probably driving the elicitation of the heterologous neutralization. Vaccinal implications of this study are numerous as the transmitted/founder virus has been used as an immunogen for several immunization studies.

In 2014, Doria-Rose and colleagues [95] successfully isolated twelve bNAbs from a single lineage, targeting the V2-Apex supersite from a donor enrolled in a South African cohort (CAPRISA). Three timepoints spanning from 15 to 51 months post infection (mpi) were sampled using a single B cell culture approach. Single-B cell culture supernatant was screened using microneutralization and RT-PCR attempted in positive wells. This labor-intensive procedure allowed the recovery of these 12 bNAbs, of V_H3-30 and V_L1-51 origin. These were lambda type Abs with SHM rates between 4 and 15%. CDR_H3 were extraordinarily long (35 AA) and was produced during intial gene rearrangement, prior to any HIV-driven selection. The combination of all 12 bNAbs recapitulated plasma neutralization. Extensive neutralization assays allowed for epitope mapping, and structural analysis confirmed the mode of

recognition similar to that of PG9-class Abs. Exploration of this lineage was further enriched with unpaired heavy- and light-chains obtained through pyrosequencing of B cells at 8 timepoints, starting at around 4 mpi. Vaccine implications were limited, as the elicitation of such bNAbs relied on the critical yet uncommon rearrangement of Ig genes to produce the long, protruding, tyrosine-rich anionic CDR_H3 responsible for breadth. This work nevertheless underlined the need to obtain precise developmental pathways of breadth, and especially the viral evolution that drives the development of breadth.

In another study, MacLeod and colleagues from our group [210] successfully isolated bNAbs targeting the HMP from an elite-neutralizer (PC76) from the Protocol C cohort. Recombinant mgp120 probes (WT and N332 mutated) were used to FACS-single-sort B cells specific for the N332 glycan in separate wells. RT-PCR and Ig gene cloning was performed without further screening. Twelve NAbs belonging to the same lineage were recovered, which used the genes IG_HV4-34*01 and IG_HJ5*01 for the heavy-chain. The light-chain was of kappa type and used the genes IG_KV3-20*01 and IG_KJ1*01. SHM rates at the AA level ranged from 8 to 26% for heavy-chains. CDR_H3 length was 22 AA. Most matured NAbs (from 33 and 38 mpi) neutralized between 65 and 70% of a 37 PV panel and the NAbs were dependent on high-mannose and hybrid glycans for binding. These bNAbs demonstrate weak to no polyreactivity, albeit with some exceptions. Several autologous env sequences were retrieved and showed the presence of PNGS at position N335, a unique feature of this viral strain. The loss of the glycan in postion N332 was thought to be the main driver of viral escape. The lineage was further enriched by heavy-chain sequences retrieved from bulk NGS sequencing of PBMCs. The neutralizing lineage seemed to have undergone an early diversification with branches that individually matured in parallel. While most branches reached a dead-end, some allowed sustained maturation supporting the development of breadth. Most broadly NAb from this donor exhibited an extended CDR_H3 loop that could make contact with the protein backbone of the HIV Env. High hopes were raised concerning vaccinal implications of this study: the relatively low SHM rate observed in isolated bNAbs seemed to be achievable through vaccination, and the bNAbs lacked some difficult-to-induce features such as large insertions or deletions. However, the use of the IGHV4-34*01 allele, known to have autoreactive properties suggested this lineage could be difficult to elicit.

In a second longitudinal study of a donor (PC64) from the IAVI Protocol C cohort, Landais and colleagues [190] isolated bNAbs targeting the V2-apex supersite. Polyclonal neutralizing activity depended on the glycan at position N160. PBMCs from six timepoint (13 to 46 mpi) were used to isolate 33 bNAbs from a single lineage (named PCT64) through single-B cell FACS sorting followed by B cell activation and supernatant screening by microneutralization. SHM rate ranged from 2.6 to 13.5% at the nucleotide level for heavy-chains that used the genes V_H3-15*01 and J_H6*03. Mapping experiments suggested that these NAbs bind a quaternary V2-apex epitope similar to CAP256-VRC26. In this study, the authors suggested that relatively few mutations could be necessary to achieve neutralization breadth. Furthermore, they claimed that the maturation over a certain threshold does not improve breadth nor potency. Again, bulk-NGS sequencing was performed on total PBMCs to enrich the neutralizing lineage. A near-germline (99.4% identity) heavy-chain sequence was recovered from a sample at 10 mpi. Here again, the phylogenetic analysis revealed a highly-branched maturation process. Maturation allowing acquisition of breadth seemed to mostly have happened in CDR_H2 and CDR_H3 regions. In this study, the autologous *env* diversity was sampled by NGS. This allowed for unprecedented resolution of the drivers of maturation towards breadth. This allowed to pinpoint the individual residues in potions 166, 167 and 169 as key drivers for the elicitation of heterologous neutralization. Finally, the UCA of the lineage was shown to bind to early autologous Env trimers when these lacked complex and hybrid glycans. The authors suggested that the early and rapid emergence of bNAbs could be encouraging from a vaccine perspective, and that Env immunogens for germline-targeting approaches should be produced in systems favoring a higher proportion of $Man_{8\text{-}9}$GlcNAc glycans.

Rantalainen and colleagues [267] further explored the neutralization of these bNAbs isolated from donor PC64. In this work, detailed cryoEM and X-ray crystallographic studies revealed key details about the structural basis of co-evolution between autologous Env proteins and nascent bNAbs. The maturation of PCT64 NAbs revealed a change in the angle of approach to the Env trimer, concomitant with a rigidification of the CDR_H3 loop. The data gathered by the authors in this study suggested that neutralizing lineages should be elicited by stimulating germline Abs with different modes of binding to the

Env, hence multiplying the chances to later develop broad neutralization.

More recently, Zhang and colleagues [367] probed a single sample from a donor (P13) of the Protocol G cohort to isolate anti-MPER bNAbs. B cell sorting was achieved using a traditional FACS approach. IgG^{+} IgD^{-} IgM^{-} B cells were selected for double-positivity against a fluorescent-labelled MPER peptide and sorted in single wells. A single NAb was successfully isolated (PGZL1) and the corresponding lineage further enriched with heavy-chain sequences obtained through bulk-NGS sequencing. PGZL1 made use of V_H1-69 and V_K3-20 genes, responsible for a high sequence homology for other anti-MPER bNAbs (namely 4E10 and VRC24.01). Neutralization was extensive, reaching 84% of a 130 PV panel, albeit with a relatively modest potency (geomean IC50 = 6.1 $\mu g.mL^{-1}$). However, the Ab with a sequence reverted to germline showed substantial neutralization capabilities, in contrast with most studies where the UCA struggles to bind to the Env glycoprotein. Furthermore, PGZL1 had limited polyreactivity compared to 4E10, with whom it shared the mode of recognition of the MPER epitope. The obtained structures in complex with full length HIV Env bound to the membrane bring valuable information to the vaccine field. Furthermore, the authors provide insights in booster designs, proposing several pathways to guide maturation of early Abs after initial elicitation through germline-targeting approach.

Umotoy and colleagues [328] probed another donor (PC63) from the Protocol C cohort. Their work allowed the unveiling of the development of a VRC01-class bNAb targeting the CD4bs. The strategy applied to B cell isolation relied on the use of WT and CD4bs-epitope knock-out recombinant mgp120 proteins. Differentially sorted B cells were isolated in single wells from three timepoints, ranging from 66 to 77 mpi. The neutralizing lineage recovered encompassed 18 NAb members and made use of the $IG_HV1\text{-}2*02$ and $IG_HJ05*02$ genes for the heavy-chains and the $IG_KV1\text{-}5*03$ and IG_KJ1*01 kappa genes for the light-chains. These harbored the 5 AA insertion in the CDR_L3, characteristic of VRC01-class NAbs. However, these NAbs were substantially less mutated (9.6 to 16% mutated at the nucleotide level), while retaining the breadth of neutralization. Bulk-NGS sequencing demonstrated that the frequency of NAbs progenitors was not higher in this donor than in HIV-negative individuals of different geographic origin. This work provided

detailed mutational pathways that led to neutralization breadth in VRC01-class NAbs from lineage elicitation. Findings from this study confirmed the design of the germline-targeting immunogen eOD-GT8 (see below) as a potential candidate for VRC01-class lineage priming.

Finally, van Schooten and colleagues [290] successfully isolated CD4bs bNAbs, albeit of limited breadth. Their sorting strategy involved FACS sorting of positive cells for at least one probe among an autologous SOSIP trimer, a heterologous SOSIP trimer and a recombinant mgp120 of heterologous origin. A transmitter/founder virus lacking a glycan at position N276 seems to have elicited the neutralizing lineage, suggesting that this could be used as an immunogen to elicit CD4bs-targeting bNAbs of this class. Interestingly, in this particular donor, large breadth of neutralization observed in the serum seemed to arise from several less broad neutralizing lineages targeting multiple epitopes [289]. Consequently, the authors suggest that eliciting a polyclonal response via immunization might be an interesting strategy.

Altogether, these studies reveal potential roadmaps to the development of neutralization breadth. Their common goal is to identify the unmutated common ancestor Ab that sparkled the development of the neutralizing lineage. After this is recovered, virions that are recognized by the UCA Ab can serve to attempt the elicitation of neutralizing lineage in other individuals.

The present study aims at isolating neutralizing lineage(s) from an elite neutralizer from the Protocol C cohort and recapitulate the maturation pathway that led to neutralization and breadth.

1.3 Interests and potential uses of bNAbs in a clinical setting

Broadly NAbs could play a pivotal role in addressing HIV infections across various fronts. Two primary domains directly benefit from the study of bNAbs: firstly, their passive applications in both preventive (prophylactic use) and therapeutic (treatment) contexts, and secondly, their existence and the mechanisms that allowed their development bring fundamental insights to the field of informed vaccine design. Concerning the therapeutic approach, two possible uses have been described: the administration in substitution or in

addition to ART to control viremia, or the use of bNAbs to help achieve the definitive elimination of the virus (cure).

I will review these uses, first in passive immunization settings and then in vaccination. I will start with prophylactic use, before addressing the therapeutic use, either in treatment approaches or in the outlook for a cure.

1.3.1 Broadly NAbs use in passive immunization settings

Prophylactic use: bNAbs as prevention

The ability for NAbs to protect against contamination in homologous viral challenges has been demonstrated in animal models of HIV infection, especially in NHP models [41]. Neutralizing Abs can therefore provide individuals with sterilizing immunity. Sterilizing immunity usually describes a natural immune response to a pathogen where this pathogen is completely eliminated upon transmission, before the infection can be established and the replication can be sustained [338]. In the case of HIV infection, sterilizing immunity is the only solution to efficiently protect the individual, as any established infection will induce the constitution of a viral reservoir, ruling out a possible control of the infection.

Given the ability of bNAbs to neutralize a large spectrum of viral strains, they could provide sterilizing immunity (therefore protection) against the diversity of circulating strains, alone, or in cocktails of bNAbs [163]. Indeed, bNAbs were shown to protect animals from viral challenge [218]. In this study, protection was achieved with relatively low titers (1:29 and 1:128). This sterilizing immunity conferred by bNAbs has been confirmed in multiple preclinical trials, and for multiple routes of contamination [245, 115]. In these later studies, protection against SHIV infection was observed for titers as low a 1:20 (for 10-1074 and 3BNC117) and 1:51 (for VRC01-LS) [233, 117, 164].

A first human trial demonstrated the diffusion of infused bNAbs to mucosal secretions and local tissues prone to be the recipient sites of infection [9]. Broadly NAbs were then used in Antibody Mediated Protection (AMP) trials to understand the protection they could confer in real-life settings. Furthermore, these trials made it possible to study the emergence of viral resistance, and helped assess pharmacokinetics related issues.

The AMP trials HVTN 704/HPTN 085 and HVTN 703/HPTN 081 conducted between 2016 and 2021 were phase IIb studies designed to assess the prevention efficacy (PE) of the CD4bs-targeting bNAb VRC01 against placebo. Unfortunately, these studies were unable to demonstrate overall protection with this single bNAb. However, in a genetic analysis of viral strains in breakthrough infections, a study highlighted the correlation between PE and the genetic distance that exists between the VRC01 epitope and the corresponding sequence in breakthrough infective strains [169]. Hence VRC01 was able to protect individuals from susceptible viral strains with a PE of 75%.

Indeed, the inhibitory concentration 80% (IC_{80}) of VRC01 against the infectious strain was strongly associated with PE. However, assessing the protective levels of infused bNAbs remained complex. A detailed analysis of the trial data allowed the calculation of protective titers and correlates of protection [119]. In this analysis, the authors calculated that achieving 50%, 75% or 95% PE required serum half-maximum inhibitory dilution (ID_{50}) titers to be of 1:116, 1:252 or 1:565, respectively. When considering ID_{80}s, this corresponded to titers of 1:32, 1:82 or 1:194, respectively. These titers are remarkably close to those found in NHP (1:91, 1:219 or 1:685 serum ID_{50}s for 50%, 75% and 90% PE) in previously undertaken studies [149]. This suggests that PE efficacy can be measured though neutralization titer assessment of the serum.

Overall, the AMP trials demonstrated that VRC01 alone did not succeed in HIV-acquisition risk reduction. But by showcasing the protection of individuals exposed to VRC01-sensitive viral strains, these trials were the first to bring evidence of Ab-mediated protection against HIV infection in humans [71]. The same VRC01 has been successfully tested in newborns, through subcutaneous injections, and could be used as an alternative to ART in a foreseeable future to prevent maternal transmission [77, 222].

Therapeutic use: bNAbs as treatment

Early investigation using first-generation bNAbs (2G12, 2F5, 4E10) demonstrated safety and capacity of these NAbs to reduce viral load in infected (human) individuals [7, 317], although eliciting the emergence of escape mutants [214]. Further studies demonstrated a significant delay in viral rebound up to 24 weeks post ART interruption [327, 229].

Second generation bNAbs were used in monotherapy in phase I clinical trials in infected individuals using either CD4bs bNABs (3BNC117 or VRC01) or V3-glycan targeting bNAbs (10-1074 or PGT121). The observed reduction of the viral load of bNAb-sensitive individuals was of 1.10 to 1.77 $\log_{10}$ viral copies.mL^{-1} [54, 208, 53, 315]. In these studies, viremia remained undetectable up to 28 days following bNAb infusion, and up to six months in some individuals with initial low-level viremia. Viral rebound with the emergence of escape mutants was however inevitable in all participants.

In early studies, bNAbs were used in the absence of ART. A novel approach assessed the combined use of both drug regimens: initial ART to lower the viral diversity and subsequent bNAb monotherapy to control viremia. In studies with the CD4bs targeting bNAbs VRC01 or 3BNC117, the viremia was controlled for between 4 and 19 weeks post ART discontinuation [286, 12, 76, 50]. Furthermore, these studies demonstrated that the viral rebound was associated with waning bNAb trough concentrations or with preexisting variants resistant to the corresponding bNAb.

Together these studies demonstrated the safety and efficacy of bNAb use in patients living with HIV (PWH). However, these studies also outlined the limitations of bNAbs in monotherapy, paving the way for bNAb use in combinations.

Several studies undertaken in infected NHPs demonstrated that combinations of bNAbs were able to achieve sustained viral suppression [272, 347, 247]. Translated into human settings, the combination of the CD4bs bNAb 3BNC117 and the V3-glycan targeting bNAb 10-1074 was shown to be well tolerated [66]. The combination achieved a sustained viral suppression for 21 weeks without inducing selection of bNAb-resistant strains in infected individuals undergoing ART interruption [230]. When initiated in viremic patients without ART use, the same combination proved efficient for up to 3 months [13].

More combinations of bNAbs are being studied and some trials have already delivered their first results. A phase I study demonstrated the safety and efficacy of a cocktail of three bNABs: PGT121, PGDM1400 and VRC07-523LS

[315]. Viremic patients had their baseline viral load reduced by approximately 2.0 $\log_{10}$ viral copies.mL^{-1} after a single injection of the bNAb mix.

The additive nature of bNAb efficacy should be noted: there seems to be no synergistic effect of bNAbs when used in combination. Instead, breadth of coverage of bNAb cocktails solely increases as a result of the sum of individual breadths. This eases the computation of the neutralizing breadth of combination of bNAbs [183]. However, and because each single bNAb has unique characteristics of manufacturability, pharmacokinetics and half-life (among others), combining these bNAbs in the most efficient way remains challenging. Determining the best combination of bNAbs, with the additional challenges of bi-specific or tri-specific Ab constructs, is one of the goals of currently ongoing studies [30]. A bispecific construct combining an anti-MPER and an anti-CD4bs specificities (10E8v4/iMab) is being evaluated for safety, tolerability and pharmacokinetics by IAVI in a small subset of around 50 infected and non-infected individuals (NCT03875209, results expected in 2024). A tri-specific molecule combining the specificities of VRC01, PGDM1400 and 10E8v4 is also undergoing testing for safety, tolerability and pharmacokinetics (NCT03705169) and raw, unconsolidated results have been published early in 2024. These results show little reduction in viral load (-0.1 and -0.38 $\log_{10}$ copies.mL^{-1}), regardless of dosage.

Together, these later studies demonstrated the potential of these combinations as well as key determinants for future successes: bNAbs used alone or in combination are generally well-tolerated and have little to no side effects, these NAbs can achieve sustained viral suppression given the therapeutic concentrations are achieved and maintained over time, and finally viral suppression can be attained given the absence of pre-existing resistant viral strains.

Therapeutic use: bNAbs as cure

Broadly NAbs could potentially be used in other therapeutic approaches aiming to achieve a functional cure of infected individuals. Two main approaches have been developed and proof-of-concept successfully obtained: the shock-and-kill approach (**Figure 1.7**) [6], and the block-and-lock approach [176].

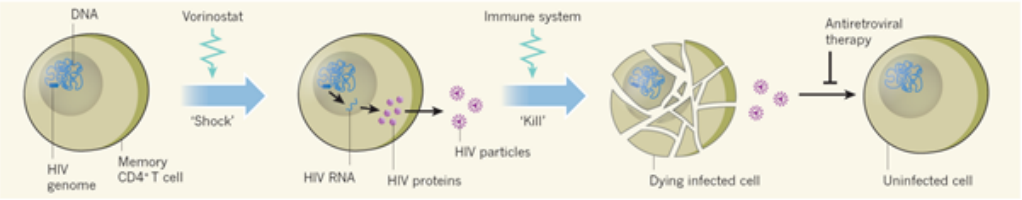

Figure 1.7. Schematic representation of the "shock'n'kill" approach to an HIV cure. Broadly neutralizing antibodies can play an important role for the 'kill' part of the cure. Adapted from [82]

In the shock-and-kill approach, bNAbs could have a role to play, helping to kill the infected cell. Hence, seminal studies have been conducted [131, 130] demonstrating the interest of bNAbs in these settings. Using latency reverting agents for the 'shock' part and the CD4bs-targeting 3BNC117 bNAb for the 'kill' part, some patients from these studies achieved ART-free sustained virological control for at least 12 weeks.

Other approaches to a functional cure are under investigation, and some of them make use of bNAbs. Among approaches of particular interest, we could cite the Bispecific T-cell Engaging antibodies (BiTEs) approach [40] and the Dual-Affinity Re-Targeting molecule (DART) approach [320, 304], both capitalizing on previously isolated bNAbs to build next-generation therapeutic tools.

1.3.2 Broadly NAbs in vaccinal approaches

Traditional vaccine approaches

Several vaccine trials have been conducted since 1998 to assess the protection conferred by different immunogens. They have been extensively reviewed, especially in [192]. Notoriously, all of them have failed to provide protection in the targeted populations. A few selected trials are summarized here.

The first vaccine trials to enter phase III studies were the VAX003 and VAX004 trials. These vaccines aimed at inducing neutralizing Ab responses directed to the gp120 subunit. The VAX003 study aimed at demonstrating the protective efficacy of a bivalent subtype B (MN) and AE (CRF01_AE) recombinant gp120-based vaccine candidate to protect from infection individuals from an at-risk-of-infection population of Thai drug users [322]. The VAX004

study had a similar design [133], but measured the efficacy of a bivalent subtype B (MN and CNE8 strains) recombinant protein vaccine candidate with alum adjuvant in an American population of Men who have sex with Men (MSM). Both studies failed to demonstrate any protection [107, 252].

The only efficacy trial to showcase some potential level of protection is known as the RV144 trial. In this study, a canarypox vector displaying the HIV Env protein and boosted twice with recombinant mgp120 proteins from clade B and E achieved 31.2% protection among study participants in Thailand [269]. An attempt to replicate these finding in a South-African population (HVTN 702, Uhambo trial, NCT02968849) failed to achieve protection, even with adapted boosting strategy for the local viral epidemiology [128]. The CRF01_AE subtype used in priming (92TH023) was replaced by a subtype C strain (96ZM651). Boosting involved two subtype C gp120 proteins (TV1.C and 1086.C). Despite successfully eliciting some specific responses and high anti-gp120 titers, no neutralizing responses were detected in the South-African study. In the original RV144 trial, and when considering efficacy in individuals with breakthrough viruses that matched the vaccinal strain, measured protection efficacy reached 48% [136]. Some authors have suggested that observed non-neutralizing responses directed towards the V1-V2 region of the Env might have played a role in this partial protection.

Among following trials are the HVTN705/Imbokodo (NCT03060629) and the HVTN706/Mosaico (NCT03964415) studies. Both were conducted between 2017 and 2024 and aimed at assessing the prevention efficacy of Ab responses elicited by an adenovirus vector prime with recombinant Env protein booster immunizations. The Imbokodo trial followed a phase I/IIa study (APPROACH) and an evaluation of the vaccine strategy in NHPs [17] where the immunogens demonstrated significant protection against repetitive challenges. However, the phase IIb trial was stopped early in August 2021 after non-efficacy was assessed at an interim review of the data. Vaccine efficacy has been estimated at 25.2 % [191], although the final analysis remains to be published. The Mosaico study used a heterologous vaccine regimen with a clade C gp140 adenoviral vector for priming and a mosaic gp140 boosting strategy. The trial was stopped early in 2023 for non-efficacy of the tested regimen [191].

bNAb-informed vaccine design: germline-targeting approaches

Outside the field of HIV, most virus-targeting vaccines successfully protect against their pathogenic target by eliciting a neutralizing response [298]. Therefore, specifically eliciting an anti-HIV Env bNAb response in healthy subjects aims at protecting uninfected individuals in the same manner. However, eliciting bNAbs by means of a vaccine has proven remarkably challenging.

An important fraction of bNAbs exhibit peculiar features (unusually long CDR_H3, high SHM rates, presence of indels, ...) (reviewed in [306]). Furthermore, some bNAbs (or their ancestors) have demonstrated poly- or autoreactive behaviors [135, 205]. Finally, for several bNAbs, corresponding precursors can be exceedingly rare [157, 134, 312]. Fortunately, this is not always true, and some (longitudinal) studies have demonstrated the existence of bNAb lacking these rare features, exhibiting no polyreactivity and for which precursors are available in healthy repertoires at higher frequencies.

A novel vaccinal route has been envisioned [156] to try to solve these challenges. This approach aims at leveraging the knowledge from longitudinal studies of Ab and viral co-evolution to try to replicate the elicitation and maturation processes that lead to broad spectrum neutralization. Env proteins isolated from early timepoints could help design immunogens able to prime the precursor of bNAbs. However, many inferred germline versions of the bNAbs have low to no binding to Env immunogens [143, 156, 303]. Thus, a successful germline-targeting (GT) approach requires heavy engineering of these GT immunogens to elicit bNAb precursors.

Germline-targeting immunogens are designed to specifically bind to B cells whose BCR sequence corresponds to the bNAb precursor of interest, or its inferred germline version. Subsequent immunizations would then shepherd the maturation of this initial B cell to induce favorable SHM, directing lineage evolution towards breadth and potency [45].

CD4bs-targeting VRC01-class bNAbs have been isolated from independent donors [369, 15], suggesting that elicitation of these neutralizing responses in healthy individuals should be feasible. VRC01-class bNAbs are defined by a IG_HV1-2 V gene and a CDR_L3 encompassing 5 AA residues. To target

these VRC01-class inferred-germline B cells, a CD4bs-mimicking immunogen has been designed, namely eOD-GT8. This immunogen is formed by a modified version of the gp120 outer-domain (eOD), specifically designed to bind germline B cells (hence the GT) capable of priming broadly neutralizing responses [156, 157, 134].

The immunogen eOD-GT8 successfully elicited VRC01-class bNAb precursors in several mouse models [158, 96, 308, 38, 323, 203]. Furthermore, a study in BCR knock-in (KI) mice showed that elicited precursors could be successfully shepherded towards broad neutralization [59].

The IAVI phase I G001 trial successfully demonstrated the feasibility of neutralizing lineage elicitation in humans with the help of this self-assembling 60mer particle eOD-GT8. This engineered trimer, designed to prime the neutralizing lineages of VRC01-class bNAbs, has proven effective in 97% of the candidate recipients [197]. These results are highly encouraging and a direct and successful use of knowledge collected in bNAb isolation studies conducted in the last decade.

In parallel, a second collaboration designed a different GT immunogen destined at simultaneously targeting the CD4bs and the V1/V2-Apex bNAb precursors [228]. This immunogen is referred to as BG505 SOSIP.GT.1.1 gp140. This GT immunogen successfully primed VRC01-like precursors in mouse models [157, 134]. However, elicited bNAb precursors had much lower affinities to BG505 SOSIP.GT.1.1 when compared to the affinities obtained by eOD-GT8. This raises the question of whether this initial affinity will play a role in development of breadth and potency, a question that will probably be answered in ongoing trials.

In the IAVI phase I C101 clinical trial [228], this immunogen is used to prime neutralizing lineages in 48 participants followed up for 12 months. This trial started in 2020 and results are not expected to be available before the end of 2024. Correspondingly, neutralizing lineages are expected to be directed against the CD4bs and V1/V2-apex supersites.

These GT immunogens have been designed to elicit bNAb precursors that could develop neutralization activity (mainly) directed towards the CD4bs.

Other designs aim at eliciting precursors of different specificity. Based on the developmental history of the N332-specific, HMP-targeting PGT121 [340, 310], a potential GT immunogen has been designed [313]. This BG505-10MUT immunogen successfully primed PGT121 precursors in a tailored knock-in mouse model and subsequent immunizations induced the SHM that conferred the breadth of neutralization of the mature PGT121 [313, 103].

Similarly, the isolation in 2016 from an infected viremic controller of the anti-V3 bNAb BG18 targeting the glycan at position N332 in a similar manner as PGT121 [110] primed the development of a corresponding GT immunogen. This has proven successful with the generation of a N332-GT2 construct that primed BG18 precursors in an adoptive model mouse [312]. Moving to human settings, the undergoing HVTN 144 study is a phase I clinical trial aiming at demonstrating the feasibility of priming bNAb-like responses using the new GT immunogen N332-GT5 gp140 adjuvanted with SMNP (ClinicalTrials.gov: HVTN144). End of recruitment period is expected around 2025 and results are to be made available shortly after.

Finally, the bNAb PGT130 served as a guide to develop the 130GT family of immunogens. Here again, pre-clinical studies are encouraging (Steichen, unpublished): in a survey of 12 naïve human repertoires, PGT130 precursors were found at a median frequency of 1 in 200,00 naïve B cells [1 in 10,000 to 1 in 1,000,000], much above the numbers found for VRC01-class or BG18-class precursors. Furthermore, 83% of the donors had detectable reactivity to the 130GT7 immunogen.

Other GT approaches were developed. Among them, the 426c also aims at eliciting VRC01-class NAbs, and successfully primed germline version of these NAbs in mice [224]. The 426c immunogen is based on a clade C gp120 subunit and an engineered version lacking the inner-domain was later generated (426cOD) [203]. The first version (426c Core) is currently undergoing a phase I trial (NCT05471076) with results expected during the second semester of 2024.

bNAb-informed vaccine design: vaccine strategies based on lineage

The existence of studies showcasing the co-evolution of bNAbs along with the Env viral protein enabled the design of sequential immunogens that can guide the maturation towards breadth and potency. After empirical immunization attempts failed to provide protection, a following approach consisted in attempting to elicite bNAbs through sequential immunization with trimer immunogens corresponding to Env sequences observed in vivo in individuals producing bNAbs. In 2013, Liao and colleagues completed the isolation of a neutralizing lineage from donor CH505 from the CHAVI001, along with the description of 53 viral Env sequences, including the transmitted/founder virus [200]. The bNAbs belonging to this lineage targeted the CD4bs. Interestingly, the UCA of this CH103 lineage was found to bind to the transmitted/founder virus. Consequently, the sequential use of trimers derived from viruses isolated from this donor, was considered as a potential strategy to elicit corresponding bNAbs in healthy individuals. Therefore, these CH505 Env-based immunogens were used in NHPs which successfully developed neutralizing responses of significant breadth [24] in 2020.

Unmutated common ancestors (UCA) from bNAb lineages represent the closest B cell to the naïve B cell that needs to be engaged to elicit those neutralizing lineages. Hence priming these lineages requires the development of immunogens that are recognized by these UCAs [28]. In the longitudinal study that isolated the previously mentioned CH103 bNAb, the UCA of the lineage retained affinity to the transmitted/founder virus CH505, thus making this Env a good candidate for GT and priming. However, recent trials with this lineage-targeting immunogen in different constructs have resulted in limited results as two studies out of three were unable to elicit strong neutralizing responses [351, 285, 284]. The strategy is undergoing phase I clinical trials (NCT03220724: HVTN115 and NCT04607408) to fully determine the potential of these immunogens. Partial preliminary results are available but a peer-reviewed consolidated analysis remains to be published. Other studies making use of these immunogens are also planned.

1.4 PhD project

1.4.1 The legacy of the IAVI Protocol C cohort

ART initiation was initially recommended after CD4 T-cell count dropped below 200 cells/mm^3, 350 cells/mm^3 and 500 cells/mm^3 successively. Recent studies however, clearly demonstrated the benefits on overall mortality and morbidity of early ART initiation, enabling a switch of global and local guidelines to immediate use of ART in all settings [111, 74]. Prior to this shift in patient management, ART was initiated on CD4 T-cell count or following clinical status of the patient, initially allowing treatment of patients presenting with later-stage AIDS.

In this context, the IAVI Protocol C study was an international cohort of 'Early HIV Infections' that recruited patients between 2006 and 2011. Participants in this cohort were screened from two other IAVI cohorts, namely Protocol B and Protocol HT, which started in 2003 and were interested in the epidemiology of HIV infections. A complete and exhaustive review of these cohorts has been published recently [259].

Between 2006 and 2011, 613 primarily HIV-1-infected donors from Eastern and South Africa were followed-up within the IAVI Protocol C longitudinal cohort. In 2016, Landais et al. evaluated the neutralizing response against HIV-1 in 439 donors from the Protocol C cohort [189]. Mounting of a neutralizing response by these donors was initially assessed using a predictive panel of heterologous viruses from all main clades [339, 340]. A heterologous neutralizing response was present in about 15% of donors and arose mainly between 2 and 4 years post infection. Using a neutralization score taking into account both potency and breadth [300], donors were ranked for their peak neutralization activity in plasma. Among top neutralizers, donor PC94 ranked second when tested against a medium-size predictive panel of 37 pseudoviruses [189].

1.4.2 Exploring the neutralizing response from an elite neutralizer

As described above, studying how bNAbs develop in certain HIV-infected individuals can yield important information for vaccine design, in particular for germline-targeting approaches. Therefore, our lab has embarked on the

study of B cell repertoires from infected individuals developing serum neutralizing activity. In particular, previous work in our lab focused on the donor PC94 [189, 274, 275]. This donor ranked second in the Protocol C cohort for the serum neutralizing activity against heterologous viruses, thus making PC94 an elite-neutralizer.

PC94 is a young woman, aged 22 at the estimated time of infection, with a recognized risk factor of HIV transmission (sexual worker) and originating from Uganda.

After depletion of the gp120-binding fraction of the serum of PC94 at 55 mpi, remaining neutralizing activity was close to null. This demonstrated that the neutralizing activity of the polyclonal serum was indeed targeting mainly epitopes present on the mgp120, thus ruling out any possible quaternary mode of recognition. Neutralizing activity directed towards gp41 was also ruled out [189]. Other major antigenic determinants such as CD4bs, MPER or the apex region were ruled out using different competition approaches.

In their work, Landais *et al.* showed that 17 broad neutralizers (40% of the individuals whose serum activity was considered broad) had a neutralizing activity significantly affected by mutations in the V3 region, surrounding the N332 N-linked glycosylation site. PC94 was among those seventeen donors, thus indicating the main target of neutralizing activity seen in this donor. Neutralization was highly affected in knock-out experiments that targeted several PNGS, thus revealing their importance for neutralization. However, the glycan at position N332 was not the main determinant of neutralization as the impact was less important than for other PNGS [189].

In other experiments, Landais and colleagues demonstrated the absence of effect on PC94 serum neutralization activity when PVs were treated with kifunensine. This molecule prevents the formation of complex glycans at PNGS and leaves unmodified the glycans with nine mannose residues attached to the N-acetylglucosamine residues ($Man_9GlcNAc_2$). Taking into account this observation, we do not expect the neutralizing activity of PC94 to target any of the complex glycans exhibiting N-acetylglucosamine residues at their extremities.

The donor PC94 was infected with a HIV-1 subtype D clade virus. Clade D is highly represented in sub-Saharan African countries with very few infections of this clade being reported outside of this region. Interestingly, while HIV-1 clade D viruses are frequently reported in Uganda, there seems to be an important fraction (69%) of viruses originating from inter-subtype recombinations, with the A1/D variant accounting for most of these recombinations [11]. In a study of HIV genomes collected in the years corresponding to those of the Protocol C follow-up period, Balinda and colleagues demonstrated the presence of viruses with highly recombinogenic *env* regions with a predominance of subtype D in the *gag/pol* region. While these recombining forms bore no difference in replication capacity, extensive heterogeneity was observed in CD4 T-cell loss and transmission rates, with highly variable and recombinogenic *env* gene viruses being linked to the highest transmission rates. This could be of interest concerning the viral determinants of the large breadth neutralization observed. Notwithstanding, the genetic characterization of the viral strain infective in PC94 was only performed on the *env* region, thus jeopardizing a full-scale comparison and integration with viral genetic data available in public databases.

Further work allowed the isolation of several NAbs from longitudinal samples of this donor [274, 275]. Previous attempts for bNAb recovery from this donor used five different procedures. The first sorting experiment used an epitope-specific approach based on a differential sorting with three recombinant mgp120 (sorting B cells double-positive for 92BR020_WT_gp120 and IAVIc22_WT_gp120 and negative for IAVIc22_N332A_gp120) as the N332 specificity was suspected. This sorting experiment spanned over three timepoints (V48, V54, V60). Subsequent sorts were performed using trimers or a combination of both strategies. The second sort used a strategy that did not target a specific epitope (epitope-agnostic). It used six trimers: CE0217 SOSIP, CNE8 SOSIP, TRO11 SOSIP, 25710 SOSIP (KO), BG5050 T332N SOSIP and JR-FL NFL. The third and fourth sorts used a combination of both strategies: two mgp120 (92BR020_WT and 92BR020_N332A) were used in association with four of the previously listed trimers, in different combinations. Timepoints used here spanned V54, V60, V66 and V78 samples. Finally, a fifth sorting experiment used an epitope-agnostic approach based on a panel of four trimers against five timepoints (V30, V36, V42, V48 and

V60). Trimers were BJOX2000 SOSIP, TRO11 SOSIP, BG505 T332N SOSIP and JR-FL NFL.

Overall, heterologous neutralization from isolated NAbs was not very potent and of limited breadth in comparison with the exceptional neutralization activity measured from the polyclonal serum, as initially mapped against a small PV panel [189]. Furthermore, isolated NAbs did not recapitulate the magnitude of the breadth and potency as seen in the serum when further tested against a larger PV panel [274, 275]. Together, this suggested the presence of undiscovered bNAbs. Moreover, the limited breadth and potency of previously isolated NAbs suggested that the yet-to-be-isolated bNAbs could demonstrate exceptional neutralization activity.

To better understand the processes leading to the outstanding neutralizing activity seen in PC94, we further studied this donor aiming to isolate bNAbs that would recapitulate the polyclonal serum neutralizing activity. We sought to use novel techniques to isolate mAbs from this donor compared to previous studies. To our knowledge, the use of single-cell RNA sequencing (scRNA-seq) to isolate bNAbs from longitudinal samples has not been attempted in the context of HIV. However, the relatively scarce use of the scRNA-seq techniques for bNAb isolation raised questions concerning this approach.

1.4.3 Available techniques: from FACS to scRNA-seq

The isolation of most bNAbs described above was made possible thanks to the use of FACS sorting techniques coupled to immunoglobulin gene amplification, sequencing and cloning from single B cells. In this low-throughput setting, FACS has been used alone or in combination with B cell activation techniques. When used alone, sorting strategies mostly relied on the sorting of IgG^+ MBC specific to viral probes. This prevents the recovery of other isotypes, such as IgA^+ or IgM^+ B cells. This strategy also reduces the ability to sort bNAbs ancestor B cells, as early B cells are expected to be closer to the naïve phenotype IgD^+ IgG^-.

Concerning viral probes, first, recombinant mgp120 protein have been used owing to the ease of production. However, by exhibiting epitopes that are usually masked, an important number of recovered B cells translated into

NNAbs. A solution to this has been the use of differential sorting strategies. In this approach, the epitope of interest is targeted by the differential binding to wild-type (WT) and knock-out (KO) versions of a given mgp120. This differential sorting strategy has been used for our top-neutralizer donor [274, 275]. This approach however requires previous knowledge about the putative target of the broad neutralization.

The advent of soluble native-like trimers allowed for better presentation of the antigenic sites, as well as agnostic sorting strategies. In these strategies, trimers can be used without expected prior knowledge of the specificity of the neutralization activity. Differential sorting approaches can be also used with these constructs. This has been intended for our donor in several attempts to isolate bNAbs using SOSIPs [275].

With these native-like baits, broad neutralizing responses can be isolated by increasing the number of baits to which a B cell is required to bind to in order to be sorted out. While this approach proved to be achievable and successfully helped isolate some of the aforementioned bNAbs, it has a practical limit. The number of baits to be used is strictly limited, in accordance with the available sources of coherent light and detection capabilities of the FACS machines. Even if in the past decade it has been possible to reach around 20 fluorochromes, the mandatory use of certain channels to correctly identify live B-lymphocytes from the memory compartment, leaves the number of fluorochromes limited.

When used in combination with B cell activation and paired with microneutralization screening, this proved incredibly labor-intensive and prohibited increased throughput. Despite this low throughput, this technique allows for epitope-agnostic, probe-free sorting of single B cells.

Single-cell RNA sequencing was introduced in 2009 [321]. The year 2011 saw the integration of oligonucleotide barcode [154] and 2013 the first microfluidic system allowing for automated preparation of the samples [34, 83]. The advent of droplet-based methods dates from 2015 [177, 211] with the 10X Genomics Chromium platform being released in 2016. Nowadays, scRNA-seq enables analysis of a large population of cells without prior knowledge of the markers

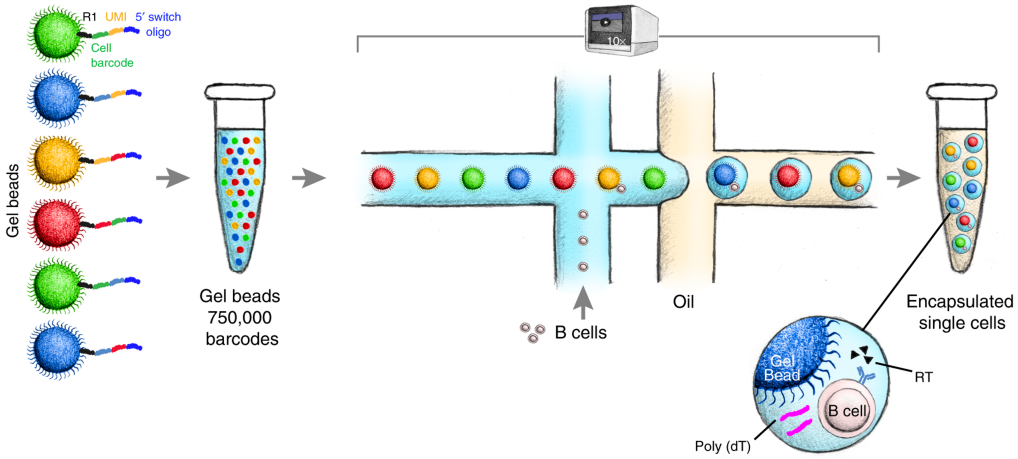

Figure 1.8. Schematic overview of the single-cell pipeline commercialized by 10X-Genomics. A microfluidic system encloses single cells with gel beads covered with hundreds of thousands of barcodes enabling the labelling of individual mRNA transcripts during a reverse-transcription reaction taking place in single-cell droplets.

or genes involved in the biological process of interest. Hence, this approach is as close as possible to an unbiased exploration of cell populations, yielding unprecedented details in several fields of study. Furthermore, these approaches allow the recovery of paired heavy- and light-chains from B cells, thus allowing a high-throughput recovery of B cells and the BCR/Ab repertoire.

This scRNA-seq technology is readily available commercially. 10X-Genomics kits use a microfluidic system to link each cell to a single bead coated with hundreds of thousands of identical oligonucleotide barcodes (**Figure 1.8**). The process allows for the recovery of the cellular identity as the corresponding barcode is sequenced. In addition, barcodes bound to cellular mRNA transcripts enable the identification of expressed genes and their relative levels of expression, thus revealing the transcriptomic state of the cell. Furthermore, copies of the same barcode can be used to bind other sequences of interest, such as molecular tags, oligonucleotide labels encoding for the presence or absence of a desired molecule or spatially encoded localization of the cell. This altogether reveals unprecedent details about the cells in a given population with single-cell resolution.

In the present work we have leveraged this technique to identify the specificity of circulating B cells in a HIV-infected elite-neutralizer over multiple

timepoints of a follow-up study. Recovered specificities were then used to fuel the discovery of novel bNAbs, recapitulating the neutralizing activity seen in the polyclonal serum.

Chapter 2

METHODS

2.1 Patient samples

Patient samples originate from the Protocol C cohort from IAVI, an international cohort of primarily HIV-infected patients followed up for several years. The participants were informed and gave their consent. Details of the ethics statement and approval of the study by several boards are available in [189].

Samples from PC94 were used in the past for initial screening for neutralizing activity, specificity assessment [189] and viral sequencing, as well as for anterior Ab isolation attempts. Remaining samples are listed in **Table 2.1** below. PBMC aliquots were conserved in liquid nitrogen. Each vial contained about 10 x 10^6 cells.

We chose to focus on the latest available samples to isolate potential bNAbs. For this, we used the samples collected at 50, 55, 61 and 73 months post-infection (mpi), corresponding to visits V54, V60, V66 and V78. On the other hand, we were interested in unveiling the origins of such bNAbs. To do so we focused part of our analysis on earlier timepoints. In this approach we selected the samples collected at 17, 22, 28 and 33 months post-infection, that corresponded to visits V18, V24, V30 and V36.

Table 2.1: Follow-up visit timepoints and attended visits

Visit code	V12	V18	V24	V30	V36	V42	V48	V54	V60	V66	V72	V78
Attended	✓	✓	✓	✓	✓	✓	✓	✓	✓	✓		✓
ART	no	no	no	no	no	no	no	no	no	no	no	no
Date	2006-09	2007-03	2007-08	2008-02	2008-07	2009-01	2009-07	2009-12	2010-06	2010-11	-	2011-12
Mpi	-	17	22	28	33	39	44	50	55	61	-	73
Samples	-	3	1	1	1	2	1	1	1	1	-	1

mpi: months post-infection; ART: anti-retroviral therapy

In this study, these two different batches of samples corresponding to different approaches will be referred to as 'early timepoints' (V18, V24, V30 and V36), and 'late timepoints' (V54, V60, V66 and V78).

2.2 Cell lines

Cultured cell lines were used to produce both antibodies and pseudoviruses (PVs) or to perform assays, such as neutralization assays. All human cell lines were cultured at 37°C and with 5 % CO2 atmospheric content.

2.2.1 HEK 293 cells

HEK 293 cells are of human origin and are especially suited for recombinant protein production [124]. The HEK 293T cell line was derived from the HEK 293 culture by transfection with a neomycin resistance gene as well as a viral antigen that provide a favorable environment for viral protein synthesis [98, 270]. These cells are adherent to culture substrate and were passaged twice a week using NaPyr Dulbecco's Modified Eagle Medium (DMEM FisherScientific, Gibco ♯11995065) completed with 10 % FBS, Penicillin, Streptomycin and Glutamine. Cell passage required the use of 0.25 % EDTA Trypsin for 2 to 5 min before inactivation in 3 to 5 volumes of completed DMEM (DMEMc). Cells were then centrifuged for 10 mins at 400 g and resuspended in fresh media at a concentration of 0.5 x 10^6 cells.mL^{-1}. These cells were used for pseudovirus production.

In contrast to the previous cell line, HEK 293F are cultivated in suspension. These cells are best suited for recombinant protein production and were used for antibody and HIV Env trimer synthesis [256]. HEK 293F cells were seeded at a concentration of 0.5 x 10^6 cells.mL^{-1} in 293-FreeStyleTM (ThermoFisher Gibco ♯R79007) medium under agitation (110-120 rpm). Cells can grow up to a density of 3.5 x 10^6 cells.mL^{-1}.

2.2.2 TZM-bl cells

This cell line derives from the HeLa cells. Firstly, JC53 cells were obtained after transfection of the CCR5 HIV co-receptor in CD4 positive clones, thus rendering these initial cells permissive to HIV infection [253]. Secondly, these

JC53 cells were further engineered to embark a reporter system for HIV infection [344]. This reporting system is based on the induction of the expression of a firefly luciferase by the HIV-1 long terminal repeat (LTR). These cells are cultivated as an adherent cell line, seeded at a concentration of 0.5 x 10^6 cells.mL^{-1} in DMEMc media. Passaging of the TZM-bl cell line was similar to the HEK293T.

2.3 B single-cell sorting, sequencing and analysis

We used the 10X-Genomics Chromium kit to perform single-cell analysis of the anti-HIV Env antibody repertoire. In a nutshell, experimental design was as follows: we produced recombinant HIV Env trimer baits corresponding to several wild-type or mutated viral strains encompassing six different clades, and further biotinylated these constructs. The biotin allowed us to bind non-specific fluorescent labels and unique oligonucleotide barcodes to each recombinant bait. Biotinylated baits were used in a FACS-based sort to enrich the PBMC fraction in either naïve B cells, memory B cells, or antigen-specific B cells. Once sorted in bulk, cells of interest were single-cell sorted using the 10X-Genomics Chromium pipeline. After single-cell separation, cDNA synthesis and library preparation, recovered material was sequenced to obtain both transcriptome information with single-cell resolution, paired heavy- and light-chains for BCR/antibodies and external features such as antigenicity, sample barcodes, and cell-surface markers. This general experimental design is illustrated in **Figure 2.1**.

2.3.1 HIV Env baits preparation and validation

HIV-1 Env sequences selection

Sequences coding for the *env* gene from nine heterologous HIV strains belonging to four different clades were retrieved, modified and inserted into a suitable vector to make natively-conformed soluble trimers. These sequences corresponded to those of PVs neutralized by the serum of PC94 [274, 275]. For five sequences out of nine, our colleagues isolated mAbs capable of neutralization. Selected strains are detailed in **Table 2.2**. Two sequences corresponded to clade A viruses, two belonged to the clade AE, three to the clade B and two to the clade C. No clade D heterologous viral sequence was used as autologous PVs belonged to this clade. All these heterologous sequences corresponded

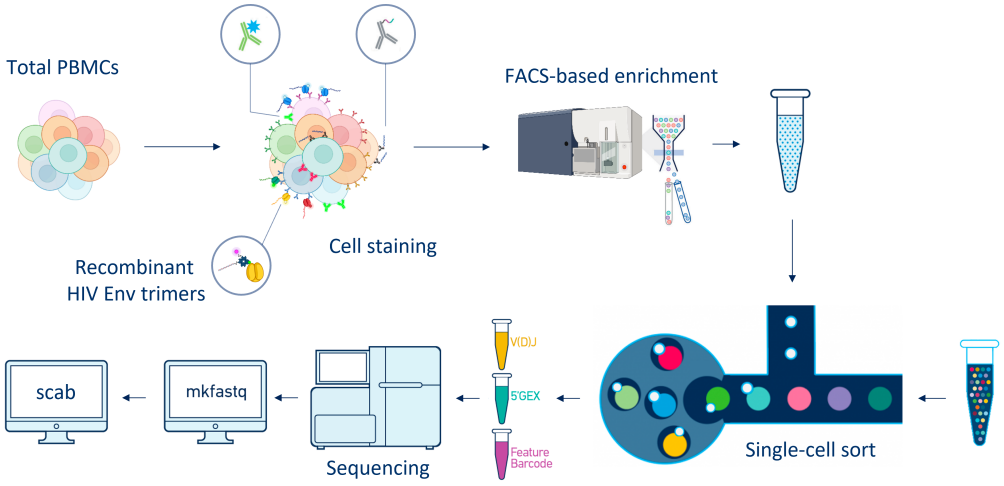

Figure 2.1. Overall experimental design used for single B cell isolation. Cells from total PBMCs were stained with barcode- and fluorochrome-labelled recombinant HIV-1 Env trimers and enriched for different cell fractions by FACS. Obtained cells were then single-cell sorted before library preparation allowed sequencing. Downstream analysis required an important bioinformatic deconvolution using several software programs, among which *scab* was developed in the lab. PBMC: Peripheral Blood Mononuclear Cell

to tier 2 or 3 viruses. Neutralization of the corresponding PVs by the serum of PC94 ranged from 1:495 to $\geq$1:3200 and the sera showing most potent neutralization were collected from timepoints ranging from 39 to 73 mpi. In contrast, mAbs previously isolated from PC94 were only able to neutralize five out of nine PVs when tested against the corresponding PVs. The mAbs exhibiting the best IC_{50}s for each of these PVs were isolated from timepoints corresponding to 33 or 31 mpi exclusively.

Concerning autologous viruses, we selected five *env* sequences to express corresponding trimers. These sequences are listed in **Table 2.2**. They corresponded to viruses isolated from samples obtained at visits V12, V18, V48, V60 and V78 of the follow-up. These sequences were selected for their timely distribution across infection. We used neutralization data from previously isolated mAbs [274, 275] to selected sequences for which neutralization was achieved at a great potency (PC94 v12 c007 and PC94 v18 c046) as well as sequences for which neutralization of corresponding PVs was low (PC94 v48 c028) or almost nonexistent (PC94 v60 c037 and PC94 v78 c040).

Table 2.2: Selected HIV-1 Env sequences for bait production and previously isolated neutralizing mAbs

Origin	Virus name	Clade	Tier	Best Serum IC_{50}	Best serum visit code	Best mAb IC_{50}	mAb visit code	mAb lineage	Neutralization by other lineages
Heterologous	BG505 WT	A	2	1:495	V48	0.0289	V66	C	Lineages A and B neutralize
	BG505 T332N	A	2	1:3988	V66	*None*	∅	∅	No mAbs isolated
	CNE55	AE	2	≥1:3200	V54, V78	*None*	∅	∅	No mAbs isolated
	CNE8	AE	2 or 3	≥1:3200	V78	*None*	∅	∅	No mAbs isolated
	92BR020	B	2	1:3010	V60	0.0574	V36	A	Lineages B and C neutralize
	JRCSF	B	2	1:2070	V48	0.9262	V66	A	Lineages B and C do not neutralize
	JRFL	B	3	1:2321	V66	0.0683	V66	C	Lineages A and B do not neutralize
	IAVI c22	C	2	1:2872	V42	0.5964	V36	A	Lineages B and C do not neutralize
	CE0217	C	?	≥1:3200	V78	*None*	∅	∅	No mAbs isolated
Autologous	PC94 V12 c007	D	?			0.01	V48, V60	A, B	Lineage C neutralizes
	PC94 V24 c046	D	?			0.21	V48, V60	A	Lineage B and C neutralize
	PC94 V48 c028	D	?			2.22	V60	B	Lineage A does not neutralize
	PC94 V60 c037	D	?			28.44	V60	B	Lineages A, C and D do not neutralize
	PC94 V78 c040	D	?			20.71	V78	D	Lineages A, B and C do not neutralize

mAb: monoclonal antibody, IC_{50}: Inhibitory Concentration 50%, ID_{50}: Inhibitory Dilution 50%, IC_{50} are expressed in $\mu g.mL^{-1}$

HIV-1 Env trimer expression platform

We chose to use the disulfide substitution (DS) chimera platform for HIV Env soluble trimer production as it was suggested to result in reduced binding to non-NAbs targeting the V3 and CD4bs [187]. DS-chimeras were constructed using gp120 elements of the virus of interest and a modified version of the gp41 subunit derived from the original BG505 SOSIP.664 construction to serve as a scaffold, as per described in [162]. In this particular construct, the SOSIP.6R.664 design previously described is used as a supporting system to accommodate the central part of the gp120 subunit. N- and C-terminal

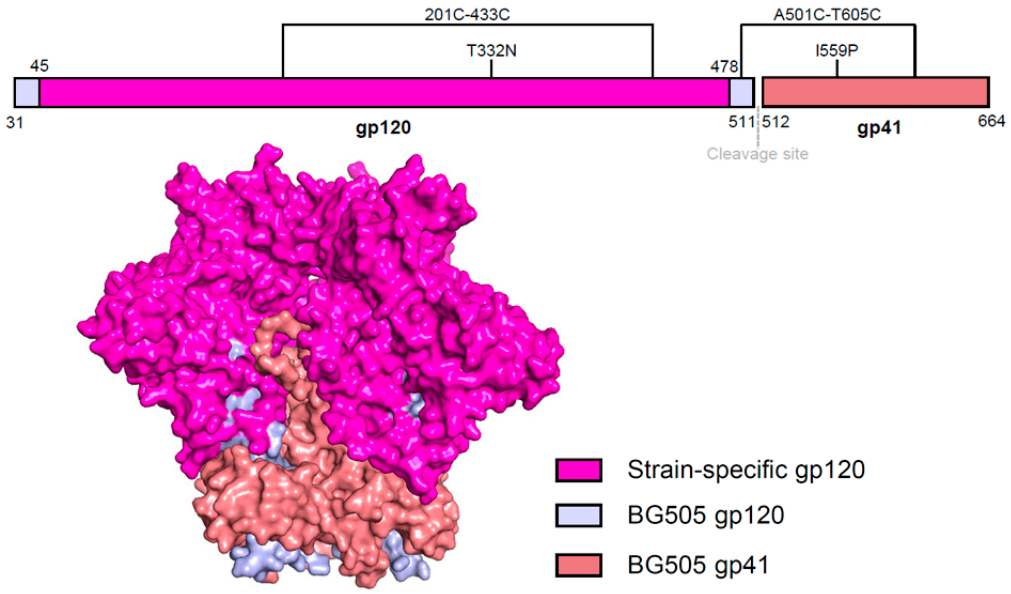

Figure 2.2. Elements from BG505.SOSIP.664 (light red and light blue) and strain-specific gp120 (pink) concur to form DS-Chimera stabilized trimers (adapted from [162]). The DS-Chimera platform makes use of two supplementary cystein residues to form an additional pre-fusion conformation stabilizing disulfide bond.

sequences from BG505 gp120 are retained to help stabilize the trimer. Furthermore, prefusion-stabilizing mutations 201C and 433C (DS) are incorporated as shown in **Figure 2.2**. No further modifications were introduced in the construct described by [162].

HIV-1 Env trimer production

Trimer production followed up the steps shown at **Figure 2.3**. Details of each step are provided in the following paragraphs.

DNA design and synthesis Selected sequences corresponding to heterologous Env proteins were retrieved from the HIV Sequence Database from Los Alamos National Laboratory (HIV Sequence Database). Autologous *env* sequences were obtained previously by our group using a single-genome sequencing (SGS) approach in plasma samples and performed by Monogram (San Francisco, CA, USA). In-silico sequence manipulations were performed using the Geneious software (Boston, MA, USA). An AVI-Tag sequence was added to the C-terminal portion of the protein to allow for subsequent biotinylation. Chimeric sequences were then synthesized by GenScript (Pis-

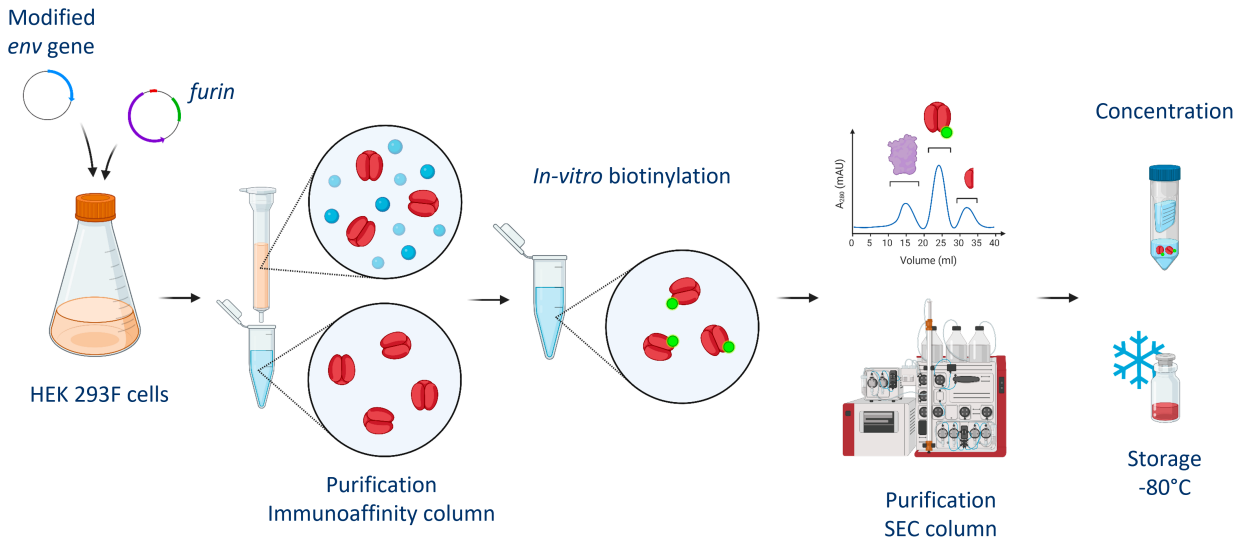

Figure 2.3. Schematic view of the HIV Env trimer production process. Trimers are obtained by the co-transfection of dedicated plasmids containing the *env* modified gene with furin-encoding plasmids. The initial purification is achieved by means of immunoaffinity columns. After enzymatic biotinylation, trimers are further purified on a SEC before final concentration. Trimers are shown in red. Biotin is depicted as green spheres. SEC: Size-exclusion chromatography

cataway, NJ, USA). DNA plasmids were transformed in DH-5αcells for amplification and purified using the NucleoBond PC 10000 EF giga prep kit (Macherey-Nagel, ♯740548). Final DNA concentrations were measured using a NanoDrop One instrument, sequences were verified by Sanger sequencing (Eton Biosciences, San Diego, CA, USA) and plasmids were stored at -20°C for future transfections.

Trimer protein production The selected HIV Env trimers were produced by the co-transfection of one of the obtained DS-chimera DNA plasmids (**Figure 2.4**) with a second plasmid encoding the Furin protease. The produced Furin allowed for physiologic cleavage of the trimers and helped render the tridimensional structure close to the native configuration. Transfection was performed as follow: 350 µg of DS-chimera DNA was mixed with 150 µg of Furin DNA and filtered through a 0.22 µm filter in 25 mL OptiMEM media. In a separate tube, lab-made PEI 40K was incubated for 5 min at room temperature (RT) in 25 mL OptiMEM media. After incubation, separate tubes were mixed and further incubated for 25 min at RT. Finally, DNA

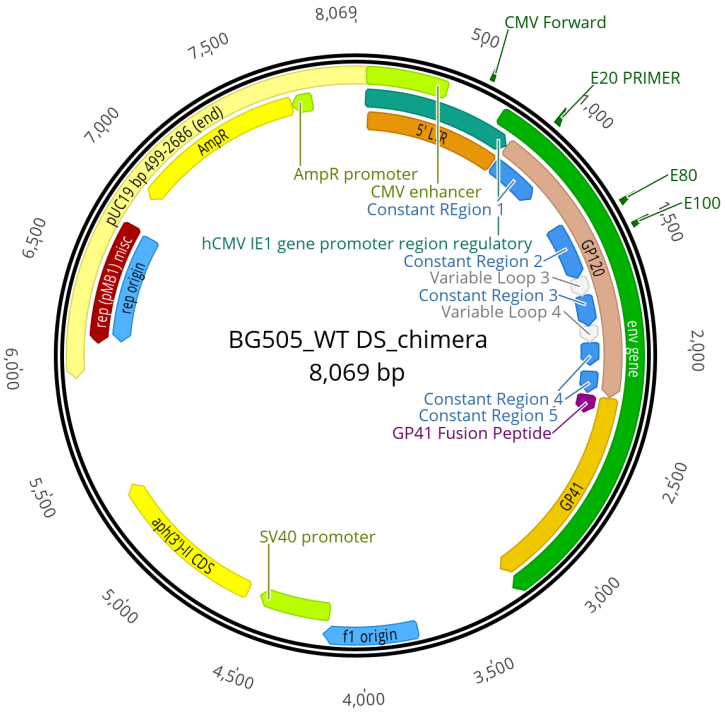

Figure 2.4. Plasmid map for one of DS-chimera construct used (BG505 WT). Resistance gene for selection is shown (AmpR). Produced with Geneious Prime 2023.01

and transfectant mix was added to 1 L HEK 293F cells in suspension at 1.2 x 10^6 cells.mL^{-1} with at least 50% fresh media. Cells and supernatant were harvested at day five.

Trimer bait purification (1/2) On harvest day, cells were collected and spun down. Cells were centrifuged a first time at low speeds (80-150 g) for 10 min to remove live cells, followed by a subsequent centrifugation at higher speeds (2000-3000 g) for 20 min to eliminate any remaining cell debris. Supernatant was filtered using a vacuum-driven 0.22 µm filter with a 500 mL bottle-top vacuum filter. Trimer purification was performed on lab-made immunoaffinity columns using a conformational antibody directed against the V2-apex supersite of the Env protein: PGT145 [78]. Prior to this, we verified that selected Env sequences corresponded to viruses neutralized by PGT145. Immunoaffinity columns were made as usually performed in our lab. Before adding supernatant, columns were rinsed with 100 mL of 1X cold TBS. Super-

natant was then loaded onto the column at slow flow speed (0.5-1 mL.min^{-1}) at 4°C. After loading, the columns were washed with 200 mL of 1X cold TBS and 50 mL of cold TN75 (TrisHCl, 0.75 mM NaCl at pH = 8). Elution was achieved with 50 mL of 3M MgCl, 20 mM TrisHCl at pH = 7.2 (elution buffer) into the same volume of 20 mM TN75 solution at 4°C. Finally, purified trimers were concentrated in 100K Amicon ultra-centrifugal filters at 4°C and buffer-exchanged into a TBS 1X solution. Subsequent biotinylation steps were performed immediately to avoid trimer degradation.

Trimer bait biotinylation Biotinylation of the HIV Env trimers was performed using the BirA500 dedicated kit (Avidity) following the manufacturer's instructions. In a nutshell, recombinant proteins were brought to an initial concentration of 40 µM maximum, and reagents (BioMix A and B, BirA enzyme and free biotin) were added to the purified protein. Reaction was left to happen overnight at 4°C and under slow agitation. Final purification was performed without delay on the following day.

Trimer bait purification 2/2 HIV Env trimers were retrieved and set to final purification step on a size exclusion chromatography column to eliminate the unwanted BirA enzyme from biotinylation step. This procedure also helped in separating monomeric and dimeric HIV Env complexes from actual trimers. Freshly biotinylated trimers were injected into a SuperDex200 (GE Healthcare) column at a flow rate of 0.5 mL.min^{-1} and 500 µL fractions were collected. Properly folded trimers passed through the column first, exiting the filtering bed in around one column volume. Peak absorbance of the trimer-filled fraction was observed at 20.4 mL. Fractions of interest were collected and pooled. Purified biotinylated trimers were buffer-exchanged to 1X TBS and concentrated to approximately 1 mg.mL^{-1} using small centrifugal filter units. Purified trimers were aliquoted in small 10 µL fractions and immediately stored at -80°C.

Quality control of trimer baits

We tested these trimers before using them as baits to recover HIV Env-specific antibodies. We conducted three different assessments of the purified trimers to confirm their antigenic profile, their folding state, and their potential polyreactivity to human PBMCs from uninfected individuals. Biotinyla-

tion was also controlled prior to this, hence confirming the correct binding to biotin on the purpose-designed AVI-Tag.

Antigenic profiling We evaluated the antigenicity of the obtained trimers by measuring binding responses to various antibodies with known neutralizing abilities using the biolayer interferometry (BLI) technique. Using a Sartorius Octet analyzer, we loaded the trimers on individual streptavidin-coated probes (Sartorius, ♯18-5019) and measured the association (binding) and dissociation kinetics of selected antibodies. These antibodies were selected to test for specific features of the HIV Env trimer and to confirm their correct folding and expected antigenic profile. Antibodies used in these experiments encompassed the following: F105 is an anti-monomeric-gp120 and was used to distinguish the presence of monomers from trimers. Anti-DEN3 targets an epitope from the Dengue virus subtype 3; it served as a negative control in our experiments. NC-Cow1 and VRC01 are directed towards the CD4bs and checked for the correct availability of this epitope. PG16 and PGT145 controlled the V2-apex region of the trimer, also confirming the close conformation of the constructs for PGT145 as it has a quaternary epitope. Other HIV Env supersites were probed with PGT121 and PGT128 for the V3-region, PGT151 for the gp41:gp120 interface site and 4E10 for the MPER region. All these antibodies were locally provided by collaborators or purposedly produced and purified (See below "Antibody production" section). Kinetic response was evaluated individually for each trimer/antibody pair and compared with neutralization data available from the CATNAP database [364].
The previously obtained trimers were extensively tested to confirm their antigenicity against these Abs. An example of obtained results is shown in the **Figure 2.5**. This evaluation examined whether the expected epitopes are present in the selected HIV Env trimers, and whether these epitopes exhibited a correct tridimensional structure. Furthermore, mAbs targeting the quaternary structure of the trimers were used to confirm the close conformation of the trimers. All batches of expressed trimers were individually tested for their antigenicity as displayed above. When the antigenic responses (binding kinetic) observed in BLI differed substantially from the expected results for a given trimer, the corresponding batch was discarded and removed from any further use. Overall, at least one batch of each construct matched the expected results and was retained for further use. Subsequently, we proceeded

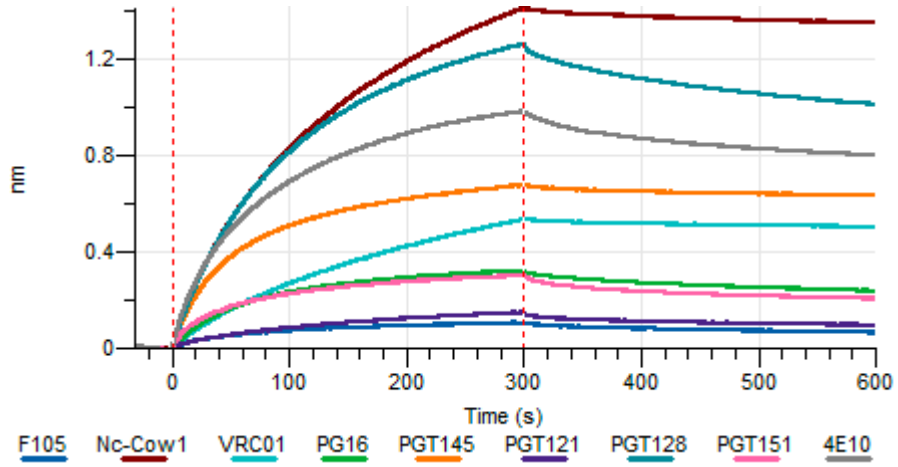

Figure 2.5. Binding and release kinetic profiles of several antibodies against one HIV Env trimer obtained in biolayer interferometry (BLI) experiments. Trimers were bound to streptavidin-coated probes and tested antibodies were in solution.

with a structural analysis of these trimers to probe for the presence of dimeric and monomeric forms.

Electron microscopy Conformational stability of HIV Env trimeric constructs was validated by acquisition of structural data. We conducted negative staining followed by single-molecule acquisition using an electron microscope. Multiple micrographs were obtained from different areas of the grid to ensure representative sampling and obtention of correct orientations for all tested trimers. In total, around 10,000 [7213; 14115] single-molecule micrographs were examined per trimer and classified. Proportions of well folded, native-like trimers were evaluated on small-scale large micrographs and from higher resolution individual micrographs of single-molecule trimers. The proportion of fully-folded trimers, as well as the proportion of monomeric and dimeric forms was calculated. Batches of expressed baits that exhibited more than 1.0% monomeric or dimeric forms were excluded. Only trimers harboring $\geq$99.0% of correctly conformed molecules were subsequently used for antigen-positive B cell enrichment in the following experiments. While trimers can exhibit a correct conformation at a given instant, the degradation rate can be significantly elevated allowing for open-conformations [234] and hypo-oligomerized forms to appear. To balance this effect, trimers were kept at room temperature for a few hours before image acquisition.
An example of the obtained results is displayed below in **Figure 2.6**. Native-

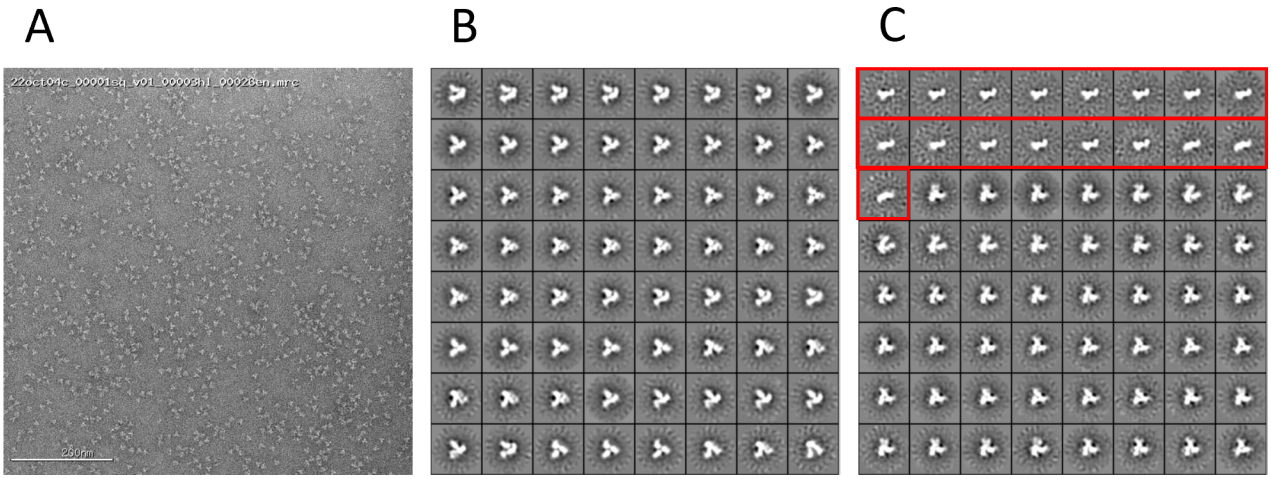

Figure 2.6. Negative-stain electron microscopy images of HIV Env recombinant proteins. **A.** Low resolution micrograph showing trimers in different orientations, **B.** high-resolution single-molecule images of a well-conformed trimer, and **C.** of an unstable construct (73% trimers, 27% dimers)

like trimeric shapes (B) are easily distinguished from monomers or dimers (C) in single-molecule images. At least one batch of trimers matched the criterion fixed for all twelve expressed trimers.

In open conformations and hypo-oligomerized forms, inner sides of the gp120 monomers are displayed and accessible for immune recognition. Consequently, we decided to perform a last evaluation on the remaining trimers to verify their polyreactivity against human PBMCs from uninfected individuals.

Testing trimer polyreactivity in healthy patient PBMCs Correctly folded trimers with accurate antigenic profiles were tested against healthy human PBMCs to ensure the absence of abnormal stickiness. Each trimer was used twice, labeled with alternatively one of the two fluorescent probes: PE or APC. Human PBMCs from healthy subjects (StemCell, ♯70025, lot n° D326651) were stained using the same experimental procedure as described below for mAbs isolation. Cell-surface markers are presented in **Table 2.3**.

Cell population determination and signal acquisition was performed utilizing a BD FACS-Melody cell sorter. Gating was set to isolate in this order, and from all events: the lymphocyte population (SSC-W vs SSC-H), the single-cell droplets (FSC-W vs FSC-H), the live cells BV510- (SSC-A vs BV510), the B cells $CD3^-$ $CD14^-$ $CD19^+$ and quantifying for double-positivity (APC

Table 2.3: Cell surface markers and FACS antibodies

Marker	Origin	Fluorophore	Reference	Clone
Live/dead		BV510	Brilliant Violet	
CD3	mouse anti-human	APC-Cyanine-7	BD Pharmingen, ♯557757	SP34-2
CD14	mouse anti-human	APC-H7	BD Pharmingen, ♯561384	M5E2
CD19	mouse anti-human	PerCP-Cyanine-5.5	BD Pharmingen, ♯561295	HIB19
Bait ♯1	in-house	PE	BioLegend, ♯405245	
Bait ♯2	in-house	APC	BioLegend, ♯405207	

vs PE) to baits. Threshold for antigen positivity was set at 10^3 arbitrary units (**Figure 2.7**). Flow rate was adapted to match an event rate of between 250-500 events per second.

In the present example, lymphocytes represented about 20.0% of the total PBMCs, within the physiologic and expected range [241]. B cells totalized about 26.4% of these lymphocytes (5.28% of all cells). Among these B cells, less than 0.1% were positive for both PE- and APC-labelled autologous trimer PC94 v18 c046. These results suggested the lack of unspecific binding between this construct and B cells from a healthy uninfected donor, hence confirming that this particular batch of trimers was amenable for specific Ab isolation. Overall, this allowed us to confirm the absence of polyreactive and unspecific binding for all constructs.

Conclusion on bait preparation and validation

Altogether, twelve trimers were produced, purified and verified. Among them, four trimers corresponded to autologous viruses, and eight corresponded to heterologous viruses. A list of these trimers is shown in **Figure 2.8**. Additionally, the region surrounding the PNGS in position 332 (HxB2 numbering, highlighted in yellow) is shown for the corresponding trimers. The heterologous trimer 92BR020 could never be expressed despite multiple attempts. We observed the same issues with the autologous trimer PC94 v60 c037. In both cases no explanation was found for the absence of production.

At the 5' side of the 332 PNGS we can notice the presence of a motif widely shared across trimers: the $_{324}$[**GDIR**]$_{327}$ motif. It was demonstrated that this motif is part of the V3 epitope and contains essential contact residues for some bNAbs [307, 16, 186]. In our case, 9 sequences out of 12 bear the aspartic

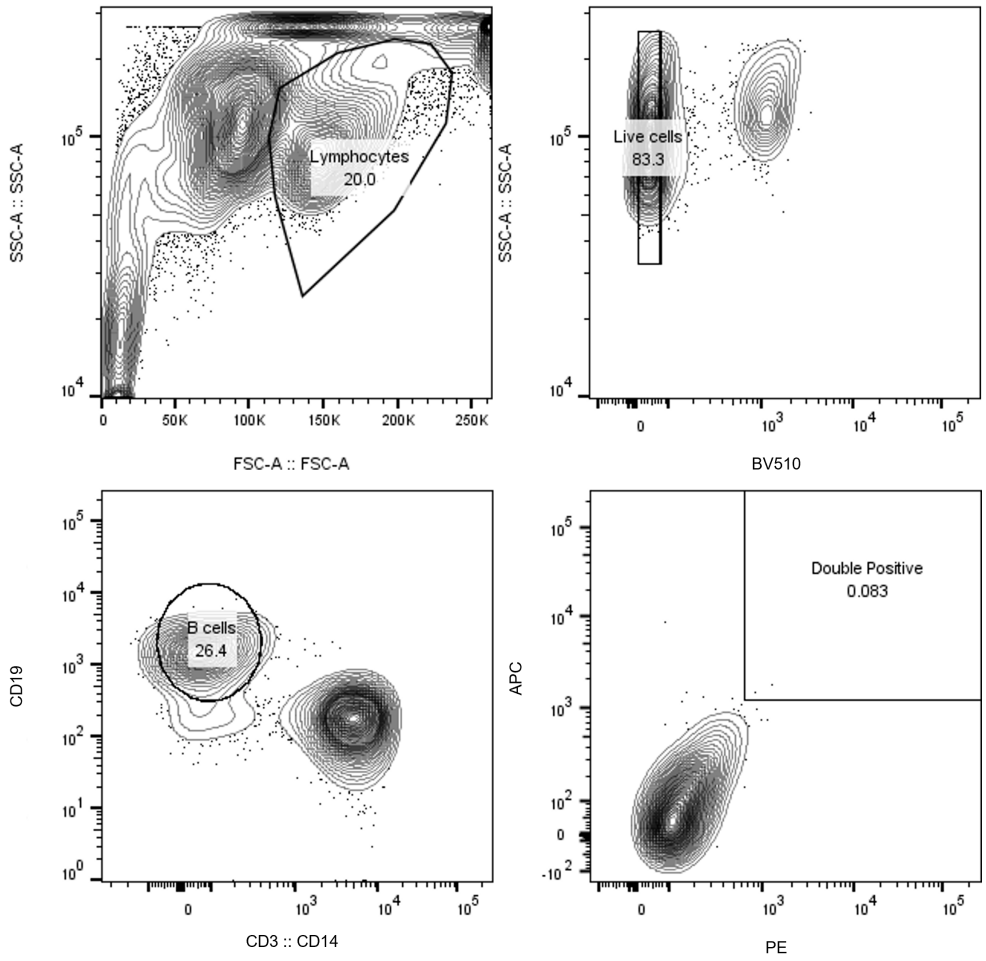

Figure 2.7. FACS gating parameters for healthy human PBMC sort. In this example, the trimer used as a bait displayed the HIV Env sequence of autologous PC94 v18 c046 virus. FACS: fluorescence-activated cell sorting, PBMC: peripheral blood mononuclear cells, SSC: side-scatter, FCS: forward-scatter.

acid (D) in position 325, while three of the autologous sequences had this residue replaced with an asparagine (N), thus potentially impairing potential bNAb access to these residues. To be noted, two of these constructs displayed a PNGS in position 334: CNE8 and PC94 v78 c040. For the sequences corresponding to the autologous virus, this may be the hallmark of an escape mechanism, as this latter construct corresponds to a virus isolated 6.5 years after infection and for which no isolated mAb showed neutralization.

gp120 strain	Clade	Tier	332 N-glycosylation site
BG505 WT	A	2	
BG505 T33N	A	2	
CE0217	C	2	
CNE8	AE	2 or 3	
CNE55	AE	2	
IAVI c22	C	2	
JRCSF	B	2	
JRFL	B	2	
PC94 v12 c007	D	#N/A	
PC94 v18 c046	D	#N/A	
PC94 v48 c028	D	#N/A	
PC94 v78 c040	D	#N/A	

Figure 2.8. Definitive list of trimers produced and used as baits for antibody isolation. Corresponding clades and tiers are shown, along with amino acids surrounding position 332 highlighted in yellow (HxB2 numbering)

2.3.2 FACS enrichment, single-cell B-lymphocyte sequencing and analysis

This procedure was previously described and used in our lab [152]. Samples from PC94 were recovered from long-term liquid nitrogen (-196°C) storage at IAVI's Neutralizing Antibody Center (NAC). To ensure cross-contamination, separate batches were processed on separate days. Retrieved PBMCs were placed on ice. Cells containing infectious material were manipulated in a suitable BSL2 facility. Once thawed, cells were placed in 10 mL pre-warmed RPMI supplemented with 50% FBS at +37°C. Cells were subsequently pelleted at 400 g for 5 mins and the supernatant was discarded to remove all traces of DMSO. Cells were resuspended in 5 mL FACS buffer and counted while spun down with the same setting. Supernatant was discarded and pelleted cells were readily available for staining.

FACS enrichment

HIV Env trimer labelling Prepared HIV Env trimers were used as baits to allow for specific antibody recovery. Baits were labelled with unspecific fluorochromes and unique oligonucleotide barcodes, enabling bait recognition through sequencing. Pre-assembled labels from BioLengend TotalSeq product line were used. Baits were separately labelled with one out of the two fluorochromes described above: PE and APC. PE-streptavidin tags belonged to the BioLegend TotalSeq-C series (♯C0961 to ♯C0970), as well as the APC ones (♯C0956 to ♯C0960; ♯C0971 to ♯C0980). Nine microliters of each bait at a concentration of 1000 µg.mL^{-1} were conjugated with 2.2 µL of corresponding TotalSeq-C labelling reagent and incubated for 30 min on ice and in the dark. Free biotin (Avidity BIO200, ♯E1122) was added (5 µL) after labelling to quench remaining biotin-free streptavidin sites and prevent bait aggregation.

PBMC staining A staining master mix was prepared extemporaneously as follows: HIV Env trimers (baits) were pooled using 2.5 µL of each per 10 million PBMC to stain. Cell hashtags were used for sample demultiplexing in downstream analysis of 'early timepoint' samples only, and in this case, these were added at this step. Those were BioLegend TotalSeq reagents (BioLegend, ♯C0251 to ♯C0258), used at a concentration of 500 µg.mL^{-1} and with a volume of 2.5 µL per 10 x 10^6 PBMCs. Fluorescent-labelled cell-surface markers were added to the master mix: 1.25 µL of each fluorochrome was added for each 10 x 10^6 cells to stain. Cells were stained with this master mix for 30 mins on ice and in the dark. Meanwhile, a working solution of live/dead stain was prepared from stock (1:300 dilution in sort buffer). After an initial 15-minute staining, live/dead stain was added to the cells. At the end of the 30 min incubation period, 10 mL of sort buffer were added to the cells and spun down for 5 min at 400 g to wash out unbound labels and markers. A second, identical washing step was performed, and, after removing the supernatant, cells were resuspended in 500 µL of sort buffer per 20 x 10^6 cells. When using cell hashes, cells from separate samples were pooled at this stage. Finally, samples were filtered twice using mesh caps from FACS tubes and stored on ice in the dark until sorting. In addition to the previously described cell-surface markers, a mouse anti-human CD27 was used in sorts concerning the 'early timepoint' samples, paired with the FITC fluorochrome reporter (BioLegend, ♯B358854, clone n°O323), and prepared in the same conditions as other markers.

FACS enrichment During cell staining and the incubation period, the FACS instrument was set up and calibrated. Tight timing in these steps revealed to be crucial for high cell recovery rates in the 10X-Genomics single-cell downstream analysis. A BD FACSMelody sorter was used in all our experiments. Due to the infectious nature of the sorted samples, the setting included working under a BSL2 biosafety cabinet during all the procedure. The calibration process included calibration of flow with BD FACS CS&T beads (lot n°1182462) and BD FACS Acudrop beads (lot n°2073806). For beads, voltages were set up at 90 mV for both FSC and SSC measures. When sorting lymphocytes, voltages were adjusted to 75 mV for the FSC output and 135 mV for the SSC parameter to account for cell size. After calibration and before attempting any sort, fluorochrome compensation was performed using staining markers individually as per local standard operative procedures.
Samples were sorted individually for 'late timepoint samples' or pooled for 'early timepoint' samples, using sample hashtags. Cell populations of interest were sorted in bulk into 96-well plates. About 25,000 cells were sorted in each well to avoid sample overflow. To enhance cell survival, the wells were pre-coated with FBS. Two hundred microliters of sterile FBS were added to the wells and incubated for between 10 to 30 minutes. FBS was then aspirated and fresh FBS (20 µL) was added to the bottom of the well to accommodate sorted cells. Finally, to speed up the sorting process and allow for better recovery rates, sorting was set up in "yield" mode, instead of the traditional "purity" mode). This enabled a higher event rate at the expense of false positive detections.
In a first experiment, we separately sorted the four timepoints belonging to the 'late timepoints' batch. Vials corresponding to the visit codes V54, V60, V66 and V78 were thawed and stained individually as described. Because these samples were sorted separately, no sample hash tags were added. These cells were sorted for HIV Env double-antigen-positive B cells to ensure specificity of recovered cells. Gating was set as follows: from total cells, we selected the lymphocyte population. After removing dead cells ($BV510^+$), we gated for B cells ($CD19^+$) while eliminating other unwanted cell populations ($CD3^+$, $CD14^+$, $CD19^-$). Finally, cells positive for both PE- and APC-labelled trimers with a threshold of 10^3 arbitrary units were sorted in bulk. This threshold was set deliberately low to minimize the false-negative detection rate. We calculated expected recovered cells to be as many as 25,000 cells per sample

(**Figure 2.9** right).

The samples from earlier timepoints (V18, V24, V30 and V36) were sorted with a different approach. Instead, we leveraged the FACS sorting step to enrich the cell population in B cells, either MBCs or naïve B cells. The samples from visits V18, V24, V30 and V36 were thawed and stained with a similar approach to the previous sort. To decrease sample handling times, we labeled the cells from different samples with sample hashtags, pooled the cells, and proceeded with FACS sorting. This sorting procedure was completed in a two-step fashion (**Figure 2.9 left**).

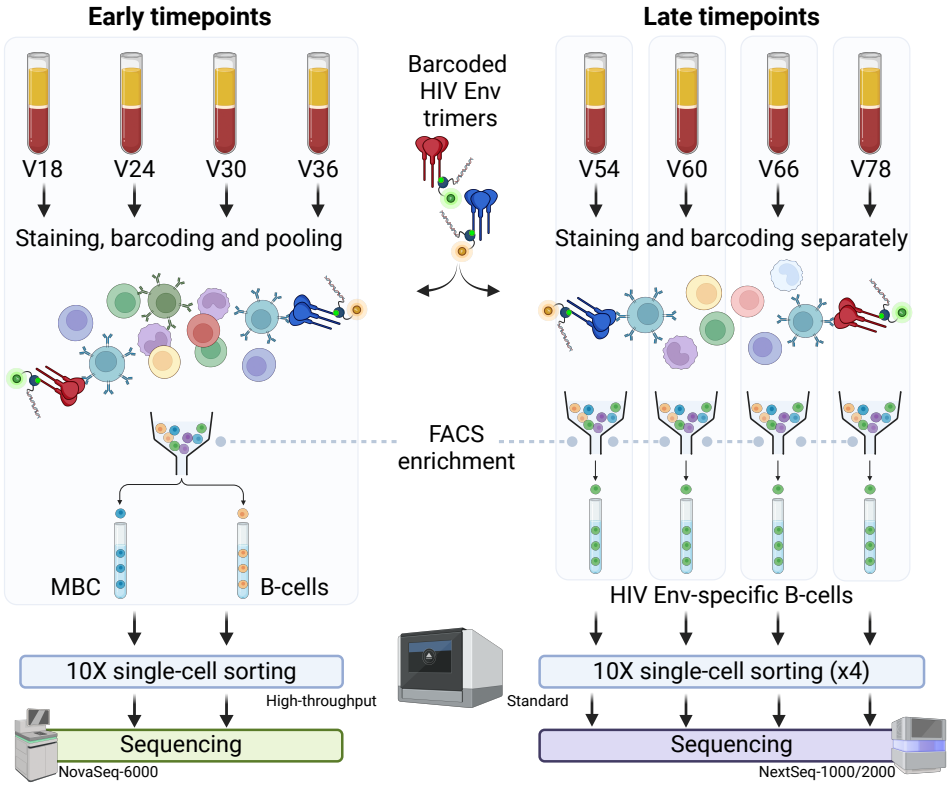

Figure 2.9. Detailed experimental procedures. Early timepoint samples and late timepoint samples were processed differently. Early timepoint samples were barcoded and pooled before enrichment for MBCs first and total B cells. Late timepoint samples were barcoded and sorted separately for antigen positive cells. MBC: memory B cells

First, we sorted memory B cells, regardless of their antigen specificity. Gating was set up to select for lymphocytes, live cells ($BV510^-$), B cells ($CD3^-$

$CD4^-$ $CD19^+$) and those harboring the cell surface marker specific to the memory compartment ($CD27^+$). We expected to sort around 200,000 memory B cells with this agnostic approach before switching to the second phase of our sort.
The second step aimed at completing the present sort with a broader sampling of the B cell population. The gating for the memory B cell specific surface marker ($CD27^+$) was removed and B cells from all sub-populations (naïve B cells, activated B cells, PCs, MBCs, ...) were sorted in bulk in separate wells. During this second phase we aimed at sorting 200,000 cells in addition to the previous contingent (**Figure 2.9 left**).

Single-cell sorting

After samples had been enriched for desired cell populations, we proceeded with the single-cell sort. We used the single-cell immune profiling kit (10X-Genomics, Chromium Next GEM Single Cell 5' v2, ♯1000263) and its high-throughput version (10X-Genomics, Chromium Next GEM Single Cell 5' HT v2, ♯1000356). Single-cell sorting was performed according to the manufacturer's instructions. We collected the FACS-enriched cells in 96-wells plates and cells were loaded onto the corresponding 10X-Genomics chip. Single-cell barcoding was achieved aboard the 10X-Genomics Chromium X instrument. Bead emulsions were recovered and transferred into PCR tubes for cDNA synthesis and library preparation. Reverse transcription for cDNA synthesis was performed on the sorting day. Once DNA had been obtained, samples were conserved at +4°C.

Late timepoints samples (V54, V60, V66 and V78) were barcoded separately using low-throughput (standard) kits and reagents. The four samples were loaded onto four separate lanes from a single chip (Next GEM Chip K, ♯2000182, lot n°160506), and emulsions were recovered without delay to proceed with cDNA synthesis. Cells from early timepoint samples (V18, V24, V30 and V36) were separated into 5 wells of a high-throughput chip (Next GEM, Chip N, ♯1000375, lot n°012128). Emulsion creation was only partial and we recovered usable material from 4 out of the 5 wells loaded. Pellet concentration after clean-up ranged from [342; 2152] $pg.\mu L^{-1}$ in the four usable wells. The 4 wells corresponded to the two enriched cell populations: memory B cells ($CD27^+$) on one side and bulk B cells on the other (**Figure 2.9**).

Library preparation followed up the manufacturer's instructions. All three libraries, for gene expression monitoring (GEX), BCR/antibody chains recovery (VDJ), and antigen specificity and cell surface markers sequencing (FBC, for Feature BarCodes) were used and prepared. Quantification of libraries during purification steps was done either with the 2100 BioAnalyzer instrument (Agilent, ♯G2939BA) using High Sensitivity DNA Assays chips, or with the 4200 TapeStation instrument (Agilent, ♯G2991A) and corresponding chips, depending on the availability of analyzers. The GEX library only encompasses short reads of each gene beside barcodes and is, therefore, a relatively small library in fragment length. The typical size is expected to peak around 400 bp. Conversely, the FBC library solely contains barcodes, which are between 10 to 30 bp. Final library size peaks at about 220 bp. The biggest library is the VDJ library, which contains the sequence of the variable part of immunoglobulins. Size of fragments is separated into two different peaks (one for the light chains, one for the heavy chains), both comprised between 650 and 750 bp. Final quantifications for pooling and loading on the sequencer were done using the Qubit 30 Fluorometer (Life Technologies, ♯Q33238).

Sequencing

Sequencing reagents were prepared according to Illumina's recommendations. Specifically, PhiX reagent was added as per protocol to ensure heterogeneity of the sequences and higher quality of reads. Sequencing was performed using Illumina's short-read technology. The NovaSeq-6000 was used for 'early timepoint' samples and the NextSeq-1000/2000 instruments were used to deliver DNA sequences from prepared 'late timepoint' samples. The sequencing depth – and therefore sequencing flow cells – depended on the desired output. Recovery of paired heavy- and light-chains for BCR/antibodies typically requires about 5,000 reads per cell (VDJ library). Another 5,000 reads per cells are usually necessary for the FBC library. Transcriptome exploration, making use of the GEX library, requires the most sequencing depth, with as many as 20,000 reads per cell. For instance, sequencing depth for information recovery and correct interpretation for 50,000 cells would require about 150,000,000 reads.

To achieve such sequencing depth, we made use of Illumina's S4 flow-cells. Those are the most powerful flow-cells on their higher-end sequencer. Sequenc-

ing was achieved using the chemistry 1.5 of these flow-cells with a 2 x 150 bp cycle capacity, programmed as follow: 26-10-10-90, corresponding to cell barcodes and UMIs, i7 sample indexes, i5 sample indexes, and insert, respectively. Sequencing data was automatically uploaded to the Illumina BaseSpace tool, from which downstream computational analysis took place. Libraries corresponding to 'late timepoints' samples were sequenced aboard the Illumina NextSeq-1000/2000 machine using a P2 100 cycles flow cell (♯20027770, lot n° 20490244), whereas libraries coming from early timepoints samples were sequenced on an Illumina NovaSeq-6000 instrument upon loading on an S4 flow cell (♯20015843, lot n° 20657719) with chemistry v1.5 reagents allowing for 200 cycles. Upon sequencing, this second run generated 1.52 Tbp with high quality reads: 96.1% of reads had a Phred score above Q30.

2.3.3 Bioinformatic analysis

Due to the consequent size of data files, non-trivial computational power was used for the following workflow. The initial process of data handling can be recapitulated here: raw data was acquired and primary analysis (basecalling and FASTQ preparation) was performed. The next step consisted in the secondary analysis, with scRNA-seq specificities: this encompassed the demultiplexing of both samples and single-cell information as well as the gene counting process. Finally, tertiary analysis consisting of both quality assessment and scientific analysis of refined data was achieved. A table of all software and scripts used is available in the Supplementary Data (See **Table 6.1**).
Considerable part of my work here was undertaken in the laboratory of Dr Bryan Briney (Scripps Research), who has specialized in these bioinformatic questions.

Data preprocessing

Data preprocessing took place on a lab-hosted server using custom-tailored scripts for initial steps. Base calling and FASTQ file generation were performed by the 10X-Genomics dedicated tool **cellranger** (GitHub: cellranger). This tool wraps the Illumina core engine **bcl2fastq** script to process the raw sequencing data. After FASTQ files are generated, cellranger performs the demultiplexing and gene counting steps, generating three main files for subsequent use:

- Filtered barcode counts are readily available in a dedicated file organizing gene counts for each single cell from the processed sample;

- Reconstructed contigs are collected in a FASTA file mainly containing the VDJ sequences from BCR/antibodies of interest;

- An annotation file is generated containing the antigen specificities and eventual cell-surface markers or sample hashtags in a comma-separated value (*.csv*) form.

Automation of this process was made possible thanks to a custom command line interface wrapper termed **scabranger**, thus allowing for flawless end-to-end processing of the raw sequencing data. The scabranger tool is readily available within the **scab** package (GitHub: scab) used for single-cell data consolidation, manipulation and binning, as described in previous work from our lab [152].

Demultiplexing the gene counts and barcodes for different features was performed using **scab**. To do so, thresholds for each barcode were individually optimized to find the best threshold. An example of this threshold is shown in **Figure 2.10**. Briefly, UMI counts for all cells were jointly analyzed for each bait. The optimal cut-off threshold to distinguish between negative and positive cells was obtained by calculating the derivative of Gaussian function that fits the barcode density estimate. The cutoff was then based on the local minima (where the derivative changes sign) of the kernel density estimate (KDE) of the dataset within specified minimum and maximum thresholds.

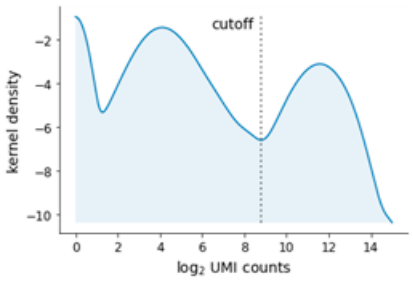

Figure 2.10. Individual cut-off finding was performed using a built-in optimizer for each barcode. UMI: unique molecular identifier

We then filtered this dataset as follows: doublets were removed as they embed two different cells with a single barcode. Cells binding to the negative control (HSA) were subsequently removed. A novel data subset was created to account for the cells that were double-positives (PE- and APC-equivalent) for any of the HIV Env trimer and that contained a single heavy-chain paired with a single light-chain sequence. These double-antigen-positive paired cells were at the base of our approach to select for potential bNAbs. The dataset was termed "HIV Env-specific recovered B cells".

Exploration of the Adaptive Immune Receptor Repertoire

Exploration of the Adaptative Immune Receptor Repertoire (AIRR) has mainly been performed using the following tools: **AbStar** [35] for VDJ gene assignment, **scab** for single-cell data handling and **Clonify** [36] to infer lineages, in line with the AIRR community standards. AbStar assignment of VDJ segments of genes and in silico characterization of antibody sequences relies on **IgBlast** algorithms [362] and IMGT germline sequence repertoire that is also used by IGMT/V-QUEST and IMGT/highV-QUEST tools [195, 196, 215]. We chose to use AbStar over IMGT V-QUEST tools on practical concerns: for the large datasets we worked with, the Ig gene assignment was faster with AbStar. The amplification and sequencing of the BCR/antibody VDJ sequences is performed thanks to primers situated in the 5'-end of the constant part. Those primers sit far enough from the start of the constant region to correctly infer the isotype of the recovered antibody.

To explore B cell specificity, we took two different approaches. A first approach consisted in an agnostic exploration of the dataset. A second approach consisted in a more systematic review and hit ranking upon selected criteria. This systematic review allowed us to select a limited number of B cells to characterize their corresponding neutralization capabilities. We will now review the process that we chose to handpick the BCR sequences that were used for Ab production and purification, and in-depth characterization, from neutralization assays up to structural determination of molecular determinants of HIV Env trimer contacts. Details about the cell transcriptome analysis at population levels with single-cell resolution can be found further down in the present manuscript (See the "Cell population and transcriptome analysis" section below).

Selection of antibody sequences

To isolate bNAbs from the entire repertoire of recovered Ab sequences, we set up an exhaustive sieving algorithm. This allowed us to rank each one of the recovered sequences into priority categories. The first category was designed to group the least Abs but with the highest probability of neutralization, breadth and potency. Conversely, the last category corresponded to sequences with a very low probability of encoding a bNAb. Setting up this ranking approach was an important task in my work and here are details of the resulting algorithm we propose.

These five categories were set up with the following definitions:

- The first category (P1) grouped BCR sequences from B cells that bind multiple baits from both autologous and heterologous viruses, corresponding to multiple clades. This binding to baits had to be observed for both labels (PE- and APC-equivalent labelled baits) and using heightened thresholds for positivity (threshold = 0.999985 percentile). Moreover, these sequences had to be strict pairs: only one single heavy-chain was allowed with a single light-chain

- The second category (P2) encompassed BCR sequences that fulfilled the same criteria described above with one exception: binding to the baits with both labels was not necessary, and cells binding to only the PE- or the APC-equivalent version of the baits could be conserved

- Third and fourth categories (P3 and P4) matched the previously described P1 and P2 groups but relied on a lower threshold for binding assessment (threshold = 0.999000 percentile). P3 grouped cells binding to baits with both labels, and P4 did not have to match this criterion

- Finally, the last pool of BCR sequences (P5) had a negative definition: any of the sequences not falling under any of the other four categories was collected here.

When one BCR was classified in multiple categories, the highest priority (lowest category number) was conserved. Any BCR that showed binding to the negative control (HSA) was immediately set for the least important category (P5).

To complete this approach, we introduced lineage information to the previously described classification. We hypothesized that neutralization would be present in large lineages, with single mAbs having lower probability of harboring strong neutralizing activity. We enriched the fraction of Abs to test with members of large lineages. However, we did not produce and test all members of selected lineages. Conversely, if a single Ab from a large lineage was retained, maybe because other mAb members were tagged as potentially autoreactive (binding to negative control) or not broad enough, relative mAbs were sometimes rescued based on their binding patterns. Furthermore, lineages that were known to be neutralizing from previous sorts were broadly tested regardless of the priority of the mAbs they encompassed.

scRNA-seq: Cell population and transcriptome analysis

Cell population analysis making use of the transcriptomic data available was performed using the **scab** tool [152] mainly. Other tools encompassed the **ScanPy** package [352] used for gene-ranking studies, as well as **citocypher** [10] for cell population cluster assessment and **CellTypist** [89] for automated cell type assignment.

Individual cells were collected and preprocessed using the following parameters: cells with fewer than 200 gene records were eliminated, genes found in less than 41 cells were ruled out. Cellular data in which more than 10% of the reads mapped to the mitochondrial genome were removed as these corresponded to poor quality or apoptotic cells according to 10X Genomics (10X Genomics knowledge base). Dimension reduction was performed using the UMAP algorithm [225] with default settings. Individual cells were grouped into Leiden clusters of cells and manually annotated for cell type according to gene expression of canonical cell surface markers (**Table 2.4**). Monocytes and T-cells were removed for downstream analysis.

B cells and plasma cells were analyzed together. The B cell compartment was devised into naïve B cells and memory B cells based on the differential expression of genes IG_HA1, IG_HG1, IG_HD, IG_HM, but also CD38 and CD27. Further sub-populations could be explored and resting memory B cells were separated from activated memory B cells and transitional B cells.

Table 2.4: Gene markers used for cell population separation

Population	Gene markers
T-cells	$CD3^+$ ($CD4^+$ or $CD8^+$)
Monocytes	$CD14^+$
B cells	$CD19^+$ $CD20^+$
Naïve B cells	$CD19^+$ $CD20^+$ $IGHD^+$
Memory B cells	$CD19^+$ $CD27^+$ $CD38^+$ ($IGHA1^+$ or $IGHG1^+$) $IGHD^-$
Plasma cells	$CD19^+$ $CD38^{++}$ $CD74^-$ $CD79^-$

2.4 Antibody production

2.4.1 Antibody sequence construction

Selected antibody sequences were trimmed to their minimal variable part. Codon usage was optimized for yield when expressed in human cells with the DNA Chisel tool [375]. Overlapping 5' and 3' sequences were added to allow for seamless cloning into the corresponding expression vector (**Table 2.5**). The 5' seamless adapter comprised part of the leader sequence and translocation signal, while the 3' seamless adapter allowed for in-frame junction of the constant part of the immunoglobulin ('backbone') contained in the expressing vector. The vectors used were derived from Tiller and colleagues' work [324]. Vectors included an ampicillin-associated resistance gene allowing for easy selection of transformed clones.

Table 2.5: Overhang sequences used for seamless cloning of variable antibody regions into corresponding expression vectors

Position	Chain	Sequence
5'-OH	Heavy	GCTGGGTTTTCCTTGTTGCTATTCTCGAGGGTGTCCAGTGT
5'-OH	Kappa	ATCCTTTTTCTAGTAGCAACTGCAACCGGTGTACAC
5'-OH	Lambda	ATCCTTTTTCTAGTAGCAACTGCAACCGGTGTACAC
3'-OH	Heavy	GCTAGCACCAAGGGCCCATCGGTCTTCC
3'-OH	Kappa	CGTACGGTGGCTGCACCATCTGTCTTCATC
3'-OH	Lambda	GGTCAGCCCAAGGCTGCCCCCTCGGTCACT

Codon-optimizing strategies to enhance productivity included k-mer uniqueness enforced along all variable sequences with a length of 10 nt, codon usage adapted to match that of human cells, and GC content optimized to remain below 56% at a global level and under 60% over 60 nt-long sliding windows.

In silico-generated sequences were sent for gene synthesis. We relied on IDT DNA eBlocks Gene Fragments (https://eu.idtdna.com) services for production. Upon reception of newly synthesized gene fragments, variable parts of antibodies were cloned into corresponding backbones as described below.

2.4.2 Antibody cloning

Plasmid vectors encoding the constant parts of IgG1 heavy, lambda and kappa chains were prepared as described: suitable vectors were linearized using corresponding restriction enzymes (2.5 µL each for 20 µg of vector DNA) and remaining extremities were dephosphorylated to avoid recircularization using 12 µL recombinant shrimp alkaline phosphatase (New-England Biolabs, ♯M0371S) per 20 µg of vector DNA. Enzymatic preparation was performed in a single step, for 4.5h at 37°C. To maximize cloning efficiency, vectors were linearized using three enzymatic digestions. Two restriction enzymes flanking the variable sequence on both sides allowed for insert removal. A third restriction enzyme further degraded the insert to prevent unwanted recircularization. Dephosphorylated and linearized DNA was then purified using the NucleoSpin Gel Purification kit (Macherey-Nagel, ♯740609) after DNA migration on a 2 % agarose gel and following manufacturer's instructions. Final elution was performed with 50 µL molecular-grade pre-warmed H_2O. Concentration was assessed and aliquots were stored at -20°C for further use.

The cloning reaction allowed recombination of the insert with the previously prepared linearized and dephosphorylated vector by means of seamless flanking regions. In a 96-well plate, 50 ng of corresponding empty linearized vector were added to 10 ng of antibody-specific insert, along with 6 µL of In-Fusion enzyme mix (Takara Bio, ♯638947). The reaction plate was incubated for 15 min at 50°C in a PCR block before cooling down to +4°C. Immediate transformation in ultra-competent Stellar cells (HST08) was achieved in PCR block and spread after recovery on LB agar petri dishes supplemented with the corresponding antibiotic. Transformed bacteria were left to grow overnight at 37°C.

On the following day, a single bacterial colony was handpicked and further grown in antibiotic-rich LB media under agitation for 16h. After bacterial growth and DNA amplification, heavy- and light-chain encoding DNAs were

purified to obtain ≈100 µL at 800 ng.µL^{-1} on average. After miniprep, purified DNA was sent for Sanger sequencing using SP6 universal primers. Correct cloning was verified using the Geneious software and the whole process was replicated once if a mismatch with expected DNA was uncovered.

2.4.3 Antibody production

Full length human antibodies were obtained by co-transfection of matching heavy- and light-chain DNA into HEK 293F cells. Cells were brought to a concentration of 1.2 x 10^6 cells.mL^{-1} with 50 % fresh media. For 70 mL cultures, two tubes were prepared with 2 mL OptiMEM media. Tube A was spiked with 21 µg of each antibody chain DNA. Fifty microliters of 293-Fectin (Thermo-Fischer, ♯12347019) were added to tube B. After 5 min of incubation to allow lipid distribution, tube A and tube B were mixed together and left for incubation at RT for another 30 min. DNA and transfectant were then added to the cells and antibody synthesis allowed for 5 days. Abs were initially produced from small-scale, screening-oriented 70 mL HEK 293F cultures and production scaled up if broad neutralization activity was unveiled.

2.4.4 Antibody purification

On fifth day, cells were harvested and spin down at 1200 g for 5 min to pellet cells. Supernatant was spin for 20 min at 2000 g to remove cell debris. Gravity filtration columns were prepared using protein A sepharose beads and rinsed with PBS. We ran cell supernatant through gravity column at slow pace and washed the column with 50 column volumes of PBS. Elution was performed using 9 mL of glycine solution at pH = 2.5. Eluted antibodies were buffered to physiologic pH using 1 mL 1M Tris pH = 8.0 and concentrated using Amicon ultra-centrifugal filter units (100kDa). Elution buffer was replaced by 1X PBS and final concentration was brought to 1 mg.mL^{-1}.

2.5 Pseudoviruses production

Neutralization assays allowed for functional testing of produced antibodies. These assays rely on the production of a reporter luciferase by the infection of permissive and engineered cells when put in contact with native viral strains or pseudo-virus constructs [282]. Pseudoviruses are built by co-transfection

of a *env* gene-deficient HIV-1 backbone DNA with a plasmid containing the missing *env* gene of interest.

2.5.1 Pseudovirus selection (PV panels)

Three different panels of PVs were used in the present work. A small-scale cross-clade predictive panel of 14 PVs [81] was used for initial high-throughput screening of produced antibodies. These PVs are listed in **Table 6.2**. A second panel of 37 PVs, identical to the one used in the initial Protocol C screening [189], was used to perform initial characterization of antibodies exhibiting neutralization capacities against the screening panel. Viral strains corresponding to this 37 PVs panel are listed in **Table 6.3**. Finally, a few handpicked antibodies were fully tested against a large cross-clade widely-used panel comprising 109 PVs [291] and recapitulated in **Table 6.4**. Altogether, bNAbs were tested against a maximum of 133 PVs.

2.5.2 DNA preparation

DNA plasmid of *env*-deficient HIV-1 backbone (pSG3Δ*env*) was transformed, amplified and purified as per standard procedures [344]. Due to its relatively large size (around 15 kb), plasmid amplification was achieved at 30°C instead of the traditional 37°C. On the other hand, *env*-coding DNA corresponding to viral strains of interest were cloned, amplified and purified. Sequences encoding the gp160 surface protein were available in our lab [274, 275].

2.5.3 Pseudovirus production

Pseudoviruses were produced by co-transfection of the pSG3Δ*env* plasmid with the Env-coding DNA of interest into HEK 293T cells. Transfection was performed in 10 cm-wide round culture dishes for small screening panels or in tissue-culture treated 24-wells plates for larger panels. For large cultures, 40 µg of backbone DNA pSG3Δ*env* was used along with 20 µg of Env-containing plasmid. Transfection was made possible by 90 µL HelixIN (Oz Biosciences, ♯HX11000) transfecting reagent, enhanced with 100 µL HIB (Oz Biosciences, ♯HX11000). Small-size transfections were scaled accordingly. Three days after transfection, PVs were harvested. Pseudoviruses were eventually concentrated using Amicon ultra-centrifugal filters (100 kDa) and used fresh or aliquoted

and stored at -80°C for further use. Titers obtained in neutralization assays (see below) were assessed to ensure correct infectivity and usability for antibody characterization. Measured titers ranged from 43,930 to 5,346,035 RLU and were diluted accordingly for neutralization assays. Altogether, we have synthesized 133 PVs originating from all major clades and encompassing all three tiers.

2.6 Neutralization assessment

Neutralization assays were performed according to the previously described TZM-bl assay [282]. In this assay, infection of HIV-permissive cells engineered with a reporter system activates the transcription of a gene coding for the firefly luciferase. Luciferase presence is assessed by the production of luminescent luciferin, whose luminous activity is immediately recorded.

2.6.1 Neutralization assays

Neutralization assays were performed as follows: initial antibody concentration was set at 50 $mg.mL^{-1}$ and 5-fold serial dilutions were conducted to obtain 8 points total, reaching 0.64 $ng.mL^{-1}$ at the lowest level. Background signal was assessed in the absence of infective pseudoviruses and subtracted from all infectious readouts. Maximal infection levels were assessed for each PV and corresponded to signal in the absence of antibodies. To validate the assays, PGT121 , PGT128, PGT145 [340] and PGT151 [104] bNAbs were used as control antibodies. On day one, 20 µL of antibody dilutions were put in presence of 20 µL of PV corresponding to at least 100,000 RLU in infectious titer. Antibody and PV mixes were incubated for 1h at 37°C in tissue culture-treated 96-well plates. After incubation, 4 x 10^5 TZM-bl cells/well in 20 µL DMEMc were seeded in each well and the mixture was further incubated for 24h. On day 2, cells were re-fed by addition of 40 µL of DMEMc per well, and left for a further 24h of incubation at 37°C. On day three, supernatant was aspirated and cell lysed using 45 µL of dedicated cell lysis buffer (Oz Biosciences, ♯LUC0100) under agitation for a minimum of 20 min. When ready, 30 µL of luciferase substrate (Oz Biosciences, ♯LUC0100) were added to each well and luminous activity was measured without delay.

2.6.2 Neutralization results interpretation

Neutralization was then calculated from infection readouts as follows:

$$Neutralization = \frac{RLU_{\text{virus only}} - RLU_{\text{virus + antibody}}}{RLU_{\text{virus only}}} \times 100 \tag{2.1}$$

Calculated neutralization was plotted for all dilution points and fitted with a dose-response (inhibition) model equation:

$$y = \frac{a - d}{1 + (\frac{x}{c})^b} + d \tag{2.2}$$

where y is the neutralization for any given antibody concentration x. Model parameters (a, b, c and d) were then used to calculate the IC_{50}, corresponding to the concentration of antibody needed to reduce infectivity by 50 %. Individual neutralization curves were plotted and visually checked for consistency. IC_{50} values were calculated and the presence of a plateau was verified for each tested mAb/PV pair. An example of neutralization profiles is given in **Figure 2.11**.

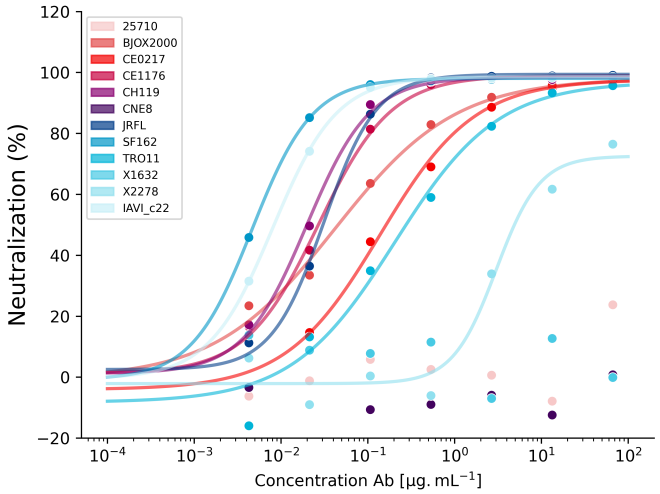

Figure 2.11. Neutralization data obtained and corresponding modeling curves for an example antibody (PC94-A.31) tested against twelve PVs during initial screening. PV: pseudovirus, Ab: antibody

If neutralization was not present, mAb was considered non-neutralized (NN). If the neutralization curve suggested the presence of a plateau, the following

procedure was used: if the plateau was above 50%, the IC_{50} was calculated based on the maximum (100%) infectivity. If the plateau was below 50%, the IC_{50} was artificially set to $\geq$ 50 $\mu g.mL^{-1}$. In the absence of a plateau, the calculated IC_{50} was used even if superior to 50 $\mu g.mL^{-1}$. This approach might underestimate both the IC_{50}s and the breadth of neutralization, especially in the presence of a plateau. However, we preferred to use this method rather than a more optimistic inverse approach were IC_{50}s are always calculated to the local maximum, even if only neutralizing a small fraction of the PV pool. Also, we did not use IC_{80}s, even though it was demonstrated that this was a better predictor of in vivo protection. In a final step, IC_{50} values obtained against multiple PVs were aggregated to obtain a two-dimensional characterization of each antibody: the breadth of coverage on one hand (number of neutralized PVs with an IC_{50} value inferior to 50 $\mu g.mL^{-1}$ divided by the total number of viral strains tested), and on the other hand, the potency of neutralization of each antibody was calculated as the geometric mean of the IC_{50} values obtained for the PVs neutralized ($geomean_{IC50}$).

2.7 ELISA assays

ELISA assays were conducted by coating 10 µL of mgp120 at 2 $\mu g.mL^{-1}$ in 1X PBS overnight at +4°C in 96-well plates. To prevent unspecific binding, 20 µL per well of a mix containing 3 % BSA in 1X PBS was applied for 1h at RT. Tested antibodies were then incubated for 1h before washing. Washing steps (x3) were performed with 50 µL 1X PBS. The secondary antibody used was a goat anti-IgG1 Fab'_2 human coupled with alkaline phosphatase (Jackson Immuno ♯109-001-008). This enzyme catalyzed the hydrolysis of p-nitrophenyl phosphate (pNP) substrate molecules into the yellow-colored p-nitrophenolate, and its concentration was measured by its absorbance at 405 nm. Substrate was added at a volume of 20 µL per well and incubated for 30 min in the dark before measurement.

2.8 Polyreactivity assays

The polyreactive nature of mAbs was assessed through two different approaches. In a first experimental setup, ELISA assays were conducted against a panel of ten antigens known to be regular targets of unspecific binding and considered hallmarks of polyreactive mAbs [178, 5, 42, 29]. The antigens used

included: single-strand DNA (ssDNA), ganglioside GD1a, lipopolysaccharide (LPS), transferrin, apotransferrin, hemocyanin, insulin, cardiolipin, albumin and histones. These antigens were coated overnight at +4°C and the ELISA assay followed the experimental protocol detailed above for mgp120.

A second approach was employed to assess the potential polyreactivity and autoreactivity of the isolated mAbs. For this, Hep2 cells were used and the binding to cellular structures was carefully controlled using indirect immunofluorescence as previously described [178].

2.9 Bulk NGS Adaptative Immune Receptor Repertoire analysis

We performed bulk-NGS analysis of the B cell repertoire. This approach allows for the sequencing and analysis of entire adaptive immune receptor repertoires (AIRR). It aims to recover circulating BCRs at a given timepoint, resulting in a snapshot of the state of the adaptive humoral immune response. This technique yields vast amounts of data, however without the paired information for heavy- and light-chains as well as other details such as the isotype.

2.9.1 BCR library preparation and sequencing

Sequencing of entire AIRR repertoires was introduced in 2009 [345, 31]. In the present work, we followed the protocol detailed in Briney *et al.* [37]. BCR heavy-chains were exclusively sequenced from total PBMCs as follows: RNA was first extracted using the RNeasy Maxi kit (Qiagen, ♯75162) from 10 x 10^6 PBMC. Antibody-coding mRNAs were reverse-transcribed using common primers situated at the 5'-end of the constant region of the heavy chain (CH1). Second-strand synthesis took place using multiplexed V-gene primers corresponding to 7 V-genes. Further amplification (25 cycles) was performed using added Illumina adapters as PCR primers to avoid preferential amplification of certain V genes. Libraries were calibrated and loaded on an Illumina NovaSeq-6000 for sequencing using a 2 x 300 bp S4 flow-cell.

2.9.2 Bioinformatic analysis

Base-calling was performed on the Illumina dedicated BaseSpace. Raw FASTQ reads were then downloaded and preprocessed on a local server using

a custom pre-processing Python script. Obtained FASTA sequences were then assigned using the **AbStar** package [35].

Antibody sequences belonging to the same mRNA were collapsed down thanks to the **AbCorrect** module of **AbUtils** package (GitHub: AbUtils). Antibody sequences belonging to shared lineages – or clonotypes – were grouped together using the Clonify package [36]. Clonotypes were defined as antibodies with shared V-gene usage, shared J-gene usage, a sequence identity level of CDR_H3 greater than 65 % pondered with penalties for length difference, and with bonuses for shared mutations in framework regions (FR).

Sequence identity between bulk-NGS antibodies heavy-chains and isolated mAbs heavy-chains was calculated using alignment tools (global alignment) from the **AbUtils** package, with underlying use of the Needleman-Wunsch algorithm [236]. Lineages of interest were recovered to perform phylogenic analysis. In depth, sequence identity of every single NGS mAb to each isolated bNAb was calculated using the global alignment method. Next, we selected the NGS mAbs with the highest identity (the threshold was set manually for each sample, usually above 90 % identity) and with a plausible SHM rate. We then recovered the entire corresponding lineage, and verified the pertinence of this approach by phylogenic analysis of the sequences.

Phylogenies were built using the **MAFFT** tool [172] for alignment (used with default settings) at the nucleotide level, and trees were built using the **FastTree** utility [260]. Phylogenies were visualized using the **Baltic** package (GitHub: Baltic). Ancestral sequences were inferred using the **IQ-Tree 2** tool [232] with model selection [171], ultrafast bootstrap [141] and the posterior mean site frequency model [341]. Presence of previously undocumented germline alleles was assessed using the **IgDiscover** toolkit [70].

Repertoire diversity was assessed by measuring alpha- and beta-diversity between timepoint sampled. Alpha- and beta-diversity metrics were calculated using the AbCompare tool from the **AbTools** package. For each measure, only the V-gene usage frequencies were used, for the heavy-chain exclusively. Each measure comprised 1,000 iterative calculations by subsampling the sequence space (n = 100,000 BCR sequences). Calculations were performed on the UMI

corrected dataset (centroids), thus corresponding to a single BCR sequence per cell. This removed the limitation arising from possible variations in depth of sequencing. Alpha-diversity was assessed using the Chao1 index and beta-diversity was assessed using both the Morisita-Horn similarity index and the Bray-Curtis similarity metric.

Computation-intensive tasks, such as AbStar assignment, AbCorrect UMI handling and Clonify lineage definition ran either locally, on an Amazon Elastic Compute Cloud (EC2) m4.xlarge instance, or on the Grenoble Alpes University Cloud Computing Cluster (GRICAD infrastructure), which is supported by Grenoble research communities.

2.10 HIV *env* evolutionary analysis

HIV *env* genes were sequenced prior to my arrival in the group as follows: plasma samples were collected from different timepoints and diluted in a 96-well plate in order to achieve 30 % positivity in an *env*-specific RT-PCR. This ensured that the positive wells contained only a single virus and therefore a single sequence. Sequencing was then performed by Monogram Biosciences using Sanger sequencing on the positive wells.

Phylogeny analysis of these sequences was conducted in collaboration with Dr. Raphaëlle Klitting (Andersen Lab, Scripps Research, USA) in the following manner. Patient's viral sequences were concatenated to the Los Alamos National Laboratory reference database (available at www.hiv.lanl.gov). Reference alignment included all complete HIV-1 sequences up to year 2020. Sequences were retrieved in DNA (nucleotide) FASTA format for the *env*-region only. This reference alignment contained 8,075 sequences (3,110 of subtype B, 751 of subtype A, 1,795 of subtype C, 148 of subtype D among others). Reference sequences and patient's viral sequences were aligned using the **MAFFT** tool [172] online server (MAFFT) with default alignment parameters. The obtained alignment was visualized using **AliView**, available from AliView. From this alignment, a first tree was constructed using a maximum-likelihood (ML) approach. This was performed using **IQ-Tree** [232] in its version 2.0.3.The obtained tree was visualized using **figtree** version 1.4.4 from Rambaut *et al.*. (source-code available at GitHub: FigTree).

Recombination events were modeled using the **RDP** (Recombination Detection Program) software developed by Martin and colleagues [217]. RDP version 4 was used to screen for recombinations within the autologous viral dataset. An exhaustive search was perform using the following model hypotheses: RDP, GENECONV, Chimaera, MaxChi and 3Seq. A bootstrap posterior analysis was performed using BootScan and SiScan models. The default options were otherwise used, including the 'Polish Breakpoints' option to reinforce validity of breakpoints localizations. Ultimately, hits were confirmed using the **GARD** algorithm from Pond *et al.* [184].

Chapter 3

RESULTS

3.1 Isolated antibodies constitute a snapshot of the HIV Env trimer specific repertoire

3.1.1 Overall characteristics of B cells identified in samples from donor PC94

We sorted separately samples from early and late timepoints. From early timepoints (visits V18, V24, V30 and V36), a total of 33 million frozen PBMC were recovered from long-term storage, thawed and processed as described in Methods (see section "B single-cell sorting, sequencing and analysis"). We hypothesized that early B cells belonging to neutralizing lineages identified previously or in later timepoints would exhibit low affinity for HIV Env trimers and would not be sorted based on trimer binding. Therefore, we decided to process early samples without FACS enrichment based on trimer binding. Sorted cell counts are shown in **Table 3.1**. Cell gating parameters are shown in **Supplementary Figure 6.1**.

Table 3.1: FACS enrichment of early timepoint samples

	Cells	Processed	Live cells	B cells	% B cells	MBC	% MBC
PC94 V18	7,960,000	16,363,560	53.24 %	589,096	6.76 %	86,922	14.76 %
PC94 V24	5,760,000						
PC94 V30	8,640,000						
PC94 V36	11,600,000						
Total	33,960,000						
Sorted cells				208,072	2.39 %	32,652	5.54 %

B cells: $CD3^-$ $CD14^-$ $CD19^+$, Memory B cells (MBC): $CD3^-$ $CD14^-$ $CD19^+$ $CD27^+$

A substantial proportion of cells were either lost during the staining procedure or filtered-out as dead cells, resulting in only a little more than a total of 8 million live PBMCs being selected at initial FACS sorting gates. From those, a total of 32,652 memory B cells were sorted in bulk. We further sorted in bulk 208,072 B cells. Together, this totalized 240,724 B cells that were collected from the FACS and further processed with the single-cell pipeline for

individual barcoding. Due to a technical failure in our sorter, we were unable to reach the forecasted number of cells for these 'early timepoint' samples.

Concerning late timepoints, we selected B cells that were positive for both PE-labelled trimers and APC-labelled trimers. These cells are referred to as double-antigen-positive B cells. We sorted in bulk a total of 54,869 double-antigen-positive B cells from these four 'late timepoint' samples. These were then transferred for single-cell sorting. Cells counts obtained from later timepoints (visits V54, V60, V66 and V78) at different steps of the experimental procedure are shown in **Table 3.2**. Cell gating parameters are shown in **Supplementary Figure 6.2**.

Table 3.2: FACS enrichment of late timepoint samples

	Cells	Live cells	B cells	% B cells	Double positive	% Double positive
PC94 V54	4,479,696	3,224,357	249,898	7.75 %	12,703	0.39 %
PC94 V60	5,150,224	3,134,767	256,066	8.17 %	11,667	0.37 %
PC94 V66	5,796,300	3,928,932	419,740	10.68 %	15,498	0.39 %
PC94 V78	6,912,908	3,942,241	370,286	9.39 %	15,001	0.38 %
Total	22,339,128					
Sorted cells					54,869	0.24 %

B cells: $CD3^-$ $CD14^-$ $CD19^+$

From both early and late timepoints, a total of 42,469 cell sequences were finally recovered from the total of 295,593 cells barcoded. This corresponded to 14.4% of the cells following FACS enrichment and before single-cell sorting. This was substantially lower than the expected range: 10X-Genomics mentions about 35% cell recovery using their pipeline. To our understanding, this could be explained by technical difficulties we have encountered, especially in the FACS sorting procedure for 'early timepoints' samples. From early timepoints, we recovered 7,801 MBCs and 19,760 B cells. From late timepoint samples, we recovered 1,450, 3,712, 5,091 and 4,655 cells from samples V54, V60, V66 and V78 respectively.

After these sequences were available, we proceeded with the barcode demultiplexing, allowing us to recover all barcode-encoded information (time-

point/sample of origin, HIV Env trimer baits bound, ...). After demultiplexing, the sample (hence the timepoint) of origin could therefore be recovered for all cells (**Figure 3.1 left**). The vast majority of cells were not sorted for their specificity against the HIV Env trimers. Therefore, a large share of the recovered cells were not HIV Env-specific cells (**Figure 3.1 right**). Some barcodes were not recovered (not properly sequenced), rendering impossible the recovery of the corresponding encoded information. For the 'early timepoint' samples for example, the absence of recovery of the sample barcode did not allow us to demultiplex the timepoint of origin for certain cells. These are labelled as 'unassigned'.

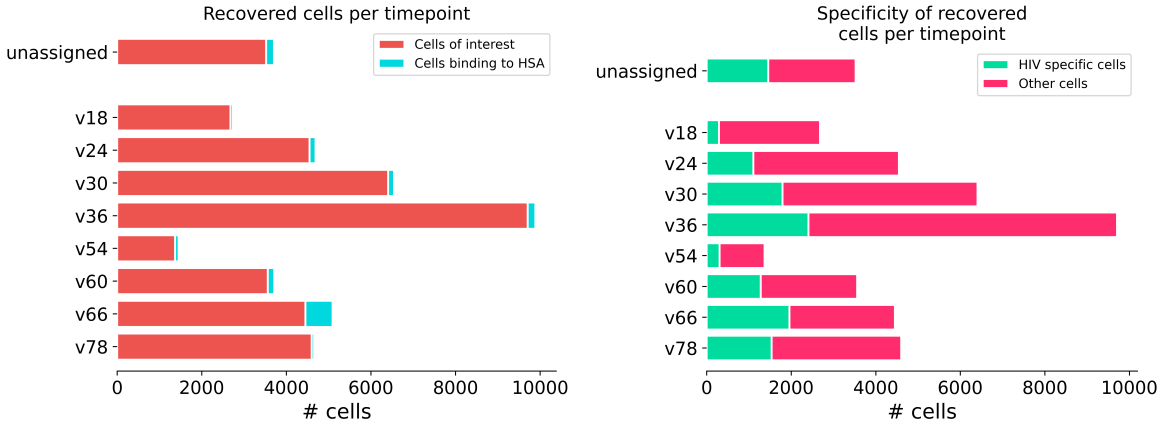

Figure 3.1. Total number of cells recovered after single-cell sorting and sequencing sorted by timepoint (left) and specificity (right). HSA: human serum albumin, mpi: months post-infection

The distibution of the number of barcode reads per cell is given in **Figure 3.2 Left**. The mean number of barcodes recovered per B cell was 13,589. This is in accordance with other estimates of the number of BCR present at the surface of each B cell [360]. Thresholds for antigen positivity were comprised between 5 and 157 barcodes. We thus considered that the difference of two to four orders of magnitude between the total number of BCR and the positivity thresholds allowed us to process B cells binding to multiple baits similarly to B cells of single specificity. Indeed, we hypothesized that the binding of multiple antigens on a B cell, and therefore multiple barcodes, would not interfere with the positivity thresholds. The frequency of cell positivity for each antigen barcode is given in **Figure 3.2 Right**.

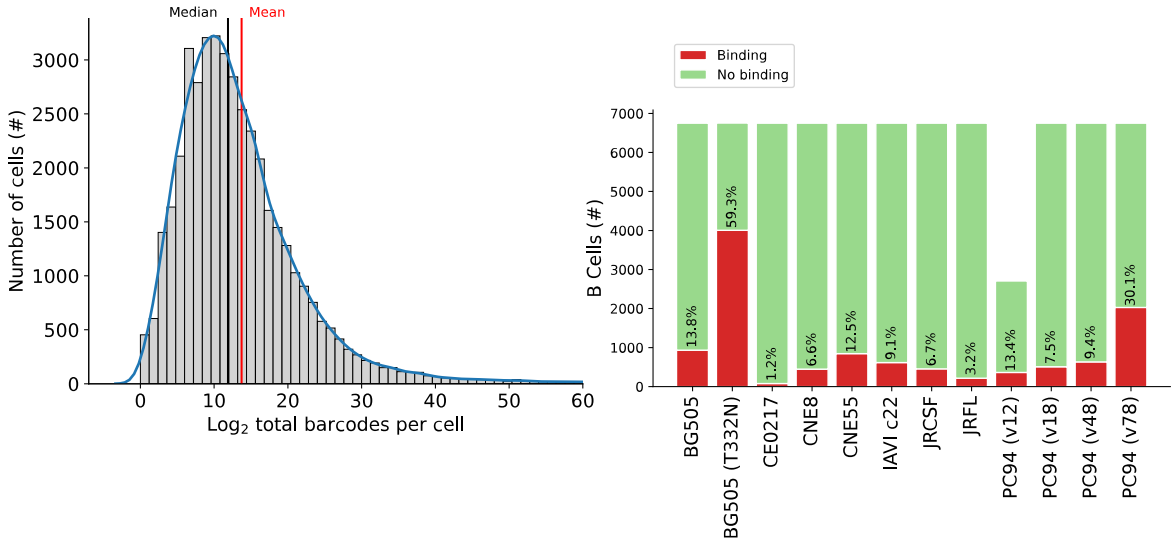

Figure 3.2. Left. Distribution of barcode reads obtained per cell. The number of barcode reads is shown as $\log_2$ reads. Median (3,744 reads) and mean (13,589 reads) are shown in black and red respectively. **Right.** The distribution of positive (red) and negative (green) cells for each bait is shown for the 6,751 HIV Env-specific B cells recovered. The high proportion of cells positive for BG505 T332N suggested an unspecific binding of this bait to a large fraction of B cells. It is worth noting that PC94 v12 was only used in the sorting procedure of 'early timepoint' samples, therefore the binding information is not available for all B cells.

From a total of 42,469 recovered cells, 1,632 showed significant binding to the human serum albumin (HAS) used as a negative control, thus resulting in a total of 40,837 cells potentially HIV Env-specific. Among them, we categorized 12,130 as specific for HIV Env trimers. These were binding to at least one of the trimer baits, labelled with both PE- and APC-corresponding barcodes. As this corresponds to the FACS population described above, these cells are referred to as HIV Env double-positive cells, regardless of the number of different baits they bind to. From these 12,130 HIV Env double-positive B cells, we identified 7,362 separate lineages with sizes ranging from 1 (singlets) to 75 B cells. A hundred and sixty-eight lineages (1.38%) had more than 12 members. The vast majority of the lineages were relatively small-sized, with 51.7% of lineages only encompassing a single mAb.

Overall, from the 42,469 recovered cells, 12,130 were double-positive B cells, and 23,749 were strict pairs, that is to say for which we recovered paired information from the heavy- and light-chains. The union of these two criteria

yielded a total of 6,751 unique, HSA-negative, paired-chain, HIV Env double-positive B cells. These 6,751 B cells were used for the forthcoming analyses, to which we will refer to as simply HIV Env-specific recovered B cells.

3.1.2 The isolated HIV Env-specific repertoire substantially differs from the unspecific repertoire

We first observed the distribution of isotypes from the HIV Env-specific recovered B cells. Results are presented in **Figure 3.3**. Unsurprisingly, B cells capable of binding to a low number of different baits were mostly of the IgM isotype. The proportion of IgD expressing B cells declined consistently with increasing breadth of binding. Finally, B cells with the largest breadth of binding were expressing IgA and most often IgG class-switched Abs. The B cells binding to 10 or 11 trimer baits were exceedingly rare, hence the distribution of the isotypes is of no relevance for these categories.

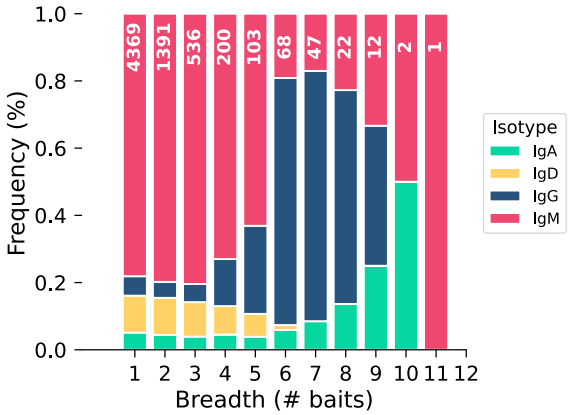

Figure 3.3. Isotypes of recovered BCR given the breadth of binding. The number of recovered HIV Env-specific B cells for each category is shown in white in the colored bars. Subclasses are not separated (IgG encompass IgG1, IgG2 and IgG3 for instance)

We then explored the binding capabilities of the recovered B cells, for both autologous and heterologous Env trimer baits (**Figure 3.4**).

One of the baits, BG505 T332N, was found to bind about 60% of the HIV Env-specific recovered B cells, much above the signal obtained from the other baits. This suggested the presence of unspecific binding, which we mapped

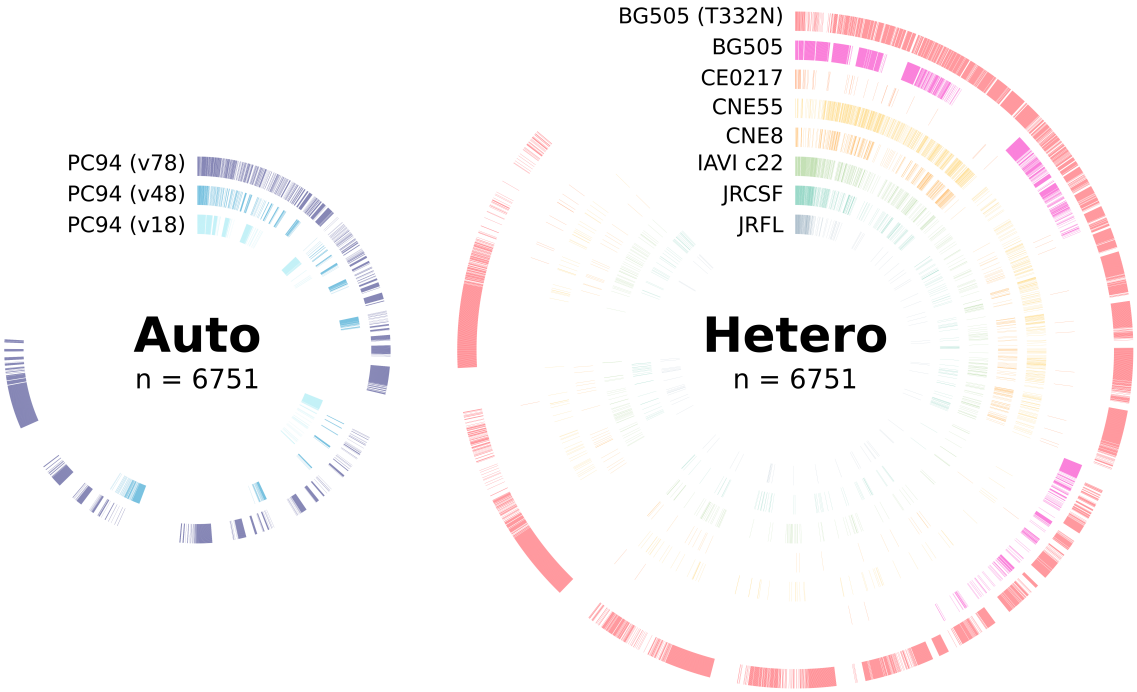

Figure 3.4. Putative antigenicity of recovered HIV Env-specific B cells. B cell specificity for autologous trimers is shown on the left, B cell specificity for heterologous trimers is depicted on the right.

to this bait. We therefore removed BG505 T332N binding information from further specific analysis.

Next, we analyzed further B cells binding to baits. We first studied binding to either all three of the autologous baits, or to all eight of the heterologous baits. The autologous trimer PC94 v12 c007 was not used for all sorting experiments and therefore was not included in the analysis here. Concerning the autologous baits, we hypothesized that they should be recognized by a large fraction of the HIV Env-specific recovered B cells. When considering the autologous baits (PC94 v18 c046, PC94 v48 c028 and PC94 v78 c040), only 122 B cells were positive for all three autologous trimers. We found this number to be unexpectedly low given our initial hypothesis. However, this might be related to the large temporal hence antigenic distance between these Env trimers: five years of evolution under selective pressure separate the trimer PC94 v18 c046 and the trimer PC94 v78 c040.

For heterologous baits, only two B cells were found that could bind to all 8 heterologous trimers, a number that was more within our expectations, considering that broadly binders are supposed to be exceedingly rare. One of these two B cells exhibited binding to 9 trimers (PC94 v78 in addition to all eight heterologous trimers). The specificity of the other B cells mapped to all 11 autologous and heterologous baits.

We further dug into the specificity of binding of these HIV Env-specific recovered B cells. First, we looked at clade specificities (**Figure 3.5**).

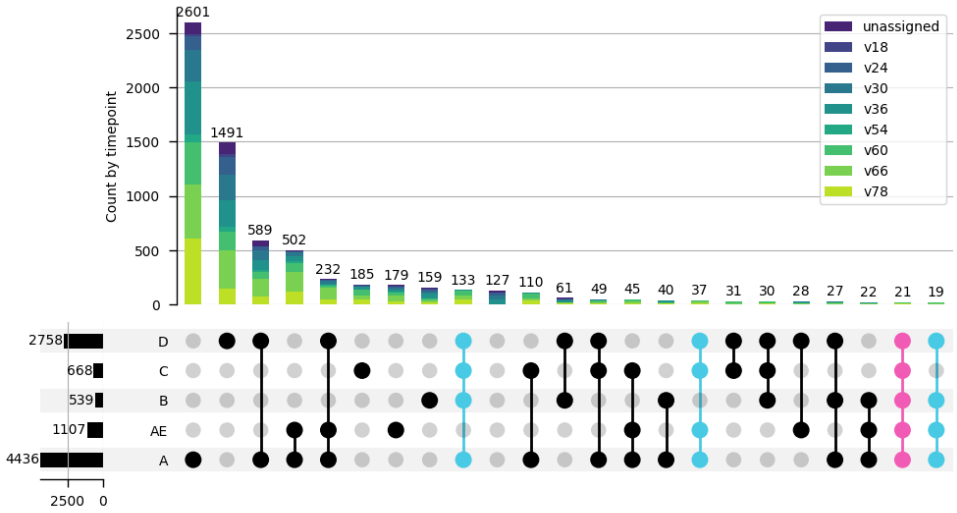

Figure 3.5. Clade specificity of recovered HIV Env-specific B cells. Cells sharing the same specificity are grouped together. Batches of cells binding to 4 different clades are highlighted in cyan, and those binding to all five clades are highlighted in pink. The distribution of the sample of origin of the cells is given in the colored histograms. Clade D baits were only represented by Env from autologous viruses.

Interestingly, most of the B cells were able to recognize clade A trimers, while a much lower number could recognize clade D trimers. Donor PC94 was infected by a clade D virus and we had expected that clade D Env would be highly recognized. Not surprisingly however, B cells specific to a single clade were far more numerous than those capable of multiclade recognition. A total of 21 B cells were able to bind to trimers from all 5 tested clades (highlighted in pink) and 198 BCRs bound 4 of the 5 tested clades (highlighted in cyan).

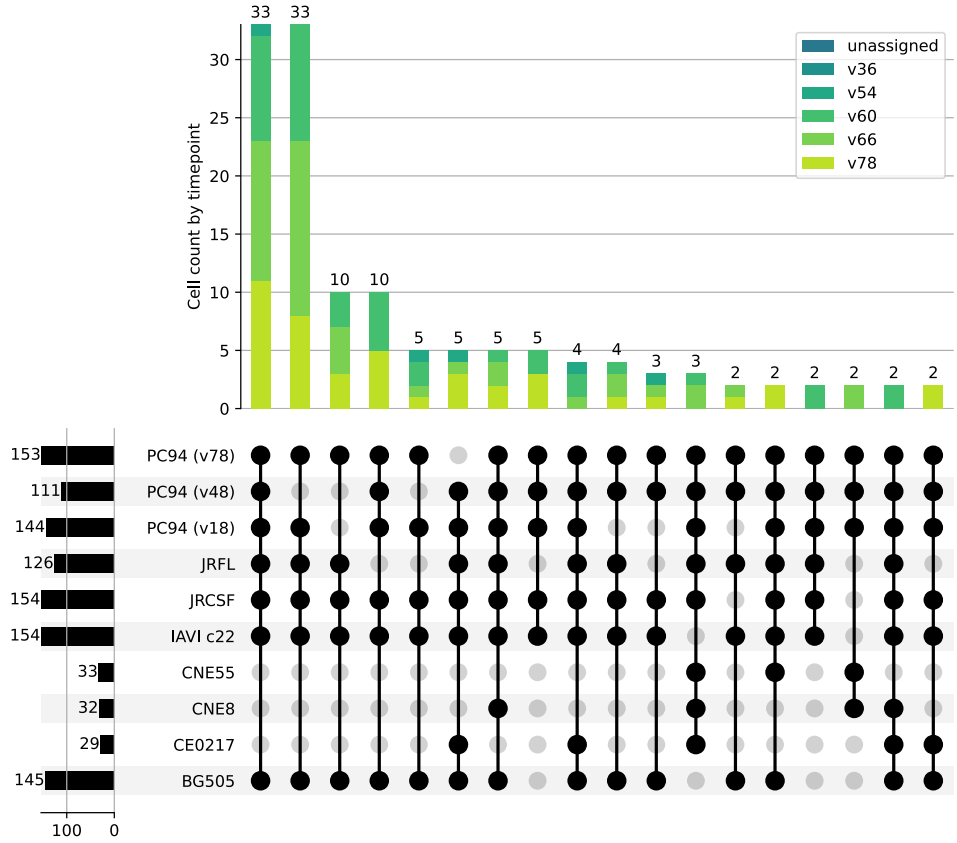

Figure 3.6. Individual specificity of binding of HIV Env-positive recovered B cells. Cells sharing the same specificity are grouped together. Only the cells binding to 5 or more baits are represented. Cells presenting a unique pattern of binding are not shown.

We further looked at the distribution of the individual viral strain specificities of HIV Env-specific recovered B cells. Results are shown in **Figure 3.6**. In this representation we have illustrated all the HIV Env-specific recovered B cells that demonstrated binding capabilities to more than four different viral strains and for which the binding motif was shared at least twice (a large number of cells harbor different binding combinations with more than four viral strains but are unique in their binding pattern, hence not represented here). Interestingly, the overall distribution of binding is similar for all viral

strains with the exception of CNE55, CNE8 and CE0217. In these cases, the number of HIV Env-specific recovered B cells able to bind to these trimers in combination with others is substantially lower. CNE55 and CNE8 are clade AE viruses and of tier 2 or 3. CE0217 is a clade C virus and also classified as a tier 2. The reasons why the baits were selectively less recolonized by B cells from our donor are not known.

The presence of cells exhibiting a great binding breadth suggested that some of these cells could correspond to bNAbs. However, not all cells were equally represented when filtering for greater breadth of binding. Overall, HIV Env-specific recovered B cells from early timepoints are under-represented. It is worth noting the absence of cells from timepoints V18 and V24 in this selection. The cells with the ability to bind to several baits were essentially isolated from the late timepoint samples. This could be in part a consequence of the experimental design, as samples from late timepoints only were sorted for antigen-positive cells, but we cannot rule out that this fact could be a hallmark of a real increased breadth of B cells circulating at these later timepoints.

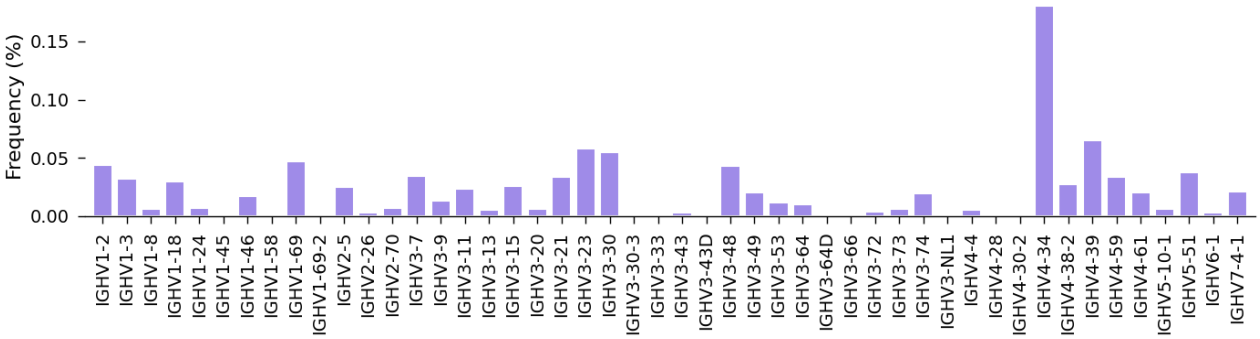

Figure 3.7. Heavy-chain V-gene usage frequencies observed in the HIV Env-specific recovered B cells. The total number of cells considered here is n = 6,751.

Regarding the immunoglobulin gene usages, **Figure 3.7** shows the overall frequencies of V-gene usage in the heavy chains of the Abs in the HIV Env-specific recovered B cells.

An overall increased proportion of BCRs making use of the IGH V4-34 gene was observed. We therefore sought to compare in more detail the gene usage

frequency in HIV Env-specific recovered B cells exhibiting a large breadth of binding ($\geq$ 5 different trimers bound) with a reference repertoire (baseline) from PC94 obtained through the high-throughput unbiased exploration of the immune repertoire. Compared frequencies in V-gene usages in heavy-chains from single-cell sort heavy binders versus the unbiased frequencies observed in PC94 is shown in **Figure 3.8**.

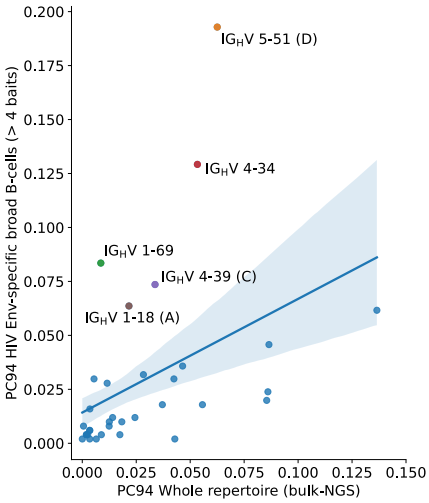

Figure 3.8. Heavy chains V-gene usage frequencies compared between HIV Env specific B cells binding at least 5 different viral strains (single-cell data) and natural frequencies observed in an unbiased sampling of the whole repertoire (bulk-NGS). Five heavy-chain V-genes are over-represented in the cells capable of greater binding breadth. Three of them correspond to V_H-genes used by neutralizing lineages previously isolated (denoted "A", "C" and "D").

Five V-genes from heavy-chains were over-represented within the population of B cells capable of broader binding to viral baits (binding more than 4 different trimers). These were the V-genes IG_H V1-18, IG_H V1-69, IG_H V4-34, IG_H V4-39 and IG_H V5-51. Three out of these five genes corresponded to V-genes found in heavy-chains of NAb lineages previously isolated from this donor [274, 275], denoted "A", "C" and "D" in **Figure 3.8**. This suggested that the B cells recovered from our experiments and exhibiting a larger breadth of binding could indeed correspond to B cells bearing Abs with neutralizing capabilities.

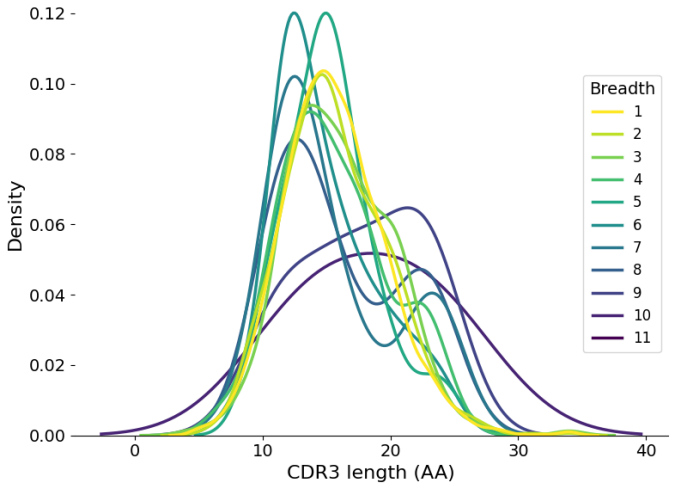

Figure 3.9. Distribution of CDR_H3 length in amino-acids (AA) by breadth of binding observed in the HIV Env-specific B cells recovered from donor PC94 (single-cell dataset). CDR_H3: complementarity-determining region 3 from heavy-chains

The frequency distribution of CDR_H3 lengths from recovered B cells in PC94 according to their binding breadth is represented in **Figure 3.9**.

Interestingly, the distribution of these CDR_H3 lengths does not follow a normal (gaussian) distribution. For each breadth category, the observed distribution exhibits a shoulder, a typical feature of double populations (except for the "breadth = 11" category, for which the sampling size is too low). Hence, while some B cells harbor typical CDR_H3 lengths, of around 15 AA, a smaller population of B cells encodes BCRs with longer CDR_H3s. Furthermore, the position of the shoulder exhibits a shift towards longer lengths of CDR_H3s as breadth increases. No association was observed between CDR_H3 length and other potential confounding variables such as timepoint, experimental batch or V_H-gene usage.

Regarding the SHM rate and its association with the binding breadth, a correlation is also noticeable, as depicted in **Figure 3.10**.

The SHM is measured here as the nucleotide-level germline-divergence of the V-gene in the heavy-chain. The association of SHM rate with increased breadth of binding is noticeable: BCRs belonging to cells capable of binding to multiple HIV Env trimers tend to exhibit a higher level of SHM, thus

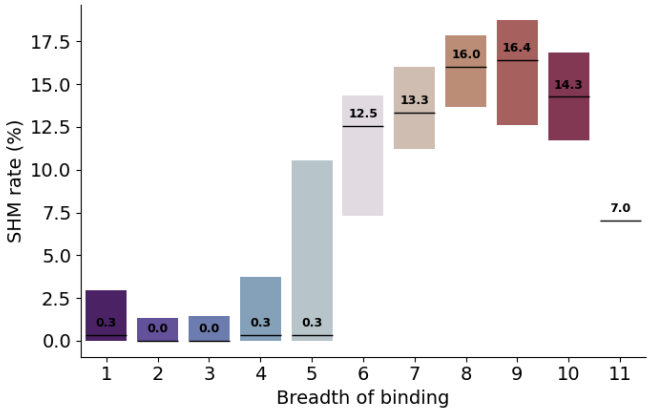

Figure 3.10. Somatic hypermutation (SHM) rates observed in V-genes from heavy-chains at the nucleotide level and grouped by binding breadth to HIV Env trimers. Horizontal lines denote the mean of each category with the corresponding value.

suggesting the prerequisite of substantial Ab maturation through SHM to achieve broad binding (and possibly broad neutralization) in this particular donor PC94.

We then compared the evolution of binding breadth by isolated HIV Env-specific B cells over time with the evolution of serum neutralization as assessed initially on a small-scale 6 PVs panel [189]. In **Figure 3.11**, we compared the maximum binding breadth of HIV Env-specific B cells recovered from each sampled timepoint (blue curve, left y-axis) with the neutralization score obtained against the small PV panel (red curve, right y-axis).

The two curves appear to follow a similar trajectory, suggesting that the increase in serum neutralization breadth parallels the emergence of B cells bearing Abs with progressively enhanced binding capacity to a diversity of Envs. This may suggest that Abs recovered from cells sorts could recapitulate the neutralizing activity observed at the serum level.

In conclusion, we successfully isolated 42,469 cells from eight different time-points of the follow-up of the elite-neutralizer PC94. Among these, 6,751 were HIV Env-reactive B cells for which we recovered both their BCR heavy- and light-chains sequences. These B cells belong to 6,131 separate lineages; the largest clone/lineage comprised 75 members and 5,198 of these B cells

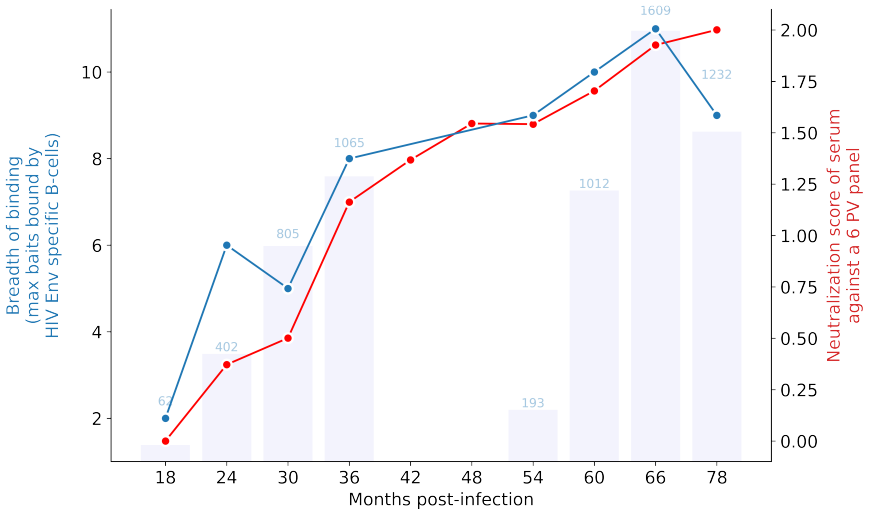

Figure 3.11. Comparison of maximum binding breadth of recovered B cells (left axis, blue curve) with the neutralization activity from the polyclonal serum (right axis, red curve). Blue histograms indicate the number of cells recovered at each timepoint. PV: pseudoviruses.

were singlets. The complete distribution of lineage sizes is illustrated in **Figure 3.12**.

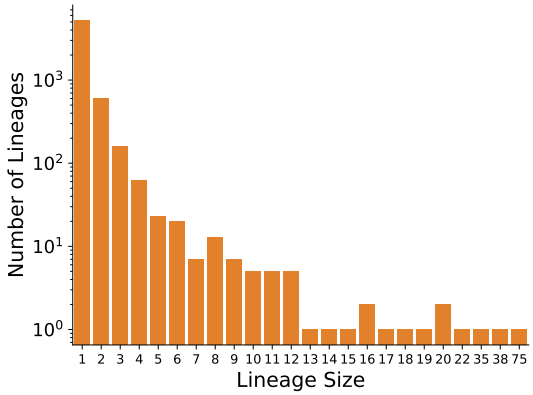

Figure 3.12. Distribution of the sizes of the lineages observed in HIV Env-specific recovered B cells. The most expanded lineage comprised 75 cells. 5,198 lineages had only one member.

We observed an increased frequency of IgGs and IgAs in BCRs displaying greater binding breadth. Additionally, we found an association between binding breadth and CDR_H3 length, as well as SHM rates. Five V-genes ap-

peared over-represented in heavy-chains of broadly binding B cells compared to the baseline repertoire. Three of these V-genes (IG_H V1-18, IG_H V4-39 and IG_H V5-51) were coincidentally those used by neutralizing lineages previously isolated from donor PC94.

3.2 Isolated antibodies exhibit heterologous neutralization capabilities

After we observed the overall characteristics of the isolated HIV Env-specific B cells, we decided to study the neutralizing capabilities of their corresponding Abs. Given the large number of cells available (6,751 HIV Env-specific recovered B cells), we first designed a sorting strategy to sieve for potential neutralizing Abs.

3.2.1 Isolated mAbs recapitulate the heterologous neutralizing activity of the serum of donor PC94

All 42,469 cells were classified using the ranking scheme described above (see Methods, "Selection of Antibody" paragraph). Briefly, cells binding to heterologous and autologous HIV Env trimer baits labelled with both PE- and APC-corresponding barcodes as assessed with stringent thresholds, and comprising a strict combination of a single heavy-chain with a single light-chain were categorized as P1.

	Number of cells
P1	249
P2	481
P3	2,205
P4	3,937
P5	35,597

From all cells, only 249 B cells were categorized as P1. Four hundred and forty-one Ab sequences fell into the P2 group (binding to either PE- or APC-corresponding labelled baits). Group P3 (mimicking group P1 but relying on less stringent thresholds) comprised 2,205 cells. Following categories comprised respectively 3,937 and 35,597 cell records (see table on the left). The P1 group contained essentially cells isolated from later timepoints. None of the cells isolated from the V18 timepoint (17 mpi) fell into this category. Also, none of the isolated cells showed binding to heterologous baits exclusively, without recognition of autologous baits. This behavior was expected.

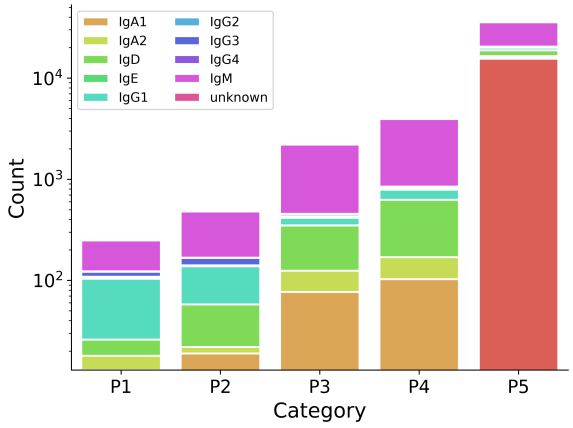

Figure 3.13. Distribution of isotypes and subtypes in different priority categories. The P1 pool was highly enriched in IgG1. For a large proportion of cells in the P5 category (red), the isotype was unavailable (recovered sequence absent or too short to correctly infer the isotype).

The distribution of isotypes was also strongly skewed between these categories (**Figure 3.13**). The P1 category was highly enriched for IgG1 antibodies. The distribution in this category was as follows: IgM: 126 isolated Abs, IgG1: 78, IgA1: 13, IgG3: 13, IgD: 8, IgG2: 5, IgA2: 5, IgG4: 1.

A total of 121 mAbs were selected for production from the 249 Abs belonging to category P1 after taking into account lineage information as described in Methods (paragraph antibody selection). All 121 selected mAbs were considered as potentially productive, as they lacked any alteration (frameshifts, stop codon, missing bases, ...) rendering them all suitable for sequence synthesis and Ab production. Overall, 104 mAbs out of the 121 selected were successfully transfected and purified as described (See Methods – Antibody production). Yields varied greatly, ranging from less than 20 µg to more than 3800 µg for 70 mL cultures (mean = 1042 µg). Among these 104 produced mAbs, the isotype distribution was as follows: IgG1: 75 mAbs, IgA1: 15 mAbs, IgM: 12 mAbs, IgG2: 2 mAbs. These were all produced as IgG1. All produced mAbs were initially screened for neutralizing activity against a 14 PV panel (**Table 6.2**).

Overall, the best mAbs neutralized about 75% of this small screening panel, while some mAbs displayed no neutralizing capabilities at all. The most potent NAb had an IC_{50} = 0.001 µg.mL^{-1} for the best neutralized PV, and a

geomean$_{IC50}$ = 0.01 µg.mL^{-1} for all 14 tested PVs. No mAb achieved neutralization against PVs CNE8 and CNE55, despite some binding capabilities of the corresponding BCR as seen by binding to the corresponding trimers in the single-cell sort data.

After this initial screening, eighteen mAbs displaying substantial neutralizing activity were further tested against the broader 37-PV panel. The corresponding IC$_{50}$ calculated for these NAbs are shown in **Figure 3.14**. The observed breadth of neutralization ranged from 15% to 70% on this panel. The most potent NAb had a geomean$_{IC50}$ = 0.058 µg.mL^{-1}.

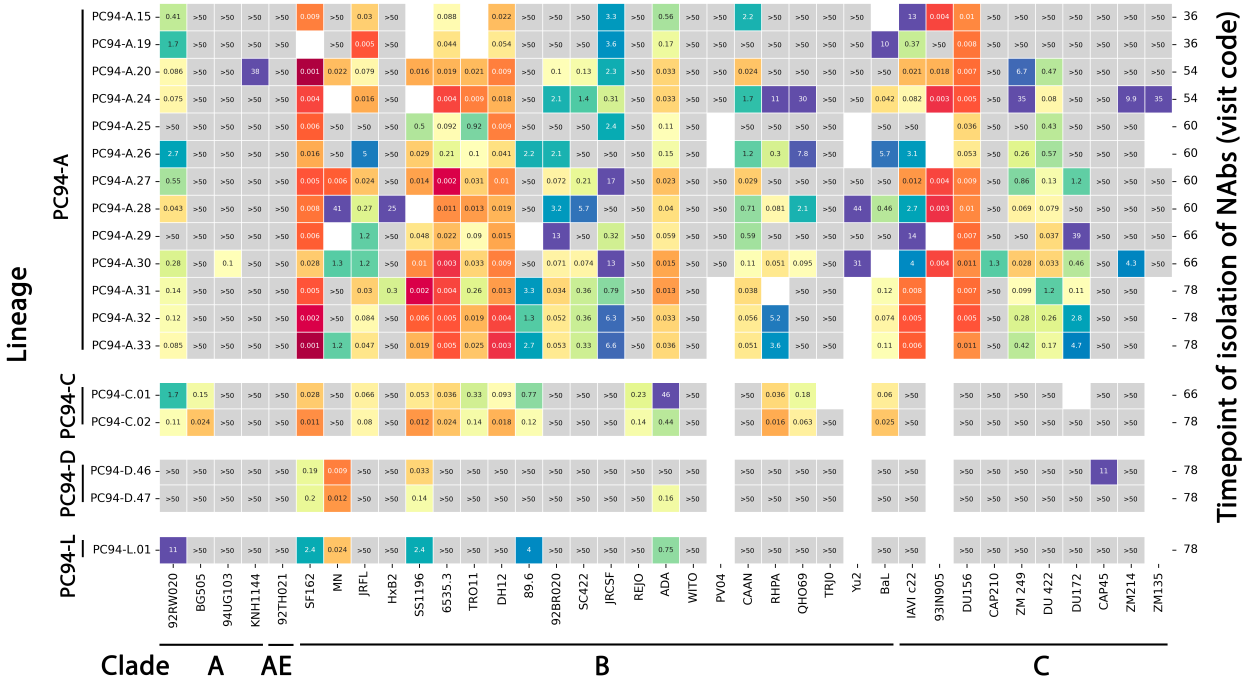

Figure 3.14. Neutralization data against a 37 PV panel. Neutralization with IC$_{50}$ above 50 µg.mL^{-1} was considered as non-neutralizing ("≥50"). Viral clades are indicated at the bottom. Lineages are mentioned on the left. Timepoints of NAb isolation are depicted on the right. PV: pseudovirus, IC$_{50}$: inhibitory concentration 50%, NAbs: neutralizing antibodies. Values are given in µg.mL^{-1}.

All 37 PVs were neutralized by the serum [189]. Four PVs were not neutralized by any of the tested antibodies: 92TH021, WITO (WITO4160_33), PVO.4 and TRJO (TRJO4551_58) despite being neutralized by the serum

(titers were 1:333, 1:82, 1:660, 1:74 respectively). These are of tier 2, except for PVO.4 which is a tier 3 virus.

We observed overall a good correlation in potency between the neutralization by the serum (as given by the ID_{50}s) and the neutralization by isolated NAbs (as given by their IC_{50}s) for a given virus. Concerning the discrepancy observed for the 4 aforementioned PVs, while the NAbs isolated in our work were unable to account for the serum neutralization activity, these four PVs were neutralized by NAbs isolated previously [274, 275] from this same donor, thus fully completing the observed serum neutralization breadth on this panel. The best NAbs from this selection were further studied against a larger PV panel, to confirm their ability to neutralize a large fraction of viral strains.

The seven best NAbs isolated (PC94-A.20, PC94-A.26, PC94-A.27, PC94-A.30, PC94-A.31, PC94-A.32, PC94-A.33) were thus tested against a larger PV panel of 109 PVs adapted from [291]. Neutralization data against the 109 PV panel is shown in **Figure 3.15**. Isolated bNAbs are shown ordered by timepoint of isolation (PC94-A.20 was isolated from sample at V54, and PC94-A.33 was isolated from sample at V78). All the tested bNAbs belong to the same lineage (PC94-Lineage A), so that the neutralization activity is similar between mAbs. For example, none of the NAbs neutralized PVs belonging to the AE clade. This is the only clade for which it is the case.

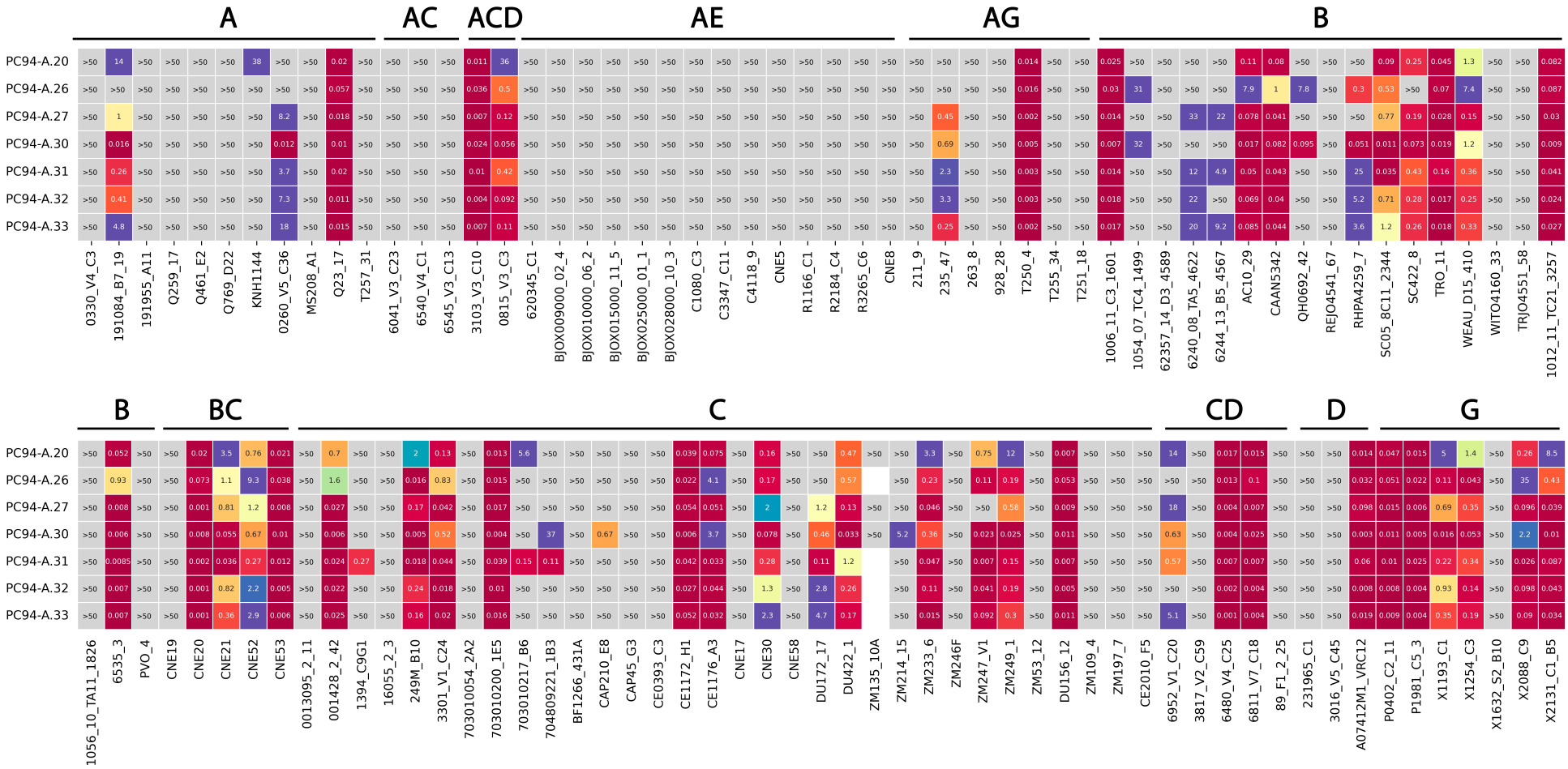

Figure 3.15. Neutralization data (IC_{50}) obtained for seven selected bNAbs against a 109-PV panel adapted from [291]. Viral clades are shown on the top of each row. PV: pseudovirus, IC_{50}: inhibitory concentration 50%, bNAbs: broadly neutralizing antibodies.

Overall potencies were relatively strong, with $\text{geomean}_{\text{IC50}}$ ranging from 0.25 to 0.053 µg.mL^{-1} for the seven bNAbs. However, breadth of neutralization was slightly inferior to the one measured against the 37-PV panel: individual coverage values ranged from 36.7% to 45.0%. In comparison, the polyclonal serum breadth reached 57.1% against the same panel. When considering the activity of all the bNAbs tested, the coverage reached 49.5% of the viral strains present in this large PV panel. We attributed this difference of breadth between the two PV panels to the known overestimation of the breadth of certain NAbs by the 37-PV panel.

In order to grasp the full extent of the heterologous neutralization that can be recapitulated by isolated NAbs, neutralization data from previously isolated NAbs from PC94 [274, 275] along with those isolated in the present study were jointly analyzed. Taken together, neutralization data are available for these NAbs for a total of 126 PVs, combining results obtained from the 14-PV panel, the 37-PV panel and the larger 109-PVs panel used in our study. The total number of PVs for which neutralization data is available is lower than the sum of the three panels due to the presence of redundant strains and to some strains for which the serum had not been tested.

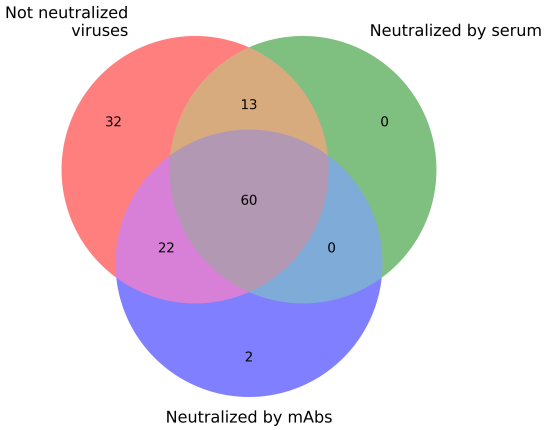

Figure 3.16. Distribution of neutralization activity observed for the serum of PC94 and isolated mAbs from this donor. Overall, the serum neutralized 73 PVs, tested mAbs neutralized 82 PVs, and 32 PVs were not neutralized by either of them. PV: pseudovirus, mAbs: monoclonal antibodies

We considered the following thresholds to define neutralization: serum was considered neutralizing if the ID_{50} was superior to 1:100, mAbs were considered neutralizing (NAbs) if the IC_{50} was lower than 50 $\mu g.mL^{-1}$. Results are shown in **Figure 3.16**. When assessed against the total 126 PVs, the serum neutralized 73/126 viral strains (57.9%). Isolated mAbs when considered together neutralized 83/126 viral strains (65.8%). There was a concordance in neutralization by the serum and isolated mAbs for 91/126 PVs (72.2%).

When looking in depth at individual mismatches, for 22 PVs (17.5%), we successfully isolated NAbs from samples from donor PC94 in spite of the absence of neutralization activity observed at the serum level. Conversely, for 13 viral strains (10.3%), serum neutralizing activity had been observed but no NAbs could be recovered.

We compared for each PV the serum ID_{50} with the best IC_{50} from all isolated NAbs (**Figure 3.17**), using either a continuous (left) or discrete (right) representation of mAb neutralization. The neutralization titer (ID_{50}) of the serum for any given PV was robustly associated with the neutralizing potential of isolated mAbs (IC_{50}) when tested against the same PV ($p = 0.0004$).

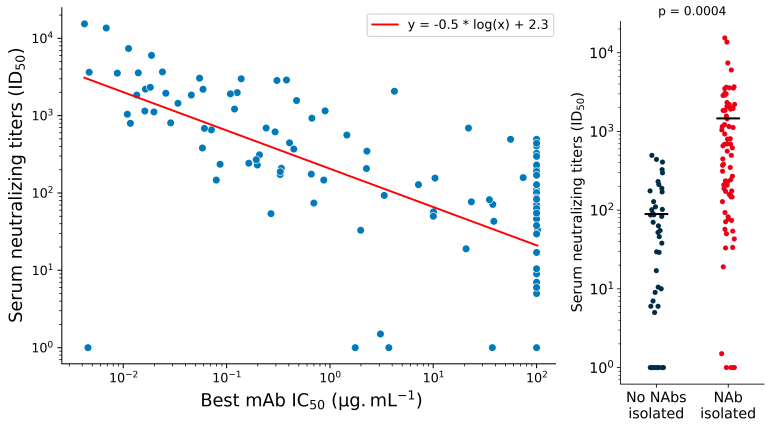

Figure 3.17. Comparison between neutralization activity of the serum (ID_{50}) and neutralization activity of isolated NAbs; **Left.** when considering a continuous approach to mAbs neutralization (IC_{50}), and **Right.** when considering a discrete approach (absence of NAbs vs successful isolation of NAbs). ID_{50} = inhibitory dilution 50%, IC_{50}: inhibitory concentration 50%, NAbs: neutralizing antibodies, mAbs: monoclonal antibodies.

Overall, the neutralization activity of bNAbs isolated from donor PC94 in this study and in previous works [274, 275] together recapitulated the neutralizing activity of the serum against the 37-PV panel. When considering a larger panel of 126 PVs, the neutralization activity of all bNAbs recapitulated 72.2% of the neutralization activity of the serum against the same panel.

3.2.2 A single antibody lineage accounts for most of the heterologous neutralization

As demonstrated above, the neutralizing activity of isolated mAbs from this donor together recapitulates a large fraction of the neutralizing activity observed in the serum. We investigated to see if this neutralization was mainly due to a single neutralizing lineage, or if this activity resulted from the sum of multiple neutralizing lineages of limited breadth. To do so, we further explored the lineages corresponding to the mAbs described above.

The 104 mAbs produced belonged to 60 different lineages with a mean size of 21 mAbs per lineage (median = 9 mAbs, max = 75 mAbs). The most represented lineage was named PC94-D. We produced 26 mAbs out of 75 available sequences from this lineage, which is also the most expanded lineage in our entire dataset (**Figure 3.12**). Abs from this lineage make use of the $IG_HV5\text{-}51*03$ allele for the V-gene and the IG_HJ4*02 for the J-gene. The corresponding CDR_H3 is relatively short, with a length varying between 12 and 13 aa. The SHM rates varied between 8.5% and 18.0% at the nucleotide level. The light chain emerges from the recombination of the $IG_LV1\text{-}51*01$ and IG_LJ3*01 alleles and is of lambda type. From this lineage, we recovered 68 IgG1 and 4 IgA1 sequences. Lineage details are recapitulated in **Table 3.3** at the end of this section. A single member of this lineage was recovered by previous work from our laboratory on this donor [275] using an epitope-agnostic approach with 4 trimers (BJOX2000_SOSIP, TRO.11_SOSIP, BG5050_T332N_SOSIP and JRFL_NFL) in a traditional FACS-based sorting approach. Interestingly, in spite of its marked expansion, lineage PC94-D was not broadly neutralizing, and thus partly questioning the strategy we used to select mAb for production and testing.

The second most represented lineage, designated PC94-A, encompasses 20 mAbs, from which 17 were produced. We recovered the heavy-chain sequence of the

three remaining mAbs from this lineage but not the paired light-chain. This lineage is characterized by the combination of $IG_HV1\text{-}18*01$ and IG_HJ6*01 along with a kappa chain using $IG_KV1\text{-}5*03$ and IG_KJ1*01. The CDR_H3, at 23 aa, is longer than that of PC94-D. The SHM rates varied between 9.9% and 21.4%. The Abs from the PC94-A lineage isolated through our approach consists of 9 IgG1 and 11 IgA1. These mAbs come in addition to 22 other mAbs isolated previously [274, 275] which exhibited narrower breadth and lower potency compared to the new ones.

Among other lineages, we expressed 2 mAbs from PC94-C out of 7 that had been recovered (IgG1 exclusively). Previous attempts at mAb isolation from our laboratory had yielded a single mAb from this lineage (PC94-C.03). Gene usage is as follows: $IG_HV4\text{-}39*07$, IG_HJ6*01, $IG_LV2\text{-}8*01$, IG_LJ1*01 and CDR_H3 length is 17 aa. Lineage PC94-C Abs did not neutralize clade C viruses, but exhibited a broader neutralization against clade A viruses. This characteristic makes lineage PC94-C valuable in conjunction with lineage PC94-A Abs for recapitulating the neutralizing breadth of the serum.

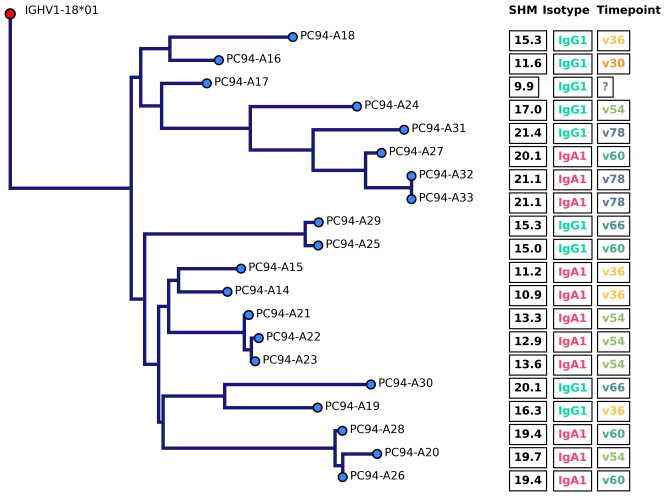

Figure 3.18. Phylogeny tree for the lineage PC94-A. Twenty antibodies are represented along with their SHM rates, isotype and timepoint from which they were isolated. One antibody has no timepoint assigned because the corresponding barcode could not be properly assessed (but belongs to 'early timepoint' samples). The phylogeny tree was rooted using the germline V_H-gene as an outgroup (in red). SHM: somatic hypermutation

The evolutive history of these lineages can be traced by elaborating the phylogenetic tree of the lineage. For this, we can leverage the paired sequences of heavy- and light-chain sequences, along with features of each antibody (SHM rates, timepoint of isolation, isotype, ...). In **Figure 3.18**, we show the phylogenetic tree for the 20 mAbs recovered from lineage PC94-A. In this lineage, mAbs were isolated from six out of eight sampled timepoints (V30, V36, V54, V60, V66 and V78).

Evolutionary distance from root increased with SHM rate. Furthermore, the isotype of recovered mAbs and position in the phylogeny were consistent with mechanisms of class-switch: IgA1 were found to be downstream of IgG1 and conversely, no IgG1 was found to be 'descending' from IgA1 precursors.

In addition to the mentioned lineages, several others were tested. However, none exhibited broad or potent neutralization. Among the 21 lineages explored, only three were considered of interest : PC94-A, PC94-C and PC94-D. The main lineages and their key characteristics are summed up in **Table 3.3**. It is worth noting that the potential polyreactive nature of isolated bNAbs that belonged to these three lineages was evaluated as described above (See Methods – Polyreactivity paragraph). Importantly, the tested NAbs did not exhibit polyreactive behaviors in both ELISA assays and cellular Hep2 anti-nuclear antibody assays

Table 3.3: Key features of selected isolated lineages. The potency is expressed as the $\text{geomean}_{\text{IC50}}$ in µg.mL^{-1}. Breadth and potency are shown for 47 PV (14 PV panel + 37 PV panel)

Lineage	**Isolated mAbs**	**Produced mAbs**	**IG_H-V**	**IG_H-J**	**Type**	**IG_L-V**	**IG_L-J**	**CDR_H3 length**	**Max breadth**	**Mean potency**
PC94-A	20	17	V_H1-18*01	J_H6*01	kappa	V_K1-5*03	J_K1*01	23	67%	1.65
PC94-C	7	2	V_H4-39*07	J_H6*01	lambda	V_L2-8*01	J_L1*01	17	38%	0.172
PC94-D	75	32	V_H5-51*03	J_H4*02	lambda	V_L1-51*01	J_L3*01	12-13	30%	1.292
PC94-E	20	4	V_H1-69*13	J_H5*02	lambda	V_L2-11*01	J_L3*02	15	0%	NN
PC94-F	19	3	V_H5-51*03	J_H5*02	lambda	V_L1-51*01	J_L3*01	12	15%	1.597

PV: pseudovirus, mAbs: monoclonal antibodies,
CDR_H3: complementary determining region, NN: non-neutralizing

The neutralization abilities of Abs from the lineages PC94-A, PC94-C and PC94-D assessed against the 37-PV panel are shown together in **Figure 3.19**.

The lineage displaying the greatest breadth and potency overall was lineage PC94-A. The other neutralizing lineages were limited in terms of breadth (lineage PC94-C reached 38% coverage of 47 PVs tested, lineage PC94-D only reached about 30% against the same 47 PVs) and potency. Lineage PC94-E Abs did not exhibit any neutralizing activity in our screening. In our work, NAbs isolated and belonging to lineage PC94-A were able to neutralize a mean of 57% PVs with the best bNAb reaching 67% of 47 screening PVs, corresponding to 47% neutralization against a total of 133 PVs tested.

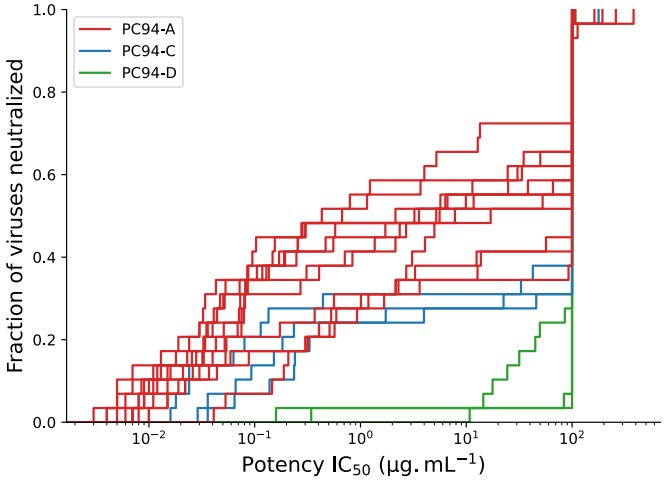

Figure 3.19. Fraction of heterologous viruses neutralized according to the IC_{50}s for the NAbs isolated from the three main lineages PC94-A, PC94-C and PC94-D. Neutralization values used here were obtained against a 37-PV panel (Table 6.3). IC_{50}: half-maximum inhibitory concentration, NAb: neutralizing antibody, PV: pseudovirus.

Overall, we isolated several thousand of HIV Env-specific B cells, from which we selected about a hundred of paired heavy- and light-chain sequences to express the corresponding Abs. These mAbs belonged to 39 different lineages. Some of these mAbs demonstrated strong neutralizing capabilities against heterologous viruses, and, together, mAbs from the main lineages recapitulated a large fraction of the serum neutralizing activity. We observed strong discrepancies between neutralizing lineages were important. A single lineage, PC94-A, demonstrated most of the neutralizing capabilities, largely surpassing the other lineages tested. This lineage comprised 42 Abs recovered either in our work (20 mAbs) or from previous sorting procedures attempted with

samples from the donor PC94 (22 mAbs).

3.2.3 The bNAbs isolated from PC94 show high potency but somehow limited breadth

We compared the neutralization breadth and potency of the bNAbs that we have isolated in this work against those of well-known bNAbs described in the literature. Using the data available from public databases [364], we gathered the values for breath and potency of selected bNAbs. The resulting comparison is shown in **Figure 3.20**.

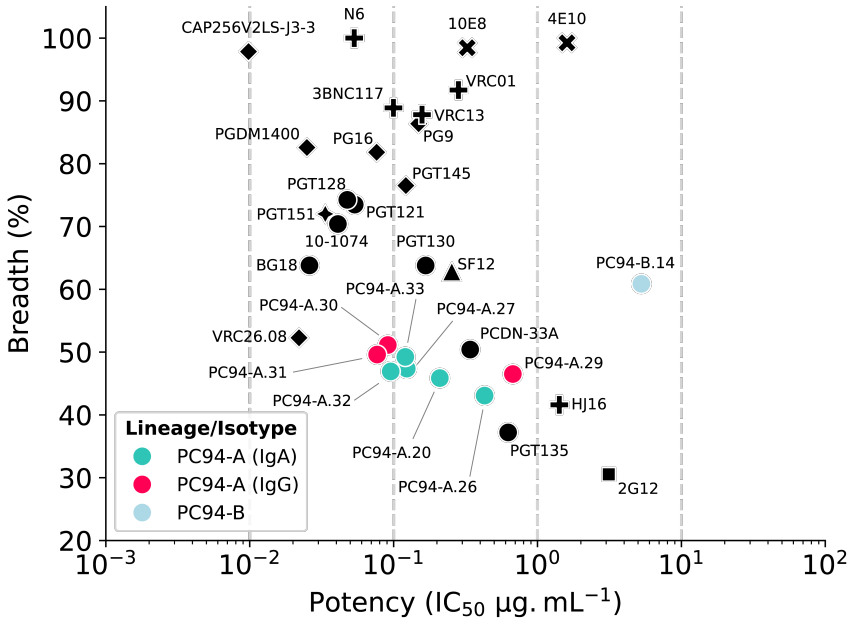

Figure 3.20. Comparison of breadth and potency between selected NAbs isolated from PC94 and several bNAbs from literature (CATNAP database). Data from 126 viruses have been used. To be noted, PC94-B.14 (blue, right) has not been evaluated against the same viruses, hence breadth is overestimated. Shapes of markers denote the targeted epitope: ◯ = V3-glycan, + = CD4bs, ♦ = V2-Apex, × = MPER, △ = Silent face.

Overall, isolated bNAbs from PC94 are not as potent nor as broad as some previously described bNAbs. However, their breadth compares with that of bNAbs such as VRC26.08 and PCDN-33A and is greater than the breadth of PGT135 or HJ16. The maximum observed potency of PC94-A Abs compares with that of PG16 and 38BNC117.

The specificity of the serum of donor PC94 being mapped to the V3-glycan region, we hypothesized that the lineage PC94-A NAbs would bear the same specificity directed towards the V3 glycan region. Therefore, we compared the NAbs from this PC94-A lineage to bNAbs targeting the same site. Among such bNAbs, 2G12, BG18, PGT121, PGT128, 10-1074, PGT121, PCDN-33A or PGT135 can be cited. All these Abs seems to be distributed along a trending line, with increasing breadth along with potency. PGT128 and 10-1074 stand at the higher-end, exhibiting the largest breadth and most potency, while 2G12 and PGT135 sit at the lowest end, both in terms of breadth and potency. Isolated bNAbs from lineage PC94-A seem to fit between the extremes of this trending line.

The fraction of virus neutralized by the best NAbs isolated from our work and in donor PC94 in general can be observed in two different representations, in comparison to selected bNAbs. In a first representation (**Figure 3.21**), we compared the neutralization of the four most potent and broadest bNAbs isolated from PC94 (all from lineage PC94-A) with four selected bNAbs, targeting either the V3-glycan supersite (PGT128, 10-1074 and 2G12) or targeting the V2-apex site (PGT145). The magnitude of the neutralization is represented for these bNAbs against 126 PV.

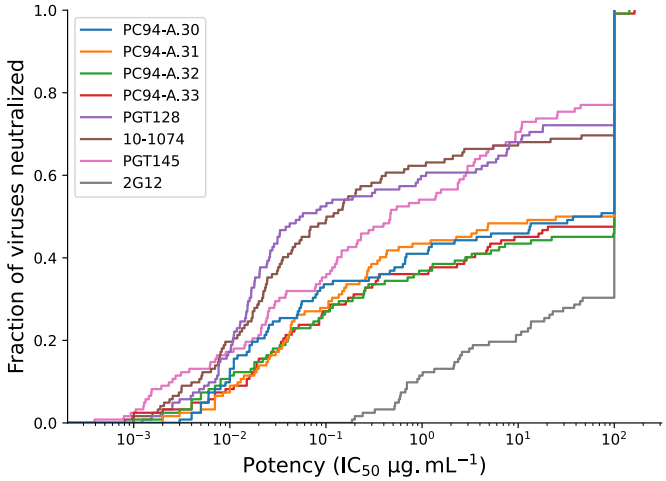

Figure 3.21. Fraction of heterologous viruses neutralized according to the IC_{50}s for the NAbs isolated from the three main lineages PC94-A, PC94-C and PC94-D. Neutralization values used here were obtained against 126 PVs. IC_{50}: half-maximum inhibitory concentration, NAb: neutralizing antibody, PV: pseudovirus.

When compared to these selected bNAbs, the neutralization capabilities of the best NAbs isolated from PC94 are below the neutralization abilities of more potent bNAbs such as PGT145, PGT128 and 10-1074, but far above those of the first generation NAb 2G12. For about a third of the tested PVs, neutralization potency by bNAbs isolated from PC94 is similar to that of these other potent bNAbs. However, our bNAbs plateau more rapidly, hence leaving a significant fraction of non-neutralized viruses (around 50%).

In a second representation (**Figure 3.22**), we focused on comparing the IC_{50}s from these four bNAbs together with bNAbs isolated from other donors and targeting the V3-Glycan region.

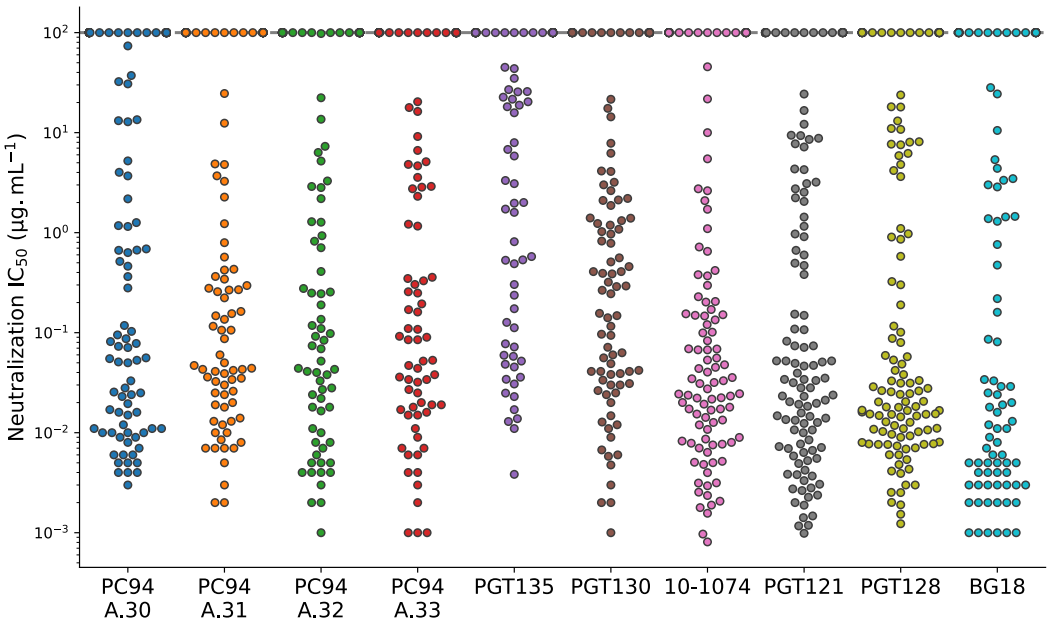

Figure 3.22. Comparison of best isolated bNAbs with anti-V3-glycan bNAbs isolated from other donors. Each dot represents the IC_{50} value obtained against one PV from a 126-PV panel. Non-neutralizing Abs are shown with an IC_{50} value of 100 µg.mL^{-1}. bNAbs: broadly neutralizing antibodies, Abs: antibodies, PV: pseudovirus

Notwithstanding the relatively limited breadth of these isolated bNAbs, they demonstrated considerable potency against neutralized strains. For these four bNAbs, the $geomean_{IC50}$ is respectively 91.1, 76.8, 95.5 and 120.5 ng.mL^{-1} (measured against 133 PVs).

Altogether, several mAbs isolated from PC94 in our approach exhibit substantial neutralizing activity against heterologous viruses. A single lineage among those tested encompassed true bNAbs, capable of demonstrating large breadth and potency.

3.3 Isolated antibodies inform on the autologous neutralization

After we explored the heterologous neutralization capabilities of isolated mAbs, we sought to study their role in the autologous neutralization observed in donor PC94. For that, we produced PVs bearing env sequences corresponding to autologous viruses isolated from donor PC94 at different timepoints of the follow-up. We selected and produced 52 PV from the 210 available autologous env sequences, and tested some of the isolated mAbs against these to assess their autologous neutralization capabilities.

3.3.1 Isolated bNAbs from lineage PC94-A neutralize autologous viruses from early timepoints

The isolated NAbs from lineage PC94-A were tested for neutralization against autologous PVs to further investigate the co-evolution of this lineage and the infective viral strain. The obtained IC_{50}s are presented in **Figure 3.23**. No autologous viral isolate was obtained prior to the V12 timepoint, thus making it impossible to determine the early co-evolution of the lineage before this timepoint.

Autologous viruses from early timepoints (V12, V18, V24) were neutralized by NAbs from PC94-A lineage. Viruses isolated from timepoint V30 were inconsistently neutralized. However, the autologous viruses consistently escaped neutralization after the V36 timepoint (33 mpi). Therefore, viral escape must have occurred between V30 (28 mpi) and V36 (33 mpi).

To explain this viral escape, and because the neutralization activity of the serum of PC94 had been mapped toward the high-mannose patch and the glycan at position N332, we sought to verify a possible correlation between the presence of a PNGS at position N332 and the neutralization.

Timepoint of isolation	mAb	PC94-A.20 V54	PC94-A.26 V60	PC94-A.27 V60	PC94-A.30 V60	PC94-A.31 V78	PC94-A.32 V78	PC94-A.33 V78
V12	c007	0,256	0,014	0,011	0,026	0,011	0,003	0,006
V18	c017	0,995	0,115	0,023	0,155	0,013	0,006	0,013
	c032	0,679	0,108	0,017	0,114	0,012	0,012	0,017
	c046	0,46	0,051	0,014	0,073	0,019	0,008	0,011
	c049	0,471	0,015	0,007	0,031	0,006	0,006	0,006
	c077	NN	NN	NN	NN	NN	NN	NN
	c095	0,788	0,089	0,011	0,076	0,007	0,011	0,013
V24	c025	0,791	0,064	0,01	0,037	0,007	0,002	0,007
	c043	0,154	0,008	0,007	0,017	0,005	0,007	0,009
	c050	0,317	0,025	0,008	0,073	0,013	0,006	0,008
	c059	0,477	0,067	0,024	0,069	0,025	0,017	0,025
	c069	0,191	0,021	0,007	0,022	0,008	0,004	0,004
	c081	0,721	0,134	0,024	0,131	0,018	0,014	0,023
	c087	0,221	0,056	0,013	0,08	0,018	0,012	0,012
	c093	0,346	0,062	0,015	0,091	0,013	0,008	0,012
V30	c003	1,083	0,038	0,023	0,088	0,037	0,017	0,039
	c030	0,004	0,002	0,009	0,011	NN	0,032	0,319
	c064	NN	0,047	NN	0,04	NN	NN	NN
	c089	NN	0,062	1,739	0,016	NN	NN	NN
	c091	NN	NN	NN	NN	NN	NN	NN
	c092	16,106	0,016	NN	0,021	NN	NN	NN
	c119	NN	NN	NN	NN	NN	NN	NN
	c122	NN	0,005	0,011	0,004	0,003	0,001	0,003
V36	c033	NN	0,455	NN	2,008	NN	NN	NN
	c076	NN	NN	NN	1,031	NN	NN	NN
	c102	NN	NN	NN	2,862	NN	NN	NN
	c152	NN	NN	NN	NN	NN	NN	NN
V42	c117	NN	NN	NN	NN	NN	NN	NN
	c143	NN	NN	NN	NN	NN	NN	NN
V48	c028	NN	NN	NN	NN	NN	NN	NN
	c055	NN	NN	NN	2,641	NN	42,104	NN
V54	c025	NN	NN	NN	NN	NN	NN	NN
	c033	NN	NN	NN	NN	NN	NN	NN
	c093	NN	NN	NN	NN	NN	NN	NN
V60	c037	NN	NN	NN	83,241	NN	NN	NN
	c142	NN	NN	NN	NN	NN	NN	NN
V66	c029	NN	NN	NN	NN	NN	NN	NN
	c045	NN	NN	NN	NN	NN	NN	NN
V78	c040	NN	NN	NN	NN	NN	NN	NN
	c058	NN	NN	NN	NN	NN	NN	NN

Figure 3.23. Heatmap of autologous neutralization for NAbs belonging to lineage PC94-A. Timepoints of isolation of these NAbs are shown below the name of the NAbs. Viruses are sorted by timepoint of isolation, shown in the first column. Values shown are IC_{50}. NN: non-neutralizing, NAbs: neutralizing antibodies.

Sensitivity to neutralization did not correlate with the presence or absence of the glycan at position N332. The loss of the PNGS in this position originates from 42 mpi, where the original asparagine in position N332 is replaced by a lysine. This is long after the autologous strains escaped from neutralization by the Abs from PC94-A lineage. Autologous viruses that exhibit a PNGS in position N334 are consistently seen after 54 mpi. Here again, there is no correlation in neutralization by these NAbs either as viral escape happened before.

One exception to this can be formulated for the viral isolate v18 c077. This virus exhibits an altered PNGS in position N332 by substitution of the serine in position N334 by a glycine. While this impairs the PNGS and abolishes all neutralization by lineage PC94-A antibodies tested here, this mutation is not found in later isolates, suggesting that, interestingly, despite the strong viral escape potential and evolutive advantage this would represent, it must also be associated with an important impact on viral fitness, or with an increased sensitivity to neutralization by other lineages, so that this sequence was not conserved.

Overall, sensitive isolates all bear the PNGS at position N332. However, the loss of the PNGS at that position does not appear to be the mechanism involved in viral escape.

For Abs belonging to the PC94-A lineage, potency seems to increase overall (corresponding to a decrease in observed IC_{50}s) with timepoint of isolation. However, the most mature NAbs originating from the latest timepoints are not the broadest NAbs, neither do they exhibit neutralizing activity for the longest period against autologous viruses. The NAb PC94-A.30, isolated from sample at V60 (55 mpi), seems to be able to retain a reduced but significant neutralizing activity months after the other Abs from this lineage have lost their neutralization capacity. The broadest NAb from lineage PC94-A against autologous viruses is also the broadest when tested against heterologous strains.

Altogether, these results suggest the large implication of mAbs from the PC94-A lineage to the autologous neutralization. Despite the broad and potent neutralizing activity of the Abs, viral escape occurs, as seen for other

bNAb lineages. The evolution of the autologous env allows for complete viral escape from lineage PC94-A after about three years of evolution.

3.3.2 Broadly neutralizing lineages exert autologous neutralization at different timepoints

These data can complete those obtained for NAbs isolated by previous colleagues and belonging to other lineages [274, 275]. Lineage PC94-A exhibits the most potent NAbs. Abs from the lineage PC94-A neutralized PVs with a much higher potency (mean IC_{50} = 0.78 µg.mL^{-1} versus 5.13 µg.mL^{-1}) than Abs from lineage PC94-B.

The timing of appearance of these NAbs also varied. As shown in **Figure 3.24**, lineage PC94-A seems to have been first to arise and quickly became the most prominent one, accounting for most of the neutralizing activity in early timepoints and demonstrating early maturation. The first NAbs isolated from this lineage PC94-A were recovered from timepoint V30. Lineage PC94-B probably appeared in a subsequent timeframe, with earliest NAbs being isolated from samples at 44 mpi (V48).

Lineages PC94-C and PC94-D have not been extensively studied for their role in autologous neutralization. Further studies on this matter will be required to draw solid conclusions. However, the data collected for a single mAb of each lineage suggests that these neutralizing lineages participated in autologous neutralization at later timepoints. The tested mAbs were isolated respectively from V66 and V78, suggesting these lineages were important for autologous neutralization after the virus had escaped the neutralization by lineage PC94-A and PC94-B Abs.

Altogether these data suggested a timely distribution of the autologous neutralization by the neutralizing lineages exhibiting the most important heterologous neutralizing activity.

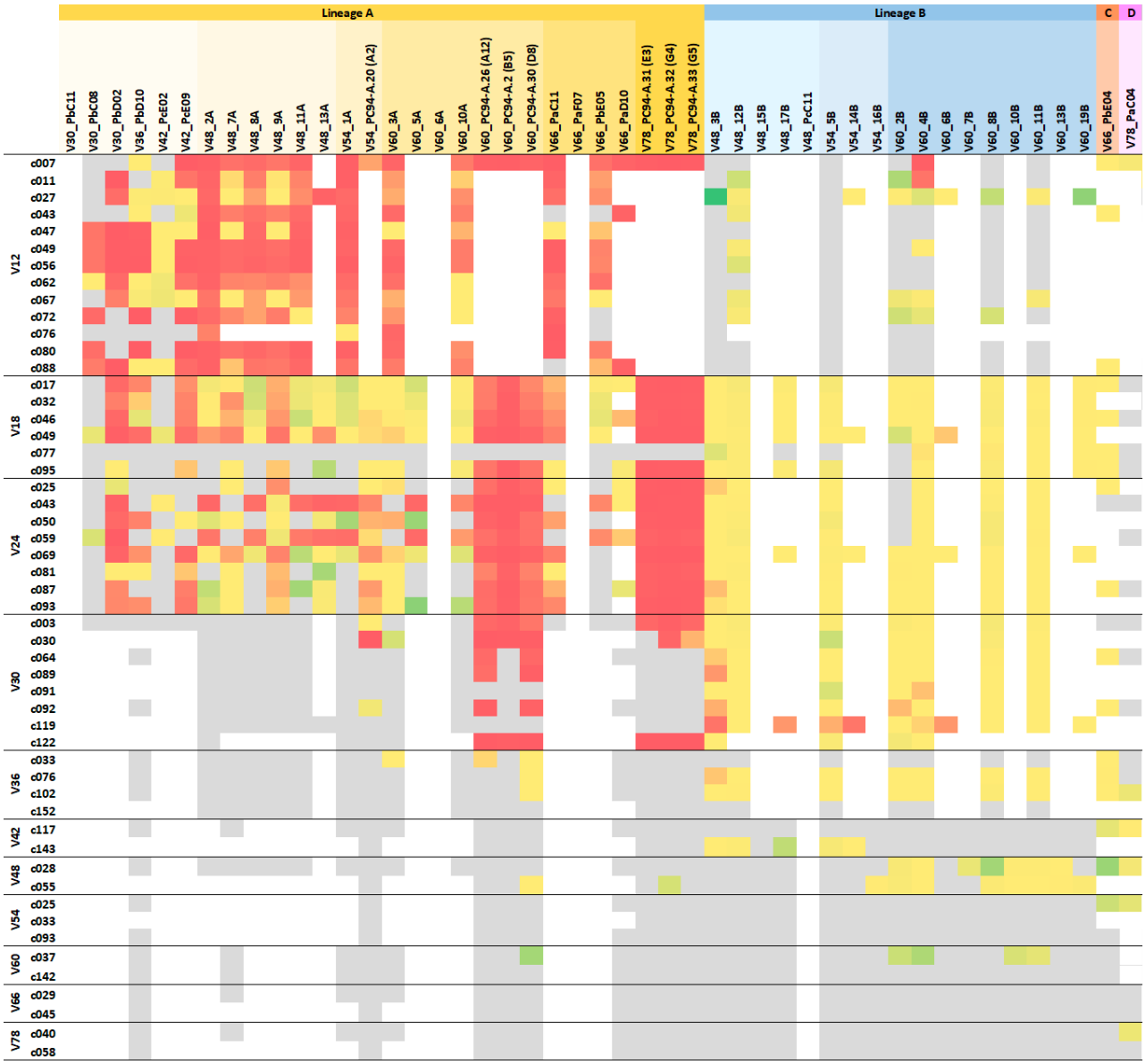

Figure 3.24. Autologous neutralization heatmap from selected recovered NAbs from PC94 using both techniques (single-cell and FACS sorting). Grey colored tiles correspond to absence of neutralization. White tiles denote the absence of testing. Both autologous viruses and recovered mAbs are organized by timepoint of isolation.

3.4 Antibody sequences from early samples reveal the maturation of neutralizing lineages

Neutralizing lineages isolated both in the present work and in previous sorts undertaken by our colleagues endorse a substantial role in both heterologous and autologous neutralization. Hence, understanding their origins and evolutionary pathways can inform on the mechanisms that allowed the development of this broad and potent neutralization. We therefore decided to study the origins and evolution of these neutralizing lineages. To do so, we performed bulk-NGS sequencing of the whole BCR repertoire from the earliest timepoints available. This helped us recapitulate the evolutionary trajectory of these lineages.

3.4.1 Evolutionary history of selected neutralizing lineages

We wanted to complete the neutralizing lineages previously described with sequences from early timepoints to better comprehend the origins of these lineages. For this, we performed bulk-NGS sequencing of the BCR repertoire at early timepoints (V18, V24, V30, V36, V42 and V48).

The heavy-chains of all BCRs were sequenced in bulk from these timepoints, as described in (see the "Methods, IX. Bulk NGS" section). A total of around 127 x 10^6 raw sequences were obtained (**Figure 3.25**) and clustered down to 1,189,082 unique sequences using UMIs. These sequences were therefore free of PCR- and sequencing errors. Sequences were annotated using AbStar and grouped into lineages with Clonify. A total of 106,647 different lineages were obtained. The largest lineage encompassed 11,730 Abs. The mean size of these lineages was 9.95 mAbs.

Among all these BCR sequences from the NGS dataset, we identified the BCR sequences that corresponded to the main neutralizing lineages isolated from single-cell sorts in this work (PC94-A, PC94-C and PC94-D) and from previous works (PC94-B) [274, 275]. We successfully recovered sequences from all four lineages in all six sampled timepoints. Therefore, all four neutralizing lineages were primed before 17 mpi. Unfortunately, the lack of samples predating this timepoint prevents us from exactly mapping the origin of these neutralizing lineages.

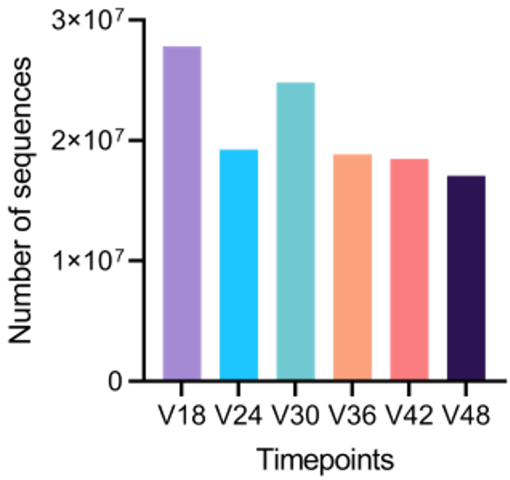

Figure 3.25. Sequence count per timepoint obtained from the bulk-NGS analysis of the BCR repertoire of PC94. Sequence counts presented here correspond to raw sequences, before UMI correction.

We next wanted to understand if the evolution of Abs within a neutralizing lineage was a constant process or if the evolution showed an irregular pace of maturation in donor PC94. To do so, we compared SHM rates of Abs originating from different timepoints in these neutralizing lineages (**Figure 3.26**).

Interestingly, different lineages exhibited very dissimilar maturation rates, with two main different profiles. Lineage PC94-A and PC94-D demonstrated a similar and relatively even evolution. In these lineages, SHM rates gradually rose from a mean 10-17% at V18 (17 mpi) up to around 30% at V48 (44 mpi). For the PC94-A lineage, for which we have extensive neutralization data, this suggests that the lineage evolved continuously over the sampled period at least. Neutralization breadth and potency of mAbs isolated from those timepoints however remains low. Potent bNAbs from this lineage were isolated from V48 to V78 and shared this mutation rate around 30%. This suggests that autologous viruses present at those timepoints might have played a role in the maturation of this neutralizing lineage toward breadth.

In contrast, SHM rates in lineages PC94-B and PC94-C remained relatively constant across all sampled timepoints. Lineage PC94-B had a distribution of SHM levels centered on 20-25% regardless of the considered timepoint. Lineage PC94-C exhibited divergent distributions at different timepoints, but

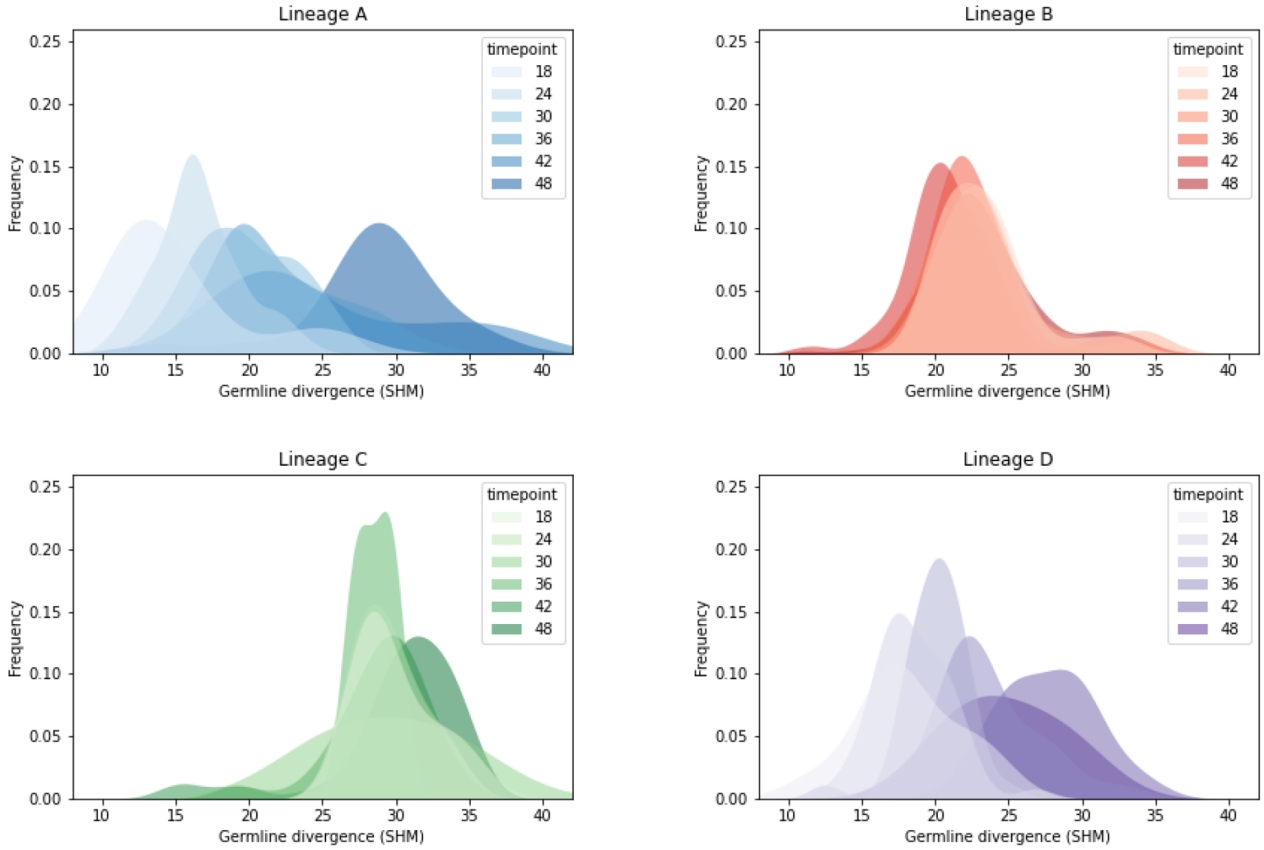

Figure 3.26. Distribution of SHM rate of BCRs at different timepoints explored. Different neutralizing lineages are shown separately. Germline divergence is shown as the nucleotide difference (%) to germline sequence within the V-gene of the heavy-chain. SHM: somatic hypermutation, BCR: B cell receptor

all of these distributions were centered around 25-30%. We formulated the following hypothesis for this observed divergence with lineages PC94-A and PC94-D: these data suggest that both lineages PC94-B and PC94-C may have evolved earlier than the first sampled timepoint at 17 mpi. The lack of sampling prior to this might be accountable for the apparent absence of evolution. Taken together then, these data suggest, for the PC94-B lineage, that this lineage evolved early in the history of the infection, fully maturating prior to 17 mpi (V18), and rapidly reaching a mutational ceiling. This might explain the relatively low breadth and potency observed, both in autologous and heterologous neutralization.

These differences should be evaluated regarding the outcome concerning neutralization. For one lineage, the evolution tended towards large breadth neutralization (PC94-A lineage), whereas the second lineage matured into a neutralizing lineage of reduced breadth (PC94-B lineage). However, these differences do not hold the comparison when taking into account the maturation of lineage PC94-D: despite a maturation history close to that of the broadly neutralizing lineage PC94-A, Abs from this family failed at developing broad and potent neutralization. Despite the high level of SHM observed in this lineage, neutralization breadth remained low.

3.4.2 Diversity of the immune receptor repertoire varied over the course of the infection

Next, we further studied the similarity of the BCR repertoire of PC94 at different timepoints when taking into account all sequences. The similarity was assessed by two different metrics: alpha diversity of the samples was assessed by the Chao1 index and the beta-diversity measured by both the Morisita-Horn distance and the Bray-Curtis dissimilarity index. The alpha diversity measures the variety of sequences present, considering both the number of distinct genetic sequences (richness) and the evenness of their distribution. High alpha-diversity indicates a greater variety of genetic material within a sample. In contrast, the beta-diversity represents the degree of similarity or dissimilarity between samples by taking into account the presence or absence and the relative abundance of different genetic sequences. High beta-diversity indicates that the genetic material in different samples is very different.

BCR repertoire rapidly changes, and we wanted to measure the distance between sampled repertoires, to put in perspective these changes in repertoire diversity with the rise of neutralization activity starting at 22 mpi (V24). Results are shown in **Figure 3.27**.

Regarding alpha-diversity, the repertoire sampled at V18 stands apart from others, underscoring a change in diversity repertoire between V18 and later timepoints. Repertoires from timepoints V24, V30 and V36 cluster together, suggesting a certain level of homogeneity within these repertoires. Finally, repertoires sampled at timepoints V42 and V48 belong to a third cluster, again denoting a change in diversity from V36. Regarding measures of beta-

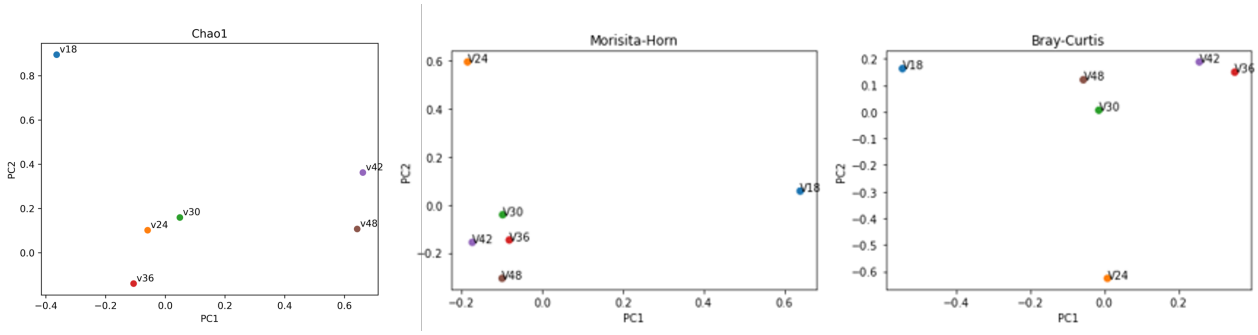

Figure 3.27. Representation of the two first components of a principal component analysis (PCA) of replicated measures of Chao1 index (alpha-diversity, left), Morisita-Horn (beta-diversity, center) and Bray-Curtis (beta-diversity, right) distances of BCR repertoires at different sampled timepoints. BCR: B cell receptor.

diversity, two samples are highly divergent from the other four, that cluster together, corresponding to a global shift in the BCR repertoire. Samples that appear at greater distance are earlier samples from visits V18 and V24. In contrast, samples collected later in the follow-up are closer together (samples from visits V30 to V78). This corresponds to the fact that distances between earlier repertoires are greater, both between them, and in respect to the later repertoires, whereas repertoires from later timepoints are less distant from each other.

We can hypothesize that the rate of evolution of the repertoire slowed down over time. This could explain the reduced distances observed in the beta-diversity measures over time. However, it is unclear if this evolution of repertoire diversity helped elicit broadly neutralizing responses.

3.4.3 Broadly neutralizing response was achieved in a repertoire built from known immunoglobulin alleles

We aimed to investigate whether donor PC94 made use of previously undocumented alleles of the immunoglobulin genes to generate the observed diversity in the immune repertoire. We used the IgDiscover tool [70] to infer germline sequences and compare those to the IMGT reference database (consulted in 2022) to assess differences. In our bulk-NGS approach, sequencing primers are situated in the 5' region of the FR1 region of the V-gene. The obtained sequences are therefore truncated at their 5' extremity. This artifact made IgDiscover consider all alleles as novel (not present in the IMGT database).

However, a manual re-analysis of the output data demonstrated that no new alleles were found, and that PC94 only used known and IMGT-listed alleles in his repertoire.

Overall, while the immune repertoire of PC94 seems to exhibit a substantial diversity, especially at timepoints contemporaneous of the elicitation of neutralization, it seems that the diversity did not arise from the use of novel, previously undocumented Ig gene alleles. Eliciting, in healthy subjects, bNAbs that resemble isolated bNAbs from PC94 would not be hindered by the required recombining alleles as these are not exceedingly rare.

3.4.4 A detailed analysis of the neutralizing lineage PC94-A

Isolated Abs from lineage PC94-A seem to bear most of the neutralizing activity and exhibit both the larger breadth and strongest potency. Therefore, we focused on this lineage to further explore this neutralization.

A continuous evolution

We first studied how the maturation of the neutralizing lineage PC94-A evolved and asked whether the evolutionary distance within lineage PC94-A reached a maximum at any point. To do so, we compared the germline divergence (or germline distance, GD) at the nucleotide level that is the Hamming distance to germline V-gene, with the evolutionary distance (ED) by calculating the ratio ED/GD. Obtained results per timepoint are presented in **Figure 3.28**.

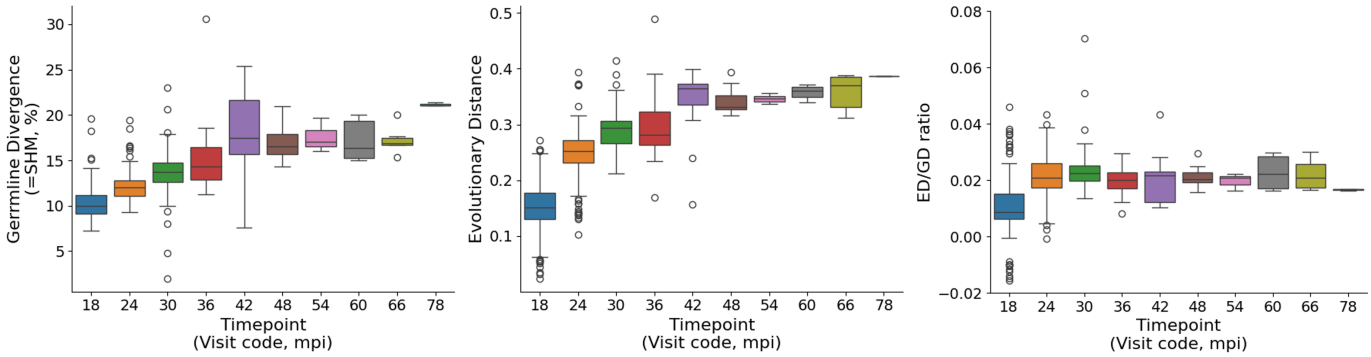

Figure 3.28. Germline Divergence (GD), Evolutionary Distance (ED) and ratio ED/GD over time observed for lineage PC94-A at different timepoints. Visit codes are used for timepoints, denoting theoretical months post-infection (mpi). SHM: somatic hypermutation.

The accumulation of mutations in the Abs from this lineage over time translates into an increased ED over the course of the 78 months studied, as seen in **Figure 3.28 left**. The GD of these same Abs also increased overtime. The ratio ED/GC remained overall constant overtime, suggesting that the maturation of the lineage continued: mutations continued to accumulate at novel positions. The overall constant ratio suggested a sustained evolution over the more than six years of follow-up. However, the rate of evolution seems to vary over the course of the infection. It appears that both the GD and ED first undergo a large increase between earlier timepoints, up to 42 mpi. After this timepoint the evolution rate seems to slow down, with both ED and GD showing relatively moderate increase. Interestingly, this slowdown in the rate of evolution seems to occur shortly after viral escape (around 36 mpi). It is therefore likely that the viral escape is responsible for a reduction in the antigenic stimulation provided to this lineage, which consequently slows down its evolution.

A progressive decline from the immune repertoire

The frequency of observed BCR sequences in the repertoire also varied over time for this lineage. For BCR sequences belonging to lineage PC94-A, frequencies observed across timepoints of follow-up are shown in **Figure 3.29**. Frequencies of sequences belonging to the neutralizing lineage PC94-A started to rise in initial timepoints sampled. Between V18 and V24, the frequency of these Abs almost doubled. This rise immediately precedes the onset of the heterologous neutralization as witnessed against a small 6-PV panel [189]. Interestingly, lineage PC94-A frequencies decreased after having peaked at V24 (22 mpi). This decrease is contemporaneous of the viral escape, as depicted in **Figure 3.24**. Frequencies of Abs belonging to this PC94-A lineage then seem to stabilize at around V42, at a frequency of 1 for every 10,000 B cell.

Complete phylogeny of lineage PC94-A

Up to this point, we have unveiled or suggested several features of the neutralizing lineage PC94-A. This lineage was elicited rapidly after the infection as it was present before V18. After heterologous neutralization was elicited, the frequency of Abs belonging to this lineage rapidly decreased in the immune repertoire, contrasting with the increasing breadth and potency. Finally, it

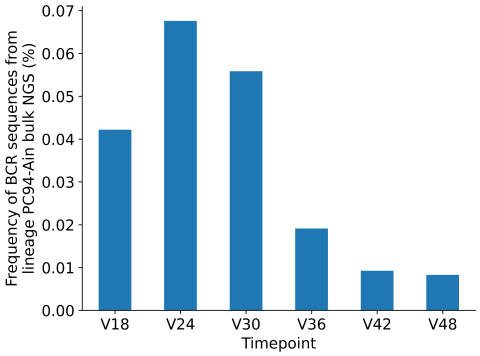

Figure 3.29. Frequencies of mAbs belonging to the lineage PC94-A per sampled timepoint as observed in the bulk-NGS sequencing dataset. mAbs: monoclonal antibodies, NGS: next-generation sequencing

seems that lineage maturation continued after viral escape, up to more than 6 years after infection.

To completely recapitulate the maturation in the PC94-A lineage, we collected all sequences available to build a large phylogeny. Collected NGS BCR sequences were grouped together with the corresponding previously isolated bNAbs both from our study and from the previous works on this donor to build a large phylogeny tree, thus recapitulating the evolution of the lineage. The phylogeny tree for lineage PC94-A is represented here in **Figure 3.30**. The tree is rooted with the germline V-gene sequence (IG_HV1-18) as an outer group. The tree seems to be divided into two regions: one spanning over later timepoints, with more mutated Abs. In this region, bNAbs isolated from both FACS sorts and single-cell sorts are homogeneously combined with sequences retrieved from bulk-NGS sequencing. The other region, exhibiting more sequences from earlier timepoints, is devoid of sequences from single-cell sorts of FACS sorts and corresponding sequences were retrieved only from bulk-NGS experiments. While this is expected (samples from timepoints V18 and V24 were never used in any of these sorting experiments), it probably also corresponds to a lower affinity to the HIV Env antigen of the less mature BCR.

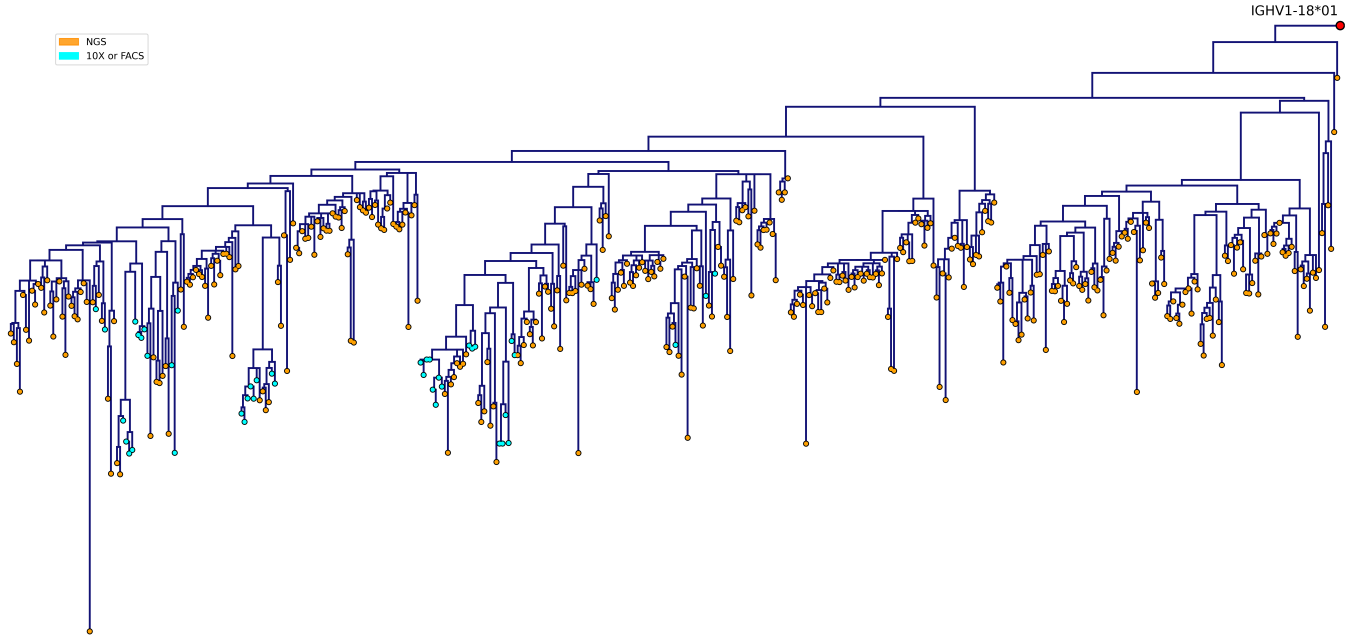

Figure 3.30. Phylogeny tree for Lineage PC94-A antibodies. These include mAbs isolated with the FACS-sorting approach or single-cell sorts (cyan) and bulk-NGS technique (orange). The tree is rooted with the germline V-gene (IG_HV1-18) as the outer group (red). Sequence alignment of heavy-chains was performed at the nucleotide level with MAFFT, the tree was reconstructed using FastTree and the representation made with Baltic (see Table 6.1). mAbs: monoclonal antibodies, NGS: next-generation sequencing.

Finally, these phylogenies allowed us to identify observed sequences close to the ancestral B cell from which these neutralizing lineages arise (UCA). The observed sequence proximal to the germline sequence exhibits a SHM rate of 2.9% at the nucleotide level, corresponding to a single mutation difference with the naive-B cell that initiated the development of this lineage.

3.5 The epitopes targeted by isolated neutralizing lineages

3.5.1 The best neutralizing lineages target the high-mannose patch and are dependent on the glycan at position N332

The serum neutralization of donor PC94 was initially mapped to the V3-Glycan region. We therefore hypothesized that lineage PC94-A was also targeting this epitope. We verified the impact of removing the N332 PNGS on the activity of newly isolated bNAbs from lineages PC94-A, PC94-B, PC94-C and PC94-D. A first assessment was performed using ELISA to test for specific binding activity to gp120 from the JR-FL strain depending on the presence of a glycan at position N332.

The results for the PC94-A lineage are shown in **Figure 3.31**. The removal of the PNGS at position N332 by substitution of the asparagine (N) for an alanine (A) nearly abolished binding of lineage PC94-A NAbs by an average 99% [96; 100]. This data strongly suggests that NAbs in this lineage target the N332 supersite, with the glycan (or side-chain) in position N332 being a major part of the antigenic determinant. Of note, these binding data are not in complete agreement with neutralization data. In the case of neutralization, the presence of the asparagine, hence the PNGS, at this position is not always required for neutralization. Indeed, some viral strains are neutralized despite the absence of the asparagine at position 332. Conversely, some PVs harbor this AA but are insensitive to neutralization.

Similarly to PC94-A lineage NAbs, NAbs from PC94-B lineage exhibited a substantial loss of binding upon substitution of the amino-acid in position N332 (**Figure 3.32 top**). This suggests that the epitope targeted is also localized within the N332-supersite. Notwithstanding, one of the NAbs tested from this lineage (PC94-B.06) seems to be capable of sustaining, at least

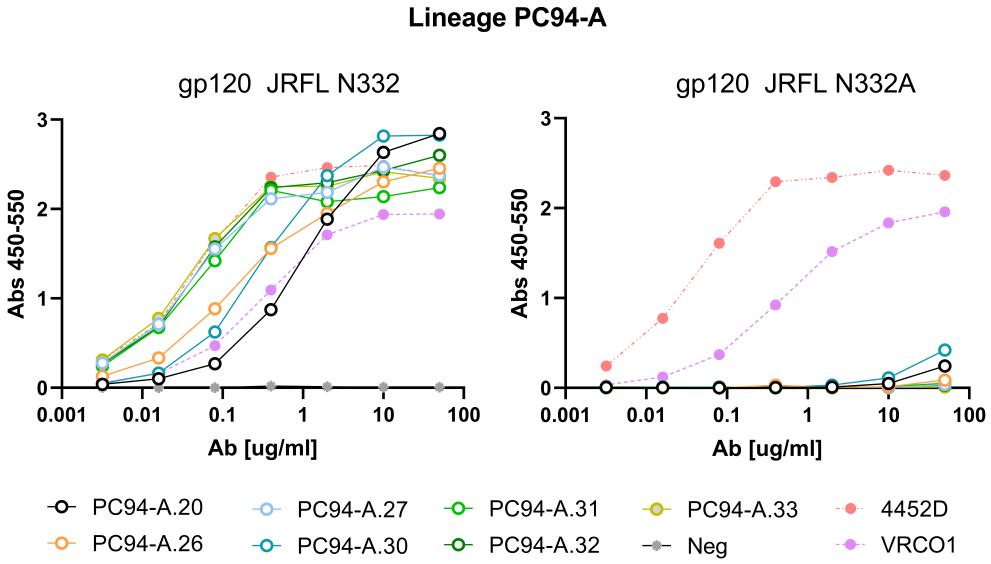

Figure 3.31. ELISA assays assessing binding capabilities of selected Lineage PC94-A mAbs to monomeric gp120 (**Left**) WT or (**Right**) mutated in position N332A. The gp120 used corresponded to the PV JR-FL. Control antibodies 4452D and VRC01 do not target the high-mannose patch and do not bind to the glycan in position N332. PV: pseudovirus

partially, the loss of the PNGS at position N332. Dependency on other glycans within the region remains to be fully determined.

3.5.2 The epitopes targeted by other lineages remain uncharacterized

Conversely, mAbs from lineages PC94-C and PC94-D appeared to be resistant to the loss of the PNGS at position N332, NAbs from both lineages showing no significant difference in binding upon removal (**Figure 3.32**). These NAbs are thus unlikely to target the high-mannose patch, and no further assumption can be made about the epitope targeted by mAbs of these two lineages.

In order to define the epitopes targeted by all four lineages (PC94-A, PC94-B, PC94-C and PC94-D) members, we are currently performing structural analysis using electron microscopy.

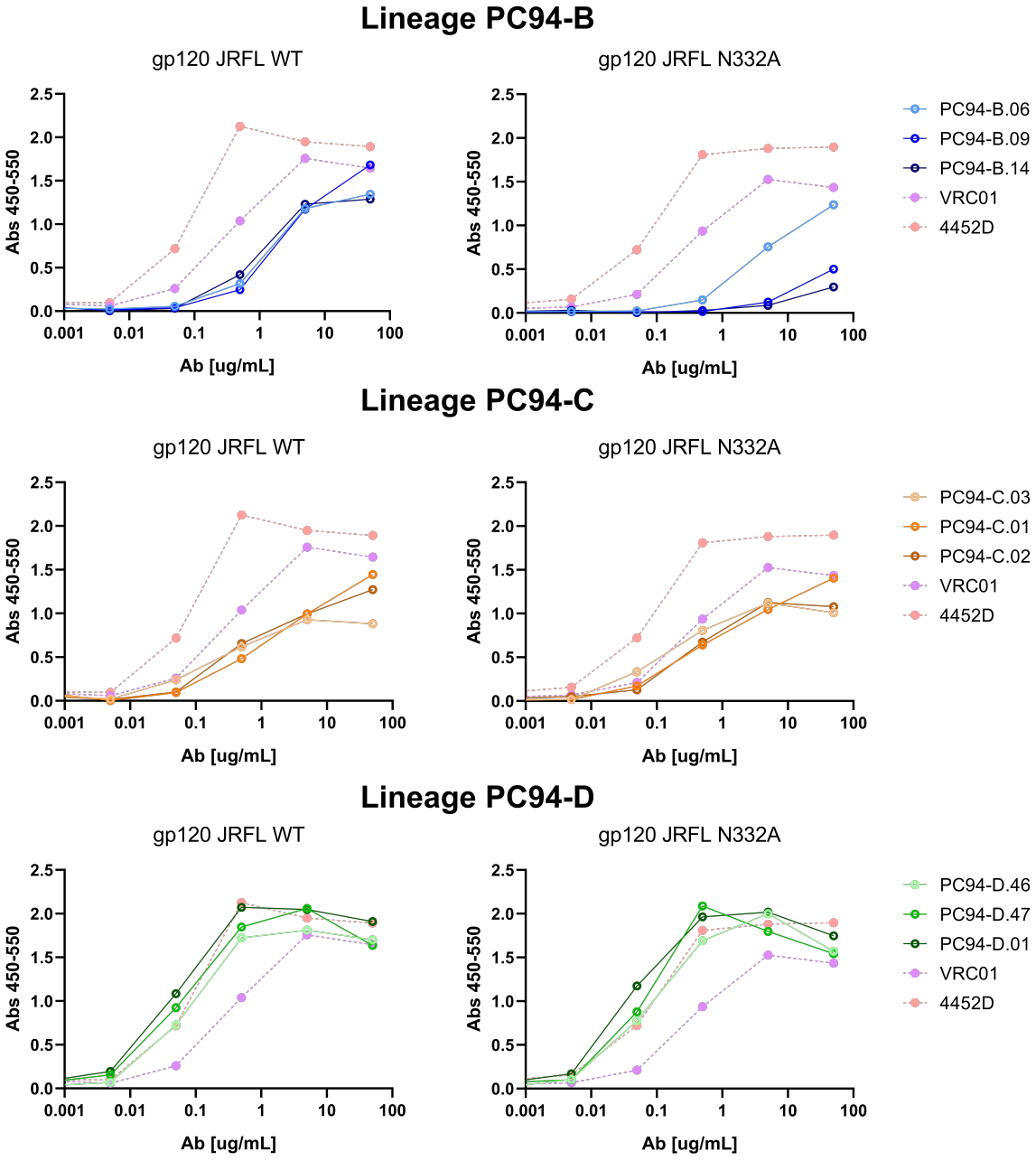

Figure 3.32. ELISA assays assessing binding capabilities of lineages PC94-B, PC94-C and PC94-D mAbs to monomeric gp120 (**Left**) WT or (**Right**) mutated in position N332A. The gp120 used corresponded to the PV JR-FL. Control antibodies 4452D and VRC01 do not target the high-mannose patch and do not bind to the glycan at position N332. PV: pseudovirus

3.6 The evolution of autologous HIV env

To determine whether specific viral features could be at the origin the broadly neutralizing lineage PC94-A, we decided to study sequences from all available autologous viral viruses. Circulating HIV strains in donor PC94 were sequenced for their env gene across several timepoints and thus reflect, in part, the viral evolution under the selective pressure driven by the immune responses. Sequencing by SGS was performed by Monogram BioSciences. A total of 210 unique sequences were obtained from all eleven timepoints of follow-up. An ancestral/founder sequence was inferred and is referred to as the most recent common ancestor (MRCA). These sequences had a mean length of 2559 nt, roughly corresponding to the full-length env sequence (GeneBank: K03455.1).

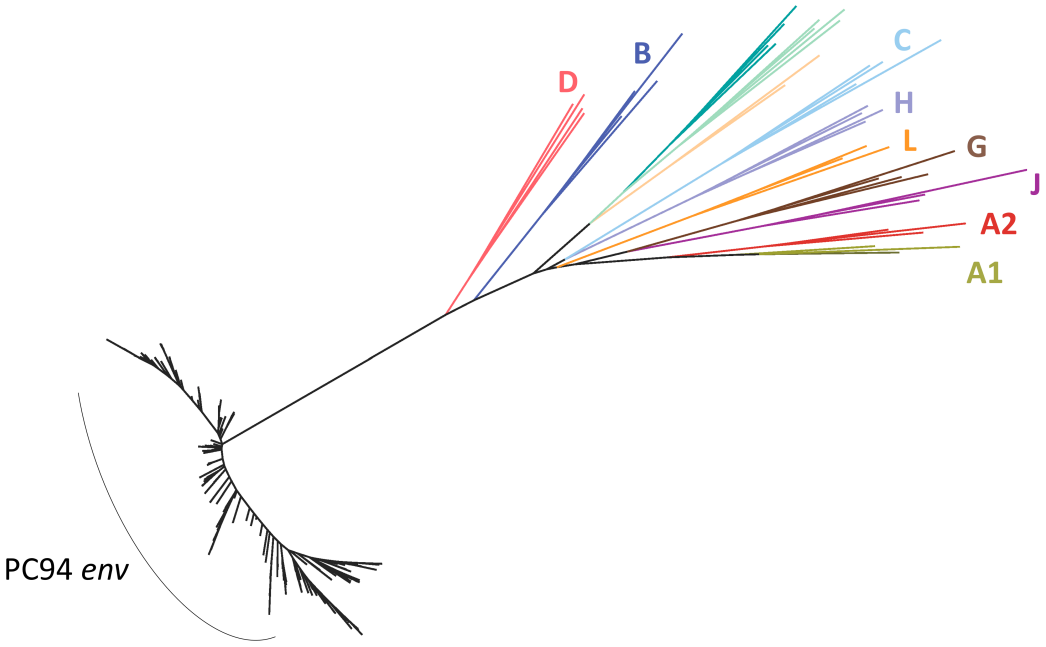

Figure 3.33. Unrooted phylogeny tree of PC94 *env* viral sequences (black) along with reference sequences from various HIV-1 group M subgroups/clades (shown with different colors). Closest to PC94 autologous viruses are sequences from clade D (shown in red). Heterologous env sequences were retrieved from the Los Alamos Reference Database.

We first wanted to verify the clade of the infective strain and place these sequences within the overall phylogeny of HIV evolution. To do so, we aligned

these sequences with a pre-computed alignment retrieved from the reference database (Los Alamos HIV database). The resulting unrooted tree is visible in **Figure 3.33**. As expected, the sequences obtained from donor PC94 clustered together, and, the sequences that clustered the closest to those of PC94 belong to clade D from HIV-1 group M.

3.6.1 A spike in diversity is contemporaneous of the elicitation of neutralization

Next, we inquired about the evolution of this HIV env gene sequence and the variation of the evolutionary rate across sampling timepoints. For each sequence we calculated the distance (Tamura-Nei distance TN93 (Tamura and Nei 1993)) to possible progenitors (i.e. sequences isolated at the previous timepoint). The obtained distances were plotted and a trend line was added along with the standard deviation error. Results are displayed in **Figure 3.34**.

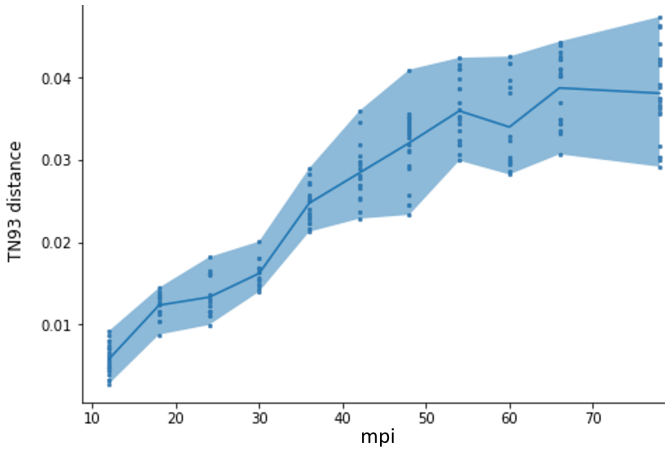

Figure 3.34. Genetic distance (TN93 distance) of autologous HIV *env* from possible progenitors (sequences from precedent timepoints) over time. Confidence interval is shown in lighter blue fill. The greatest increase in sequence distance is observed between timepoints 30 and 36.

This suggests that the evolution rate of the HIV Env gene is not constant in PC94 over time. Moreover, there seems to be a greater increase in genetic diversity between 28 mpi (V30) and 33 mpi (V36), suggesting an accelerated pace of mutation. This spark in genetic diversity is contemporaneous of the onset of the heterologous neutralization. These timepoints (V30 and V36)

are also the ones from which the first NAbs belonging to the neutralizing lineage PC94-A were isolated, suggesting that these two events (increased viral diversity and the appearance of the broad heterologous neutralization) may be related.

3.6.2 A shift in glycan occupancy could explain viral escape

As Abs from the neutralizing lineage PC94-A target the HMP and the glycan residue at position N332, we sought next to observe the modifications of glycosylation of the Env over the course of the infection. We first counted the PNGS present in the env sequences. We observed the evolution of this count according to the timepoint of isolation of these sequences. Results are illustrated at **Figure 3.35**.

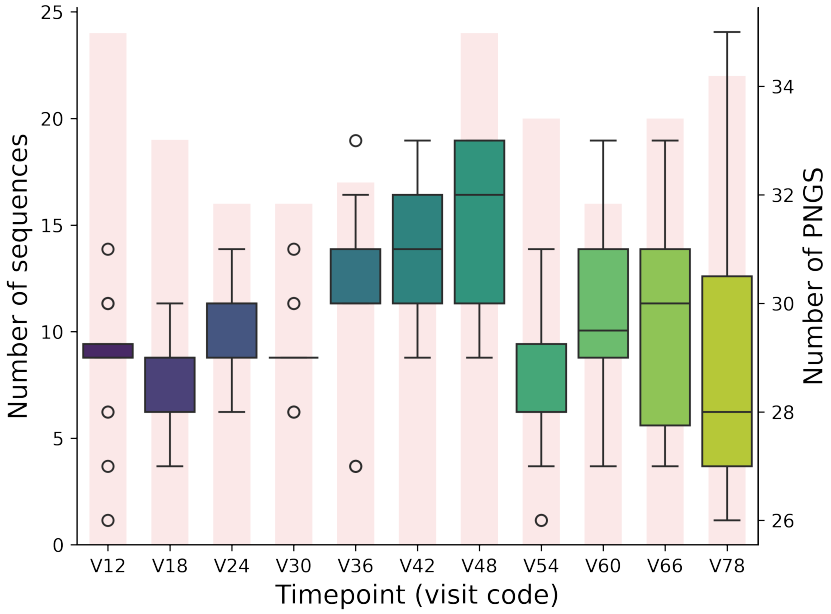

Figure 3.35. Number of PNGS in the *env* sequences per timepoint of isolation. PNGS were counted in the entire sequence, regardless of position (boxplots, right y axis). The number of sequences available is given in light-red bars (left y axis). PNGS: potential N-linked glycosylation site.

The number of PNGS available in early sequences is remarkably constrained (median = 29.0 ± 1.0 PNGS), whereas the diversity of PNGS numbers widely increases over the course of the infection, however the absolute count seems to

slightly decline (median = 28.0 ± 2.6 PNGS). Unlike the diversity of nucleotide sequence, the diversity of PNGS in these sequences does not show a strong increase between timepoint V30 and V36 (28 mpi and 33 mpi). The number of PNGS however increases. The largest increase in the distribution of PNGS numbers seems to be between the V54 and V66 timepoints (50 and 61 mpi).

We next looked at the presence or absence of specific PNGS at key positions that could be involved in the epitope targeted by Abs from neutralizing lineage PC94-A. These are mainly PNGS in the V3-glycan region (N295, N301, N332, N334). We also monitored key positions from the CD4bs (N276) and the V2-Apex (N160) supersites. We analyzed these positions in regard with the autologous neutralization provided by the bNAbs from lineage PC94-A, PC94-B or by all isolated mAbs combined. Results obtained are illustrated in **Figure 3.36**.

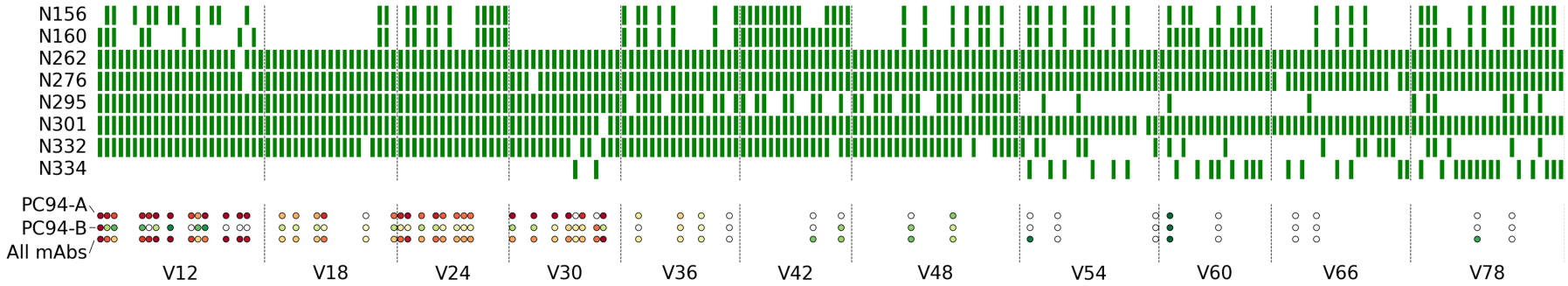

Figure 3.36. Presence of PNGS at key positions in *env* sequences isolated from our donor. For each viral isolate, a green bar denotes the presence of a PNGS. Sequences are ordered by timepoint of isolation. Corresponding autologous neutralization is shown as the geomean of half-complete inhibitory concentrations for NAbs of the lineage PC94-A (top row), PC94-B (middle row) or for all isolated mAbs (bottom row). PNGS positions are given according to the HxB2 numbering scheme. PNGS: potential N-linked glycosylation site

The presence of a PNGS at position N332 seems to correlate well with the autologous neutralization by NAbs of PC94-A lineage, as observed between V12 and V30 (28 mpi). The three autologous viral isolates devoid of a PNGS at position N332 before V36 (33 mpi) are resistant to neutralization by these NAbs. For two of them (both at V30), the PNGS at position N332 is lost to the less frequently seen PNGS at position N334. While not neutralized by any of the NAbs isolated, the viral isolate from V18 devoid of a PNGS at position N332 does not further translate into viral escape, suggesting that the viral fitness is highly impacted in this strain.

Autologous neutralization by isolated NAbs does exactly parallel the progressive loss of the PNGS at position N295. However, we suspect that the removal of this PNGS plays a role in viral escape, as this is only seen from V36 and following timepoints. PNGS at position N276 and N160 do not correlate with neutralization. This suggests that none of the isolated NAbs target the CD4bs nor the V2-Apex supersites, respectively. Or they do so in a glycan-independent manner.

Finally, the PNGS at position N334 seems to gradually replace the PNGS at position N332. This is mostly seen from V54 and ongoing timepoints.

3.7 The transcriptome of bNAb-producing B cells does not differ from the one of non-bNAb-producing B cells

Finally, we took advantage of the availability of transcriptomic data for isolated cells to explore the transcriptome of HIV Env-specific cells. We sequenced the transcriptomes of the single-sorted cells by NGS. Transcriptomic data from both 'early timepoint' samples and 'late timepoint' samples were jointly analyzed. After sequence demultiplexing and quality control of the data, cells were clustered based on their gene expression level profiles. We then identified cell types in these clusters using both manual annotation with relevant cell surface markers and automated cell type inference as described in Methods (see paragraph "Cell population and transcriptome analysis"). Cell clusters along with cell type identified are shown in **Figure 3.37**. Monocytes and T cells were removed from further analysis as our investigation focused on B cells.

Figure 3.37. Representation of cell populations after manual identification of cellular types from transcriptome data. Cell clusters were obtained after principal component analysis (PCA) and UMAP representation of the two most relevant PCA-dimensions. All 42,469 cells are represented in this figure.

We questioned whether a bNAb-producing B cell would express a different set of genes (different expression profile) from cognate cells from which the secreted corresponding mAb did not achieve significant breadth or potency. In a similar manner, we asked if HIV Env-specific B cells had a different gene expression profile from B cells of other BCR specificity (non-HIV Env).

Focusing on B cells, there were no differences in repartition in naïve and memory B cells between HIV Env specific B cells and non-specific ones. Moreover, we calculated the Morisita-Horn similarity index between these two populations (HIV Env-specific B cells and non-specific B cells). This index was equal to 0.99, acknowledging that there was no difference in these two populations.

All the cells from which we expressed NAbs belonging to the PC94-A lineage and exhibiting broad neutralizing activity arose from the activated memory B cell compartment (**Figure 3.38 Left**).

As expected, a continuous gradient was observed in the divergence from germline (SHM rate) of immunoglobulin genes between naïve B cells and

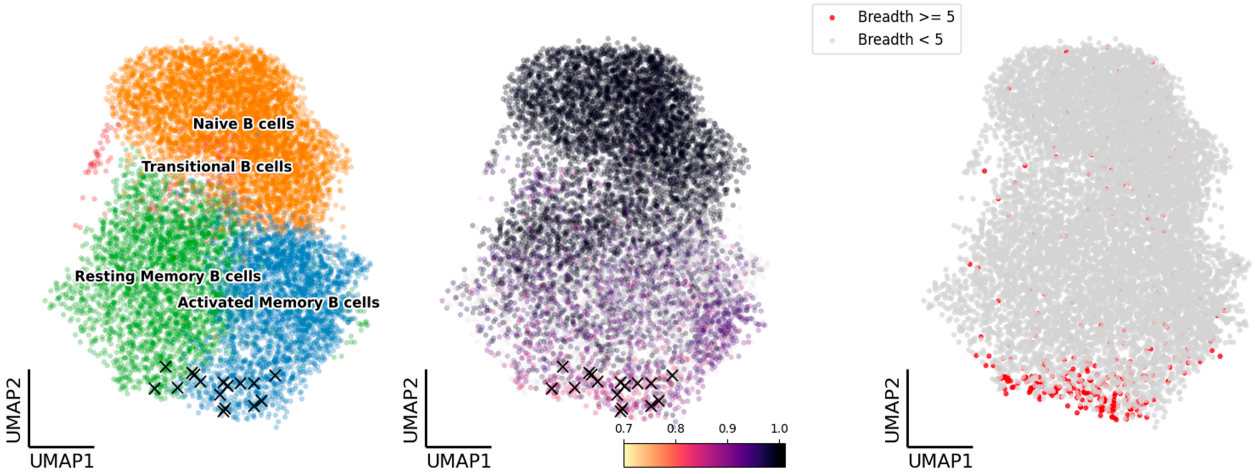

Figure 3.38. Left. Distribution of B cell populations, **Center.** Germline identity of V-genes from heavy chains and **Right.** Breadth of binding of HIV Env specific B cells. The bNAbs belonging to lineage PC94-A are highlighted with a black (X) mark. bNAbs: broadly neutralizing antibodies.

MBCs (**Figure 3.38 Center**). This was true for both resting MBCs and activated MBCs. All NAbs exhibiting breadth and potency were recovered from B cells situated at the extremity of this gradient. This underlined the length of the maturation path these cells undergo.

We then selected cells for which binding to HIV Env trimers was significantly greater (binding to more than 5 HIV Env trimer baits). Compared to others, broadly binding HIV Env-specific B cells were mainly grouped within the MBC cluster. Furthermore, if we consider the maturation gradient previously described, broadly-binding HIV Env-specific B cells were co-localized with B cells that had highly-mutated V-genes. This confirms the hypothesis that breadth is notably acquired through affinity maturation (**Figure 3.38 Right**).

Further clustering of these cells was attempted to try to isolate differential gene expression patterns between cells bearing broad neutralizing capacities and those that do not harbor such capacities. However, intra-population clusters of cells were not reliably obtained. An iterative approach used with the Cytocipher tool demonstrated highly variable cluster composition. This suggested that no differences could be found between broadly binding cells and cells exhibiting lower binding breadth.

Chapter 4

DISCUSSION

We used the Chromium Single Cell Immune Profiling approach to investigate the development of neutralization and breadth in a donor primarily infected with an HIV-1 subtype D viral strain, followed up for over 6 years without the introduction of ART. From clinical samples spanning the period of breadth development in this elite neutralizer, we identified sequences of thousands of Abs with putative specificity directed against HIV Env trimers. These Abs were ranked according to their probability of being bNAbs based on their apparent ability to bind to HIV Env trimers of different strains. Subsequently, we expressed and tested 104 of these Abs for neutralization, demonstrating the presence of neutralizing abilities in at least 21 lineages. Notably, considering previous isolated NAbs from the donor, NAbs from four lineages together recapitulated 88.7% of the breadth of neutralization of the serum when tested against a 126-PV panel. Below we discuss these findings in relation to previously obtained results for the donor and to relevant literature.

4.1 HIV Env-specific B cell repertoire

Broadly NAbs to HIV often display unusual characteristics such as high SHM rates [370, 147], presence of large insertions or deletions in the variable region [340], significant mutations in FR regions [235], or in some cases, unexpectedly long CD_HH3 [340, 95, 309]. Correspondingly, we observed in our work that B cells exhibiting large breadth of binding to trimer baits tend to have longer CDR_H3. In spite of this, B cells exhibiting large breadth of binding were extensively tested, and neutralizing lineages did not harbor especially long CDR_H3.

Despite the extensive number of studies on bNAbs, isolation of a bNAb recovered as an IgA has only been achieved recently [160]. In our work, IgA proved to be abundant, in the HIV Env-specific B cells subset. The proportion of IgA recovered tends to increase with increasing breadth of binding to trimer baits. Furthermore, broadly neutralizing lineages harbored IgA, and, in some

cases, these were among the broadest and most potent bNAbs. Recent works have studied in depth the role of IgA in HIV neutralization [207]. In this study, the IgA fraction of the serum exhibited neutralization, albeit of lower potency and restricted breadth compared to its IgG counterpart. The authors observed IgA-mediated heterologous neutralization in 30% of screened elite-neutralizers, suggesting that IgA (b)NAbs develop more rarely than their IgG siblings. They isolated IgA bNAbs that exhibited 50% breadth when tested against a small screening panel, closely recalling our findings. PC94-A.33, our best IgA bNAb, achieved 63.6% neutralization against 33 PVs.

Furthermore, they demonstrated in IgA-engrafted mice models of the infection, that the IgA bNAb significantly prolonged viremic suppression by delaying viral rebound by 37% compared to the control IgG-engrafted mice. Their data, along with the evidence we provide of significant presence of IgAs in an elite-neutralizer, suggests an important role for these IgAs in in-vivo protection. Further investigations are definitely awaited. In addition to IgAs, we recovered a substantial population of B cells of IgM subtype. In a study utilizing the same scRNA-seq approach to explore the Ab repertoire of BK virus-infected transplant recipients, Nguyen and colleagues observed similar results [237]. In our work, IgM B cells represented 48.0% of all recovered cells, regardless of the specificity. In the HIV Env specific compartment, IgMs represented 77.0% of the recovered B cells.

However, we observed an important discrepancy in the origin of these cells. Here, the overall proportion of naive IgM B cells (as defined by a V-gene sequence identical to germline, devoid of mutations) was roughly equivalent to the proportion of mutated IgM memory B cells (53.2% vs 46.8%, respectively). In the HIV Env-specific population, this proportion remained steady: 52.6% vs 47.4%. Conversely, in their BKV study, the authors reported a higher proportion of IgM memory B cell (MGM) in the BKV-specific population. They suggest that this might be driven by preferential extra-follicular maturation of BKV-specific B cells into these MGMs. This might not be the case in the context of an HIV infection, suggesting divergent immune responses to these two chronic viral infections, especially in the extra-follicular compartment.

The HIV Env-specific repertoire we isolated had nevertheless some unusual features. When comparing the frequencies in VH-gene usages between the HIV Env-specific repertoire and a baseline frequency (either from PC94 through unbiased bulk-NGS sequencing or compared to healthy donors), the overall frequency of use of the V-gene VH4-34 was significantly increased. The use of the V-gene VH4-34 was substantially higher in HIV Env-specific B cells capable of broad binding compare to those devoid of such capacity, or to non-HIV specific B cells. Intriguingly, several bNAbs isolated from other donors and targeting the V3-glycan supersite make use of this V-gene [210, 307, 161]. Furthermore, this V-gene is involved in autoreactive properties of corresponding B cells, due to the presence of a specific motif (QW AVY) in the FR1 region [257]. These B cells are rendered anergic during the immune response maturation [264], but can get activated under certain circumstances as is seen in autoimmune diseases, such as lupus, or in chronic infections, such as in our case, HIV. In this latter situation, the autoreactive motif can be eliminated in a process named clonal redemption [43].

In our case, the over-representation of this V-gene in broad binders is due to multiple lineages with few member Abs (usually one or two) rather than a single expanded lineage, and, none of the tested Abs bearing this V-gene exhibited heterologous neutralization. Almost all B cells making use of this VH gene conserved the QW AVY autoreactive motif in our dataset. Only 2.9% of these VH4-34 HIV Env-specific B cells lacked this motif, suggesting these few B cells could have undergone clonal redemption.

4.2 Strategies in scRNA-seq approaches

In our work, we have proceeded with this technique on the basis of a proof-of-concept study published a few years earlier [293]. In this study, the authors isolated bNAbs from two HIV-infected donors for whom the presence of neutralizing lineages was known. Prior to Ab isolation in these donors, they demonstrated the feasibility of the approach using cultured cells expressing BCRs of known specificity. We considered their work a striking demonstration of the validity of the approach.

In their study, they collectively used a maximum of 9 baits, 5 of HIV relevance and 4 constructs from hemagglutinin proteins from the influenza virus,

to isolate specific B cells from a single timepoint sample. In one donor, this allowed for the recovery of 1465 antigen positive B cells, from which they isolated two bNAbs, that neutralized 79% of a small 14-PV screening panel. Interestingly, they observed a good correlation between the binding observed in scRNA-seq and the neutralization, although this was only based on the data of these two NAbs and for two HIV Env sequences that were present in both assays. We have leveraged their proof-of-concept and validation study to replicate in some aspects their work, by scaling up the extent of the study in many regards. Their findings are corroborated in many ways by our results. For instance, they underlined the association between SHM rates and the number of baits bounds, as we did.

This scRNA-seq approach has also been extensively used in the context of the COVID-19 pandemic, to isolate NAbs to SARS-CoV-2. Different groups have performed this in animal models [361, 100] or in humans [52, 151]. Some of these studies were performed on longitudinal cohorts [342]. And different groups used different strategies to efficiently identify, from thousands of B cells recovered, the select few that could correspond to NAbs.

In their work, Cao and colleagues have detailed a strategy to the Ab recovery problem [52]. Isolating more than 8500 lineages from 60 different donors, they chose to produce and test Abs that fulfilled the following criteria: mAbs must belong to an expanded clonotype, as they hypothesized that neutralization would be more frequently seen in these lineages. We shared this hypothesis. Next, they selected exclusively lineages containing IgG1 Abs and devoid of IgG2 Abs, on the basis that IgG1 sustain strong responses to viral infections, as opposed to IgG2. We have not implemented this strategy. Finally, they selected sequences from MBCs only (understandably discarding naïve B cells and exhausted phenotypes) that displayed some level of SHM, based on the hypothesis of a necessary affinity maturation. Together, these criteria allowed the selection of 169 candidates out of $\geq$50,000 B cells, recalling the extent of the selection we performed (249 cells initially selected out of 42,469).

In both cases the strategy seems to have been successful: Cao and colleagues isolated 14 potent bNAbs, and we recovered several neutralizing lineages, some of which had extensive neutralization capabilities that together recapitulated

most of the serum activity. Overall, in our work, breadth of binding showed a good correlation with the neutralization breadth. B cells recovered for which the binding to HIV En trimer bait was extensive often demonstrated neutralization. However, some defects persist: for individual baits, we were unable to show a direct correlation of binding with neutralization of the corresponding PV. This suggested some limitations to the use of baits in these scRNA-seq approaches. The complete absence of recall of lineage PC94-B in our dataset further underlines these restrictions. Several hypotheses can be formulated to explain these limitations. One first hypothesis concerns the baits we used. We cannot rule out the possibility that one or more baits exhibited a conformation different from the one that is found in surface-bound native Env glycoprotein. The extent of our assessment of the correct antigenicity of the trimers remains limited, hence individual trimers could have a different antigenic profile from native Env. This was probably the case for BG505 T332N (as we mentioned, it was excluded from our analysis), but the correct conformation of the other baits cannot be strictly guaranteed.

Whether adding more bait to respond to this caveat is debatable. The final selection of mAbs that are the broadest binders could be improved with an increased number of baits. However, this would probably increase the risk of a trimer to showcase some level of polyreactivity, hence increasing the number of unwanted cells. Concerning linage PC94-B, the reasons why we were not able to recover any members of this lineage remain unclear. Almost all NAbs from the PC94-B lineage (21/22) were previously isolated using mgp120 [274]. These NAbs are capable of neutralization, albeit of low potency, hence they must be able to recognize the Env trimer on the virus. However, our trimers used as baits proved insufficient to recover any PC94-B mAb. Several hypotheses can be formulated: the soluble recombinant trimers might substantially differ from trimers at the surface of virions. However, we successfully recovered NAbs from other neutralizing lineages. The second hypothesis is that lineage PC94-B Abs are directed against an epitope that is relatively difficult to access on the trimer (e.g. with a narrow angle of approach), against an epitope that is only partially exposed, or rendered more accessible upon conformational changes following CD4 binding. This could possibly explain why it was successfully primed by mgp120 in the first sort. In our case, this could translate into a reduced affinity for the trimers. In turn, this could suggest

the presence of an affinity threshold under which isolation using trimer baits is not possible. Other hypotheses, such as a sampling bias or an amplification issue can probably be ruled out: the sampling in our case concerned more timepoints than previously achieved sorts. And the Ig genes that were used by Ab members of this lineage were successfully observed in others cells, ruling out a possible amplification bias. Overall, we have no definite explanation for this absence of recovery of PC94-B mAbs in our experiments.

4.3 Isolated bNAbs and perspectives

Notwithstanding this unrecovered lineage, we successfully isolated bNAbs with substantial breadth and potency. As seen by the heterologous neutralization of the serum, PC94 is a top neutralizer, ranking second among more than 400 donors from the Protocol C cohort. This strongly suggests that the magnitude of the serum neutralization does not necessarily translate into the presence of a single of few bNAbs of extraordinary neutralization capabilities. As it has been suggested, the extent of the neutralization by the serum might often be recapitulated by several neutralizing lineages of narrower breadth and potency [289].

Concerning the isolated bNAbs however, whether they could be further developed to translate into clinical development is debatable. Concerning passive immunization, the existence of several bNAbs with both larger breadth and increased potency tends to suggest that the perspectives of development of our bNAbs are limited. Nevertheless, Ab engineering could help enhance the characteristics of our bNAbs. On the other hand, developing immunogens to elicit bNAbs of the PC94-A class in an immunization strategy might offer a better perspective to our work. The evolutionary pathway that led to the development of breadth and potency in this lineage as depicted here could lay the ground for the development of a series of immunogens. Key arguments to support this are a relatively low SHM rate that is achievable through vaccination, the absence of insertions and deletions (indels) that are difficult to elicit, a CDR_H3 of modest length, and the absence of polyreactivity observed at different steps of the maturation process. Furthermore, the PC94-A lineage bNAbs use the IG_HV1-18 gene, whose frequency in the general population is relatively high [37]. Taken together, these features suggest that PC94-A class

bNAbs could be easier to elicit compared to some bNAbs isolated from other donors. However, the relatively limited breadth could temper this perspective. Future studies on the binding capabilities of the UCA and intermediates in the bNAb maturation could provide interesting insights on the feasibility and ease of translating this work into immunogens capable of priming and shepherding the maturation of PC94-A lineage. Ongoing structural studies should provide us with details about the epitope targeted as well as contact-making residues implicated in the paratope. This should help in clarifying potential perspectives for this work.

Beside the work achieved on donor PC94, the advent of high-throughput techniques allows us to envision future studies making use of this single-cell approach. Combinatorial approaches to barcode use were published since 2017 [51, 88] and are gaining momentum to allow an ever-increasing number of cells to be analyzed at once, raising higher limits of single-cell throughput techniques to hundreds of thousands and millions of cells probed simultaneously [273]. The next chapter of single-cell studies might be achieved by blending together other datasets while retaining single-cell resolution. Those are the genome, the epigenome, the proteome and the metabolome. In the field of immunology and for infectious diseases-targeting bNAbs, this could provide valuable information such as metabolic state of bNAbs-producing B cells, genomic segments of immune V, D and J genes, or in-vivo post-transcriptional modifications of bNAbs among others.

In the light of these technological developments, the present work could be replicated in other HIV-infected donors. The description of other bNAbs and their development in elite-neutralizer could provide valuable information to the field. For example, it is possible to screen multiple donors whose serum neutralization targets a single antigenic supersite. Comparing the responses of several donors, or even a dozen, could provide answers about their possible convergence. Furthermore, by studying, in a side-by-side approach, the immune response in an elite-neutralizer and the immune response in a donor that did not develop heterologous neutralization, we may bring insights in the determinants of the neutralization, at the single-cell level.

Chapter 5

CONCLUSION

Eliciting broadly neutralizing antibodies (bNAbs) in healthy individuals to effectively protect against HIV infection remains a top goal of the HIV vaccine research field. This PhD project aimed at investigating the development of outstanding Ab neutralizing capabilities in donor PC94, a clade-D HIV-1 primarily-infected elite-neutralizer from the IAVI Protocol C cohort.

Isolating broadly neutralizing antibodies (bNAbs) that recapitulate the activity observed in the serum was a first step to comprehend the nature of this exceptional neutralization. We used a novel high-throughput single-cell approach (scRNA-seq) to successfully isolate several bNAbs of remarkable breadth and potency. These Abs overall recapitulated serum activity. In particular, the most potent bNAb isolated neutralized 51.1% of a 126- pseudovirus panel with IC_{50}s in the range of the tenth of $ng.mL^{-1}$. Together with this bNAb, we recovered a large neutralizing lineage that targets the high-mannose patch (HMP) in the V3-glycan region of the Env. The developmental history of this lineage was reconstructed using paired heavy- and light-chains from 43 bNAbs, along with 395 unpaired heavy-chain sequences. Evidence of broad neutralization was observed in multiple branches of the lineage tree. While some bnAbs targeting the HMP exhibit features such as indels and high levels of SHM that may hinder elicitation through vaccination, our bNAbs contribute to the pool of bNAbs that target the HMP without such features. This supports the notion that the N332 glycan region may be a favorable target for vaccines. Ongoing structural studies will reveal the details of the epitope targeted by our Abs and shed light on whether they correspond to a known or novel mode of recognition.

To our knowledge, this is the first time that a high-throughput single-cell (scRNA-seq) approach has been used to explore the specificities and the development of HIV-1 bNAbs in longitudinal samples spanning several years of the course of the infection from an elite neutralizer. Our data demonstrate that the method is highly powerful, leading to a wealth of information on specific

Abs not obtained with common approaches. This approach will certainly be of great use to further explore Ab responses in natural infection and vaccine settings in the HIV field, and beyond in infections by other pathogens and in auto-immune diseases.

Chapter 6

SUPPLEMENTARY DATA

Table 6.1: List of softwares, librairies, packages and scripts used

Name	Reference	Link	Purpose
AbStar	[35]	GitHub: AbStar	Assignment of antibody sequences
AbTools	*None*	GitHub: AbTools	Comprehensive set of antibody tools
AbUtils	*None*	GitHub: AbUtils	Antibody sequence handling
AliView	*None*	AliView	Visualization of nucleotide alignments
Baltic	*None*	GitHub: Baltic	Visualization of phylogeny trees
bcl2fastq	*None*	Illumina	Basecalling of Illumina generated data
cellranger	*None*	GitHub: cellranger	10X Genomics software to demultiplex scRNA-seq data
celltypist	[89]	CellTypist	Automated labeling of cells in scRNA-seq data
cytocipher	[10]	GitHub: CytoCipher	Checks the consistency of clusters of cells in scRNA-seq data
Clonify	[36]	GitHub: Clonify	Inference of clonal B-cell lineages
FastTree	[260]	FastTree 2.1	Computes phylogeny trees from multiple sequences alignments
figtree	*None*	Uni. of Edimbrough	Visualization of phylogeny trees
GARD	[184]	Datamonkey	Assessment of genomic recombination points
igblast	[362]	NCBI IgBlast tool	Immunoglobulin gene-dedicated Blast tool
IgDiscover	[70]	GitLab: IgDiscover	Inferrence of Immunoglobuline germline genes
IQ-Tree 2	[232]	IQ-Tree 2	Computes phylogeny trees from multiple sequences alignments
mafft	[172]	MAFFT Web Server	Multiple sequence alignement
RDP 4	[217]	Uni. of Cape Town	Assessment of genomic recombination points
scab	[152]	GitHub: Scab	Integrated sc-RNA-seq and VDJ analysis
scabranger	[152]	GitHub: Scab	Wrapper for 10X Genomics cellranger
scanpy	[352]	Scanpy	scRNA-seq data handling tool in Python

Table 6.2: Pseudoviruses panel: 14 virus panel

Virus name	Clade	Tier	Year	Country	Accession
CNE55	01_AE	2	2007	China	HM215418
CNE8	01_AE	2 or 3	2006	China	HM215427
BJOX2000	07_BC	2	2007	China	HM215364
CH119	07_BC	2	2004	China	EF117261
398F1	A1	2		Tanzania	HM215312
JRFL	B	2	1986	United-States	AY669728
SF162	B	1A		United-States	EU123924
TRO.11	B	2	1995	Italy	AY835445
X2278	B	2	2007	Spain	FJ817366
25710	C	1B or 2	1999	India	EF117271
CE0217	C	2	2007	Malawi	KC894109
CE1176	C	2	2004	Malawi	FJ444437
IAVI c22	C	2			MW269981
X1632	G	2	2004	Spain	FJ817370

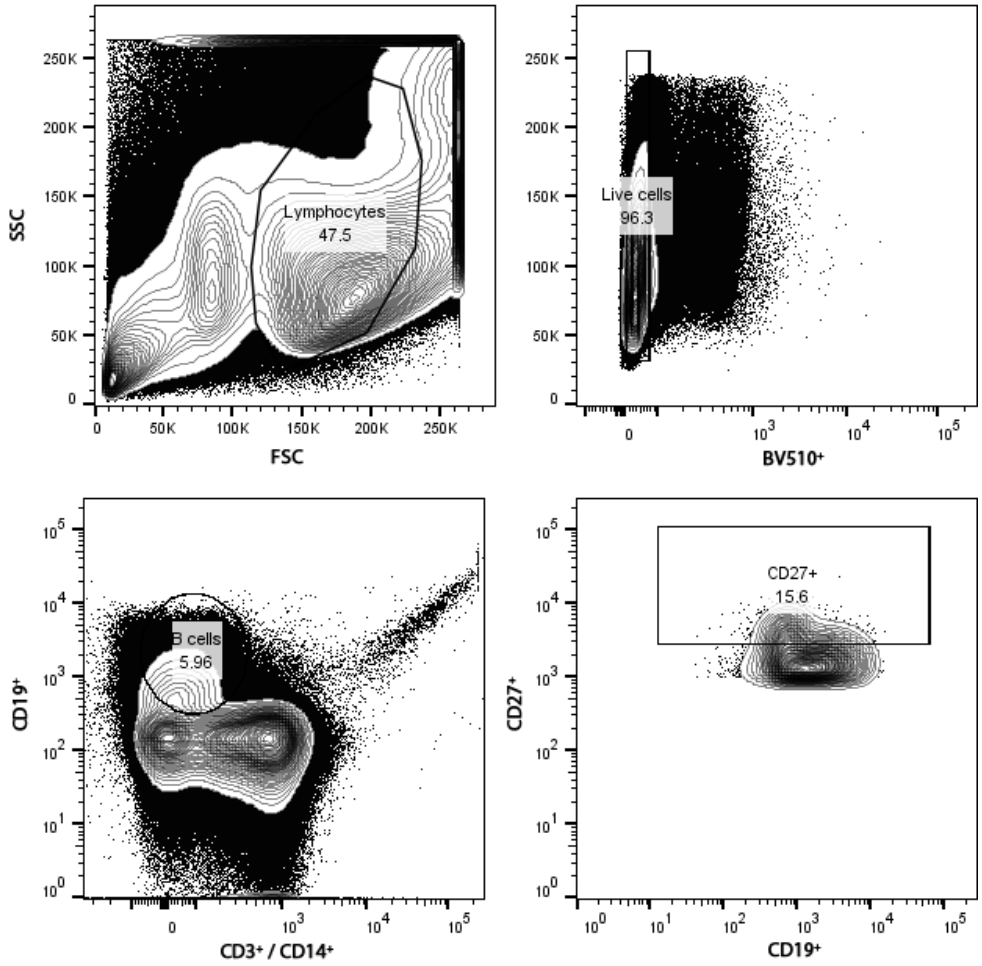

Figure 6.1. FACS gating parameters for early timepoint samples. Lymphocytes were first separated using the forward scatter (FSC) and side scatter (SSC). Live cells were then collected gating for $BV510^-$ cells. B-cells were collected using $CD3^-/CD14^-/CD19^+$ combination of markers. When memory B-cells where collected, those were gated for $CD27^+$ positivity.

Table 6.3: Pseudoviruses panel: 37 virus panel

Virus name	Clade	Tier	Year	Country	Accession
92TH021	01_AE	2	1992	Thailand	AY669775
92RW021	A		1992	Rwanda	U16236
94UG103	A1	2	1994	Uganda	AY669705
BG505_W6M_C2	A1	2	1993	Kenya	DQ208458
KNH1144	A1		2000	Kenya	AF457066
6535_3	B	1B or 2	1995	United-States	AY835438
89_6	B	2	1989	United-States	U39362
92BR020	B	1 or 2	1992	Brazil	AY669718
ADA	B		1986	United-States	AY426119
BAL_01	B	1B	1985	United-States	DQ318210
CAAN5342	B	2	2004	United-States	AY835452
DH12	B		1991	United-States	AF069140
HXB2	B	1B	1983	France	K03455
JRCSF	B	2	1986	United-States	AY669726
JRFL	B	2	1986	United-States	AY669728
MN_3	B	1A		United-States	HM215430
PVO_4	B	2 or 3	1996	Italy	AY835444
QH0692_42	B	2	1994	Trinidad-and-Tobago	AY835439
REJO4541_67	B	2	2001	United-States	AY835449
RHPA4259_7	B	2	2000	United-States	AY835447
SC422_8	B	2	1995	Trinidad-and-Tobago	AY835441
SF162	B	1A		United-States	EU123924
SS1196_1	B	1B	1997	United-States	AY835442
TRJO4551_58	B	3	2001	United-States	AY835450
TRO_11	B	2	1995	Italy	AY835445
WITO4160_33	B	2	2000	United-States	AY835451
YU2	B	2	1986	United-States	M93258
93IN905	C	2	1993	India	AY669742
CAP210_E8	C	2	2005	South Africa	DQ435683
CAP45_G3	C	2	2005	South Africa	DQ435682
DU156_12	C	1B or 2	1999	South Africa	DQ411852
DU172_17	C	2	1998	South Africa	DQ411853
DU422_1	C	2	1998	South Africa	DQ411854
ZM135_10A	C	2	1998	Zambia	AY424079
ZM214_15	C	2	2003	Zambia	DQ388516
ZM249_1	C	2	2003	Zambia	DQ388514
IAVI_C22	C	2			MW269981

Table 6.4: Pseudoviruses panel: 109 virus panel

Virus	Clade	Tier	Year	Accession	Virus	Clade	Tier	Year	Accession
620345_C1	01_AE	2	2005	JX512900	SC422_8	B	2	1995	AY835441
R3265_C6	01_AE	2	1999	JX512903	AC10_29	B	2	1998	AY835446
R2184_C4	01_AE	2	2001	JN944665	SC05_8C11_2344	B	2	1993	EU289200
C1080_C3	01_AE	2	1999	JN944660	6244_13_B5_4567	B	2	1996	EU289191
R1166_C1	01_AE	2	1998	JQ352783	TRO_11	B	2	1995	AY835445
BJOX028000_10_3	01_AE	2	2007	HM215389	6240_08_TA5_4622	B	2	1995	EU289190
BJOX025000_01_1	01_AE	2	2007	HM215386	WITO4160_33	B	2	2000	AY835451
C3347_C11	01_AE	2	1999	JX512902	62357_14_D3_4589	B	2	1997	EU289189
C4118_9	01_AE	2	2000	JQ352782	ZM246F	C	2	2003	FJ496194
BJOX010000_06_2	01_AE	2	2007	HM215373	ZM233_6	C	2	2002	DQ388517
CNE5	01_AE	2	2006	HM215415	ZM109_4	C	1B or 2	2000	AY424138
BJOX009000_02_4	01_AE	2	2007	HM215372	ZM135_10A	C	2	1998	AY424079
CNE8	01_AE	2 or 3	2006	HM215427	ZM214_15	C	2	2003	DQ388516
BJOX015000_11_5	01_AE	2	2007	HM215377	ZM247_V1	C	2	2003	FJ496204
T257_31	02A1	2 or 3	2004	EU513185	ZM197_7	C	1B or 2	2002	DQ388515
928_28	02_AG	2	1999	EU513199	0013095_2_11	C	2	2000	EF117267
T250_4	02_AG	2	2004	EU513189	CE1172_H1	C	2	2004	FJ444434
T251_18	02_AG	2 or 3	2004	EU513196	703010200_1E5	C	2	2007	FJ443999
T255_34	02_AG	2	2004	EU513184	001428_2_42	C	2	2000	EF117266
235_47	02_AG	2	2004	EU513195	1394_C9G1	C	2	2004	FJ444527
211_9	02_AG	2	2004	EU513187	16055_2_3	C	2	1999	EF117268
263_8	02_AG	2	2004	EU513182	249M_B10	C	2	2003	EU166862
CNE19	07_BC	2	2007	HM215405	3301_V1_C24	C	2	2003	HM215294
CNE20	07_BC	2	2007	HM215406	703010054_2A2	C	2	2007	FJ443808
CNE21	07_BC	2	2007	HM215407	DU422_1	C	2	1998	DQ411854
CNE52	08_BC	2	2007	HM215416	703010217_B6	C	2	2007	KC894109
CNE53	08_BC	2	2007	HM215417	704809221_1B3	C	2	2007	FJ444103
6952_V1_C20	41_CD	2	2003	HM215343	BF1266_431A	C	2	2002	HM215360
Q769_D22	A1	2	1996	AF407158	CAP210_E8	C	2	2005	DQ435683
Q461_E2	A1	2	1995	AF407156	ZM53_12	C	2	2000	AY423984
Q259_17	A1	2	1994	AF407152	CE0393_C3	C	2	2003	FJ444215
Q23_17	A1	1B	1994	AF004885	CNE30	C	2	2007	HM215411
KNH1144	A1		2000	AF457066	DU156_12	C	1B or 2	1999	DQ411852
0260_V5_C36	A1		2005	HM215256	DU172_17	C	2	1998	DQ411853
0330_V4_C3	A1	2	2005	HM215257	CAP45_G3	C	2	2005	DQ435682
191955_A11	A1	2	2007	HM215272	CNE17	C	2	2007	HM215403
191084_B7_19	A1	2	2007	HM215266	CNE58	C	2	2006	HM215421
6545_V3_C13	A1C	2	2004	HM215331	CE1176_A3	C	2	2004	FJ444437
6540_V4_C1	A1C	2	2004	HM215330	ZM249_1	C	2	2003	DQ388514
6041_V3_C23	A1C	2	2004	HM215321	CE2010_F5	C	2 or 3	2005	FJ444561
3103_V3_C10	A1CD	2	2004	HM215288	6811_V7_C18	CD	2	2006	HM215340
MS208_A1	A1D	1 or 2		DQ187010	3817_V2_C59	CD	2	2004	HM215310
0815_V3_C3	A1D	2	2004	HM215260	89_F1_2_25	CD	2		HM215349
TRJO4551_58	B	3	2001	AY835450	6480_V4_C25	CD	2	2004	HM215329
QH0692_42	B	2	1994	AY835439	3016_V5_C45	D	2	2005	HM215283
1006_11_C3_1601	B	2	1997	EU289183	231965_C1	D	2	2001	JQ361079
1054_07_TC4_1499	B	2	1997	EU289185	A07412M1_VRC12	D	2	1999	HM215357
1012_11_TC21_3257	B	1B or 2	1997	EU289184	P1981_C5_3	G	2	2008	FJ817369
PVO_4	B	2 or 3	1996	AY835444	X1254_C3	G	2	2003	EU885762
1056_10_TA11_1826	B	1B or 2	1998	EU289186	X2088_C9	G	2	2006	EU885764
REJO4541_67	B	2	2001	AY835449	X1632_S2_B10	G	2	2004	FJ817370
RHPA4259_7	B	2	2000	AY835447	X1193_C1	G	2	2002	EU885761
CAAN5342	B	2	2004	AY835452	X2131_C1_B5	G	2	2005	FJ817368
6535_3	B	1B or 2	1995	AY835438	P0402_C2_11	G	2	2002	EU885759
WEAU_D15_410	B	2	1990	EU289202					

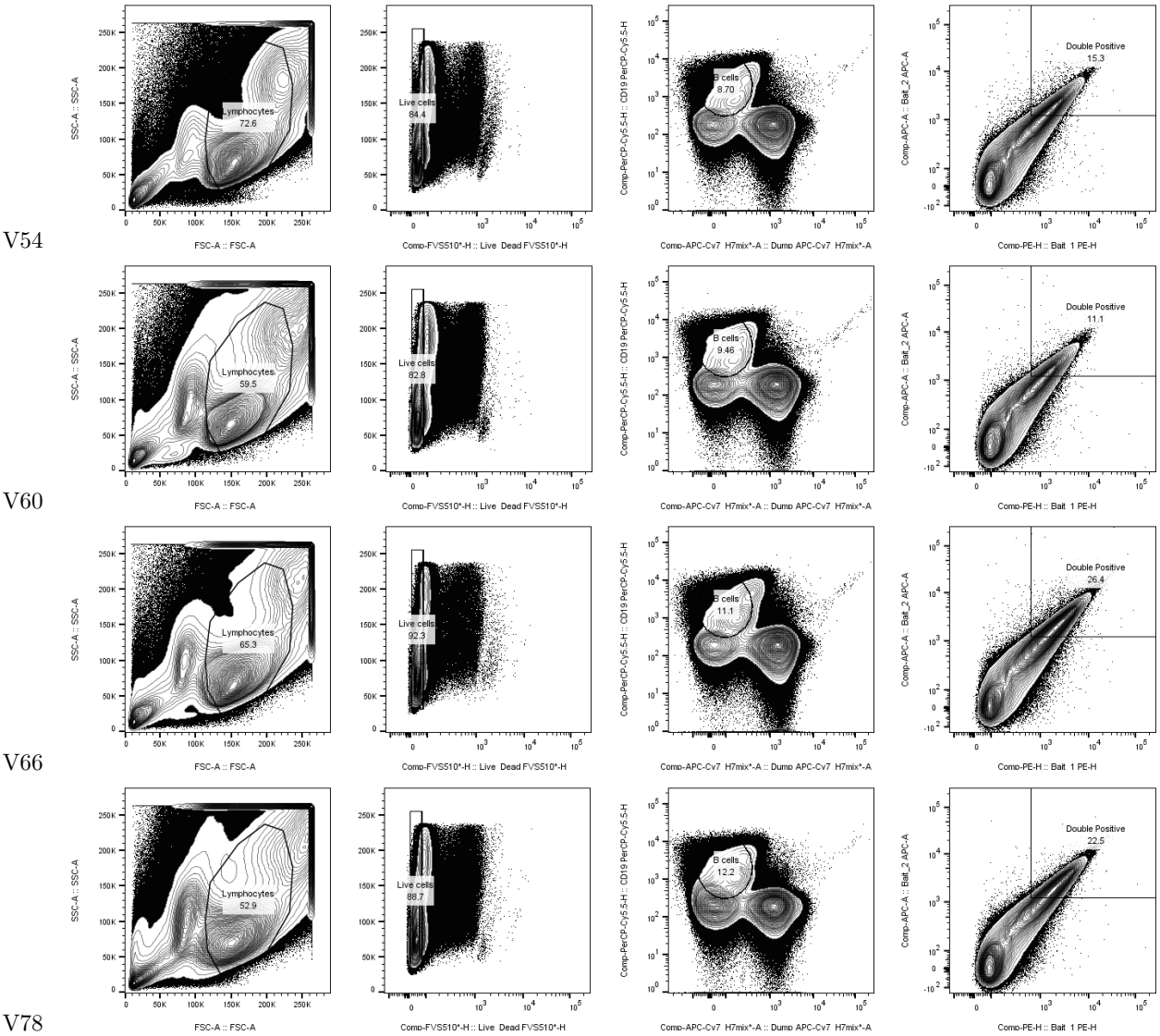

Figure 6.2. FACS gating parameters for late timepoint samples. Lymphocytes were first separated using the forward scatter (FSC) and side scatter (SSC). Live cells were then collected gating for $BV510^-$ cells. B-cells were collected using $CD3^-/CD14^-/CD19^+$ combination of markers. Finally, antigen specific cells were gated for PE^+ and APC^+ double positivity.

BIBLIOGRAPHY

[1] J Albert et al. "Rapid development of isolate-specific neutralizing antibodies after primary HIV-1 infection and consequent emergence of virus variants which resist neutralization by autologous sera". en. In: *AIDS* 4.2 (Feb. 1990), pp. 107–112. URL: http://dx.doi.org/10.1097/00002030-199002000-00002.

[2] G Alkhatib et al. "CC CKR5: a RANTES, MIP-1alpha, MIP-1beta receptor as a fusion cofactor for macrophage-tropic HIV-1". en. In: *Science* 272.5270 (June 1996), pp. 1955–1958. URL: http://dx.doi.org/10.1126/science.272.5270.1955.

[3] Christopher D C Allen and Jason G Cyster. "Follicular dendritic cell networks of primary follicles and germinal centers: phenotype and function". en. In: *Semin. Immunol.* 20.1 (Feb. 2008), pp. 14–25. URL: http://dx.doi.org/10.1016/j.smim.2007.12.001.

[4] Marcus Altfeld et al. "DCs and NK cells: critical effectors in the immune response to HIV-1". en. In: *Nat. Rev. Immunol.* 11.3 (Mar. 2011), pp. 176–186. URL: http://dx.doi.org/10.1038/nri2935.

[5] Sarah F Andrews et al. "High preexisting serological antibody levels correlate with diversification of the influenza vaccine response". en. In: *J. Virol.* 89.6 (Mar. 2015), pp. 3308–3317. URL: http://dx.doi.org/10.1128/JVI.02871-14.

[6] N M Archin et al. "Administration of vorinostat disrupts HIV-1 latency in patients on antiretroviral therapy". en. In: *Nature* 487.7408 (July 2012), pp. 482–485. URL: http://dx.doi.org/10.1038/nature11286.

[7] Christine Armbruster et al. "A phase I trial with two human monoclonal antibodies (hMAb 2F5, 2G12) against HIV-1". en. In: *AIDS* 16.2 (Jan. 2002), pp. 227–233. URL: http://dx.doi.org/10.1097/00002030-200201250-00012.

[8] Manickam Ashokkumar et al. "In vitro replicative fitness of early Transmitted founder HIV-1 variants and sensitivity to Interferon alpha". en. In: *Sci. Rep.* 10.1 (Feb. 2020), p. 2747. URL: http://dx.doi.org/10.1038/s41598-020-59596-x.

[9] Rena D Astronomo et al. "Rectal tissue and vaginal tissue from intravenous VRC01 recipients show protection against ex vivo HIV-1 challenge". en. In: *J. Clin. Invest.* 131.16 (Aug. 2021). URL: http://dx.doi.org/10.1172/JCI146975.

[10] Brad Balderson et al. "Cytocipher determines significantly different populations of cells in single-cell RNA-seq data". en. In: *Bioinformatics* 39.7 (July 2023). URL: http://dx.doi.org/10.1093/bioinformatics/btad435.

[11] Sheila N Balinda et al. "Characterization of Near Full-Length Transmitted/Founder HIV-1 Subtype D and A/D Recombinant Genomes in a Heterosexual Ugandan Population (2006-2011)". en. In: *Viruses* 14.2 (Feb. 2022). URL: http://dx.doi.org/10.3390/v14020334.

[12] Katharine J Bar et al. "Effect of HIV Antibody VRC01 on Viral Rebound after Treatment Interruption". en. In: *N. Engl. J. Med.* 375.21 (Nov. 2016), pp. 2037–2050. URL: http://dx.doi.org/10.1056/NEJMoa1608243.

[13] Yotam Bar-On et al. "Safety and antiviral activity of combination HIV-1 broadly neutralizing antibodies in viremic individuals". en. In: *Nat. Med.* 24.11 (Nov. 2018), pp. 1701–1707. URL: http://dx.doi.org/10.1038/s41591-018-0186-4.

[14] F Barin et al. "Serological evidence for virus related to simian T-lymphotropic retrovirus III in residents of west Africa". en. In: *Lancet* 2.8469-70 (1985), pp. 1387–1389. URL: http://dx.doi.org/10.1016/s0140-6736(85)92556-5.

[15] Christopher O Barnes et al. "A naturally arising broad and potent CD4-binding site antibody with low somatic mutation". en. In: *Sci Adv* 8.32 (Aug. 2022), eabp8155. URL: http://dx.doi.org/10.1126/sciadv.abp8155.

[16] Christopher O Barnes et al. "Structural characterization of a highly-potent V3-glycan broadly neutralizing antibody bound to natively-glycosylated HIV-1 envelope". en. In: *Nat. Commun.* 9.1 (Mar. 2018), p. 1251. URL: http://dx.doi.org/10.1038/s41467-018-03632-y.

[17] Dan H Barouch et al. "Evaluation of a mosaic HIV-1 vaccine in a multicentre, randomised, double-blind, placebo-controlled, phase 1/2a clinical trial (APPROACH) and in rhesus monkeys (NHP 13-19)". en. In: *Lancet* 392.10143 (July 2018), pp. 232–243. URL: http://dx.doi.org/10.1016/S0140-6736(18)31364-3.

[18] F Barré-Sinoussi et al. "Isolation of a T-lymphotropic retrovirus from a patient at risk for acquired immune deficiency syndrome (AIDS)". en. In: *Science* 220.4599 (May 1983), pp. 868–871. URL: http://dx.doi.org/10.1126/science.6189183.

[19] Nicholas Bbosa, Pontiano Kaleebu, and Deogratius Ssemwanga. "HIV subtype diversity worldwide". en. In: *Curr. Opin. HIV AIDS* 14.3 (May 2019), pp. 153–160. URL: http://dx.doi.org/10.1097/COH.0000000000000534.

[20] Anna-Janina Behrens and Max Crispin. "Structural principles controlling HIV envelope glycosylation". en. In: *Curr. Opin. Struct. Biol.* 44 (June 2017), pp. 125–133. URL: http://dx.doi.org/10.1016/j.sbi.2017.03.008.

[21] Anna-Janina Behrens et al. "Composition and antigenic effects of individual glycan sites of a trimeric HIV-1 envelope glycoprotein". en. In: *Cell Rep.* 14.11 (Mar. 2016), pp. 2695–2706. URL: http://dx.doi.org/10.1016/j.celrep.2016.02.058.

[22] A K Bhan et al. "Stages of B cell differentiation in human lymphoid tissue". en. In: *J. Exp. Med.* 154.3 (Sept. 1981), pp. 737–749. URL: http://dx.doi.org/10.1084/jem.154.3.737.

[23] J M Binley et al. "A recombinant human immunodeficiency virus type 1 envelope glycoprotein complex stabilized by an intermolecular disulfide bond between the gp120 and gp41 subunits is an antigenic mimic of the trimeric virion-associated structure". en. In: *J. Virol.* 74.2 (Jan. 2000), pp. 627–643. URL: http://dx.doi.org/10.1128/jvi.74.2.627-643.2000.

[24] Maria Blasi et al. "Immunogenicity, safety, and efficacy of sequential immunizations with an SIV-based IDLV expressing CH505 Envs". en. In: *NPJ Vaccines* 5.1 (Nov. 2020), p. 107. URL: http://dx.doi.org/10.1038/s41541-020-00252-w.

[25] S Bonhoeffer, E C Holmes, and M A Nowak. "Causes of HIV diversity". en. In: *Nature* 376.6536 (July 1995), p. 125. URL: http://dx.doi.org/10.1038/376125a0.

[26] Camille Bonomelli et al. "The glycan shield of HIV is predominantly oligomannose independently of production system or viral clade". en. In: *PLoS One* 6.8 (Aug. 2011), e23521. URL: http://dx.doi.org/10.1371/journal.pone.0023521.

[27] Mattia Bonsignori et al. "Analysis of a clonal lineage of HIV-1 envelope V2/V3 conformational epitope-specific broadly neutralizing antibodies and their inferred unmutated common ancestors". en. In: *J. Virol.* 85.19 (Oct. 2011), pp. 9998–10009. URL: http://dx.doi.org/10.1128/JVI.05045-11.

[28] Mattia Bonsignori et al. "Antibody-virus co-evolution in HIV infection: paths for HIV vaccine development". en. In: *Immunol. Rev.* 275.1 (Jan. 2017), pp. 145–160. URL: http://dx.doi.org/10.1111/imr.12509.

[29] Marta T Borowska et al. "Biochemical and biophysical characterization of natural polyreactivity in antibodies". en. In: *Cell Rep.* 42.10 (Oct. 2023), p. 113190. URL: http://dx.doi.org/10.1016/j.celrep.2023.113190.

[30] Stylianos Bournazos et al. "Bispecific anti-HIV-1 antibodies with enhanced breadth and potency". en. In: *Cell* 165.7 (June 2016), pp. 1609–1620. URL: http://dx.doi.org/10.1016/j.cell.2016.04.050.

[31] Scott D Boyd et al. "Measurement and Clinical Monitoring of Human Lymphocyte Clonality by Massively Parallel V-D-J Pyrosequencing". In: *Sci. Transl. Med.* 1.12 (2009), 12ra23–12ra23. URL: https://www.science.org/doi/abs/10.1126/scitranslmed.3000540.

[32] Oliver F Brandenberg et al. "The HIV-1 entry process: A stoichiometric view". en. In: *Trends Microbiol.* 23.12 (Dec. 2015), pp. 763–774. URL: http://dx.doi.org/10.1016/j.tim.2015.09.003.

[33] Jason M Brenchley et al. "CD4+ T cell depletion during all stages of HIV disease occurs predominantly in the gastrointestinal tract". en. In: *J. Exp. Med.* 200.6 (Sept. 2004), pp. 749–759. URL: http://dx.doi.org/10.1084/jem.20040874.

[34] Philip Brennecke et al. "Accounting for technical noise in single-cell RNA-seq experiments". en. In: *Nat. Methods* 10.11 (Nov. 2013), pp. 1093–1095. URL: http://dx.doi.org/10.1038/nmeth.2645.

[35] Bryan Briney and Dennis R Burton. "Massively scalable genetic analysis of antibody repertoires". en. Oct. 2018. URL: https://www.biorxiv.org/content/10.1101/447813v1.

[36] Bryan Briney et al. “Clonify: unseeded antibody lineage assignment from next-generation sequencing data”. en. In: *Sci. Rep.* 6 (Apr. 2016), p. 23901. URL: http://dx.doi.org/10.1038/srep23901.

[37] Bryan Briney et al. “Commonality despite exceptional diversity in the baseline human antibody repertoire”. en. In: *Nature* 566.7744 (Feb. 2019), pp. 393–397. URL: http://dx.doi.org/10.1038/s41586-019-0879-y.

[38] Bryan Briney et al. “Tailored immunogens direct affinity maturation toward HIV neutralizing antibodies”. en. In: *Cell* 166.6 (Sept. 2016), 1459–1470.e11. URL: http://dx.doi.org/10.1016/j.cell.2016.08.005.

[39] S Broder and R C Gallo. “A pathogenic retrovirus (HTLV-III) linked to AIDS”. en. In: *N. Engl. J. Med.* 311.20 (Nov. 1984), pp. 1292–1297. URL: http://dx.doi.org/10.1056/NEJM198411153112006.

[40] Johannes Brozy et al. “Antiviral Activity of HIV gp120-Targeting Bispecific T Cell Engager Antibody Constructs”. en. In: *J. Virol.* 92.14 (July 2018). URL: http://dx.doi.org/10.1128/JVI.00491-18.

[41] C Bruck et al. “HIV-1 envelope-elicited neutralizing antibody titres correlate with protection and virus load in chimpanzees”. en. In: *Vaccine* 12.12 (Sept. 1994), pp. 1141–1148. URL: http://dx.doi.org/10.1016/0264-410x(94)90185-6.

[42] Jeffrey J Bunker et al. “Natural polyreactive IgA antibodies coat the intestinal microbiota”. en. In: *Science* 358.6361 (Oct. 2017). URL: http://dx.doi.org/10.1126/science.aan6619.

[43] Deborah L Burnett et al. “Clonal redemption and clonal anergy as mechanisms to balance B cell tolerance and immunity”. en. In: *Immunol. Rev.* 292.1 (Nov. 2019), pp. 61–75. URL: http://dx.doi.org/10.1111/imr.12808.

[44] D R Burton et al. “A large array of human monoclonal antibodies to type 1 human immunodeficiency virus from combinatorial libraries of asymptomatic seropositive individuals”. en. In: *Proc. Natl. Acad. Sci. U. S. A.* 88.22 (Nov. 1991), pp. 10134–10137. URL: http://dx.doi.org/10.1073/pnas.88.22.10134.

[45] Dennis R Burton. “Advancing an HIV vaccine; advancing vaccinology”. en. In: *Nat. Rev. Immunol.* 19.2 (Feb. 2019), pp. 77–78. URL: http://dx.doi.org/10.1038/s41577-018-0103-6.

[46] Dennis R Burton. “Antiviral neutralizing antibodies: from in vitro to in vivo activity”. en. In: *Nat. Rev. Immunol.* 23.11 (Nov. 2023), pp. 720–734. URL: http://dx.doi.org/10.1038/s41577-023-00858-w.

[47] Dennis R Burton and John R Mascola. “Antibody responses to envelope glycoproteins in HIV-1 infection”. en. In: *Nat. Immunol.* 16.6 (June 2015), pp. 571–576. URL: http://dx.doi.org/10.1038/ni.3158.

[48] Isolde F Butler et al. “HIV genetic diversity: biological and public health consequences”. en. In: *Curr. HIV Res.* 5.1 (Jan. 2007), pp. 23–45. URL: http://dx.doi.org/10.2174/157016207779316297.

[49] Daniel A Calarese et al. “Antibody domain exchange is an immunological solution to carbohydrate cluster recognition”. en. In: *Science* 300.5628 (June 2003), pp. 2065–2071. URL: http://dx.doi.org/10.1126/science.1083182.

[50] Evan M Cale et al. “Neutralizing antibody VRC01 failed to select for HIV-1 mutations upon viral rebound”. en. In: *J. Clin. Invest.* 130.6 (June 2020), pp. 3299–3304. URL: http://dx.doi.org/10.1172/JCI134395.

[51] Junyue Cao et al. “Comprehensive single-cell transcriptional profiling of a multicellular organism”. en. In: *Science* 357.6352 (Aug. 2017), pp. 661–667. URL: http://dx.doi.org/10.1126/science.aam8940.

[52] Yunlong Cao et al. “Potent neutralizing antibodies against SARS-CoV-2 identified by high-throughput single-cell sequencing of convalescent patients’ B cells”. en. In: *Cell* 182.1 (July 2020), 73–84.e16. URL: http://dx.doi.org/10.1016/j.cell.2020.05.025.

[53] Marina Caskey et al. “Antibody 10-1074 suppresses viremia in HIV-1-infected individuals”. en. In: *Nat. Med.* 23.2 (Feb. 2017), pp. 185–191. URL: http://dx.doi.org/10.1038/nm.4268.

[54] Marina Caskey et al. “Viraemia suppressed in HIV-1-infected humans by broadly neutralizing antibody 3BNC117”. en. In: *Nature* 522.7557 (June 2015), pp. 487–491. URL: http://dx.doi.org/10.1038/nature14411.

[55] Centers for Disease Control (CDC). “Kaposi’s sarcoma and Pneumocystis pneumonia among homosexual men–New York City and California”. en. In: *MMWR Morb. Mortal. Wkly. Rep.* 30.25 (July 1981), pp. 305–308. URL: https://www.ncbi.nlm.nih.gov/pubmed/6789108.

[56] Centers for Disease Control (CDC). “Pneumocystis pneumonia–Los Angeles”. en. In: *MMWR Morb. Mortal. Wkly. Rep.* 30.21 (June 1981), pp. 250–252. URL: https://www.ncbi.nlm.nih.gov/pubmed/6265753.

[57] S Chakrabarti et al. “Expression of the HTLV-III envelope gene by a recombinant vaccinia virus”. en. In: *Nature* 320.6062 (1986), pp. 535–537. URL: http://dx.doi.org/10.1038/320535a0.

[58] Huan Chen et al. “BCR selection and affinity maturation in Peyer’s patch germinal centres”. en. In: *Nature* 582.7812 (June 2020), pp. 421–425. URL: http://dx.doi.org/10.1038/s41586-020-2262-4.

[59] Xuejun Chen et al. “Vaccination induces maturation in a mouse model of diverse unmutated VRC01-class precursors to HIV-neutralizing antibodies with ¿50% breadth”. en. In: *Immunity* 54.2 (Feb. 2021), 324–339.e8. URL: http://dx.doi.org/10.1016/j.immuni.2020.12.014.

[60] Xiying Chi, Yue Li, and Xiaoyan Qiu. “V(D)J recombination, somatic hypermutation and class switch recombination of immunoglobulins: mechanism and regulation”. en. In: *Immunology* 160.3 (July 2020), pp. 233–247. URL: http://dx.doi.org/10.1111/imm.13176.

[61] H Choe et al. “The beta-chemokine receptors CCR3 and CCR5 facilitate infection by primary HIV-1 isolates”. en. In: *Cell* 85.7 (June 1996), pp. 1135–1148. URL: http://dx.doi.org/10.1016/s0092-8674(00)81313-6.

[62] Bhavna Chohan et al. “Selection for human immunodeficiency virus type 1 envelope glycosylation variants with shorter V1-V2 loop sequences occurs during transmission of certain genetic subtypes and may impact viral RNA levels”. en. In: *J. Virol.* 79.10 (May 2005), pp. 6528–6531. URL: http://dx.doi.org/10.1128/JVI.79.10.6528-6531.2005.

[63] Gwo-Yu Chuang et al. "Structural Survey of Broadly Neutralizing Antibodies Targeting the HIV-1 Env Trimer Delineates Epitope Categories and Characteristics of Recognition". en. In: *Structure* 27.1 (Jan. 2019), 196–206.e6. URL: http://dx.doi.org/10.1016/j.str.2018.10.007.

[64] F Clavel et al. "Isolation of a new human retrovirus from West African patients with AIDS". en. In: *Science* 233.4761 (July 1986), pp. 343–346. URL: http://dx.doi.org/10.1126/science.2425430.

[65] Kristen Cohen et al. "Early preservation of CXCR5+ PD-1+ helper T cells and B cell activation predict the breadth of neutralizing antibody responses in chronic HIV-1 infection". en. In: *J. Virol.* 88.22 (Nov. 2014), pp. 13310–13321. URL: http://dx.doi.org/10.1128/JVI.02186-14.

[66] Yehuda Z Cohen et al. "Safety, pharmacokinetics, and immunogenicity of the combination of the broadly neutralizing anti-HIV-1 antibodies 3BNC117 and 10-1074 in healthy adults: A randomized, phase 1 study". en. In: *PLoS One* 14.8 (Aug. 2019), e0219142. URL: http://dx.doi.org/10.1371/journal.pone.0219142.

[67] Lillian B Cohn, Nicolas Chomont, and Steven G Deeks. "The Biology of the HIV-1 Latent Reservoir and Implications for Cure Strategies". en. In: *Cell Host Microbe* 27.4 (Apr. 2020), pp. 519–530. URL: http://dx.doi.org/10.1016/j.chom.2020.03.014.

[68] Philippe Colin et al. "Conformational antigenic heterogeneity as a cause of the persistent fraction in HIV-1 neutralization". en. In: *Retrovirology* 20.1 (May 2023), p. 9. URL: http://dx.doi.org/10.1186/s12977-023-00624-9.

[69] M D Cooper. "Pre-B cells; normal and abnormal development". en. In: *J. Clin. Immunol.* 1.2 (Apr. 1981), pp. 81–89. URL: http://dx.doi.org/10.1007/BF00915383.

[70] Martin M Corcoran et al. "Production of individualized V gene databases reveals high levels of immunoglobulin genetic diversity". en. In: *Nat. Commun.* 7 (Dec. 2016), p. 13642. URL: http://dx.doi.org/10.1038/ncomms13642.

[71] Lawrence Corey et al. "Two Randomized Trials of Neutralizing Antibodies to Prevent HIV-1 Acquisition". en. In: *N. Engl. J. Med.* 384.11 (Mar. 2021), pp. 1003–1014. URL: http://dx.doi.org/10.1056/NEJMoa2031738.

[72] Marion Cornelissen et al. "The Neutralizing Antibody Response in an Individual with Triple HIV-1 Infection Remains Directed at the First Infecting Subtype". en. In: *AIDS Res. Hum. Retroviruses* 32.10-11 (Feb. 2016), pp. 1135–1142. URL: http://dx.doi.org/10.1089/aid.2015.0324.

[73] Valerie Cortez et al. "HIV-1 superinfection in women broadens and strengthens the neutralizing antibody response". en. In: *PLoS Pathog.* 8.3 (Mar. 2012), e1002611. URL: http://dx.doi.org/10.1371/journal.ppat.1002611.

[74] Alessandro Cozzi-Lepri et al. "Rate of response to initial antiretroviral therapy according to level of pre-existing HIV-1 drug resistance detected by next-generation sequencing in the strategic timing of antiretroviral treatment (START) study". en. In: *HIV Med.* (Sept. 2023). URL: http://dx.doi.org/10.1111/hiv.13556.

[75] Amanda M Crooks et al. “Precise quantitation of the latent HIV-1 reservoir: Implications for eradication strategies”. en. In: *J. Infect. Dis.* 212.9 (Nov. 2015), pp. 1361–1365. URL: http://dx.doi.org/10.1093/infdis/jiv218.

[76] Trevor A Crowell et al. “Safety and efficacy of VRC01 broadly neutralising antibodies in adults with acutely treated HIV (RV397): a phase 2, randomised, double-blind, placebo-controlled trial”. en. In: *Lancet HIV* 6.5 (May 2019), e297–e306. URL: http://dx.doi.org/10.1016/S2352-3018(19)30053-0.

[77] Coleen K Cunningham et al. “Safety, tolerability, and pharmacokinetics of the broadly neutralizing human immunodeficiency virus (HIV)-1 monoclonal antibody VRC01 in HIV-exposed newborn infants”. en. In: *J. Infect. Dis.* 222.4 (July 2020), pp. 628–636. URL: http://dx.doi.org/10.1093/infdis/jiz532.

[78] Albert Cupo et al. “Optimizing the production and affinity purification of HIV-1 envelope glycoprotein SOSIP trimers from transiently transfected CHO cells”. en. In: *PLoS One* 14.4 (Apr. 2019), e0215106. URL: http://dx.doi.org/10.1371/journal.pone.0215106.

[79] Mirela D’arc et al. “Origin of the HIV-1 group O epidemic in western lowland gorillas”. en. In: *Proc. Natl. Acad. Sci. U. S. A.* 112.11 (Mar. 2015), E1343–52. URL: http://dx.doi.org/10.1073/pnas.1502022112.

[80] Kim-Marie A Dam et al. “HIV-1 CD4-binding site germline antibody-Env structures inform vaccine design”. en. In: *Nat. Commun.* 13.1 (Oct. 2022), p. 6123. URL: http://dx.doi.org/10.1038/s41467-022-33860-2.

[81] Allan deCamp et al. “Global panel of HIV-1 Env reference strains for standardized assessments of vaccine-elicited neutralizing antibodies”. en. In: *J. Virol.* 88.5 (Mar. 2014), pp. 2489–2507. URL: http://dx.doi.org/10.1128/JVI.02853-13.

[82] Steven G Deeks. “HIV: Shock and kill”. en. In: *Nature* 487.7408 (July 2012), pp. 439–440. URL: http://dx.doi.org/10.1038/487439a.

[83] Daniel M DeLaughter. “The use of the Fluidigm C1 for RNA expression analyses of single cells”. en. In: *Curr. Protoc. Mol. Biol.* 122.1 (Apr. 2018), e55. URL: http://dx.doi.org/10.1002/cpmb.55.

[84] H Deng et al. “Identification of a major co-receptor for primary isolates of HIV-1”. en. In: *Nature* 381.6584 (June 1996), pp. 661–666. URL: http://dx.doi.org/10.1038/381661a0.

[85] Cynthia A Derdeyn et al. “Envelope-constrained neutralization-sensitive HIV-1 after heterosexual transmission”. en. In: *Science* 303.5666 (Mar. 2004), pp. 2019–2022. URL: http://dx.doi.org/10.1126/science.1093137.

[86] Javier M Di Noia and Michael S Neuberger. “Molecular mechanisms of antibody somatic hypermutation”. en. In: *Annu. Rev. Biochem.* 76.1 (2007), pp. 1–22. URL: http://dx.doi.org/10.1146/annurev.biochem.76.061705.090740.

[87] Zanele Ditse et al. “HIV-1 subtype C-infected children with exceptional neutralization breadth exhibit polyclonal responses targeting known epitopes”. en. In: *J. Virol.* 92.17 (Sept. 2018). URL: http://dx.doi.org/10.1128/JVI.00878-18.

[88] Silvia Domcke et al. "A human cell atlas of fetal chromatin accessibility". en. In: *Science* 370.6518 (Nov. 2020), eaba7612. URL: http://dx.doi.org/10.1126/science.aba7612.

[89] C Domínguez Conde et al. "Cross-tissue immune cell analysis reveals tissue-specific features in humans". en. In: *Science* 376.6594 (May 2022), eabl5197. URL: http://dx.doi.org/10.1126/science.abl5197.

[90] Katie J Doores. "The HIV glycan shield as a target for broadly neutralizing antibodies". en. In: *FEBS J.* 282.24 (Dec. 2015), pp. 4679–4691. URL: http://dx.doi.org/10.1111/febs.13530.

[91] Katie J Doores and Dennis R Burton. "Variable loop glycan dependency of the broad and potent HIV-1-neutralizing antibodies PG9 and PG16". en. In: *J. Virol.* 84.20 (Oct. 2010), pp. 10510–10521. URL: http://dx.doi.org/10.1128/JVI.00552-10.

[92] Katie J Doores et al. "Two classes of broadly neutralizing antibodies within a single lineage directed to the high-mannose patch of HIV envelope". en. In: *J. Virol.* 89.2 (Jan. 2015), pp. 1105–1118. URL: http://dx.doi.org/10.1128/JVI.02905-14.

[93] B J Doranz et al. "A dual-tropic primary HIV-1 isolate that uses fusin and the beta-chemokine receptors CKR-5, CKR-3, and CKR-2b as fusion cofactors". en. In: *Cell* 85.7 (June 1996), pp. 1149–1158. URL: http://dx.doi.org/10.1016/s0092-8674(00)81314-8.

[94] Nicole A Doria-Rose. "HIV neutralizing antibodies: clinical correlates and implications for vaccines". en. In: *J. Infect. Dis.* 201.7 (Apr. 2010), pp. 981–983. URL: http://dx.doi.org/10.1086/651143.

[95] Nicole A Doria-Rose et al. "Developmental pathway for potent V1V2-directed HIV-neutralizing antibodies". en. In: *Nature* 509.7498 (May 2014), pp. 55–62. URL: http://dx.doi.org/10.1038/nature13036.

[96] Pia Dosenovic et al. "Immunization for HIV-1 broadly neutralizing antibodies in human ig knockin mice". en. In: *Cell* 161.7 (June 2015), pp. 1505–1515. URL: http://dx.doi.org/10.1016/j.cell.2015.06.003.

[97] T Dragic et al. "HIV-1 entry into CD4+ cells is mediated by the chemokine receptor CC-CKR-5". en. In: *Nature* 381.6584 (June 1996), pp. 667–673. URL: http://dx.doi.org/10.1038/381667a0.

[98] R B DuBridge et al. "Analysis of mutation in human cells by using an Epstein-Barr virus shuttle system". en. In: *Mol. Cell. Biol.* 7.1 (Jan. 1987), pp. 379–387. URL: http://dx.doi.org/10.1128/mcb.7.1.379-387.1987.

[99] P L Earl, R W Doms, and B Moss. "Oligomeric structure of the human immunodeficiency virus type 1 envelope glycoprotein". en. In: *Proc. Natl. Acad. Sci. U. S. A.* 87.2 (Jan. 1990), pp. 648–652. URL: http://dx.doi.org/10.1073/pnas.87.2.648.

[100] Roy A Ehling et al. "SARS-CoV-2 reactive and neutralizing antibodies discovered by single-cell sequencing of plasma cells and mammalian display". en. In: *Cell Rep.* 38.3 (Jan. 2022), p. 110242. URL: http://dx.doi.org/10.1016/j.celrep.2021.110242.

[101] A D Elbein et al. “Kifunensine, a potent inhibitor of the glycoprotein processing mannosidase I”. en. In: *J. Biol. Chem.* 265.26 (Sept. 1990), pp. 15599–15605. URL: https://www.ncbi.nlm.nih.gov/pubmed/2144287.

[102] Rebecca A Elsner and Mark J Shlomchik. “Germinal Center and Extrafollicular B Cell Responses in Vaccination, Immunity, and Autoimmunity”. en. In: *Immunity* 53.6 (Dec. 2020), pp. 1136–1150. URL: http://dx.doi.org/10.1016/j.immuni.2020.11.006.

[103] Amelia Escolano et al. “Sequential immunization elicits broadly neutralizing anti-HIV-1 antibodies in ig knockin mice”. en. In: *Cell* 166.6 (Sept. 2016), 1445–1458.e12. URL: http://dx.doi.org/10.1016/j.cell.2016.07.030.

[104] Emilia Falkowska et al. “Broadly neutralizing HIV antibodies define a glycan-dependent epitope on the prefusion conformation of gp41 on cleaved envelope trimers”. en. In: *Immunity* 40.5 (May 2014), pp. 657–668. URL: http://dx.doi.org/10.1016/j.immuni.2014.04.009.

[105] Nuno R Faria et al. “HIV epidemiology. The early spread and epidemic ignition of HIV-1 in human populations”. en. In: *Science* 346.6205 (Oct. 2014), pp. 56–61. URL: http://dx.doi.org/10.1126/science.1256739.

[106] Y Feng et al. “HIV-1 entry cofactor: functional cDNA cloning of a seven-transmembrane, G protein-coupled receptor”. en. In: *Science* 272.5263 (May 1996), pp. 872–877. URL: http://dx.doi.org/10.1126/science.272.5263.872.

[107] Neil M Flynn et al. “Placebo-controlled phase 3 trial of a recombinant glycoprotein 120 vaccine to prevent HIV-1 infection”. en. In: *J. Infect. Dis.* 191.5 (Mar. 2005), pp. 654–665. URL: http://dx.doi.org/10.1086/428404.

[108] Genevieve G Fouda et al. “Immunological mechanisms of inducing HIV immunity in infants”. en. In: *Vaccine* 38.3 (Jan. 2020), pp. 411–415. URL: http://dx.doi.org/10.1016/j.vaccine.2019.11.011.

[109] Christophe Fraser et al. “Virulence and pathogenesis of HIV-1 infection: an evolutionary perspective”. en. In: *Science* 343.6177 (Mar. 2014), p. 1243727. URL: http://dx.doi.org/10.1126/science.1243727.

[110] Natalia T Freund et al. “Coexistence of potent HIV-1 broadly neutralizing antibodies and antibody-sensitive viruses in a viremic controller”. en. In: *Sci. Transl. Med.* 9.373 (Jan. 2017). URL: http://dx.doi.org/10.1126/scitranslmed.aal2144.

[111] Delphine Gabillard et al. “Virological failure and drug resistance in West African HIV-infected adults who started ART immediately or deferred ART initiation”. en. In: *J. Antimicrob. Chemother.* 76.10 (Sept. 2021), pp. 2666–2674. URL: http://dx.doi.org/10.1093/jac/dkab225.

[112] R C Gallo and F Wong-Staal. “A human T-lymphotropic retrovirus (HTLV-III) as the cause of the acquired immunodeficiency syndrome”. en. In: *Ann. Intern. Med.* 103.5 (Nov. 1985), pp. 679–689. URL: http://dx.doi.org/10.7326/0003-4819-103-5-679.

[113] F Gao et al. “Origin of HIV-1 in the chimpanzee Pan troglodytes troglodytes”. en. In: *Nature* 397.6718 (Feb. 1999), pp. 436–441. URL: http://dx.doi.org/10.1038/17130.

[114] Yang Gao et al. “Immunological and virological characteristics of human immunodeficiency virus type 1 superinfection: implications in vaccine design”. en. In: *Front. Med.* 11.4 (Dec. 2017), pp. 480–489. URL: http://dx.doi.org/10.1007/s11684-017-0594-8.

[115] David A Garber et al. “Durable protection against repeated penile exposures to simian-human immunodeficiency virus by broadly neutralizing antibodies”. en. In: *Nat. Commun.* 11.1 (June 2020), p. 3195. URL: http://dx.doi.org/10.1038/s41467-020-16928-9.

[116] P Garside et al. “Visualization of specific B and T lymphocyte interactions in the lymph node”. en. In: *Science* 281.5373 (July 1998), pp. 96–99. URL: http://dx.doi.org/10.1126/science.281.5373.96.

[117] Rajeev Gautam et al. “A single injection of anti-HIV-1 antibodies protects against repeated SHIV challenges”. en. In: *Nature* 533.7601 (May 2016), pp. 105–109. URL: http://dx.doi.org/10.1038/nature17677.

[118] Syna Kuriakose Gift et al. “Functional Stability of HIV-1 Envelope Trimer Affects Accessibility to Broadly Neutralizing Antibodies at Its Apex”. en. In: *J. Virol.* 91.24 (Dec. 2017). URL: http://dx.doi.org/10.1128/JVI.01216-17.

[119] Peter B Gilbert et al. “Neutralization titer biomarker for antibody-mediated prevention of HIV-1 acquisition”. en. In: *Nat. Med.* 28.9 (Sept. 2022), pp. 1924–1932. URL: http://dx.doi.org/10.1038/s41591-022-01953-6.

[120] S Gnanakaran et al. “Recurrent signature patterns in HIV-1 B clade envelope glycoproteins associated with either early or chronic infections”. en. In: *PLoS Pathog.* 7.9 (Sept. 2011), e1002209. URL: http://dx.doi.org/10.1371/journal.ppat.1002209.

[121] Eden P Go et al. “Comparative analysis of the glycosylation profiles of membrane-anchored HIV-1 envelope glycoprotein trimers and soluble gp140”. en. In: *J. Virol.* 89.16 (Aug. 2015), pp. 8245–8257. URL: http://dx.doi.org/10.1128/JVI.00628-15.

[122] Eden P Go et al. “Glycosylation benchmark profile for HIV-1 envelope glycoprotein production based on eleven Env trimers”. en. In: *J. Virol.* 91.9 (May 2017). URL: http://dx.doi.org/10.1128/jvi.02428-16.

[123] Leslie Goo et al. “Early development of broadly neutralizing antibodies in HIV-1-infected infants”. en. In: *Nat. Med.* 20.6 (June 2014), pp. 655–658. URL: http://dx.doi.org/10.1038/nm.3565.

[124] F L Graham et al. “Characteristics of a Human Cell Line Transformed by DNA from Human Adenovirus Type 5”. In: *J. Gen. Virol.* 36.1 (July 1977), pp. 59–72. URL: https://www.microbiologyresearch.org/content/journal/jgv/10.1099/0022-1317-36-1-59.

[125] Elin S Gray et al. “4E10-resistant variants in a human immunodeficiency virus type 1 subtype C-infected individual with an anti-membrane-proximal external region-neutralizing antibody response”. en. In: *J. Virol.* 82.5 (Mar. 2008), pp. 2367–2375. URL: http://dx.doi.org/10.1128/JVI.02161-07.

[126] Elin S Gray et al. "Antibody specificities associated with neutralization breadth in plasma from human immunodeficiency virus type 1 subtype C-infected blood donors". en. In: *J. Virol.* 83.17 (Sept. 2009), pp. 8925–8937. URL: http://dx.doi.org/10.1128/JVI.00758-09.

[127] Elin S Gray et al. "The neutralization breadth of HIV-1 develops incrementally over four years and is associated with CD4+ T cell decline and high viral load during acute infection". en. In: *J. Virol.* 85.10 (May 2011), pp. 4828–4840. URL: http://dx.doi.org/10.1128/JVI.00198-11.

[128] Glenda E Gray et al. "Vaccine Efficacy of ALVAC-HIV and Bivalent Subtype C gp120-MF59 in Adults". en. In: *N. Engl. J. Med.* 384.12 (Mar. 2021), pp. 1089–1100. URL: http://dx.doi.org/10.1056/NEJMoa2031499.

[129] Sarah A Griffith and Laura E McCoy. "To bnAb or Not to bnAb: Defining Broadly Neutralising Antibodies Against HIV-1". en. In: *Front. Immunol.* 12 (Oct. 2021), p. 708227. URL: http://dx.doi.org/10.3389/fimmu.2021.708227.

[130] Henning Gruell et al. "Effect of 3BNC117 and romidepsin on the HIV-1 reservoir in people taking suppressive antiretroviral therapy (ROADMAP): a randomised, open-label, phase 2A trial". en. In: *Lancet Microbe* 3.3 (Mar. 2022), e203–e214. URL: http://dx.doi.org/10.1016/S2666-5247(21)00239-1.

[131] Jesper D Gunst et al. "Early intervention with 3BNC117 and romidepsin at antiretroviral treatment initiation in people with HIV-1: a phase 1b/2a, randomized trial". en. In: *Nat. Med.* 28.11 (Nov. 2022), pp. 2424–2435. URL: http://dx.doi.org/10.1038/s41591-022-02023-7.

[132] M Guyader et al. "Genome organization and transactivation of the human immunodeficiency virus type 2". en. In: *Nature* 326.6114 (1987), pp. 662–669. URL: http://dx.doi.org/10.1038/326662a0.

[133] Clayton D Harro et al. "Recruitment and baseline epidemiologic profile of participants in the first phase 3 HIV vaccine efficacy trial". en. In: *J. Acquir. Immune Defic. Syndr.* 37.3 (Nov. 2004), pp. 1385–1392. URL: http://dx.doi.org/10.1097/01.qai.0000122983.87519.b5.

[134] Colin Havenar-Daughton et al. "The human naive B cell repertoire contains distinct subclasses for a germline-targeting HIV-1 vaccine immunogen". en. In: *Sci. Transl. Med.* 10.448 (July 2018). URL: http://dx.doi.org/10.1126/scitranslmed.aat0381.

[135] Barton F Haynes et al. "Cardiolipin polyspecific autoreactivity in two broadly neutralizing HIV-1 antibodies". en. In: *Science* 308.5730 (June 2005), pp. 1906–1908. URL: http://dx.doi.org/10.1126/science.1111781.

[136] Barton F Haynes et al. "Immune-correlates analysis of an HIV-1 vaccine efficacy trial". en. In: *N. Engl. J. Med.* 366.14 (Apr. 2012), pp. 1275–1286. URL: http://dx.doi.org/10.1056/NEJMoa1113425.

[137] Balthasar A Heesters, Riley C Myers, and Michael C Carroll. "Follicular dendritic cells: dynamic antigen libraries". en. In: *Nat. Rev. Immunol.* 14.7 (July 2014), pp. 495–504. URL: http://dx.doi.org/10.1038/nri3689.

[138] Nina Hertoghs et al. “Sexually transmitted founder HIV-1 viruses are relatively resistant to Langerhans cell-mediated restriction”. en. In: *PLoS One* 14.12 (Dec. 2019), e0226651. URL: http://dx.doi.org/10.1371/journal.pone.0226651.

[139] Rebecca Heß et al. “Glycosylation of HIV Env impacts IgG subtype responses to vaccination”. en. In: *Viruses* 11.2 (Feb. 2019), p. 153. URL: http://dx.doi.org/10.3390/v11020153.

[140] V M Hirsch et al. “Molecular cloning of SIV from sooty mangabey monkeys”. en. In: *J. Med. Primatol.* 18.3-4 (1989), pp. 279–285. URL: http://dx.doi.org/10.1111/j.1600-0684.1989.tb00230.x.

[141] Diep Thi Hoang et al. “UFBoot2: Improving the Ultrafast Bootstrap Approximation”. en. In: *Mol. Biol. Evol.* 35.2 (Feb. 2018), pp. 518–522. URL: http://dx.doi.org/10.1093/molbev/msx281.

[142] T Déirdre Hollingsworth et al. “High Transmissibility During Early HIV Infection Among Men Who Have Sex With Men-San Francisco, California”. en. In: *J. Infect. Dis.* 211.11 (June 2015), pp. 1757–1760. URL: http://dx.doi.org/10.1093/infdis/jiu831.

[143] Sam Hoot et al. “Recombinant HIV envelope proteins fail to engage germline versions of anti-CD4bs bNAbs”. en. In: *PLoS Pathog.* 9.1 (Jan. 2013), e1003106. URL: http://dx.doi.org/10.1371/journal.ppat.1003106.

[144] Chih-Chin Huang et al. “Structure of a V3-containing HIV-1 gp120 core”. en. In: *Science* 310.5750 (Nov. 2005), pp. 1025–1028. URL: http://dx.doi.org/10.1126/science.1118398.

[145] G Y Huang et al. “Structural survey of broadly neutralizing antibodies targeting the HIV-1 Env trimer delineates epitope categories and characteristics of recognition”. In: *Structure* (2019).

[146] Jinghe Huang et al. “Broad and potent HIV-1 neutralization by a human antibody that binds the gp41-gp120 interface”. en. In: *Nature* 515.7525 (Nov. 2014), pp. 138–142. URL: http://dx.doi.org/10.1038/nature13601.

[147] Jinghe Huang et al. “Broad and potent neutralization of HIV-1 by a gp41-specific human antibody”. en. In: *Nature* 491.7424 (Nov. 2012), pp. 406–412. URL: http://dx.doi.org/10.1038/nature11544.

[148] Jinghe Huang et al. “Identification of a CD4-Binding-Site Antibody to HIV that Evolved Near-Pan Neutralization Breadth”. en. In: *Immunity* 45.5 (Nov. 2016), pp. 1108–1121. URL: http://dx.doi.org/10.1016/j.immuni.2016.10.027.

[149] Yunda Huang et al. “Modeling cumulative overall prevention efficacy for the VRC01 phase 2b efficacy trials”. en. In: *Hum. Vaccin. Immunother.* 14.9 (May 2018), pp. 2116–2127. URL: http://dx.doi.org/10.1080/21645515.2018.1462640.

[150] Isabella Huettner et al. “Cross-reactivity of glycan-reactive HIV-1 broadly neutralizing antibodies with parasite glycans”. en. In: *Cell Rep.* 38.13 (Mar. 2022), p. 110611. URL: http://dx.doi.org/10.1016/j.celrep.2022.110611.

[151] Jonathan Hurtado et al. “Deep repertoire mining uncovers ultra-broad coronavirus neutralizing antibodies targeting multiple spike epitopes”. en. Mar. 2023. URL: https://www.biorxiv.org/content/10.1101/2023.03.28.534602v2.

[152] Jonathan Hurtado et al. “Efficient isolation of rare B cells using next-generation antigen barcoding”. en. In: *Front. Cell. Infect. Microbiol.* 12 (2022), p. 962945. URL: http://dx.doi.org/10.3389/fcimb.2022.962945.

[153] International AIDS Society Scientific Working Group on HIV Cure et al. “Towards an HIV cure: a global scientific strategy”. en. In: *Nat. Rev. Immunol.* 12.8 (July 2012), pp. 607–614. URL: http://dx.doi.org/10.1038/nri3262.

[154] Saiful Islam et al. “Characterization of the single-cell transcriptional landscape by highly multiplex RNA-seq”. en. In: *Genome Res.* 21.7 (July 2011), pp. 1160–1167. URL: http://dx.doi.org/10.1101/gr.110882.110.

[155] Muzafar Jan and Sunil K Arora. “Innate sensing of HIV-1 by dendritic cell-specific ICAM-3 grabbing nonintegrin on dendritic cells: Degradation and presentation versus transmission of virus to T cells is determined by glycan composition of viral envelope”. en. In: *AIDS Res. Hum. Retroviruses* 33.8 (Aug. 2017), pp. 765–767. URL: http://dx.doi.org/10.1089/aid.2016.0290.

[156] Joseph Jardine et al. “Rational HIV immunogen design to target specific germline B cell receptors”. en. In: *Science* 340.6133 (May 2013), pp. 711–716. URL: http://dx.doi.org/10.1126/science.1234150.

[157] Joseph G Jardine et al. “HIV-1 broadly neutralizing antibody precursor B cells revealed by germline-targeting immunogen”. en. In: *Science* 351.6280 (Mar. 2016), pp. 1458–1463. URL: http://dx.doi.org/10.1126/science.aad9195.

[158] Joseph G Jardine et al. “HIV-1 VACCINES. Priming a broadly neutralizing antibody response to HIV-1 using a germline-targeting immunogen”. en. In: *Science* 349.6244 (July 2015), pp. 156–161. URL: http://dx.doi.org/10.1126/science.aac5894.

[159] K Javaherian et al. “Broadly neutralizing antibodies elicited by the hypervariable neutralizing determinant of HIV-1”. en. In: *Science* 250.4987 (Dec. 1990), pp. 1590–1593. URL: http://dx.doi.org/10.1126/science.1703322.

[160] Manxue Jia et al. “VSV-displayed HIV-1 envelope identifies broadly neutralizing antibodies class-switched to IgG and IgA”. en. In: *Cell Host Microbe* 27.6 (June 2020), 963–975.e5. URL: http://dx.doi.org/10.1016/j.chom.2020.03.024.

[161] Collin Joyce et al. “Antigen pressure from two founder viruses induces multiple insertions at a single antibody position to generate broadly neutralizing HIV antibodies”. en. In: *PLoS Pathog.* 19.6 (June 2023), e1011416. URL: http://dx.doi.org/10.1371/journal.ppat.1011416.

[162] M Gordon Joyce et al. “Soluble Prefusion Closed DS-SOSIP.664-Env Trimers of Diverse HIV-1 Strains”. en. In: *Cell Rep.* 21.10 (Dec. 2017), pp. 2992–3002. URL: http://dx.doi.org/10.1016/j.celrep.2017.11.016.

[163] Boris Julg and Dan Barouch. “Broadly neutralizing antibodies for HIV-1 prevention and therapy”. en. In: *Semin. Immunol.* 51 (Jan. 2021), p. 101475. URL: http://dx.doi.org/10.1016/j.smim.2021.101475.

[164] Boris Julg et al. “Protective efficacy of broadly neutralizing antibodies with incomplete neutralization activity against simian-human immunodeficiency virus in rhesus monkeys”. en. In: *J. Virol.* 91.20 (Oct. 2017). URL: http://dx.doi.org/10.1128/JVI.01187-17.

[165] Jean-Philippe Julien et al. “Asymmetric recognition of the HIV-1 trimer by broadly neutralizing antibody PG9”. en. In: *Proc. Natl. Acad. Sci. U. S. A.* 110.11 (Mar. 2013), pp. 4351–4356. URL: http://dx.doi.org/10.1073/pnas.1217537110.

[166] Jean-Philippe Julien et al. “Broadly neutralizing antibody PGT121 allosterically modulates CD4 binding via recognition of the HIV-1 gp120 V3 base and multiple surrounding glycans”. en. In: *PLoS Pathog.* 9.5 (May 2013), e1003342. URL: http://dx.doi.org/10.1371/journal.ppat.1003342.

[167] Jean-Philippe Julien et al. “Broadly neutralizing antibody PGT121 allosterically modulates CD4 binding via recognition of the HIV-1 gp120 V3 base and multiple surrounding glycans”. en. In: *PLoS Pathog.* 9.5 (May 2013), e1003342. URL: http://dx.doi.org/10.1371/journal.ppat.1003342.

[168] Jean-Philippe Julien et al. “Crystal structure of a soluble cleaved HIV-1 envelope trimer”. en. In: *Science* 342.6165 (Dec. 2013), pp. 1477–1483. URL: http://dx.doi.org/10.1126/science.1245625.

[169] Michal Juraska et al. “Prevention efficacy of the broadly neutralizing antibody VRC01 depends on HIV-1 envelope sequence features”. en. In: *Proc. Natl. Acad. Sci. U. S. A.* 121.4 (Jan. 2024), e2308942121. URL: http://dx.doi.org/10.1073/pnas.2308942121.

[170] Alexis Kafando et al. “HIV-1 envelope glycoprotein amino acids signatures associated with clade B transmitted/founder and recent viruses”. en. In: *Viruses* 11.11 (Nov. 2019), p. 1012. URL: http://dx.doi.org/10.3390/v11111012.

[171] Subha Kalyaanamoorthy et al. “ModelFinder: fast model selection for accurate phylogenetic estimates”. en. In: *Nat. Methods* 14.6 (June 2017), pp. 587–589. URL: http://dx.doi.org/10.1038/nmeth.4285.

[172] Kazutaka Katoh et al. “MAFFT: a novel method for rapid multiple sequence alignment based on fast Fourier transform”. en. In: *Nucleic Acids Res.* 30.14 (July 2002), pp. 3059–3066. URL: http://dx.doi.org/10.1093/nar/gkf436.

[173] Samuel W Kazer, Bruce D Walker, and Alex K Shalek. “Evolution and Diversity of Immune Responses during Acute HIV Infection”. en. In: *Immunity* 53.5 (Nov. 2020), pp. 908–924. URL: http://dx.doi.org/10.1016/j.immuni.2020.10.015.

[174] Brandon F Keele et al. “Identification and characterization of transmitted and early founder virus envelopes in primary HIV-1 infection”. en. In: *Proc. Natl. Acad. Sci. U. S. A.* 105.21 (May 2008), pp. 7552–7557. URL: http://dx.doi.org/10.1073/pnas.0802203105.

[175] T B Kepler and A S Perelson. “Cyclic re-entry of germinal center B cells and the efficiency of affinity maturation”. en. In: *Immunol. Today* 14.8 (Aug. 1993), pp. 412–415. URL: http://dx.doi.org/10.1016/0167-5699(93)90145-B.

[176] Cari F Kessing et al. “In Vivo Suppression of HIV Rebound by Didehydro-Cortistatin A, a “Block-and-Lock” Strategy for HIV-1 Treatment”. en. In: *Cell Rep.* 21.3 (Oct. 2017), pp. 600–611. URL: http://dx.doi.org/10.1016/j.celrep.2017.09.080.

[177] Allon M Klein et al. “Droplet barcoding for single-cell transcriptomics applied to embryonic stem cells”. en. In: *Cell* 161.5 (May 2015), pp. 1187–1201. URL: http://dx.doi.org/10.1016/j.cell.2015.04.044.

[178] Kristi Koelsch et al. “Mature B cells class switched to IgD are autoreactive in healthy individuals”. en. In: *J. Clin. Invest.* 117.6 (June 2007), pp. 1558–1565. URL: http://dx.doi.org/10.1172/JCI27628.

[179] Leopold Kong et al. “Expression-system-dependent modulation of HIV-1 envelope glycoprotein antigenicity and immunogenicity”. en. In: *J. Mol. Biol.* 403.1 (Oct. 2010), pp. 131–147. URL: http://dx.doi.org/10.1016/j.jmb.2010.08.033.

[180] Leopold Kong et al. “Supersite of immune vulnerability on the glycosylated face of HIV-1 envelope glycoprotein gp120”. en. In: *Nat. Struct. Mol. Biol.* 20.7 (July 2013), pp. 796–803. URL: http://dx.doi.org/10.1038/nsmb.2594.

[181] Rui Kong et al. “Antibody Lineages with Vaccine-Induced Antigen-Binding Hotspots Develop Broad HIV Neutralization”. en. In: *Cell* 178.3 (July 2019), 567–584.e19. URL: http://dx.doi.org/10.1016/j.cell.2019.06.030.

[182] Rui Kong et al. “Fusion peptide of HIV-1 as a site of vulnerability to neutralizing antibody”. en. In: *Science* 352.6287 (May 2016), pp. 828–833. URL: http://dx.doi.org/10.1126/science.aae0474.

[183] Rui Kong et al. “Improving neutralization potency and breadth by combining broadly reactive HIV-1 antibodies targeting major neutralization epitopes”. en. In: *J. Virol.* 89.5 (Mar. 2015), pp. 2659–2671. URL: http://dx.doi.org/10.1128/JVI.03136-14.

[184] Sergei L Kosakovsky Pond et al. “GARD: a genetic algorithm for recombination detection”. en. In: *Bioinformatics* 22.24 (Dec. 2006), pp. 3096–3098. URL: http://dx.doi.org/10.1093/bioinformatics/btl474.

[185] J Kulkosky and A M Skalka. “HIV DNA integration: observations and interferences”. en. In: *J. Acquir. Immune Defic. Syndr.* 3.9 (1990), pp. 839–851. URL: https://www.ncbi.nlm.nih.gov/pubmed/2166782.

[186] Sanjeev Kumar et al. “Recognition determinants of improved HIV-1 neutralization by a heavy chain matured pediatric antibody”. In: *iScience* 26.9 (Sept. 2023), p. 107579. URL: https://www.sciencedirect.com/science/article/pii/S2589004223016565.

[187] Young Do Kwon et al. “Crystal structure, conformational fixation and entry-related interactions of mature ligand-free HIV-1 Env”. en. In: *Nat. Struct. Mol. Biol.* 22.7 (July 2015), pp. 522–531. URL: http://dx.doi.org/10.1038/nsmb.3051.

[188] P D Kwong et al. “Structure of an HIV gp120 envelope glycoprotein in complex with the CD4 receptor and a neutralizing human antibody”. en. In: *Nature* 393.6686 (June 1998), pp. 648–659. URL: http://dx.doi.org/10.1038/31405.

[189] Elise Landais et al. “Broadly Neutralizing Antibody Responses in a Large Longitudinal Sub-Saharan HIV Primary Infection Cohort”. en. In: *PLoS Pathog.* 12.1 (Jan. 2016), e1005369. URL: http://dx.doi.org/10.1371/journal.ppat.1005369.

[190] Elise Landais et al. “HIV Envelope Glycoform Heterogeneity and Localized Diversity Govern the Initiation and Maturation of a V2 Apex Broadly Neutralizing Antibody Lineage”. en. In: *Immunity* 47.5 (Nov. 2017), 990–1003.e9. URL: http://dx.doi.org/10.1016/j.immuni.2017.11.002.

[191] Raphael J Landovitz, Hyman Scott, and Steven G Deeks. “Prevention, treatment and cure of HIV infection”. en. In: *Nat. Rev. Microbiol.* 21.10 (Oct. 2023), pp. 657–670. URL: http://dx.doi.org/10.1038/s41579-023-00914-1.

[192] Jeong Hyun Lee and Shane Crotty. “HIV vaccinology: 2021 update”. en. In: *Semin. Immunol.* 51 (Jan. 2021), p. 101470. URL: http://dx.doi.org/10.1016/j.smim.2021.101470.

[193] Jeong Hyun Lee et al. “Antibodies to a conformational epitope on gp41 neutralize HIV-1 by destabilizing the Env spike”. en. In: *Nat. Commun.* 6 (Sept. 2015), p. 8167. URL: http://dx.doi.org/10.1038/ncomms9167.

[194] M P Lefranc. “Nomenclature of the human immunoglobulin heavy (IGH) genes”. en. In: *Exp. Clin. Immunogenet.* 18.2 (2001), pp. 100–116. URL: http://dx.doi.org/10.1159/000049189.

[195] M P Lefranc et al. “IMGT, the international ImMunoGeneTics database”. en. In: *Nucleic Acids Res.* 27.1 (Jan. 1999), pp. 209–212. URL: http://dx.doi.org/10.1093/nar/27.1.209.

[196] Marie-Paule Lefranc et al. “IMGT, the international ImMunoGeneTics information system”. en. In: *Nucleic Acids Res.* 37.Database issue (Jan. 2009), pp. D1006–12. URL: http://dx.doi.org/10.1093/nar/gkn838.

[197] David J Leggat et al. “Vaccination induces HIV broadly neutralizing antibody precursors in humans”. en. In: *Science* 378.6623 (Dec. 2022), eadd6502. URL: http://dx.doi.org/10.1126/science.add6502.

[198] J A Levy et al. “Isolation of lymphocytopathic retroviruses from San Francisco patients with AIDS”. en. In: *Science* 225.4664 (Aug. 1984), pp. 840–842. URL: http://dx.doi.org/10.1126/science.6206563.

[199] H X Liao et al. “Vaccine Induction of Antibodies against a Structurally Heterogeneous Site of Immune Pressure within HIV-1 Envelope Protein Variable Regions 1 and 2”. In: *Immunity* 38 (2013), pp. 176–186.

[200] Hua-Xin Liao et al. “Co-evolution of a broadly neutralizing HIV-1 antibody and founder virus”. en. In: *Nature* 496.7446 (Apr. 2013), pp. 469–476. URL: http://dx.doi.org/10.1038/nature12053.

[201] J D Lifson et al. “AIDS retrovirus induced cytopathology: giant cell formation and involvement of CD4 antigen”. en. In: *Science* 232.4754 (May 1986), pp. 1123–1127. URL: http://dx.doi.org/10.1126/science.3010463.

[202] J D Lifson et al. “Induction of CD4-dependent cell fusion by the HTLV-III/LAV envelope glycoprotein”. en. In: *Nature* 323.6090 (1986), pp. 725–728. URL: http://dx.doi.org/10.1038/323725a0.

[203] Yu-Ru Lin et al. "HIV-1 VRC01 germline-targeting immunogens select distinct Epitope-specific B cell receptors". en. In: *Immunity* 53.4 (Oct. 2020), 840–851.e6. URL: http://dx.doi.org/10.1016/j.immuni.2020.09.007.

[204] Jun Liu et al. "Molecular architecture of native HIV-1 gp120 trimers". en. In: *Nature* 455.7209 (Sept. 2008), pp. 109–113. URL: http://dx.doi.org/10.1038/nature07159.

[205] Mengfei Liu et al. "Polyreactivity and autoreactivity among HIV-1 antibodies". en. In: *J. Virol.* 89.1 (Jan. 2015), pp. 784–798. URL: http://dx.doi.org/10.1128/JVI.02378-14.

[206] Michela Locci et al. "Human circulating PD-1+CXCR3-CXCR5+ memory Tfh cells are highly functional and correlate with broadly neutralizing HIV antibody responses". en. In: *Immunity* 39.4 (Oct. 2013), pp. 758–769. URL: http://dx.doi.org/10.1016/j.immuni.2013.08.031.

[207] Valérie Lorin et al. "Epitope convergence of broadly HIV-1 neutralizing IgA and IgG antibody lineages in a viremic controller". en. In: *J. Exp. Med.* 219.3 (Mar. 2022). URL: http://dx.doi.org/10.1084/jem.20212045.

[208] Rebecca M Lynch et al. "Virologic effects of broadly neutralizing antibody VRC01 administration during chronic HIV-1 infection". en. In: *Sci. Transl. Med.* 7.319 (Dec. 2015), 319ra206. URL: http://dx.doi.org/10.1126/scitranslmed.aad5752.

[209] Dmitry Lyumkis et al. "Cryo-EM structure of a fully glycosylated soluble cleaved HIV-1 envelope trimer". en. In: *Science* 342.6165 (Dec. 2013), pp. 1484–1490. URL: http://dx.doi.org/10.1126/science.1245627.

[210] Daniel T MacLeod et al. "Early Antibody Lineage Diversification and Independent Limb Maturation Lead to Broad HIV-1 Neutralization Targeting the Env High-Mannose Patch". en. In: *Immunity* 44.5 (May 2016), pp. 1215–1226. URL: https://www.cell.com/immunity/pdf/S1074-7613(16)30145-5.pdf.

[211] Evan Z Macosko et al. "Highly parallel genome-wide expression profiling of individual cells using nanoliter droplets". en. In: *Cell* 161.5 (May 2015), pp. 1202–1214. URL: http://dx.doi.org/10.1016/j.cell.2015.05.002.

[212] P J Maddon et al. "HIV infection does not require endocytosis of its receptor, CD4". en. In: *Cell* 54.6 (Sept. 1988), pp. 865–874. URL: http://dx.doi.org/10.1016/s0092-8674(88)91241-x.

[213] B Mandel. "Neutralization of animal viruses". en. In: *Adv. Virus Res.* 23 (1978), pp. 205–268. URL: http://dx.doi.org/10.1016/s0065-3527(08)60101-3.

[214] Amapola Manrique et al. "In vivo and in vitro escape from neutralizing antibodies 2G12, 2F5, and 4E10". en. In: *J. Virol.* 81.16 (Aug. 2007), pp. 8793–8808. URL: http://dx.doi.org/10.1128/JVI.00598-07.

[215] Taciana Manso et al. "IMGT® databases, related tools and web resources through three main axes of research and development". en. In: *Nucleic Acids Res.* 50.D1 (Jan. 2022), pp. D1262–D1272. URL: http://dx.doi.org/10.1093/nar/gkab1136.

[216] Leonid Margolis and Robin Shattock. "Selective transmission of CCR5-utilizing HIV-1: the 'gatekeeper' problem resolved?" en. In: *Nat. Rev. Microbiol.* 4.4 (Apr. 2006), pp. 312–317. URL: http://dx.doi.org/10.1038/nrmicro1387.

[217] Darren P Martin et al. "RDP4: Detection and analysis of recombination patterns in virus genomes". In: *Virus Evol* 1.1 (Mar. 2015). URL: https://academic.oup.com/ve/article-pdf/1/1/vev003/50562961/ve_1_1_vev003.pdf.

[218] J R Mascola et al. "Protection of macaques against vaginal transmission of a pathogenic HIV-1/SIV chimeric virus by passive infusion of neutralizing antibodies". en. In: *Nat. Med.* 6.2 (Feb. 2000), pp. 207–210. URL: http://dx.doi.org/10.1038/72318.

[219] John R Mascola and Barton F Haynes. "HIV-1 neutralizing antibodies: understanding nature's pathways". en. In: *Immunol. Rev.* 254.1 (July 2013), pp. 225–244. URL: http://dx.doi.org/10.1111/imr.12075.

[220] L M Mayr et al. "Epitope mapping of conformational V2-specific anti-HIV human mono- clonal antibodies reveals an immunodominant site in V2". In: *PloS One* 8 (2013).

[221] Laura E McCoy et al. "Incomplete Neutralization and Deviation from Sigmoidal Neutralization Curves for HIV Broadly Neutralizing Monoclonal Antibodies". en. In: *PLoS Pathog.* 11.8 (Aug. 2015), e1005110. URL: http://dx.doi.org/10.1371/journal.ppat.1005110.

[222] Elizabeth J McFarland et al. "Safety, tolerability, and pharmacokinetics of a long-acting broadly neutralizing human immunodeficiency virus type 1 (HIV-1) monoclonal antibody VRC01LS in HIV-1-exposed newborn infants". en. In: *J. Infect. Dis.* 224.11 (Dec. 2021), pp. 1916–1924. URL: http://dx.doi.org/10.1093/infdis/jiab229.

[223] Andrew T McGuire et al. "Engineering HIV envelope protein to activate germline B cell receptors of broadly neutralizing anti-CD4 binding site antibodies". en. In: *J. Exp. Med.* 210.4 (Apr. 2013), pp. 655–663. URL: http://dx.doi.org/10.1084/jem.20122824.

[224] Andrew T McGuire et al. "Specifically modified Env immunogens activate B-cell precursors of broadly neutralizing HIV-1 antibodies in transgenic mice". en. In: *Nat. Commun.* 7 (Feb. 2016), p. 10618. URL: http://dx.doi.org/10.1038/ncomms10618.

[225] Leland McInnes, John Healy, and James Melville. "UMAP: Uniform Manifold Approximation and Projection for Dimension Reduction". In: (Feb. 2018). arXiv: 1802.03426 [stat.ML]. URL: http://arxiv.org/abs/1802.03426.

[226] Jason S McLellan et al. "Structure of HIV-1 gp120 V1/V2 domain with broadly neutralizing antibody PG9". en. In: *Nature* 480.7377 (Nov. 2011), pp. 336–343. URL: http://dx.doi.org/10.1038/nature10696.

[227] Andrew J McMichael et al. "The immune response during acute HIV-1 infection: clues for vaccine development". en. In: *Nat. Rev. Immunol.* 10.1 (Jan. 2010), pp. 11–23. URL: http://dx.doi.org/10.1038/nri2674.

[228] Max Medina-Ramírez et al. "Design and crystal structure of a native-like HIV-1 envelope trimer that engages multiple broadly neutralizing antibody precursors in vivo". en. In: *J. Exp. Med.* 214.9 (Sept. 2017), pp. 2573–2590. URL: http://dx.doi.org/10.1084/jem.20161160.

[229] Saurabh Mehandru et al. "Adjunctive passive immunotherapy in human immunodeficiency virus type 1-infected individuals treated with antiviral therapy during acute and early infection". en. In: *J. Virol.* 81.20 (Oct. 2007), pp. 11016–11031. URL: http://dx.doi.org/10.1128/JVI.01340-07.

[230] Pilar Mendoza et al. "Combination therapy with anti-HIV-1 antibodies maintains viral suppression". en. In: *Nature* 561.7724 (Sept. 2018), pp. 479–484. URL: http://dx.doi.org/10.1038/s41586-018-0531-2.

[231] Christopher J Miller et al. "Propagation and dissemination of infection after vaginal transmission of simian immunodeficiency virus". en. In: *J. Virol.* 79.14 (July 2005), pp. 9217–9227. URL: http://dx.doi.org/10.1128/JVI.79.14.9217-9227.2005.

[232] Bui Quang Minh et al. "IQ-TREE 2: New Models and Efficient Methods for Phylogenetic Inference in the Genomic Era". en. In: *Mol. Biol. Evol.* 37.5 (May 2020), pp. 1530–1534. URL: http://dx.doi.org/10.1093/molbev/msaa015.

[233] Brian Moldt et al. "Highly potent HIV-specific antibody neutralization in vitro translates into effective protection against mucosal SHIV challenge in vivo". en. In: *Proc. Natl. Acad. Sci. U. S. A.* 109.46 (Nov. 2012), pp. 18921–18925. URL: http://dx.doi.org/10.1073/pnas.1214785109.

[234] David C Montefiori et al. "Neutralization tiers of HIV-1". en. In: *Curr. Opin. HIV AIDS* 13.2 (Mar. 2018), pp. 128–136. URL: http://dx.doi.org/10.1097/COH.0000000000000442.

[235] Hugo Mouquet et al. "Complex-type N-glycan recognition by potent broadly neutralizing HIV antibodies". en. In: *Proc. Natl. Acad. Sci. U. S. A.* 109.47 (Nov. 2012), E3268–77. URL: http://dx.doi.org/10.1073/pnas.1217207109.

[236] S B Needleman and C D Wunsch. "A general method applicable to the search for similarities in the amino acid sequence of two proteins". en. In: *J. Mol. Biol.* 48.3 (Mar. 1970), pp. 443–453. URL: http://dx.doi.org/10.1016/0022-2836(70)90057-4.

[237] Ngoc-Khanh Nguyen et al. "A cluster of broadly neutralizing IgG against BK polyomavirus in a repertoire dominated by IgM". en. In: *Life Sci Alliance* 6.4 (Apr. 2023). URL: http://dx.doi.org/10.26508/lsa.202201567.

[238] Vladimir Novitsky et al. "Viral load and CD4+ T-cell dynamics in primary HIV-1 subtype C infection". en. In: *J. Acquir. Immune Defic. Syndr.* 50.1 (Jan. 2009), pp. 65–76. URL: http://dx.doi.org/10.1097/QAI.0b013e3181900141.

[239] J Overbaugh and C R Bangham. "Selection forces and constraints on retroviral sequence variation". en. In: *Science* 292.5519 (May 2001), pp. 1106–1109. URL: http://dx.doi.org/10.1126/science.1059128.

[240] Matthew Pace and John Frater. "A cure for HIV: is it in sight?" en. In: *Expert Rev. Anti. Infect. Ther.* 12.7 (July 2014), pp. 783–791. URL: http://dx.doi.org/10.1586/14787210.2014.910112.

[241] Kathleen Deska Pagana, Timothy J Pagana, and Theresa Noel Pagana. *Mosby's Diagnostic and Laboratory Test Reference*. en. Elsevier, Nov. 2022. URL: https://play.google.com/store/books/details?id=nvD4zgEACAAJ.

[242] Marie Pancera et al. "Structural basis for diverse N-glycan recognition by HIV-1-neutralizing V1-V2-directed antibody PG16". en. In: *Nat. Struct. Mol. Biol.* 20.7 (July 2013), pp. 804–813. URL: http://dx.doi.org/10.1038/nsmb.2600.

[243] Didrik Paus et al. "Antigen recognition strength regulates the choice between extrafollicular plasma cell and germinal center B cell differentiation". en. In: *J. Exp. Med.* 203.4 (Apr. 2006), pp. 1081–1091. URL: http://dx.doi.org/10.1084/jem.20060087.

[244] Rushad Pavri and Michel C Nussenzweig. "AID targeting in antibody diversity". en. In: *Adv. Immunol.* 110 (2011), pp. 1–26. URL: http://dx.doi.org/10.1016/B978-0-12-387663-8.00005-3.

[245] Amarendra Pegu et al. "A meta-analysis of passive immunization studies shows that serum-neutralizing antibody titer associates with protection against SHIV challenge". en. In: *Cell Host Microbe* 26.3 (Sept. 2019), 336–346.e3. URL: http://dx.doi.org/10.1016/j.chom.2019.08.014.

[246] Amarendra Pegu et al. "Antibodies targeting the fusion peptide on the HIV envelope provide protection to rhesus macaques against mucosal SHIV challenge". en. In: *Sci. Transl. Med.* 16.730 (Jan. 2024), eadh9039. URL: http://dx.doi.org/10.1126/scitranslmed.adh9039.

[247] Amarendra Pegu et al. "Potent anti-viral activity of a trispecific HIV neutralizing antibody in SHIV-infected monkeys". en. In: *Cell Rep.* 38.1 (Jan. 2022), p. 110199. URL: http://dx.doi.org/10.1016/j.celrep.2021.110199.

[248] Jonathan U Peled et al. "The biochemistry of somatic hypermutation". en. In: *Annu. Rev. Immunol.* 26.1 (2008), pp. 481–511. URL: http://dx.doi.org/10.1146/annurev.immunol.26.021607.090236.

[249] Kerui Peng et al. "Diversity in immunogenomics: the value and the challenge". en. In: *Nat. Methods* 18.6 (June 2021), pp. 588–591. URL: http://dx.doi.org/10.1038/s41592-021-01169-5.

[250] Matthieu Perreau, Yves Levy, and Giuseppe Pantaleo. "Immune response to HIV". en. In: *Curr. Opin. HIV AIDS* 8.4 (July 2013), pp. 333–340. URL: http://dx.doi.org/10.1097/COH.0b013e328361faf4.

[251] Anne Piantadosi et al. "Breadth of neutralizing antibody response to human immunodeficiency virus type 1 is affected by factors early in infection but does not influence disease progression". en. In: *J. Virol.* 83.19 (Oct. 2009), pp. 10269–10274. URL: http://dx.doi.org/10.1128/JVI.01149-09.

[252] Punnee Pitisuttithum et al. "Randomized, double-blind, placebo-controlled efficacy trial of a bivalent recombinant glycoprotein 120 HIV-1 vaccine among injection drug users in Bangkok, Thailand". en. In: *J. Infect. Dis.* 194.12 (Dec. 2006), pp. 1661–1671. URL: http://dx.doi.org/10.1086/508748.

[253] E J Platt et al. "Effects of CCR5 and CD4 cell surface concentrations on infections by macrophagetropic isolates of human immunodeficiency virus type 1". en. In: *J. Virol.* 72.4 (Apr. 1998), pp. 2855–2864. URL: http://dx.doi.org/10.1128/JVI.72.4.2855-2864.1998.

[254] G Poli, G Pantaleo, and A S Fauci. "Immunopathogenesis of human immunodeficiency virus infection". en. In: *Clin. Infect. Dis.* 17 Suppl 1 (Aug. 1993), S224–9. URL: https://www.ncbi.nlm.nih.gov/pubmed/8104513.

[255] M Popovic et al. "Detection, isolation, and continuous production of cytopathic retroviruses (HTLV-III) from patients with AIDS and pre-AIDS". en. In: *Science* 224.4648 (May 1984), pp. 497–500. URL: http://dx.doi.org/10.1126/science.6200935.

[256] Nicola Portolano et al. "Recombinant protein expression for structural biology in HEK 293F suspension cells: a novel and accessible approach". en. In: *J. Vis. Exp.* 92 (Oct. 2014), e51897. URL: http://dx.doi.org/10.3791/51897.

[257] K N Potter et al. "Molecular characterization of a cross-reactive idiotope on human immunoglobulins utilizing the VH4-21 gene segment". en. In: *J. Exp. Med.* 178.4 (Oct. 1993), pp. 1419–1428. URL: http://dx.doi.org/10.1084/jem.178.4.1419.

[258] J Poudrier et al. "The AIDS disease of CD4C/HIV transgenic mice shows impaired germinal centers and autoantibodies and develops in the absence of IFN-gamma and IL-6". en. In: *Immunity* 15.2 (Aug. 2001), pp. 173–185. URL: http://dx.doi.org/10.1016/s1074-7613(01)00177-7.

[259] Matt A Price et al. "Cohort Profile: IAVI's HIV epidemiology and early infection cohort studies in Africa to support vaccine discovery". en. In: *Int. J. Epidemiol.* 50.1 (Mar. 2021), pp. 29–30. URL: http://dx.doi.org/10.1093/ije/dyaa100.

[260] Morgan N Price, Paramvir S Dehal, and Adam P Arkin. "FastTree 2–approximately maximum-likelihood trees for large alignments". en. In: *PLoS One* 5.3 (Mar. 2010), e9490. URL: http://dx.doi.org/10.1371/journal.pone.0009490.

[261] Laura K Pritchard et al. "Cell- and protein-directed glycosylation of native cleaved HIV-1 envelope". en. In: *J. Virol.* 89.17 (Sept. 2015), pp. 8932–8944. URL: http://dx.doi.org/10.1128/JVI.01190-15.

[262] Laura K Pritchard et al. "Glycan clustering stabilizes the mannose patch of HIV-1 and preserves vulnerability to broadly neutralizing antibodies". en. In: *Nat. Commun.* 6 (June 2015), p. 7479. URL: http://dx.doi.org/10.1038/ncomms8479.

[263] Laura K Pritchard et al. "Structural constraints determine the glycosylation of HIV-1 envelope trimers". en. In: *Cell Rep.* 11.10 (June 2015), pp. 1604–1613. URL: http://dx.doi.org/10.1016/j.celrep.2015.05.017.

[264] A E Pugh-Bernard et al. "Regulation of inherently autoreactive VH4-34 B cells in the maintenance of human B cell tolerance". en. In: *J. Clin. Invest.* 108.7 (Oct. 2001), pp. 1061–1070. URL: http://dx.doi.org/10.1172/JCI12462.

[265] Srinika Ranasinghe et al. "HIV-1 Antibody Neutralization Breadth Is Associated with Enhanced HIV-Specific CD4+ T Cell Responses". en. In: *J. Virol.* 90.5 (Dec. 2015), pp. 2208–2220. URL: http://dx.doi.org/10.1128/JVI.02278-15.

[266] A Ranki et al. “Neutralizing antibodies in HIV (HTLV-III) infection: correlation with clinical outcome and antibody response against different viral proteins”. en. In: *Clin. Exp. Immunol.* 69.2 (Aug. 1987), pp. 231–239. URL: https://www.ncbi.nlm.nih.gov/pubmed/3652531.

[267] Kimmo Rantalainen et al. “Co-evolution of HIV Envelope and Apex-Targeting Neutralizing Antibody Lineage Provides Benchmarks for Vaccine Design”. en. In: *Cell Rep.* 23.11 (June 2018), pp. 3249–3261. URL: http://dx.doi.org/10.1016/j.celrep.2018.05.046.

[268] Andrew D Redd et al. “Previously transmitted HIV-1 strains are preferentially selected during subsequent sexual transmissions”. en. In: *J. Infect. Dis.* 206.9 (Nov. 2012), pp. 1433–1442. URL: http://dx.doi.org/10.1093/infdis/jis503.

[269] Supachai Rerks-Ngarm et al. “Vaccination with ALVAC and AIDSVAX to prevent HIV-1 infection in Thailand”. en. In: *N. Engl. J. Med.* 361.23 (Dec. 2009), pp. 2209–2220. URL: http://dx.doi.org/10.1056/NEJMoa0908492.

[270] D C Rio, S G Clark, and R Tjian. “A mammalian host-vector system that regulates expression and amplification of transfected genes by temperature induction”. en. In: *Science* 227.4682 (Jan. 1985), pp. 23–28. URL: http://dx.doi.org/10.1126/science.2981116.

[271] Julia Roider et al. “High-frequency, functional HIV-specific T-follicular helper and regulatory cells are present within germinal centers in children but not adults”. en. In: *Front. Immunol.* 9 (Sept. 2018), p. 1975. URL: http://dx.doi.org/10.3389/fimmu.2018.01975.

[272] Miriam Rosás-Umbert et al. “Administration of broadly neutralizing anti-HIV-1 antibodies at ART initiation maintains long-term CD8+ T cell immunity”. en. In: *Nat. Commun.* 13.1 (Oct. 2022), p. 6473. URL: http://dx.doi.org/10.1038/s41467-022-34171-2.

[273] Alexander B Rosenberg et al. “Single-cell profiling of the developing mouse brain and spinal cord with split-pool barcoding”. en. In: *Science* 360.6385 (Apr. 2018), pp. 176–182. URL: http://dx.doi.org/10.1126/science.aam8999.

[274] Claire Rousset. *Coévolution entre les glycoprotéines d’enveloppe du VIH et les anticorps neutralisants à large spectre ciblant la région du glycane N332*. fr. https://theses.hal.science/tel-02127494. Accessed: 2024-1-15. Dec. 2018. URL: https://theses.hal.science/tel-02127494.

[275] Romy Rouzeau. “Broadly neutralizing antibodies against HIV : design of isolation strategies and application to two elite neutralizers”. en. PhD thesis. Université Grenoble Alpes [2020-....], June 2021. URL: https://theses.hal.science/tel-03375033.

[276] Rebecca S Rudicell et al. “Enhanced potency of a broadly neutralizing HIV-1 antibody in vitro improves protection against lentiviral infection in vivo”. en. In: *J. Virol.* 88.21 (Nov. 2014), pp. 12669–12682. URL: http://dx.doi.org/10.1128/JVI.02213-14.

[277] Claudia R Ruprecht et al. “MPER-specific antibodies induce gp120 shedding and irreversibly neutralize HIV-1”. en. In: *J. Exp. Med.* 208.3 (Mar. 2011), pp. 439–454. URL: http://dx.doi.org/10.1084/jem.20101907.

[278] Peter Rusert et al. "Determinants of HIV-1 broadly neutralizing antibody induction". en. In: *Nat. Med.* 22.11 (Nov. 2016), pp. 1260–1267. URL: http://dx.doi.org/10.1038/nm.4187.

[279] Manish Sagar. "HIV-1 transmission biology: selection and characteristics of infecting viruses". en. In: *J. Infect. Dis.* 202 Suppl 2.Suppl 2 (Oct. 2010), S289–96. URL: http://dx.doi.org/10.1086/655656.

[280] Manish Sagar et al. "Selection of HIV variants with signature genotypic characteristics during heterosexual transmission". en. In: *J. Infect. Dis.* 199.4 (Feb. 2009), pp. 580–589. URL: http://dx.doi.org/10.1086/596557.

[281] Rogier W Sanders et al. "A next-generation cleaved, soluble HIV-1 Env trimer, BG505 SOSIP.664 gp140, expresses multiple epitopes for broadly neutralizing but not non-neutralizing antibodies". en. In: *PLoS Pathog.* 9.9 (Sept. 2013), e1003618. URL: http://dx.doi.org/10.1371/journal.ppat.1003618.

[282] Marcella Sarzotti-Kelsoe et al. "Optimization and validation of the TZM-bl assay for standardized assessments of neutralizing antibodies against HIV-1". en. In: *J. Immunol. Methods* 409 (July 2014), pp. 131–146. URL: http://dx.doi.org/10.1016/j.jim.2013.11.022.

[283] D Noah Sather et al. "Factors associated with the development of cross-reactive neutralizing antibodies during human immunodeficiency virus type 1 infection". en. In: *J. Virol.* 83.2 (Jan. 2009), pp. 757–769. URL: http://dx.doi.org/10.1128/JVI.02036-08.

[284] Kevin O Saunders et al. "Targeted selection of HIV-specific antibody mutations by engineering B cell maturation". en. In: *Science* 366.6470 (Dec. 2019). URL: http://dx.doi.org/10.1126/science.aay7199.

[285] Kevin O Saunders et al. "Vaccine induction of heterologous tier 2 HIV-1 neutralizing antibodies in animal models". en. In: *Cell Rep.* 21.13 (Dec. 2017), pp. 3681–3690. URL: http://dx.doi.org/10.1016/j.celrep.2017.12.028.

[286] Johannes F Scheid et al. "HIV-1 antibody 3BNC117 suppresses viral rebound in humans during treatment interruption". en. In: *Nature* 535.7613 (July 2016), pp. 556–560. URL: http://dx.doi.org/10.1038/nature18929.

[287] J E Schmitz et al. "Control of viremia in simian immunodeficiency virus infection by CD8+ lymphocytes". en. In: *Science* 283.5403 (Feb. 1999), pp. 857–860. URL: http://dx.doi.org/10.1126/science.283.5403.857.

[288] Philipp Schommers et al. "Dynamics and durability of HIV-1 neutralization are determined by viral replication". en. In: *Nat. Med.* 29.11 (Nov. 2023), pp. 2763–2774. URL: http://dx.doi.org/10.1038/s41591-023-02582-3.

[289] Jelle van Schooten et al. "Complementary antibody lineages achieve neutralization breadth in an HIV-1 infected elite neutralizer". en. In: *PLoS Pathog.* 18.11 (Nov. 2022), e1010945. URL: http://dx.doi.org/10.1371/journal.ppat.1010945.

[290] Jelle van Schooten et al. "Identification of IOMA-class neutralizing antibodies targeting the CD4-binding site on the HIV-1 envelope glycoprotein". en. In: *Nat. Commun.* 13.1 (Aug. 2022), p. 4515. URL: http://dx.doi.org/10.1038/s41467-022-32208-0.

[291] Michael S Seaman et al. "Tiered categorization of a diverse panel of HIV-1 Env pseudoviruses for assessment of neutralizing antibodies". en. In: *J. Virol.* 84.3 (Feb. 2010), pp. 1439–1452. URL: http://dx.doi.org/10.1128/JVI.02108-09.

[292] Jennifer Serwanga et al. "HIV-1 superinfection can occur in the presence of broadly neutralizing antibodies". en. In: *Vaccine* 36.4 (Jan. 2018), pp. 578–586. URL: http://dx.doi.org/10.1016/j.vaccine.2017.11.075.

[293] Ian Setliff et al. "High-Throughput Mapping of B Cell Receptor Sequences to Antigen Specificity". en. In: *Cell* 179.7 (Dec. 2019), 1636–1646.e15. URL: http://dx.doi.org/10.1016/j.cell.2019.11.003.

[294] Alexander M Sevy et al. "Immune repertoire fingerprinting by principal component analysis reveals shared features in subject groups with common exposures". en. In: *BMC Bioinformatics* 20.1 (Dec. 2019), p. 629. URL: http://dx.doi.org/10.1186/s12859-019-3281-8.

[295] Daniel J Sheward et al. "HIV Superinfection Drives De Novo Antibody Responses and Not Neutralization Breadth". en. In: *Cell Host Microbe* 24.4 (Oct. 2018), 593–599.e3. URL: http://dx.doi.org/10.1016/j.chom.2018.09.001.

[296] Ryo Shinnakasu et al. "Regulated selection of germinal-center cells into the memory B cell compartment". en. In: *Nat. Immunol.* 17.7 (July 2016), pp. 861–869. URL: http://dx.doi.org/10.1038/ni.3460.

[297] Mackenzie M Shipley et al. "Functional development of a V3/glycan-specific broadly neutralizing antibody isolated from a case of HIV superinfection". en. In: *Elife* 10 (July 2021). URL: http://dx.doi.org/10.7554/eLife.68110.

[298] Claire-Anne Siegrist. "Vaccine Immunology". In: *Plotkin's Vaccines*. Elsevier, 2018, 16–34.e7. URL: http://dx.doi.org/10.1016/b978-0-323-35761-6.00002-x.

[299] Melissa D Simek et al. "Human immunodeficiency virus type 1 elite neutralizers: individuals with broad and potent neutralizing activity identified by using a high-throughput neutralization assay together with an analytical selection algorithm". en. In: *J. Virol.* 83.14 (July 2009), pp. 7337–7348. URL: http://dx.doi.org/10.1128/JVI.00110-09.

[300] Melissa D Simek et al. "Human immunodeficiency virus type 1 elite neutralizers: individuals with broad and potent neutralizing activity identified by using a high-throughput neutralization assay together with an analytical selection algorithm". en. In: *J. Virol.* 83.14 (July 2009), pp. 7337–7348. URL: http://dx.doi.org/10.1128/JVI.00110-09.

[301] Viviana Simon, David D Ho, and Quarraisha Abdool Karim. "HIV/AIDS epidemiology, pathogenesis, prevention, and treatment". en. In: *Lancet* 368.9534 (Aug. 2006), pp. 489–504. URL: http://dx.doi.org/10.1016/S0140-6736(06)69157-5.

[302] Cassandra A Simonich et al. "HIV-1 Neutralizing Antibodies with Limited Hypermutation from an Infant". en. In: *Cell* 166.1 (June 2016), pp. 77–87. URL: http://dx.doi.org/10.1016/j.cell.2016.05.055.

[303] Kwinten Sliepen et al. “Binding of inferred germline precursors of broadly neutralizing HIV-1 antibodies to native-like envelope trimers”. en. In: *Virology* 486 (Dec. 2015), pp. 116–120. URL: http://dx.doi.org/10.1016/j.virol.2015.08.002.

[304] Derek D Sloan et al. “Targeting HIV Reservoir in Infected CD4 T Cells by Dual-Affinity Re-targeting Molecules (DARTs) that Bind HIV Envelope and Recruit Cytotoxic T Cells”. en. In: *PLoS Pathog.* 11.11 (Nov. 2015), e1005233. URL: http://dx.doi.org/10.1371/journal.ppat.1005233.

[305] Devin Sok and Dennis R Burton. “HIV broadly neutralizing antibodies: Taking good care of the 98”. en. In: *Immunity* 45.5 (Nov. 2016), pp. 958–960. URL: http://dx.doi.org/10.1016/j.immuni.2016.10.033.

[306] Devin Sok and Dennis R Burton. “Recent progress in broadly neutralizing antibodies to HIV”. en. In: *Nat. Immunol.* 19.11 (Nov. 2018), pp. 1179–1188. URL: http://dx.doi.org/10.1038/s41590-018-0235-7.

[307] Devin Sok et al. “A Prominent Site of Antibody Vulnerability on HIV Envelope Incorporates a Motif Associated with CCR5 Binding and Its Camouflaging Glycans”. en. In: *Immunity* 45.1 (July 2016), pp. 31–45. URL: http://dx.doi.org/10.1016/j.immuni.2016.06.026.

[308] Devin Sok et al. “Priming HIV-1 broadly neutralizing antibody precursors in human Ig loci transgenic mice”. en. In: *Science* 353.6307 (Sept. 2016), pp. 1557–1560. URL: http://dx.doi.org/10.1126/science.aah3945.

[309] Devin Sok et al. “Recombinant HIV envelope trimer selects for quaternary-dependent antibodies targeting the trimer apex”. en. In: *Proc. Natl. Acad. Sci. U. S. A.* 111.49 (Dec. 2014), pp. 17624–17629. URL: http://dx.doi.org/10.1073/pnas.1415789111.

[310] Devin Sok et al. “The effects of somatic hypermutation on neutralization and binding in the PGT121 family of broadly neutralizing HIV antibodies”. en. In: *PLoS Pathog.* 9.11 (Nov. 2013), e1003754. URL: http://dx.doi.org/10.1371/journal.ppat.1003754.

[311] Maura Statzu et al. “CD8+ lymphocytes do not impact SIV reservoir establishment under ART”. en. In: *Nat Microbiol* 8.2 (Feb. 2023), pp. 299–308. URL: http://dx.doi.org/10.1038/s41564-022-01311-9.

[312] Jon M Steichen et al. “A generalized HIV vaccine design strategy for priming of broadly neutralizing antibody responses”. en. In: *Science* 366.6470 (Dec. 2019). URL: http://dx.doi.org/10.1126/science.aax4380.

[313] Jon M Steichen et al. “HIV Vaccine Design to Target Germline Precursors of Glycan-Dependent Broadly Neutralizing Antibodies”. en. In: *Immunity* 45.3 (Sept. 2016), pp. 483–496. URL: http://dx.doi.org/10.1016/j.immuni.2016.08.016.

[314] B S Stein et al. “pH-independent HIV entry into CD4-positive T cells via virus envelope fusion to the plasma membrane”. en. In: *Cell* 49.5 (June 1987), pp. 659–668. URL: http://dx.doi.org/10.1016/0092-8674(87)90542-3.

[315] Kathryn E Stephenson et al. "Safety, pharmacokinetics and antiviral activity of PGT121, a broadly neutralizing monoclonal antibody against HIV-1: a randomized, placebo-controlled, phase 1 clinical trial". en. In: *Nat. Med.* 27.10 (Oct. 2021), pp. 1718–1724. URL: http://dx.doi.org/10.1038/s41591-021-01509-0.

[316] G Stiegler et al. "A potent cross-clade neutralizing human monoclonal antibody against a novel epitope on gp41 of human immunodeficiency virus type 1". en. In: *AIDS Res. Hum. Retroviruses* 17.18 (Dec. 2001), pp. 1757–1765. URL: http://dx.doi.org/10.1089/08892220152741450.

[317] Gabriela Stiegler et al. "Antiviral activity of the neutralizing antibodies 2F5 and 2G12 in asymptomatic HIV-1-infected humans: a phase I evaluation". en. In: *AIDS* 16.15 (Oct. 2002), pp. 2019–2025. URL: http://dx.doi.org/10.1097/00002030-200210180-00006.

[318] Dan Suan et al. "CCR6 defines memory B cell precursors in mouse and human germinal centers, revealing light-zone location and predominant low antigen affinity". en. In: *Immunity* 47.6 (Dec. 2017), 1142–1153.e4. URL: http://dx.doi.org/10.1016/j.immuni.2017.11.022.

[319] Christopher Sundling et al. "High-resolution definition of vaccine-elicited B cell responses against the HIV primary receptor binding site". en. In: *Sci. Transl. Med.* 4.142 (July 2012), 142ra96. URL: http://dx.doi.org/10.1126/scitranslmed.3003752.

[320] Julia A M Sung et al. "Dual-Affinity Re-Targeting proteins direct T cell-mediated cytolysis of latently HIV-infected cells". en. In: *J. Clin. Invest.* 125.11 (Nov. 2015), pp. 4077–4090. URL: http://dx.doi.org/10.1172/JCI82314.

[321] Fuchou Tang et al. "mRNA-Seq whole-transcriptome analysis of a single cell". en. In: *Nat. Methods* 6.5 (May 2009), pp. 377–382. URL: http://dx.doi.org/10.1038/nmeth.1315.

[322] S Tappero et al. "Recruitment, screening and characteristics of injection drugusersparticipatingintheAIDSVAXB/EHIVvaccinetrial". In: *AIDS* 18 (2004), pp. 311–316.

[323] Ming Tian et al. "Induction of HIV Neutralizing Antibody Lineages in Mice with Diverse Precursor Repertoires". en. In: *Cell* 166.6 (Sept. 2016), 1471–1484.e18. URL: http://dx.doi.org/10.1016/j.cell.2016.07.029.

[324] Thomas Tiller et al. "Efficient generation of monoclonal antibodies from single human B cells by single cell RT-PCR and expression vector cloning". en. In: *J. Immunol. Methods* 329.1-2 (Jan. 2008), pp. 112–124. URL: http://dx.doi.org/10.1016/j.jim.2007.09.017.

[325] Georgia D Tomaras et al. "Initial B-cell responses to transmitted human immunodeficiency virus type 1: virion-binding immunoglobulin M (IgM) and IgG antibodies followed by plasma anti-gp41 antibodies with ineffective control of initial viremia". en. In: *J. Virol.* 82.24 (Dec. 2008), pp. 12449–12463. URL: http://dx.doi.org/10.1128/JVI.01708-08.

[326] A Trkola et al. "Human monoclonal antibody 2G12 defines a distinctive neutralization epitope on the gp120 glycoprotein of human immunodeficiency virus type 1". en. In: *J. Virol.* 70.2 (Feb. 1996), pp. 1100–1108. URL: http://dx.doi.org/10.1128/JVI.70.2.1100-1108.1996.

[327] Alexandra Trkola et al. "Delay of HIV-1 rebound after cessation of antiretroviral therapy through passive transfer of human neutralizing antibodies". en. In: *Nat. Med.* 11.6 (June 2005), pp. 615–622. URL: http://dx.doi.org/10.1038/nm1244.

[328] Jeffrey Umotoy et al. "Rapid and Focused Maturation of a VRC01-Class HIV Broadly Neutralizing Antibody Lineage Involves Both Binding and Accommodation of the N276-Glycan". en. In: *Immunity* 51.1 (July 2019), 141–154.e6. URL: http://dx.doi.org/10.1016/j.immuni.2019.06.004.

[329] UNAIDS. *UNAIDS Report 2023*. https://thepath.unaids.org/wp-content/themes/unaids2023/assets/files/2023_report.pdf. Accessed: 2024-2-25. 2023. URL: https://thepath.unaids.org/wp-content/themes/unaids2023/assets/files/2023_report.pdf.

[330] L A Vanoff et al. "V3 loop region of the HIV-1 gp120 envelope protein is essential for virus infectivity". In: *Virology* 187 (1992), pp. 423–432.

[331] Néstor Vázquez Bernat et al. "High-Quality Library Preparation for NGS-Based Immunoglobulin Germline Gene Inference and Repertoire Expression Analysis". en. In: *Front. Immunol.* 10 (Apr. 2019), p. 660. URL: http://dx.doi.org/10.3389/fimmu.2019.00660.

[332] F D Veronese et al. "Characterization of gp41 as the transmembrane protein coded by the HTLV-III/LAV envelope gene". en. In: *Science* 229.4720 (Sept. 1985), pp. 1402–1405. URL: http://dx.doi.org/10.1126/science.2994223.

[333] Charlotte Viant et al. "Antibody affinity shapes the choice between memory and germinal center B cell fates". en. In: *Cell* 183.5 (Nov. 2020), 1298–1311.e11. URL: http://dx.doi.org/10.1016/j.cell.2020.09.063.

[334] Gabriel D Victora and Michel C Nussenzweig. "Germinal Centers". en. In: *Annu. Rev. Immunol.* 40 (Apr. 2022), pp. 413–442. URL: http://dx.doi.org/10.1146/annurev-immunol-120419-022408.

[335] Gabriel D Victora et al. "Germinal center dynamics revealed by multiphoton microscopy with a photoactivatable fluorescent reporter". en. In: *Cell* 143.4 (Nov. 2010), pp. 592–605. URL: http://dx.doi.org/10.1016/j.cell.2010.10.032.

[336] Benoit Visseaux et al. "Hiv-2 molecular epidemiology". en. In: *Infect. Genet. Evol.* 46 (Dec. 2016), pp. 233–240. URL: http://dx.doi.org/10.1016/j.meegid.2016.08.010.

[337] Kshitij Wagh et al. "Completeness of HIV-1 envelope glycan shield at transmission determines neutralization breadth". en. In: *Cell Rep.* 25.4 (Oct. 2018), 893–908.e7. URL: http://dx.doi.org/10.1016/j.celrep.2018.09.087.

[338] Ilka Wahl and Hedda Wardemann. "Sterilizing immunity: Understanding COVID-19". en. In: *Immunity* 55.12 (Dec. 2022), pp. 2231–2235. URL: http://dx.doi.org/10.1016/j.immuni.2022.10.017.

[339] Laura M Walker et al. “Broad and potent neutralizing antibodies from an African donor reveal a new HIV-1 vaccine target”. en. In: *Science* 326.5950 (Oct. 2009), pp. 285–289. URL: http://dx.doi.org/10.1126/science.1178746.

[340] Laura M Walker et al. “Broad neutralization coverage of HIV by multiple highly potent antibodies”. en. In: *Nature* 477.7365 (Sept. 2011), pp. 466–470. URL: http://dx.doi.org/10.1038/nature10373.

[341] Huai-Chun Wang et al. “Modeling Site Heterogeneity with Posterior Mean Site Frequency Profiles Accelerates Accurate Phylogenomic Estimation”. en. In: *Syst. Biol.* 67.2 (Mar. 2018), pp. 216–235. URL: http://dx.doi.org/10.1093/sysbio/syx068.

[342] Yi Wang et al. “Single-cell transcriptomic atlas reveals distinct immunological responses between COVID-19 vaccine and natural SARS-CoV-2 infection”. en. In: *J. Med. Virol.* 94.11 (Nov. 2022), pp. 5304–5324. URL: http://dx.doi.org/10.1002/jmv.28012.

[343] Andrew B Ward and Ian A Wilson. “Insights into the trimeric HIV-1 envelope glycoprotein structure”. en. In: *Trends Biochem. Sci.* 40.2 (Feb. 2015), pp. 101–107. URL: http://dx.doi.org/10.1016/j.tibs.2014.12.006.

[344] Xiping Wei et al. “Emergence of resistant human immunodeficiency virus type 1 in patients receiving fusion inhibitor (T-20) monotherapy”. en. In: *Antimicrob. Agents Chemother.* 46.6 (June 2002), pp. 1896–1905. URL: http://dx.doi.org/10.1128/AAC.46.6.1896-1905.2002.

[345] Joshua A Weinstein et al. “High-Throughput Sequencing of the Zebrafish Antibody Repertoire”. In: *Science* 324.5928 (2009), pp. 807–810. URL: https://www.science.org/doi/abs/10.1126/science.1170020.

[346] W Weissenhorn et al. “Structural basis for membrane fusion by enveloped viruses”. en. In: *Mol. Membr. Biol.* 16.1 (1999), pp. 3–9. URL: http://dx.doi.org/10.1080/096876899294706.

[347] Hugh C Welles et al. “Broad coverage of neutralization-resistant SIV strains by second-generation SIV-specific antibodies targeting the region involved in binding CD4”. en. In: *PLoS Pathog.* 18.6 (June 2022), e1010574. URL: http://dx.doi.org/10.1371/journal.ppat.1010574.

[348] James B Whitney et al. “Rapid seeding of the viral reservoir prior to SIV viraemia in rhesus monkeys”. en. In: *Nature* 512.7512 (Aug. 2014), pp. 74–77. URL: http://dx.doi.org/10.1038/nature13594.

[349] Alexandria Williams et al. “Geographic and Population Distributions of Human Immunodeficiency Virus (HIV)-1 and HIV-2 Circulating Subtypes: A Systematic Literature Review and Meta-analysis (2010-2021)”. en. In: *J. Infect. Dis.* 228.11 (Nov. 2023), pp. 1583–1591. URL: http://dx.doi.org/10.1093/infdis/jiad327.

[350] Katherine L Williams et al. “Superinfection Drives HIV Neutralizing Antibody Responses from Several B Cell Lineages that Contribute to a Polyclonal Repertoire”. en. In: *Cell Rep.* 23.3 (Apr. 2018), pp. 682–691. URL: http://dx.doi.org/10.1016/j.celrep.2018.03.082.

[351] Wilton B Williams et al. "Initiation of HIV neutralizing B cell lineages with sequential envelope immunizations". en. In: *Nat. Commun.* 8.1 (Nov. 2017), p. 1732. URL: http://dx.doi.org/10.1038/s41467-017-01336-3.

[352] F Alexander Wolf, Philipp Angerer, and Fabian J Theis. "SCANPY: large-scale single-cell gene expression data analysis". en. In: *Genome Biol.* 19.1 (Feb. 2018), p. 15. URL: http://dx.doi.org/10.1186/s13059-017-1382-0.

[353] T F Wolfs et al. "HIV-1 genomic RNA diversification following sexual and parenteral virus transmission". en. In: *Virology* 189.1 (July 1992), pp. 103–110. URL: http://dx.doi.org/10.1016/0042-6822(92)90685-i.

[354] Joseph K Wong et al. "In vivo CD8+ T-cell suppression of siv viremia is not mediated by CTL clearance of productively infected cells". en. In: *PLoS Pathog.* 6.1 (Jan. 2010), e1000748. URL: http://dx.doi.org/10.1371/journal.ppat.1000748.

[355] Rachel Wong et al. "Affinity-restricted memory B cells dominate recall responses to heterologous flaviviruses". en. In: *Immunity* 53.5 (Nov. 2020), 1078–1094.e7. URL: http://dx.doi.org/10.1016/j.immuni.2020.09.001.

[356] F Wong-Staal et al. "Molecular characterization of human T-lymphotropic leukemia virus type III associated with the acquired immunodeficiency syndrome". en. In: *Princess Takamatsu Symp.* 15 (1984), pp. 291–300. URL: https://www.ncbi.nlm.nih.gov/pubmed/6100646.

[357] Xueling Wu et al. "Focused evolution of HIV-1 neutralizing antibodies revealed by structures and deep sequencing". en. In: *Science* 333.6049 (Sept. 2011), pp. 1593–1602. URL: http://dx.doi.org/10.1126/science.1207532.

[358] Xueling Wu et al. "Rational design of envelope identifies broadly neutralizing human monoclonal antibodies to HIV-1". en. In: *Science* 329.5993 (Aug. 2010), pp. 856–861. URL: http://dx.doi.org/10.1126/science.1187659.

[359] R Wyatt et al. "The antigenic structure of the HIV gp120 envelope glycoprotein". en. In: *Nature* 393.6686 (June 1998), pp. 705–711. URL: http://dx.doi.org/10.1038/31514.

[360] Jianying Yang and M. Reth. "Oligomeric organization of the B-cell antigen receptor on resting cells". In: *Nature* 467 (2010), pp. 465–469. DOI: 10.1038/nature09357.

[361] Xi Yang et al. "Discovery and characterization of SARS-CoV-2 reactive and neutralizing antibodies from humanized CAMouseHG mice through rapid hybridoma screening and high-throughput single-cell V(D)J sequencing". en. In: *Front. Immunol.* 13 (Sept. 2022), p. 992787. URL: http://dx.doi.org/10.3389/fimmu.2022.992787.

[362] Jian Ye et al. "IgBLAST: an immunoglobulin variable domain sequence analysis tool". en. In: *Nucleic Acids Res.* 41.Web Server issue (July 2013), W34–40. URL: http://dx.doi.org/10.1093/nar/gkt382.

[363] Leng-Siew Yeap et al. "Sequence-intrinsic mechanisms that target AID mutational outcomes on antibody genes". en. In: *Cell* 163.5 (Nov. 2015), pp. 1124–1137. URL: http://dx.doi.org/10.1016/j.cell.2015.10.042.

[364] Hyejin Yoon et al. “CATNAP: a tool to compile, analyze and tally neutralizing antibody panels”. en. In: *Nucleic Acids Res.* 43.W1 (July 2015), W213–9. URL: http://dx.doi.org/10.1093/nar/gkv404.

[365] Clara Young and Robert Brink. “The unique biology of germinal center B cells”. en. In: *Immunity* 54.8 (Aug. 2021), pp. 1652–1664. URL: http://dx.doi.org/10.1016/j.immuni.2021.07.015.

[366] L Q Zhang et al. “Selection for specific sequences in the external envelope protein of human immunodeficiency virus type 1 upon primary infection”. en. In: *J. Virol.* 67.6 (June 1993), pp. 3345–3356. URL: http://dx.doi.org/10.1128/JVI.67.6.3345-3356.1993.

[367] Lei Zhang et al. “An MPER antibody neutralizes HIV-1 using germline features shared among donors”. en. In: *Nat. Commun.* 10.1 (Nov. 2019), p. 5389. URL: http://dx.doi.org/10.1038/s41467-019-12973-1.

[368] M Zhang. “Tracking global patterns of N-linked glycosylation site variation in highly variable viral glycoproteins: HIV, SIV, and HCV envelopes and influenza hemagglutinin”. en. In: *Glycobiology* 14.12 (July 2004), pp. 1229–1246. URL: http://dx.doi.org/10.1093/glycob/cwh106.

[369] Tongqing Zhou et al. “Multidonor analysis reveals structural elements, genetic determinants, and maturation pathway for HIV-1 neutralization by VRC01-class antibodies”. en. In: *Immunity* 39.2 (Aug. 2013), pp. 245–258. URL: http://dx.doi.org/10.1016/j.immuni.2013.04.012.

[370] Tongqing Zhou et al. “Structural basis for broad and potent neutralization of HIV-1 by antibody VRC01”. en. In: *Science* 329.5993 (Aug. 2010), pp. 811–817. URL: http://dx.doi.org/10.1126/science.1192819.

[371] Ping Zhu et al. “Distribution and three-dimensional structure of AIDS virus envelope spikes”. en. In: *Nature* 441.7095 (June 2006), pp. 847–852. URL: http://dx.doi.org/10.1038/nature04817.

[372] Ping Zhu et al. “Electron tomography analysis of envelope glycoprotein trimers on HIV and simian immunodeficiency virus virions”. en. In: *Proc. Natl. Acad. Sci. U. S. A.* 100.26 (Dec. 2003), pp. 15812–15817. URL: http://dx.doi.org/10.1073/pnas.2634931100.

[373] T Zhu et al. “Genotypic and phenotypic characterization of HIV-1 patients with primary infection”. en. In: *Science* 261.5125 (Aug. 1993), pp. 1179–1181. URL: http://dx.doi.org/10.1126/science.8356453.

[374] S Zolla-Pazner and T Cardozo. “Structure-function relationships of HIV-1 envelope sequence-variable regions refocus vaccine design”. In: *Nat Rev* 10 (2011), pp. 527–535.

[375] Valentin Zulkower and Susan Rosser. “DNA Chisel, a versatile sequence optimizer”. en. In: *Bioinformatics* 36.16 (Aug. 2020), pp. 4508–4509. URL: http://dx.doi.org/10.1093/bioinformatics/btaa558.

[376] M B Zwick et al. “Broadly neutralizing antibodies targeted to the membrane-proximal external region of human immunodeficiency virus type 1 glycoprotein gp41”. en. In: *J. Virol.* 75.22 (Nov. 2001), pp. 10892–10905. URL: http://dx.doi.org/10.1128/JVI.75.22.10892-10905.2001.

[377] Michael B Zwick et al. “A novel human antibody against human immunodeficiency virus type 1 gp120 is V1, V2, and V3 loop dependent and helps delimit the epitope of the broadly neutralizing antibody immunoglobulin G1 b12”. en. In: *J. Virol.* 77.12 (June 2003), pp. 6965–6978. URL: http://dx.doi.org/10.1128/jvi.77.12.6965-6978.2003.